Multicomponent diffusion in natural silicate melts: Toward a universal eigenvector matrix

Bobo Bai*, Youxue Zhang
Department of Earth and Environmental Sciences, The University of Michigan, Ann Arbor, MI 48109-1005, USA

Concentration profiles of oxide components and eigen-components from 160 diffusion couple or mineral dissolution experiments are shown in Figs. 1-160.

* Corresponding author. Email: bbai@umich.edu

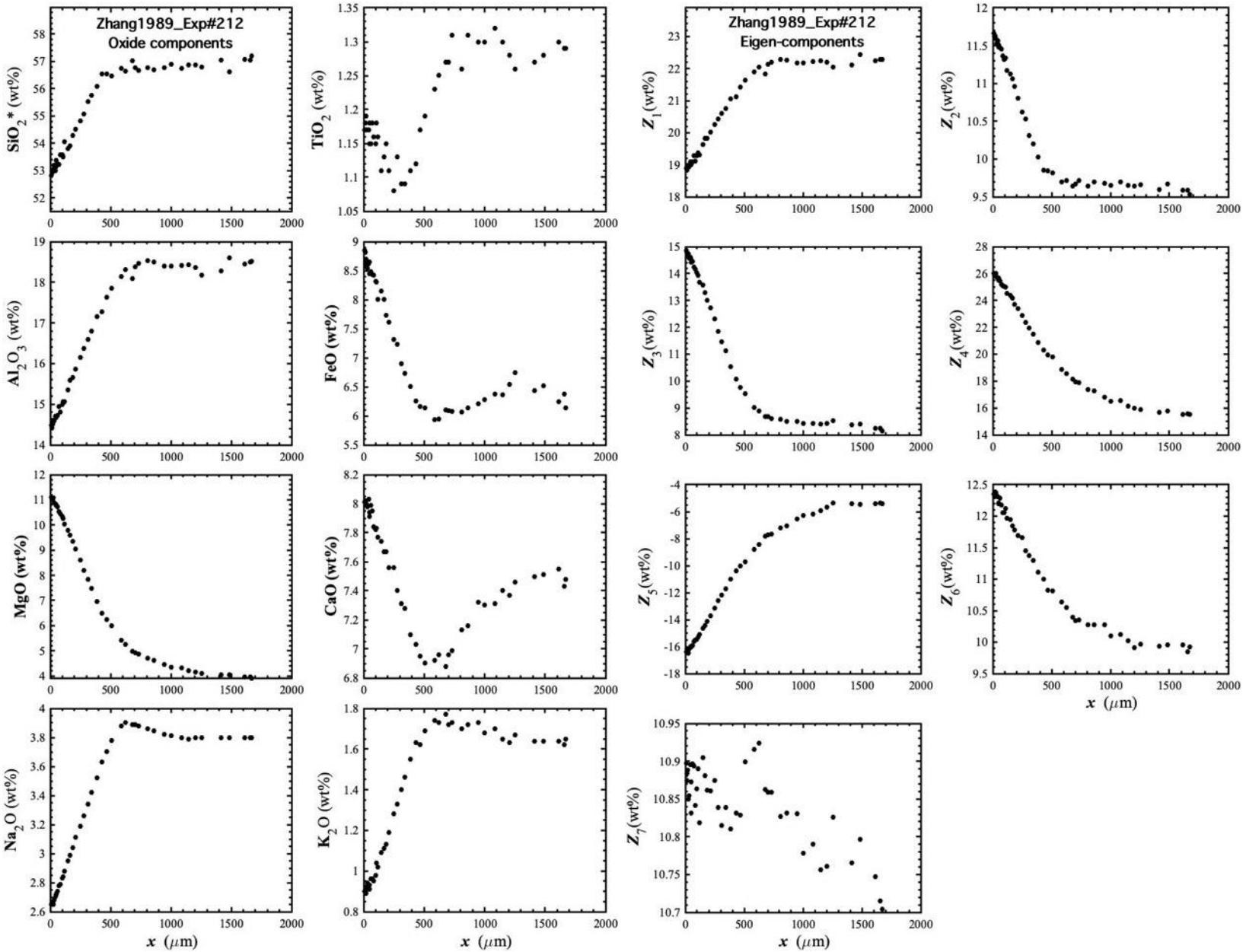

Figure 1. Concentration profiles of oxide components in wt% (left panel) and eigen-components (right panel) of Zhang1989_Exp#212, which is an olivine dissolution experiment in andesite (Zhang et al., 1989).

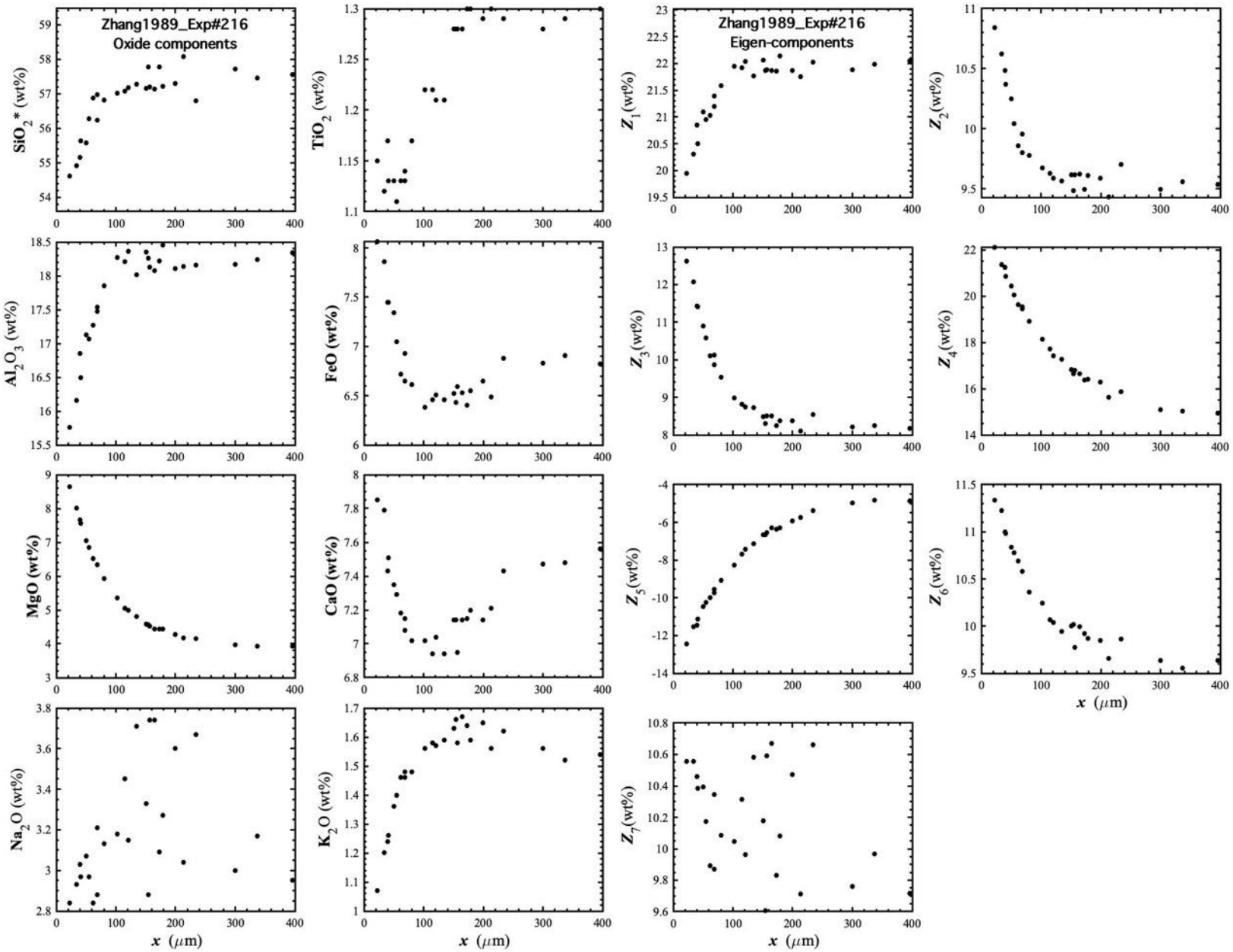

Figure 2. Concentration profiles of oxide components in wt% (left panel) and eigen-components (right panel) of Zhang1989_Exp#216, which is an olivine dissolution experiment in andesite (Zhang et al., 1989).

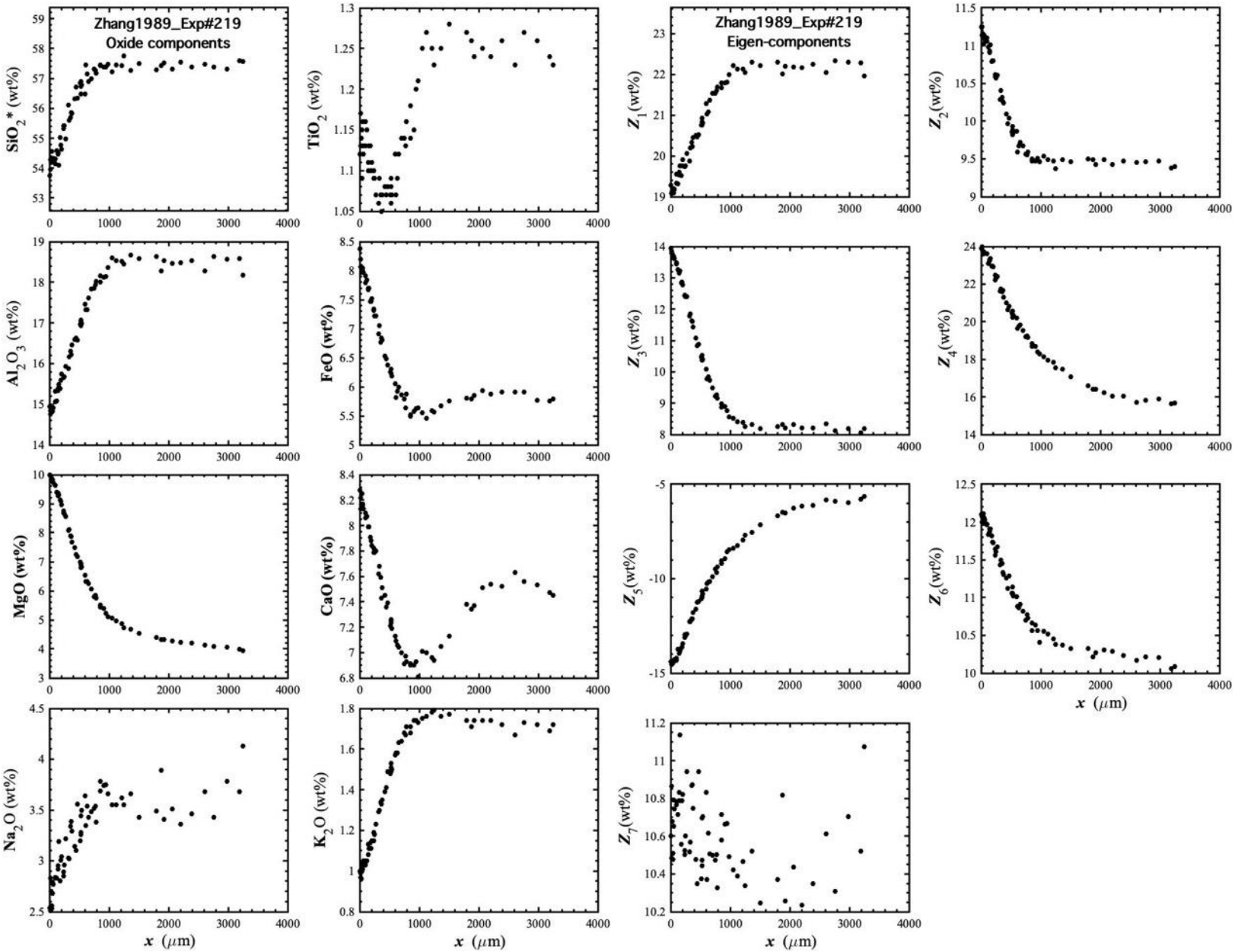

Figure 3. Concentration profiles of oxide components in wt% (left panel) and eigen-components (right panel) of Zhang1989_Exp#219, which is an olivine dissolution experiment in andesite (Zhang et al., 1989).

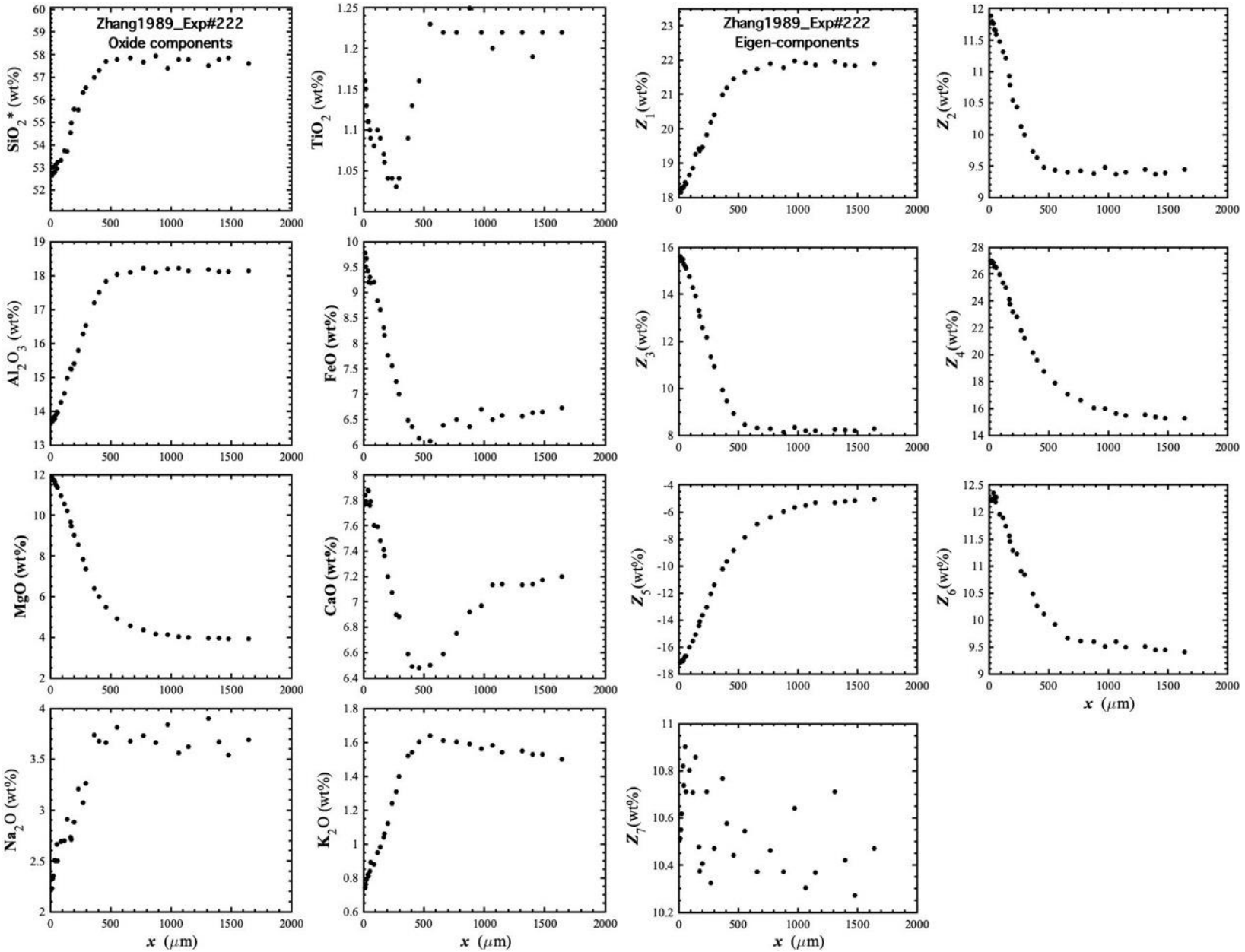

Figure 4. Concentration profiles of oxide components in wt% (left panel) and eigen-components (right panel) of Zhang1989_Exp#222, which is an olivine dissolution experiment in andesite (Zhang et al., 1989).

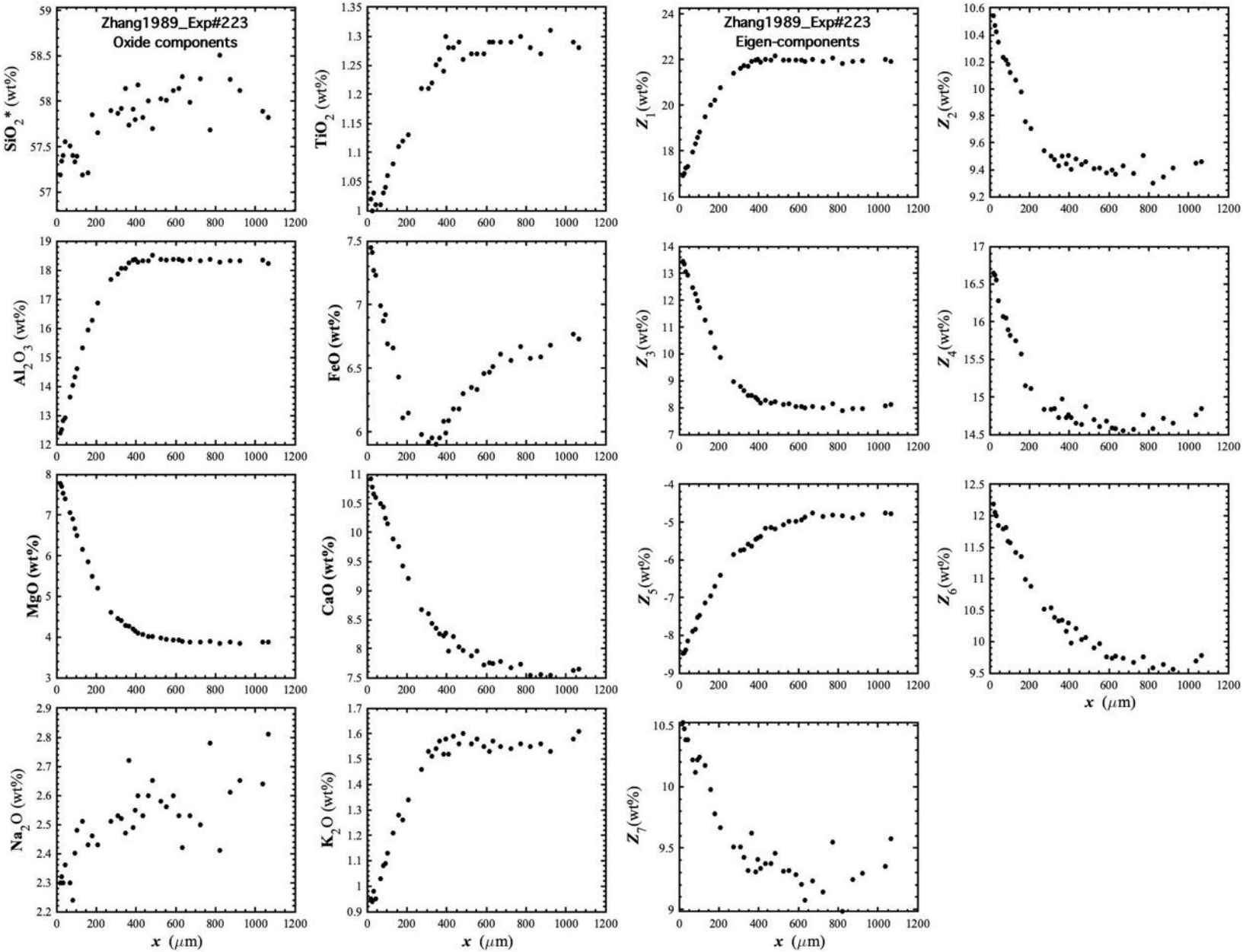

Figure 5. Concentration profiles of oxide components in wt% (left panel) and eigen-components (right panel) of Zhang1989_Exp#223, which is a diopside dissolution experiment in andesite (Zhang et al., 1989).

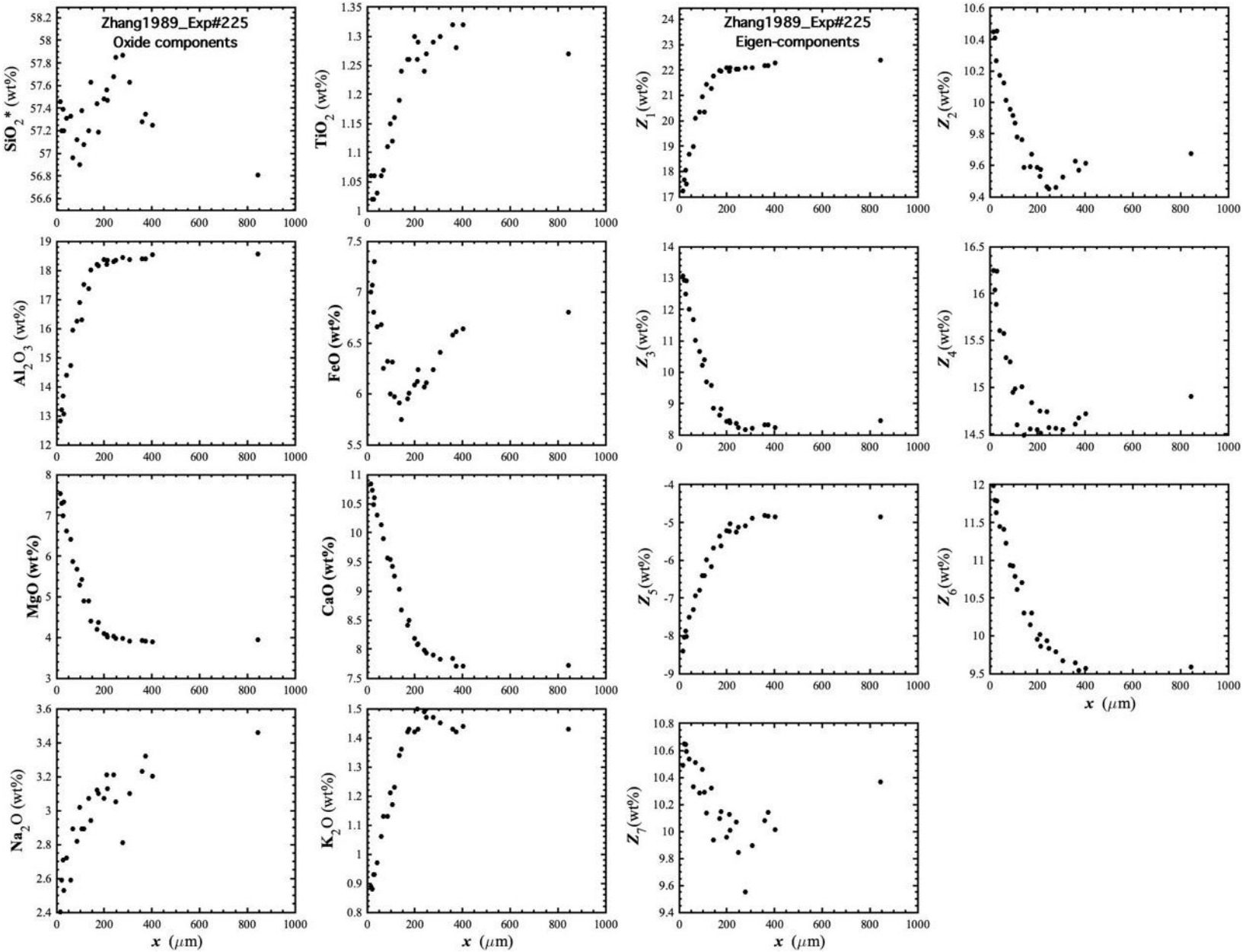

Figure 6. Concentration profiles of oxide components in wt% (left panel) and eigen-components (right panel) of Zhang1989_Exp#225, which is a diopside dissolution experiment in andesite (Zhang et al., 1989).

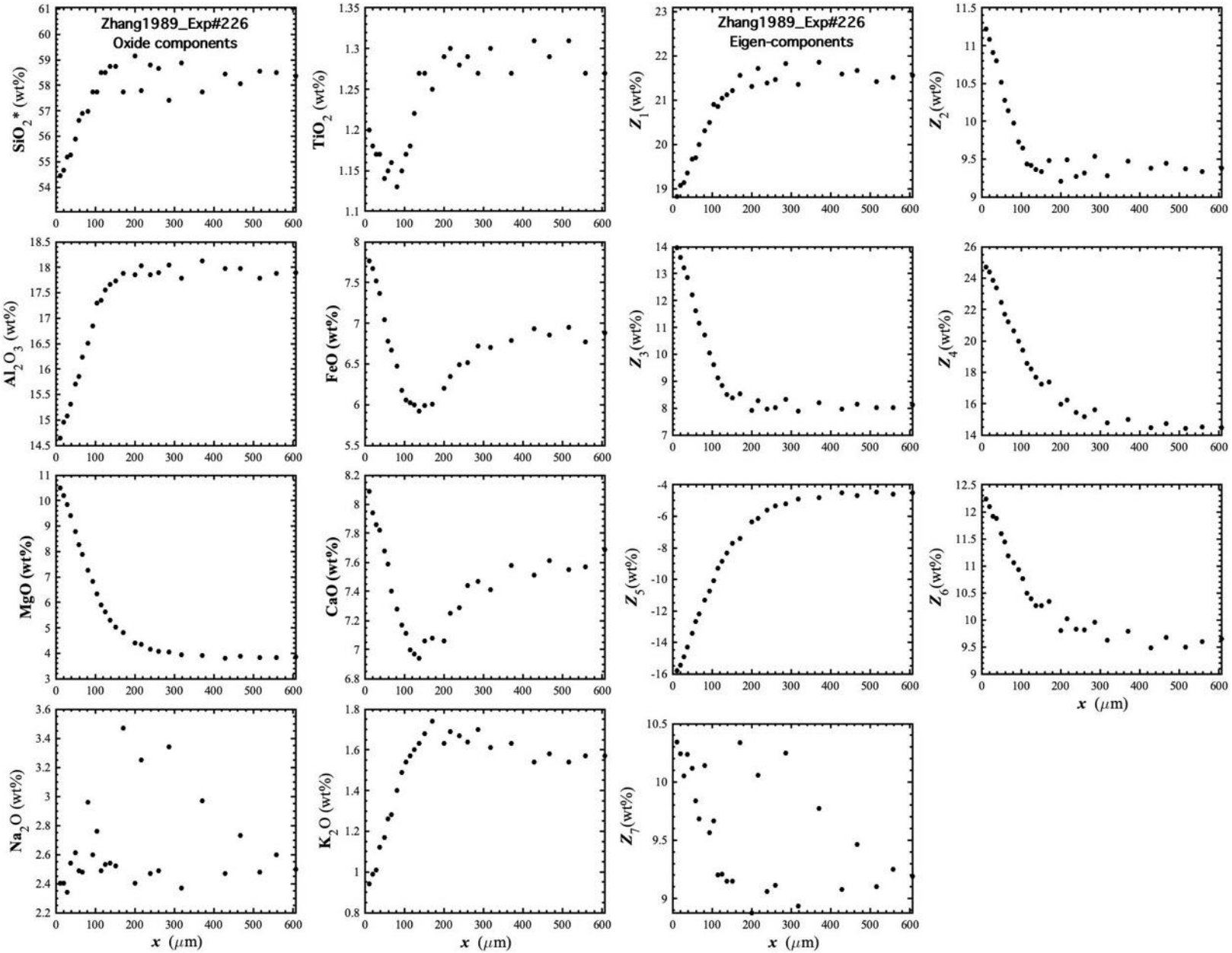

Figure 7. Concentration profiles of oxide components in wt% (left panel) and eigen-components (right panel) of Zhang1989_Exp#226, which is a forsterite dissolution experiment in andesite (Zhang et al., 1989).

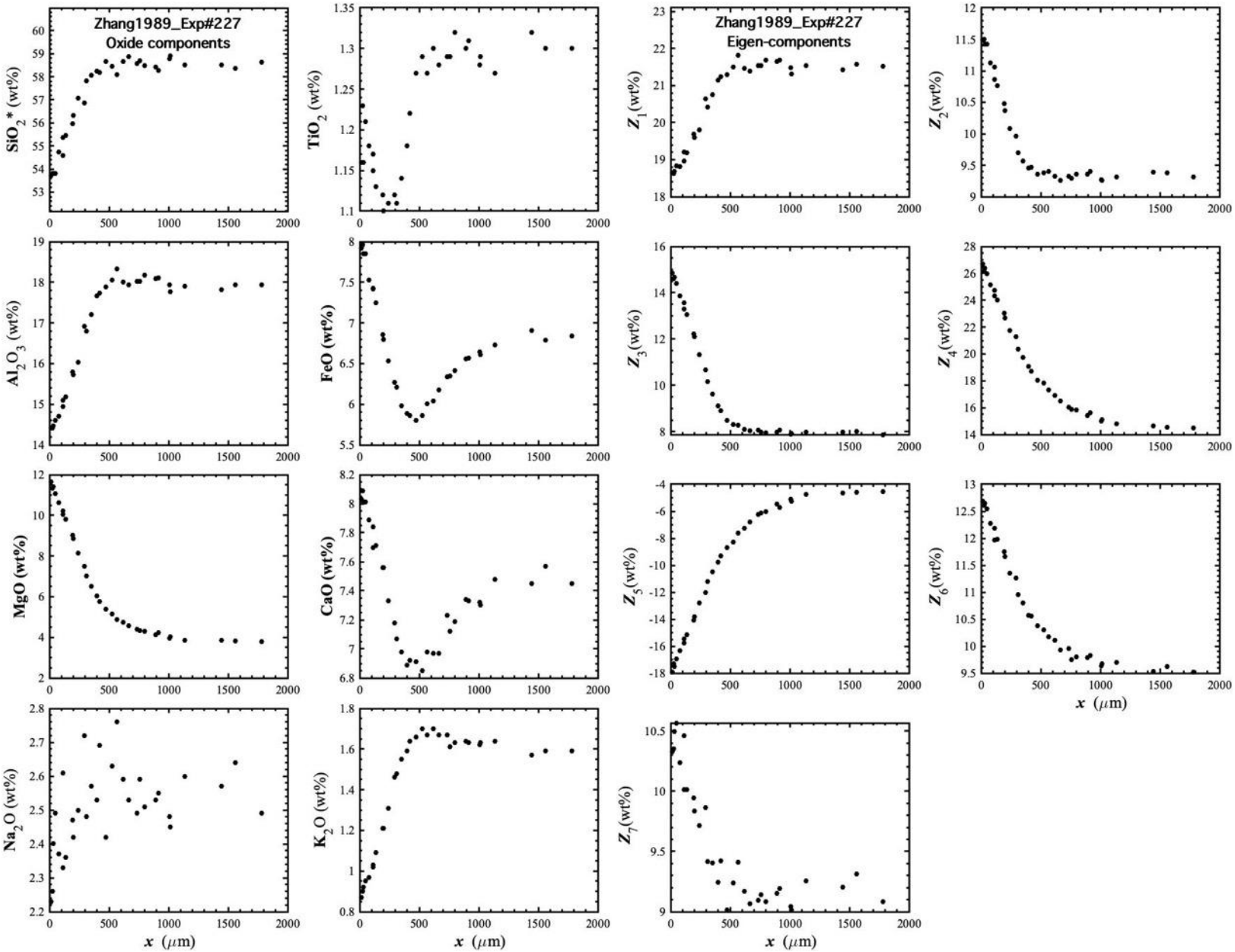

Figure 8. Concentration profiles of oxide components in wt% (left panel) and eigen-components (right panel) of Zhang1989_Exp#227, which is a forsterite dissolution experiment in andesite (Zhang et al., 1989).

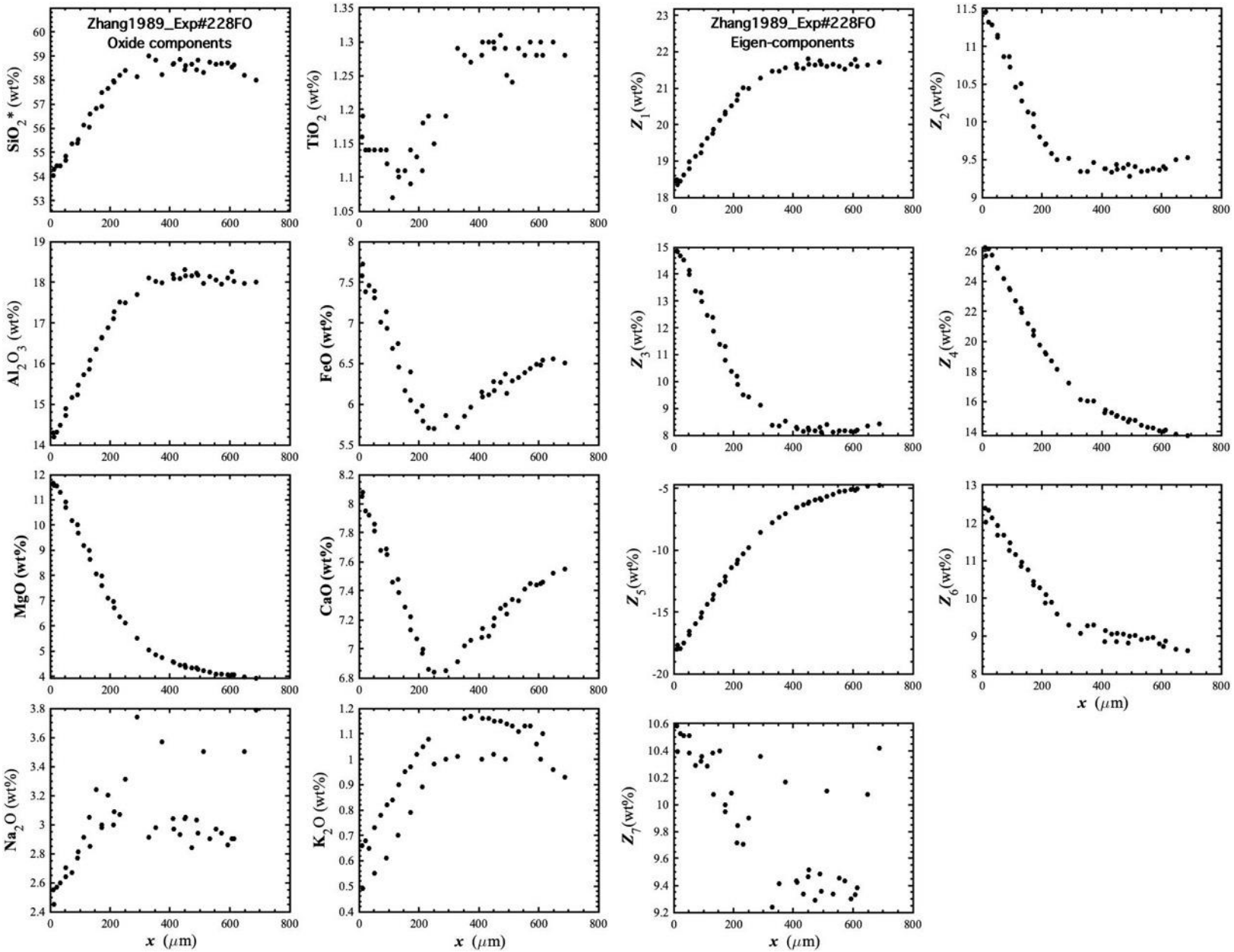

Figure 9. Concentration profiles of oxide components in wt% (left panel) and eigen-components (right panel) of Zhang1989_Exp#228FO, which is a forsterite dissolution experiment in andesite (Zhang et al., 1989).

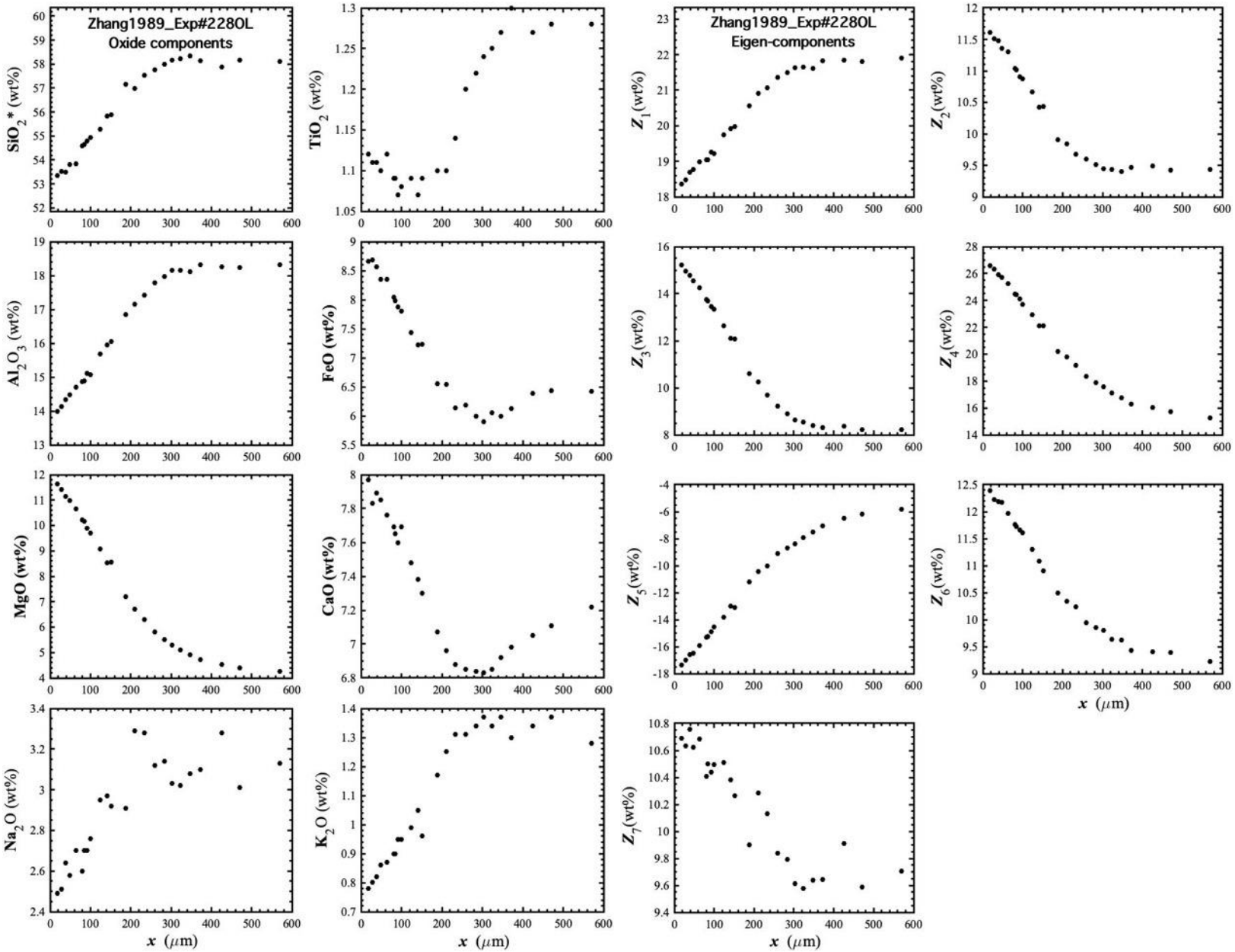

Figure 10. Concentration profiles of oxide components in wt% (left panel) and eigen-components (right panel) of Zhang1989_Exp#228OL, which is an olivine dissolution experiment in andesite (Zhang et al., 1989).

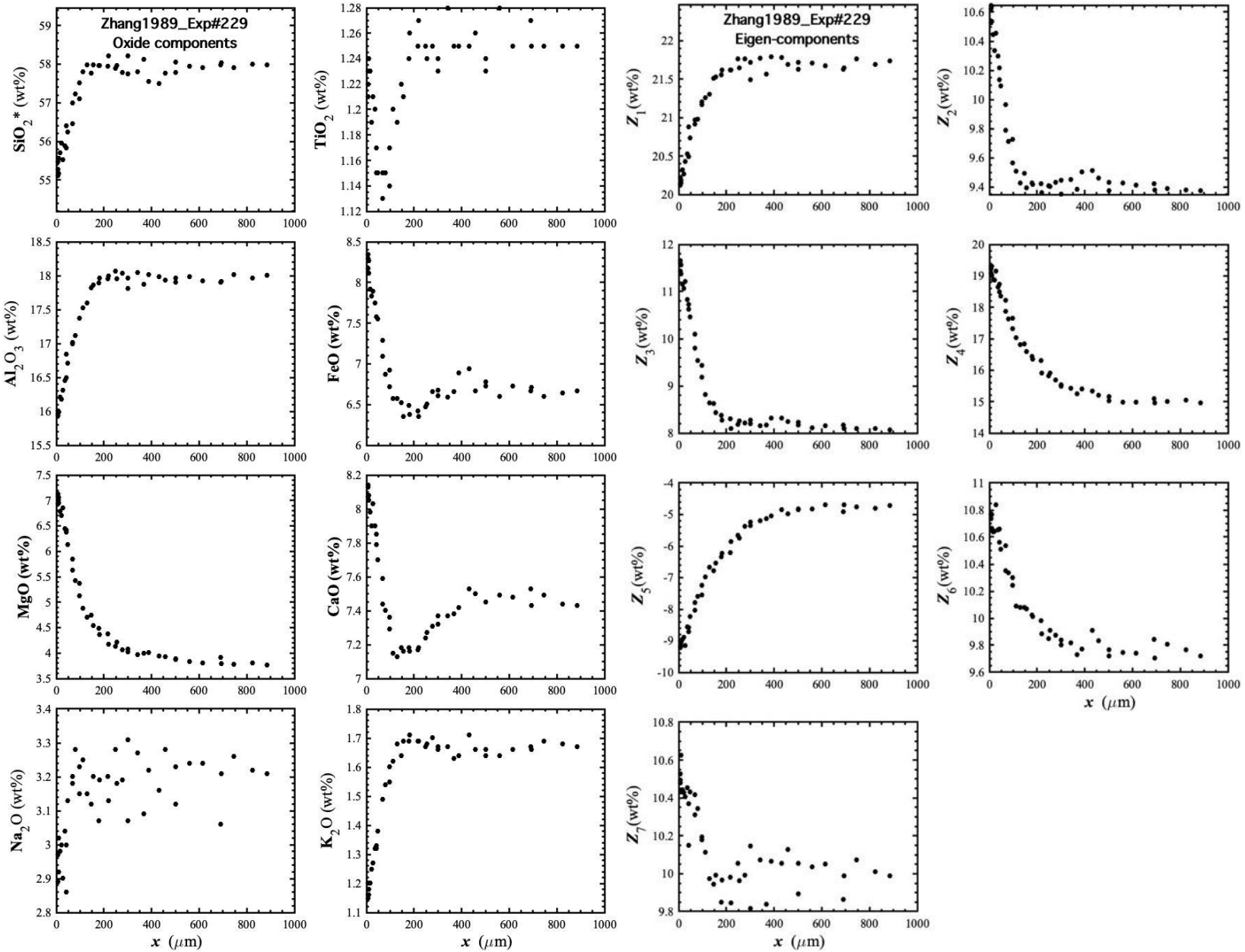

Figure 11. Concentration profiles of oxide components in wt% (left panel) and eigen-components (right panel) of Zhang1989_Exp#229, which is an olivine dissolution experiment in andesite (Zhang et al., 1989).

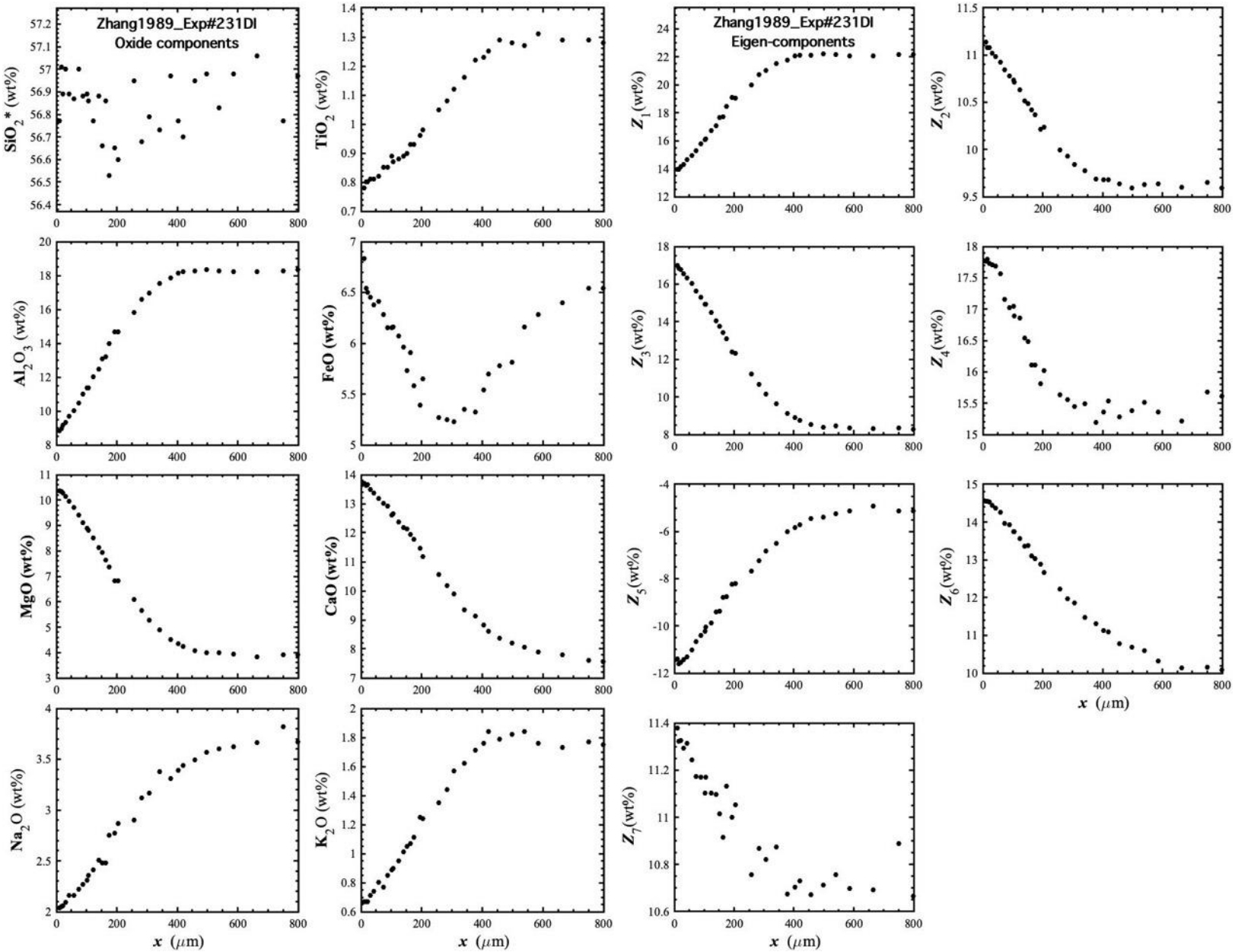

Figure 12. Concentration profiles of oxide components in wt% (left panel) and eigen-components (right panel) of Zhang1989_Exp#231DI, which is a diopside dissolution experiment in andesite (Zhang et al., 1989).

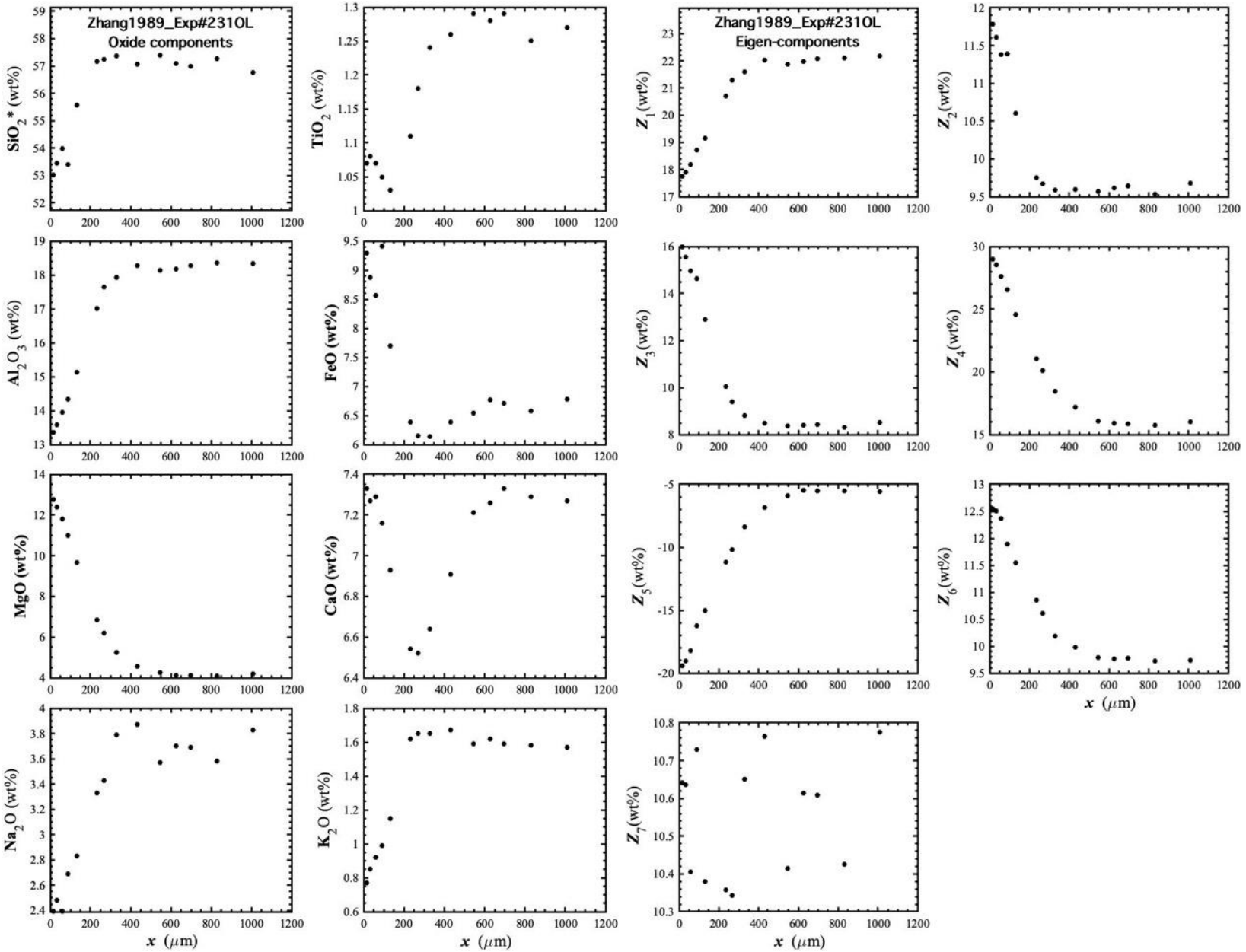

Figure 13. Concentration profiles of oxide components in wt% (left panel) and eigen-components (right panel) of Zhang1989_Exp#231OL, which is an olivine dissolution experiment in andesite (Zhang et al., 1989).

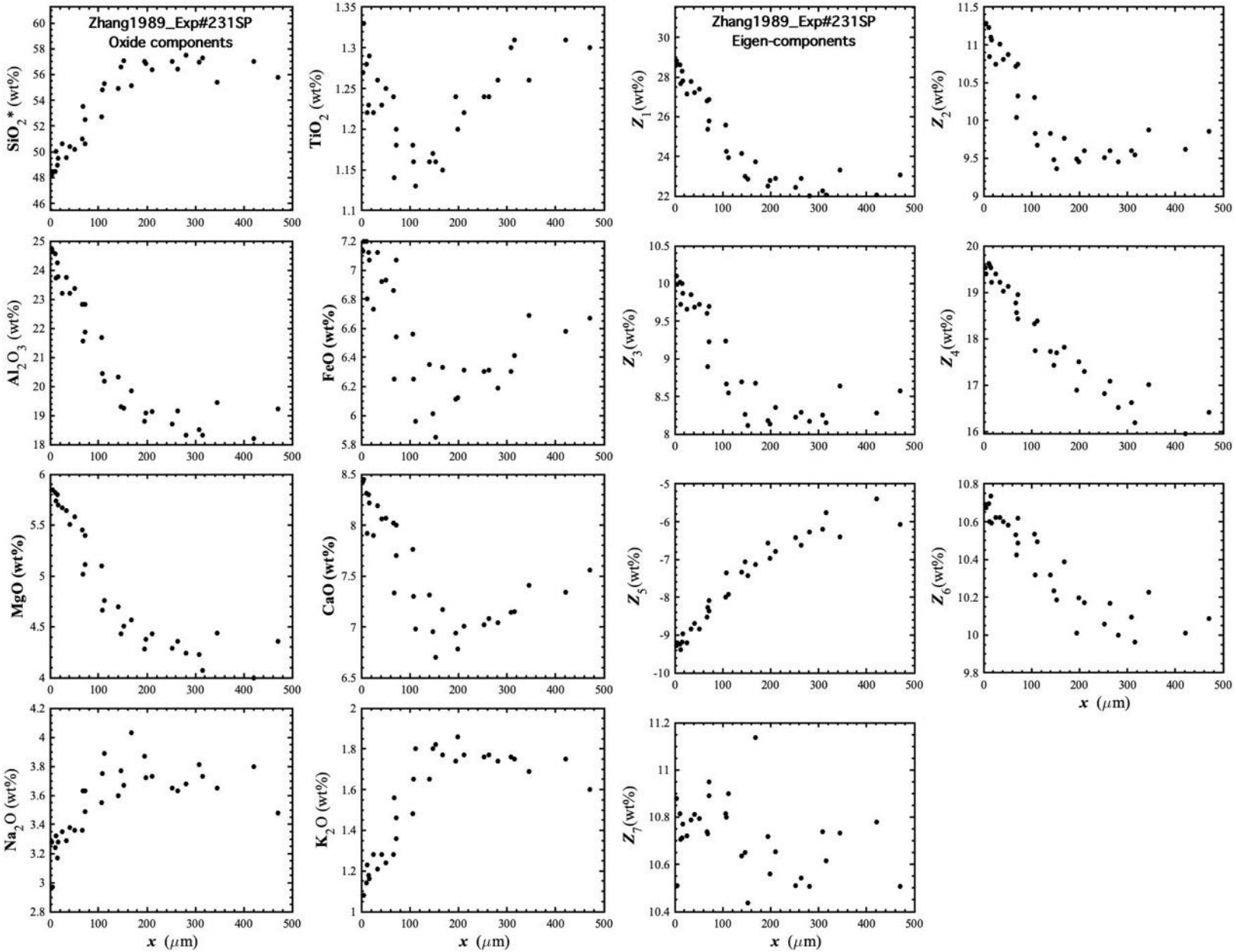

Figure 14. Concentration profiles of oxide components in wt% (left panel) and eigen-components (right panel) of Zhang1989_Exp#231SP, which is a spinel dissolution experiment in andesite (Zhang et al., 1989).

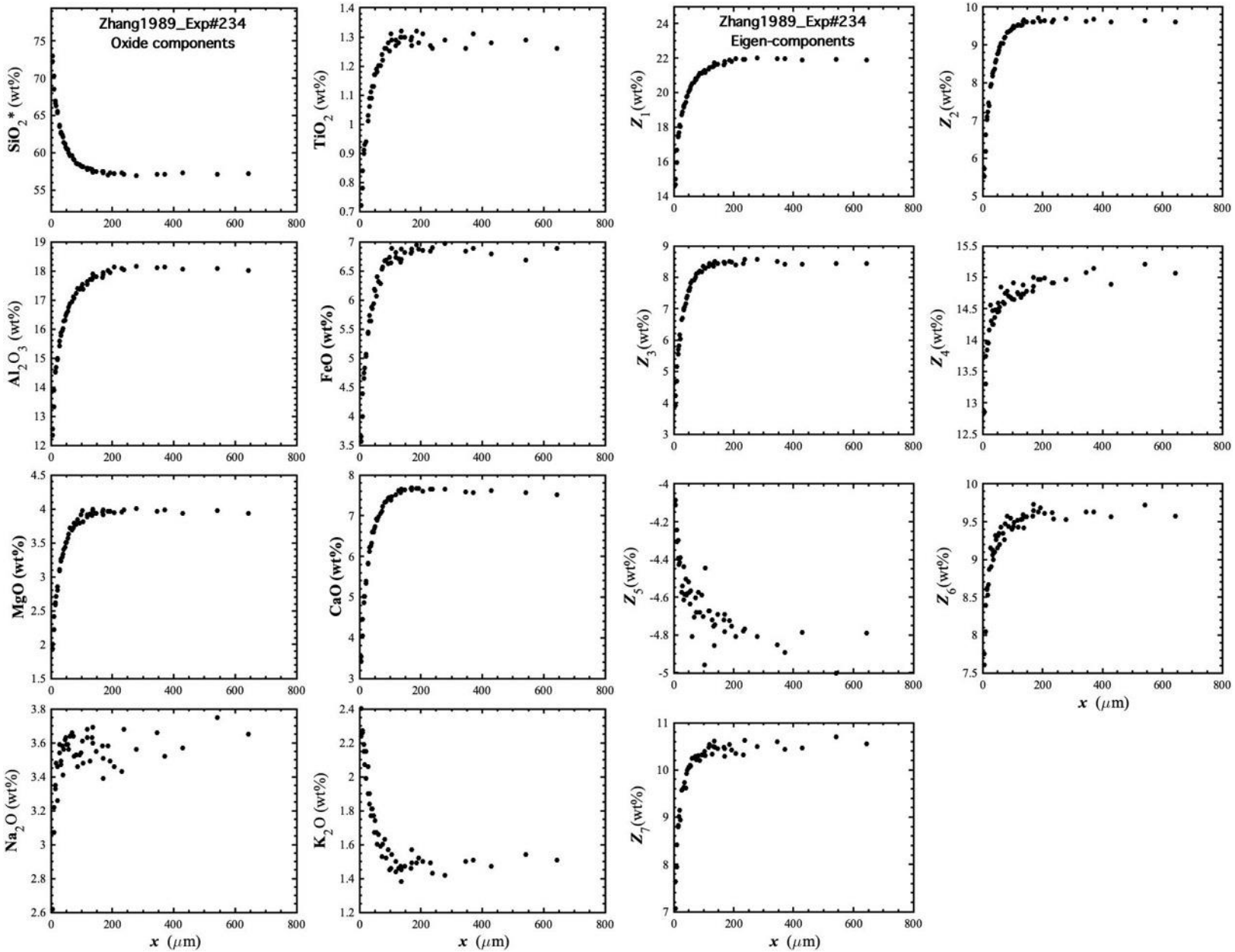

Figure 15. Concentration profiles of oxide components in wt% (left panel) and eigen-components (right panel) of Zhang1989_Exp#234, which is a quartz dissolution experiment in andesite (Zhang et al., 1989).

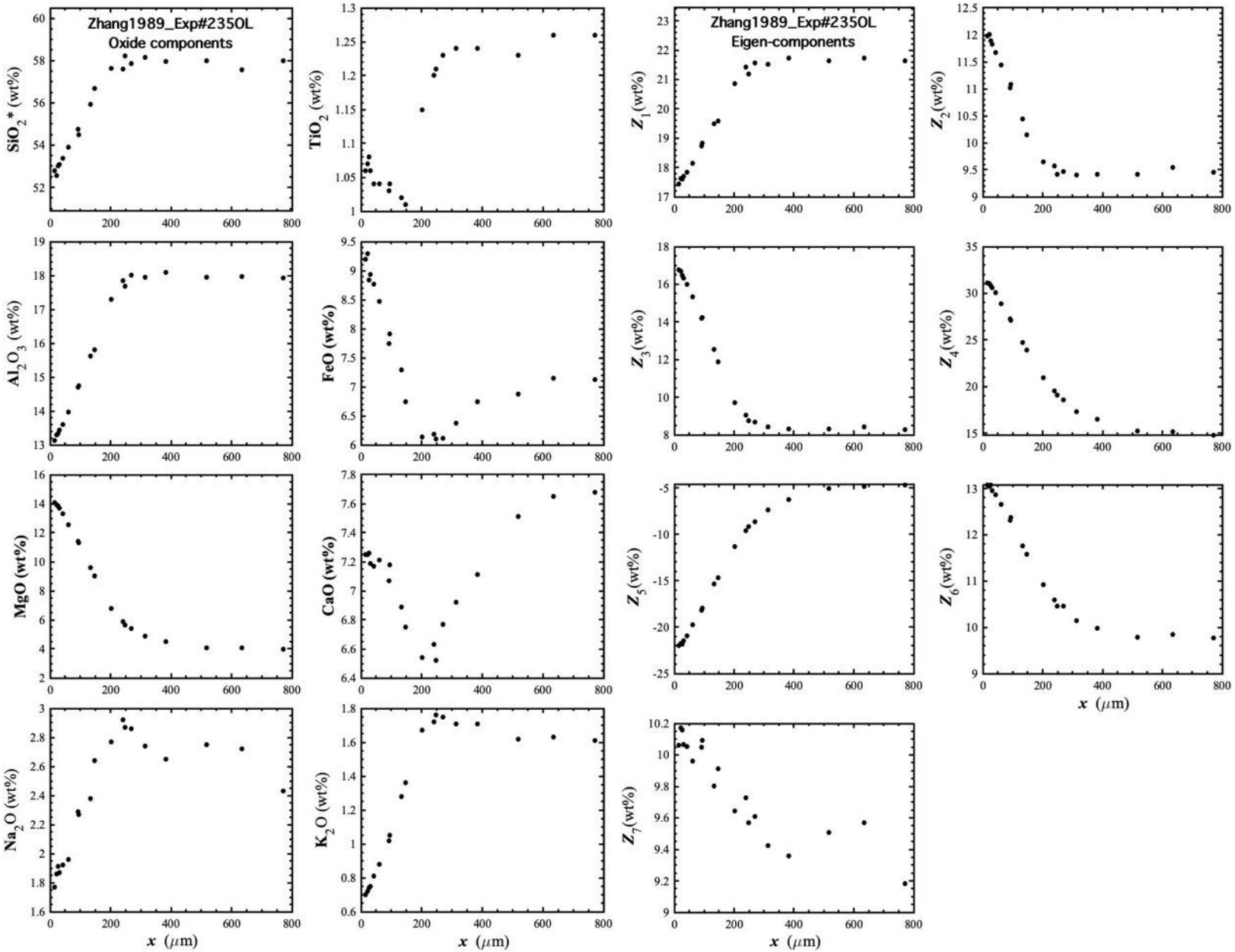

Figure 16. Concentration profiles of oxide components in wt% (left panel) and eigen-components (right panel) of Zhang1989_Exp#235OL, which is an olivine dissolution experiment in andesite (Zhang et al., 1989).

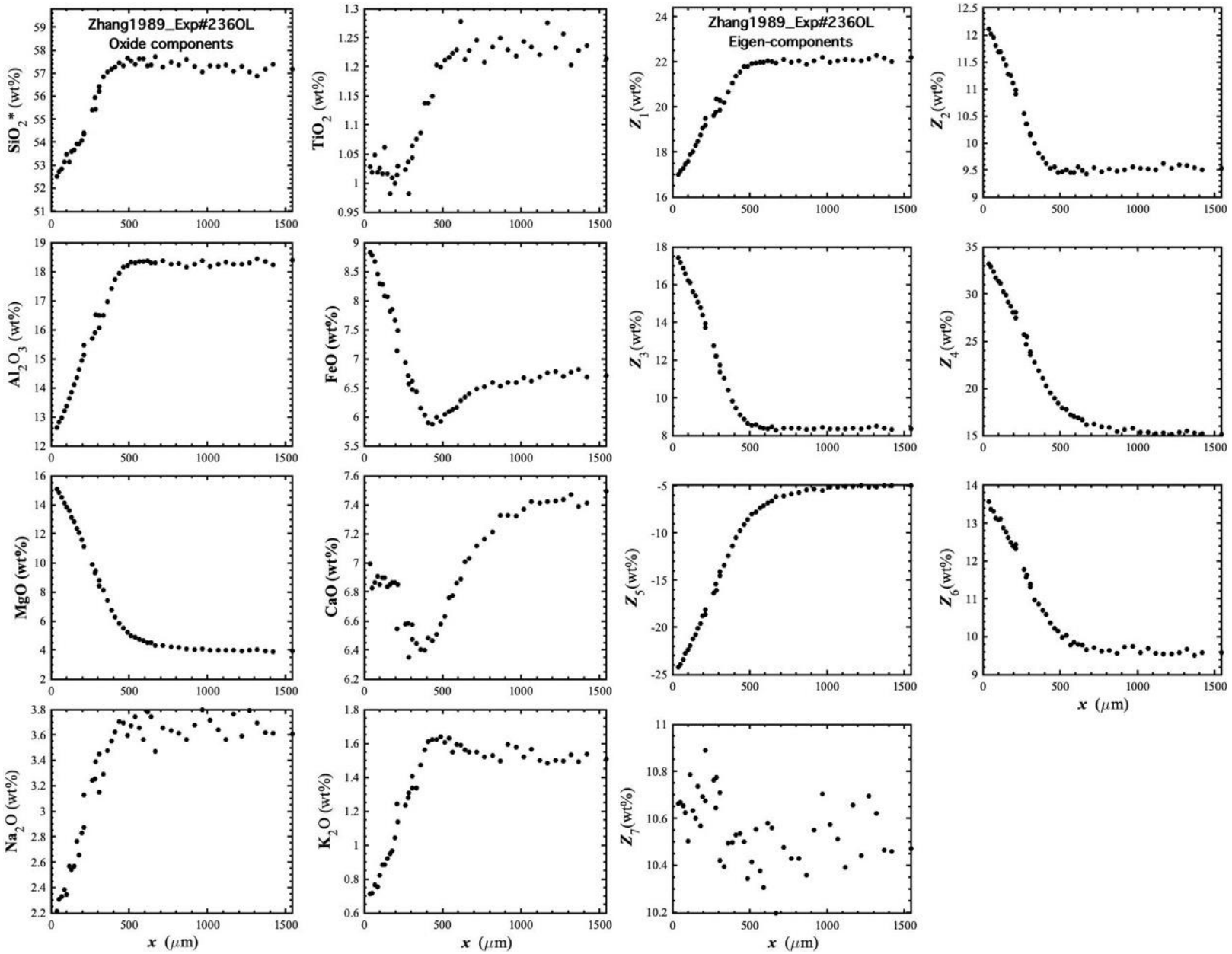

Figure 17. Concentration profiles of oxide components in wt% (left panel) and eigen-components (right panel) of Zhang1989_Exp#236OL, which is an olivine dissolution experiment in andesite (Zhang et al., 1989).

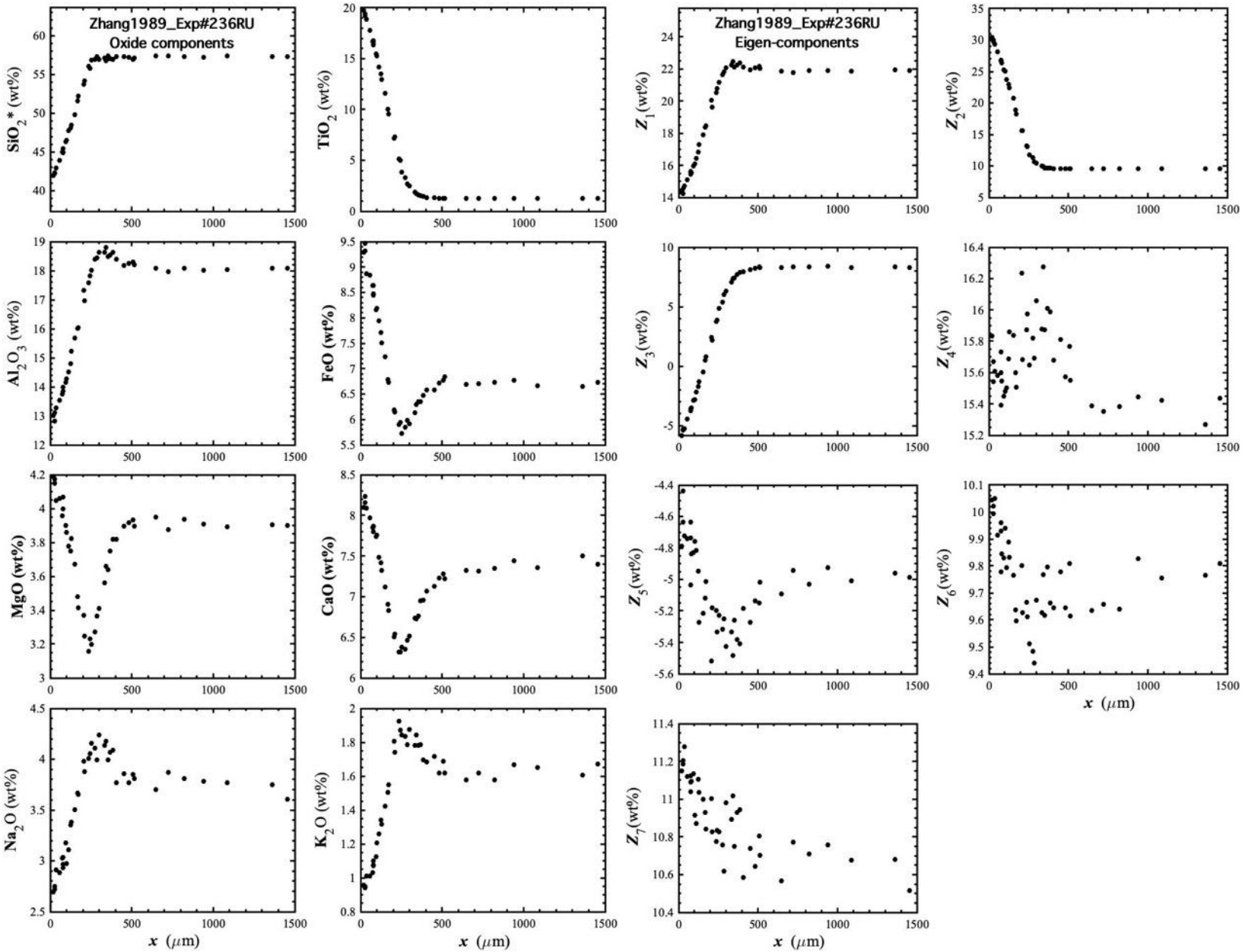

Figure 18. Concentration profiles of oxide components in wt% (left panel) and eigen-components (right panel) of Zhang1989_Exp#236RU, which is a rutile dissolution experiment in andesite (Zhang et al., 1989).

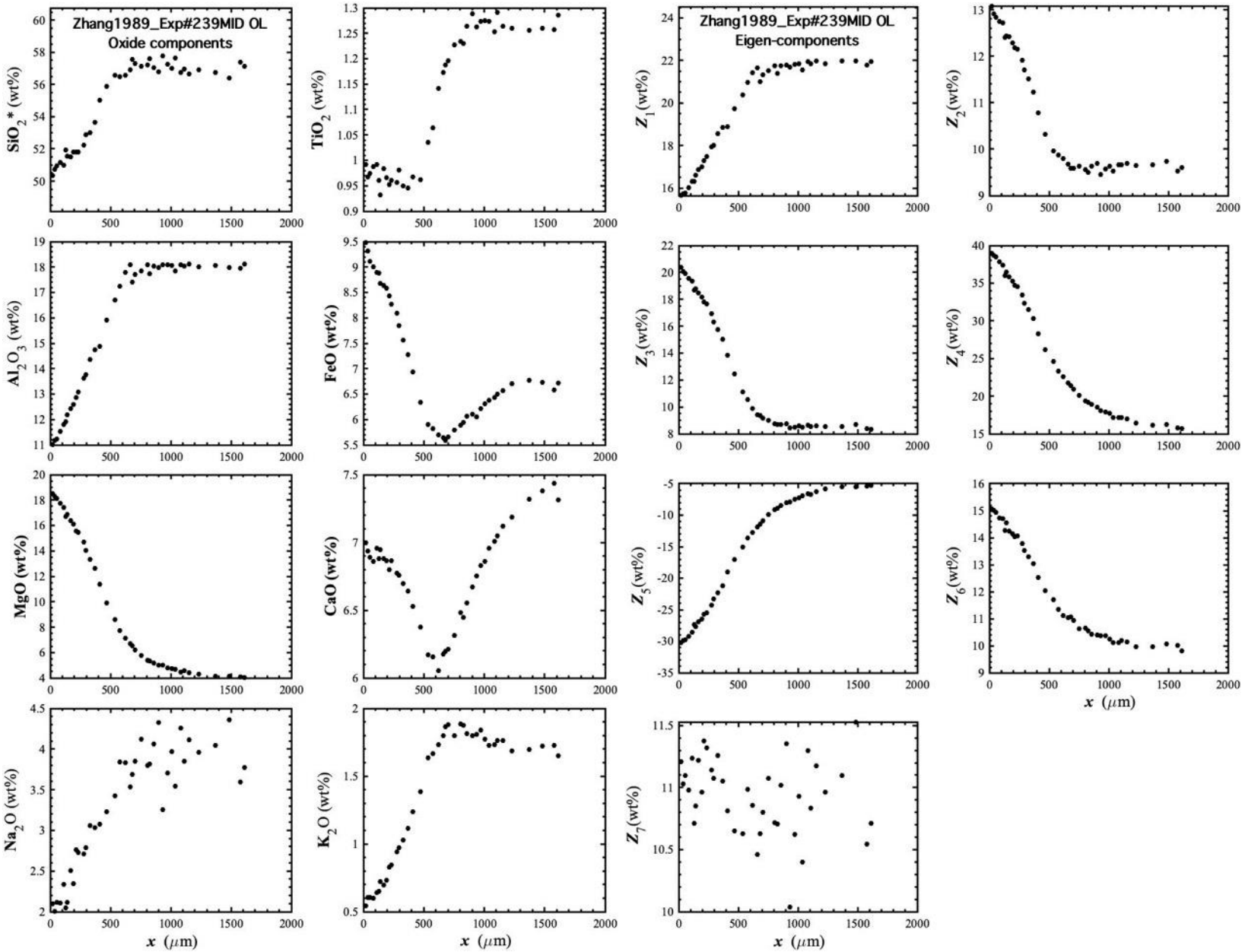

Figure 19. Concentration profiles of oxide components in wt% (left panel) and eigen-components (right panel) of Zhang1989_Exp#239MID OL, which is an olivine dissolution experiment in andesite (Zhang et al., 1989).

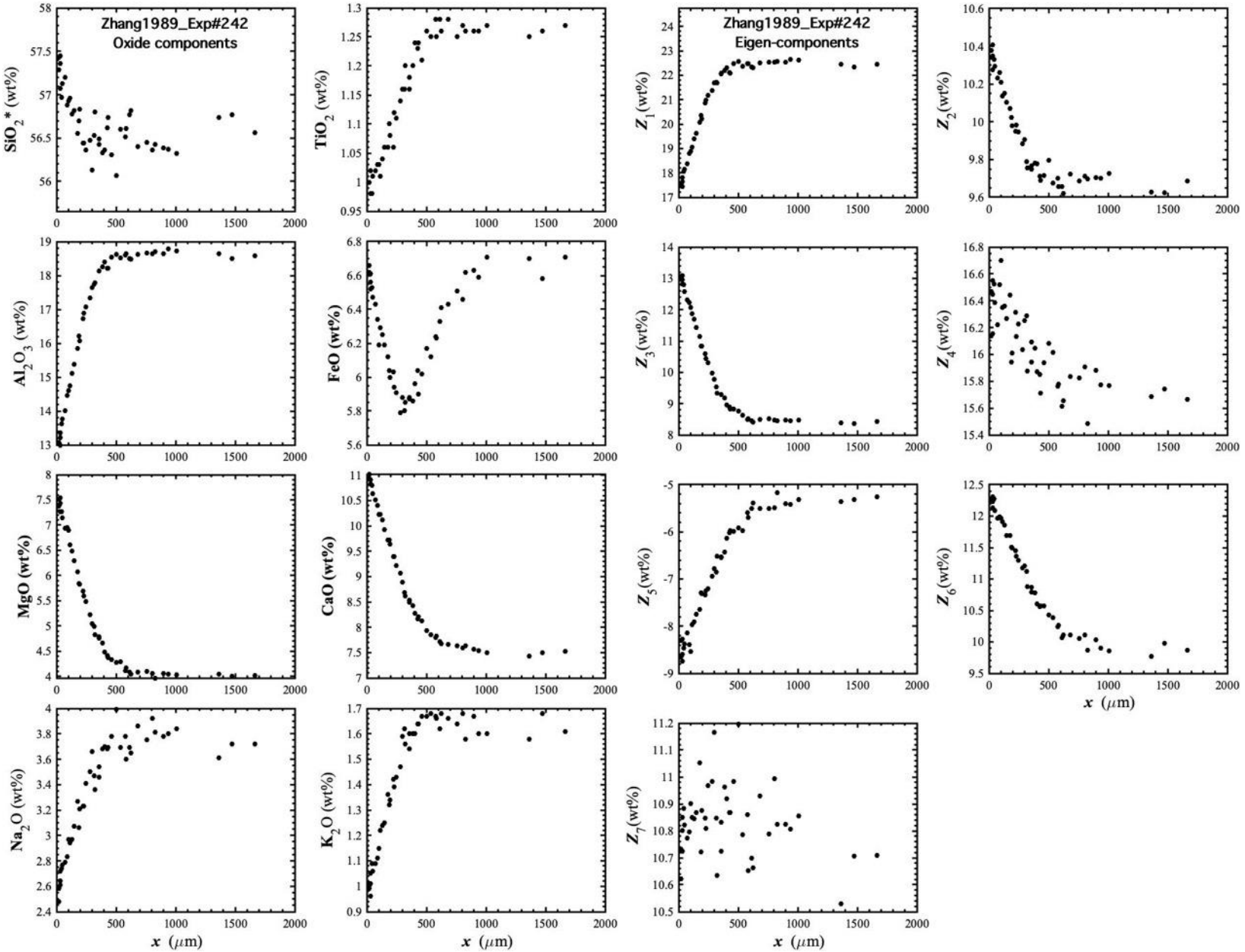

Figure 20. Concentration profiles of oxide components in wt% (left panel) and eigen-components (right panel) of Zhang1989_Exp#242, which is a diopside dissolution experiment in andesite (Zhang et al., 1989).

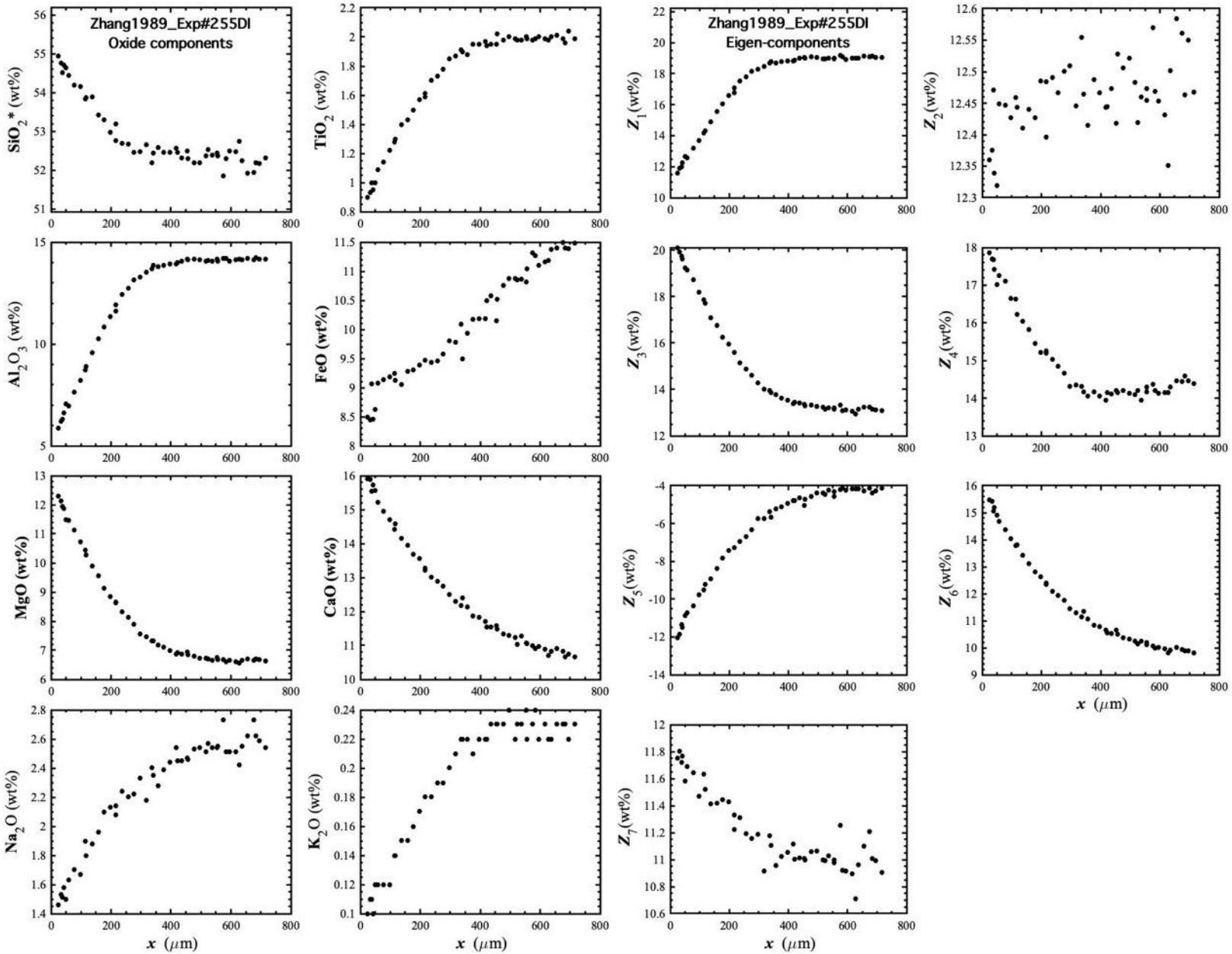

Figure 21. Concentration profiles of oxide components in wt% (left panel) and eigen-components (right panel) of Zhang1989_Exp#255DI, which is a diopside dissolution experiment in andesite (Zhang et al., 1989).

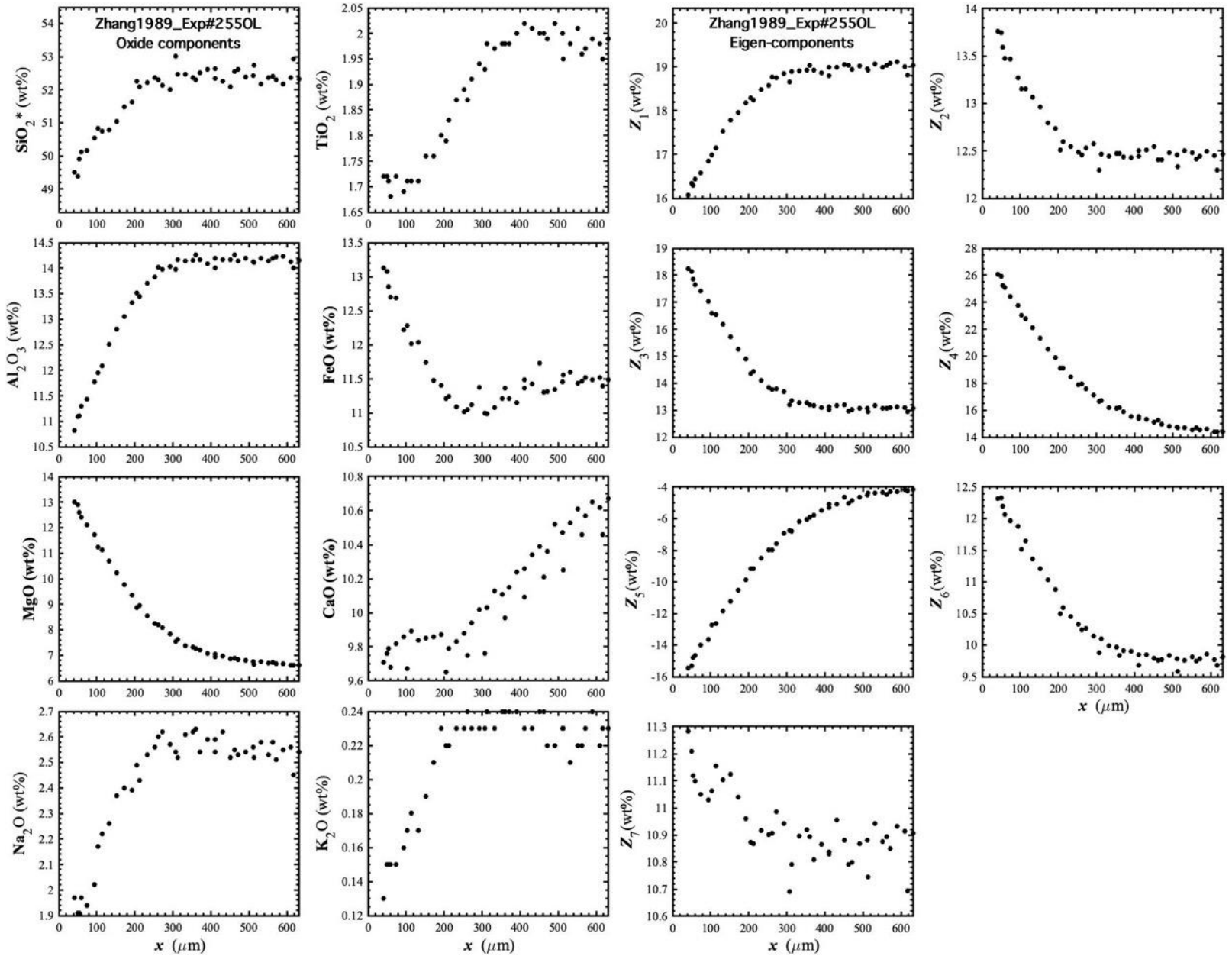

Figure 22. Concentration profiles of oxide components in wt% (left panel) and eigen-components (right panel) of Zhang1989_Exp#255OL, which is an olivine dissolution experiment in andesite (Zhang et al., 1989).

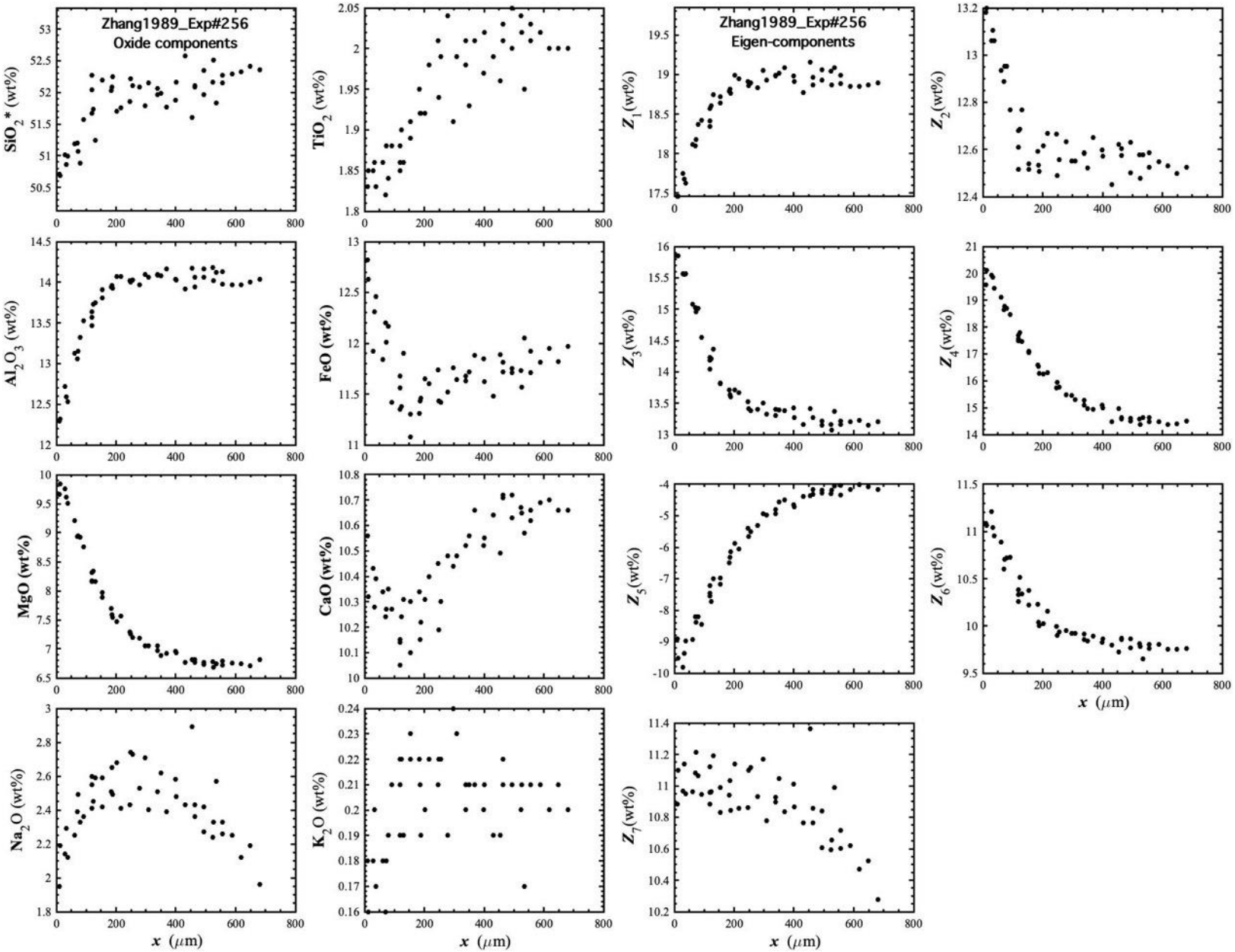

Figure 23. Concentration profiles of oxide components in wt% (left panel) and eigen-components (right panel) of Zhang1989_Exp#256, which is an olivine dissolution experiment in andesite (Zhang et al., 1989).

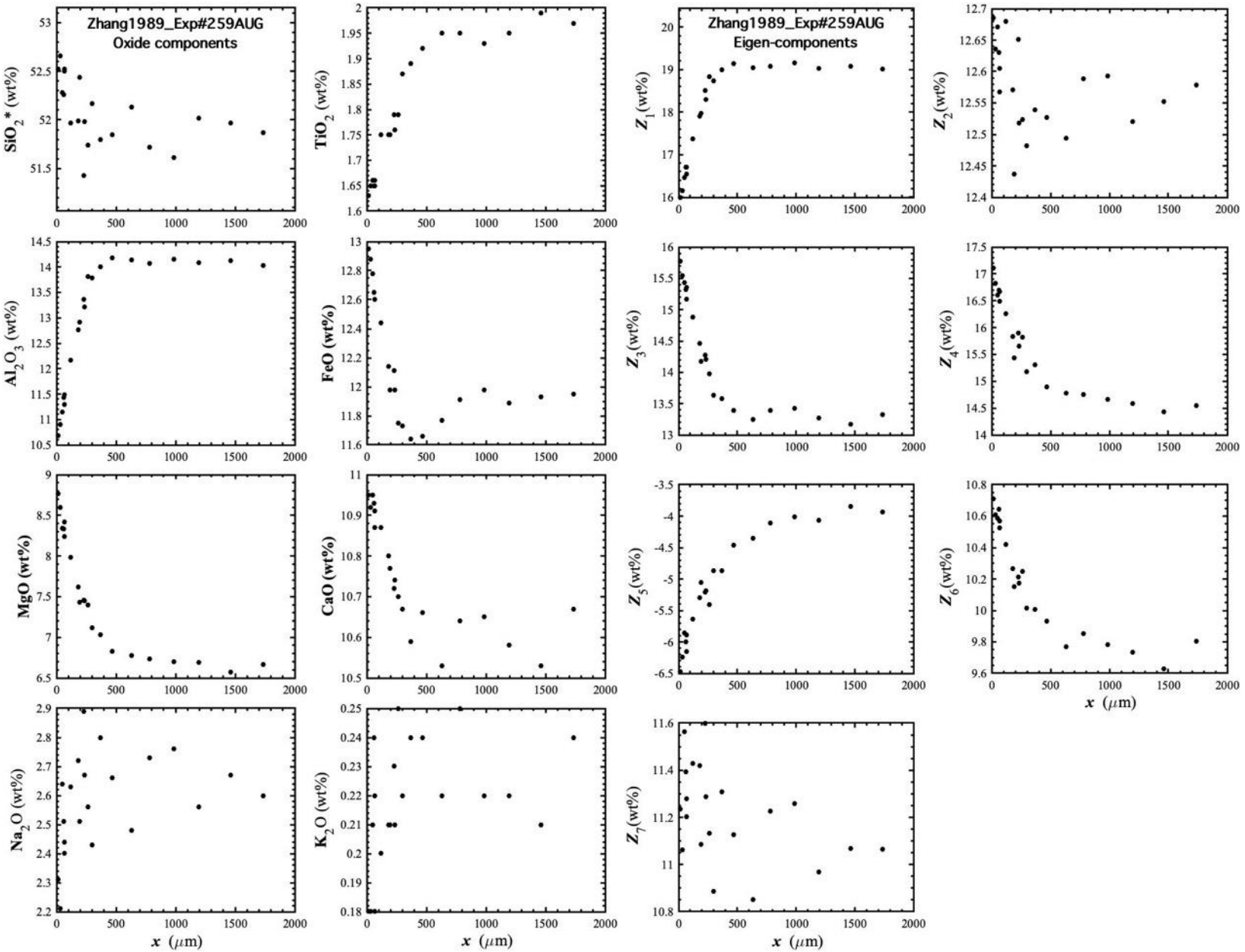

Figure 24. Concentration profiles of oxide components in wt% (left panel) and eigen-components (right panel) of Zhang1989_Exp#259AUG, which is an augite dissolution experiment in andesite (Zhang et al., 1989).

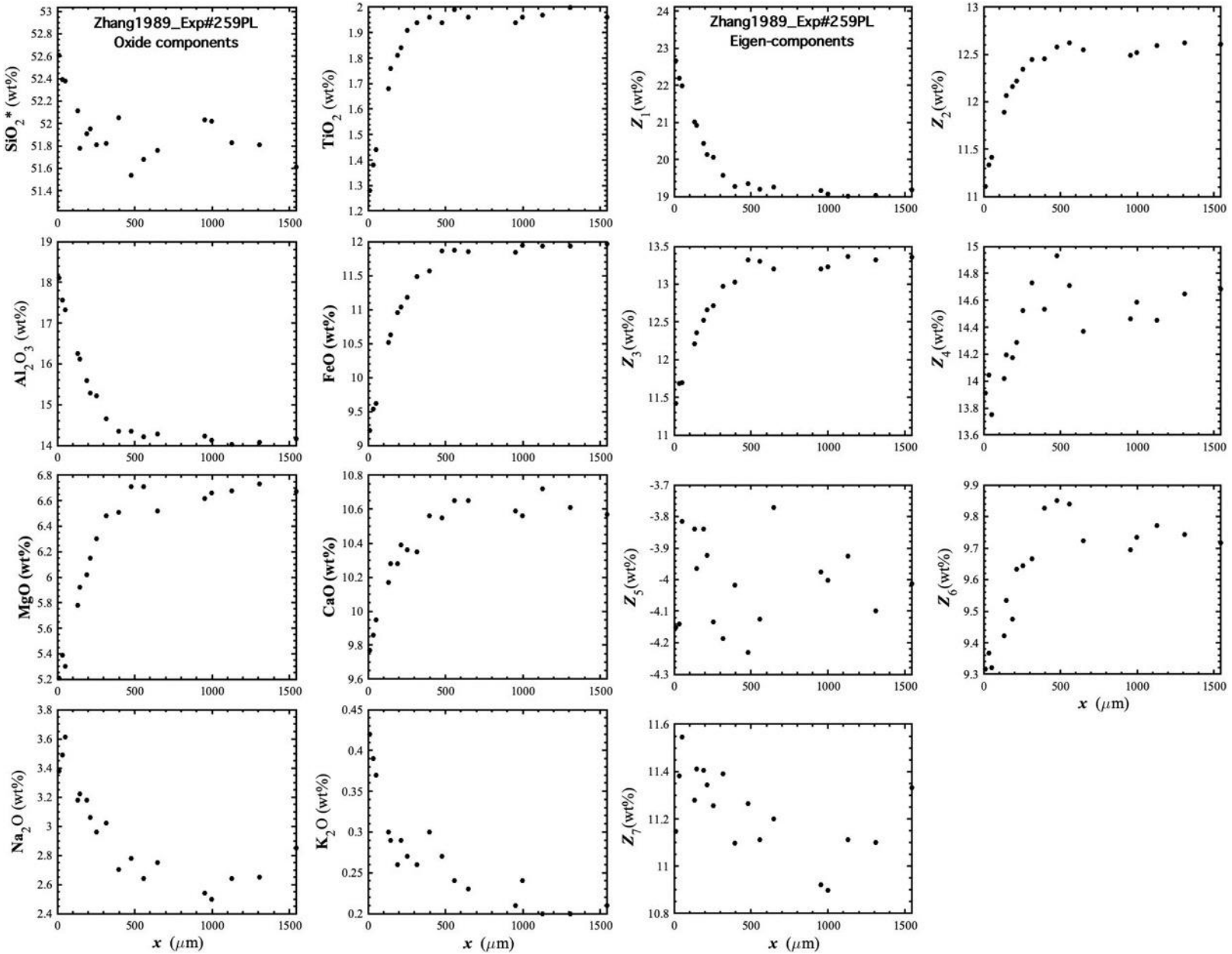

Figure 25. Concentration profiles of oxide components in wt% (left panel) and eigen-components (right panel) of Zhang1989_Exp#259PL, which is a plagioclase dissolution experiment in andesite (Zhang et al., 1989).

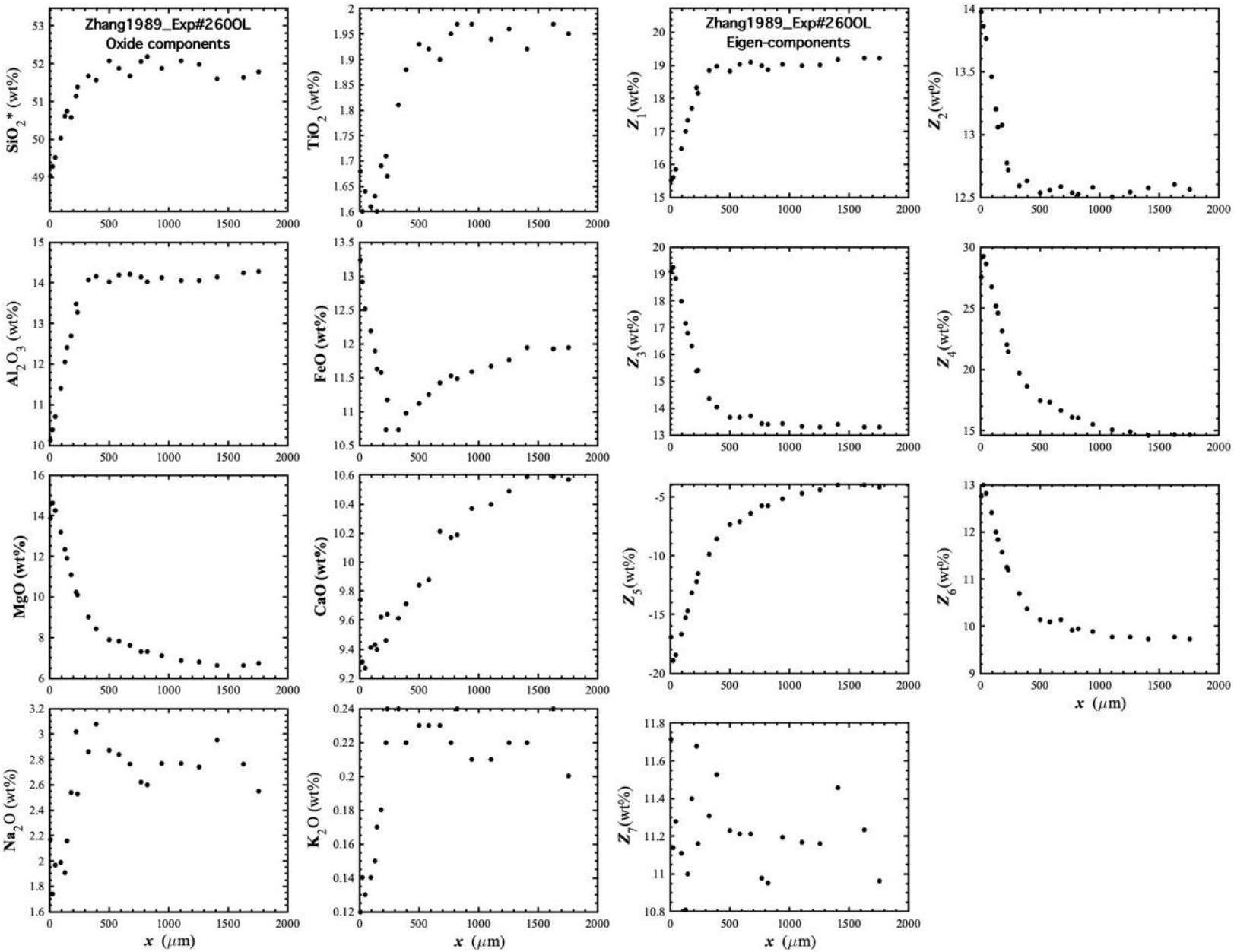

Figure 26. Concentration profiles of oxide components in wt% (left panel) and eigen-components (right panel) of Zhang1989_Exp#260OL, which is an olivine dissolution experiment in andesite (Zhang et al., 1989).

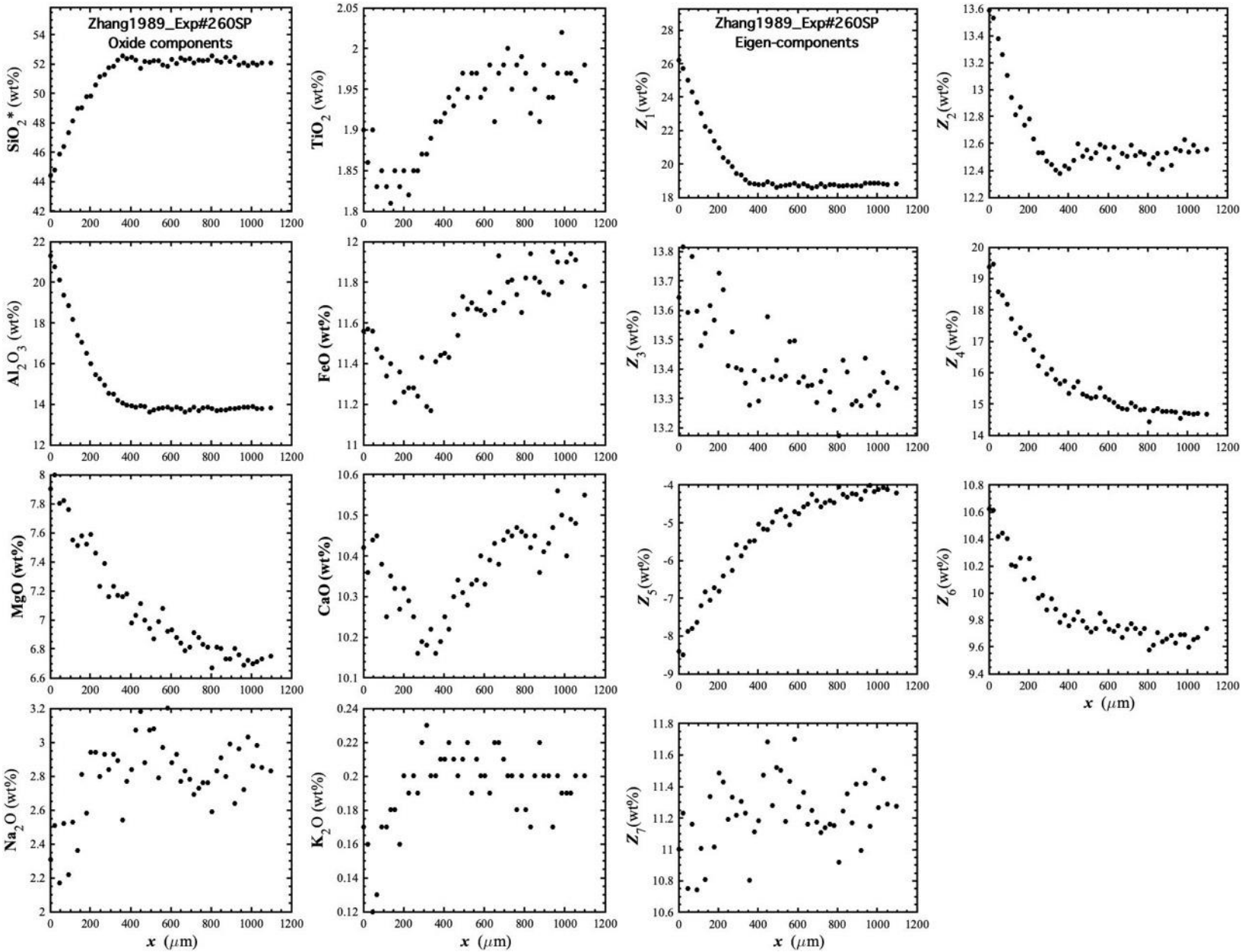

Figure 27. Concentration profiles of oxide components in wt% (left panel) and eigen-components (right panel) of Zhang1989_Exp#260SP, which is a spinel dissolution experiment in andesite (Zhang et al., 1989).

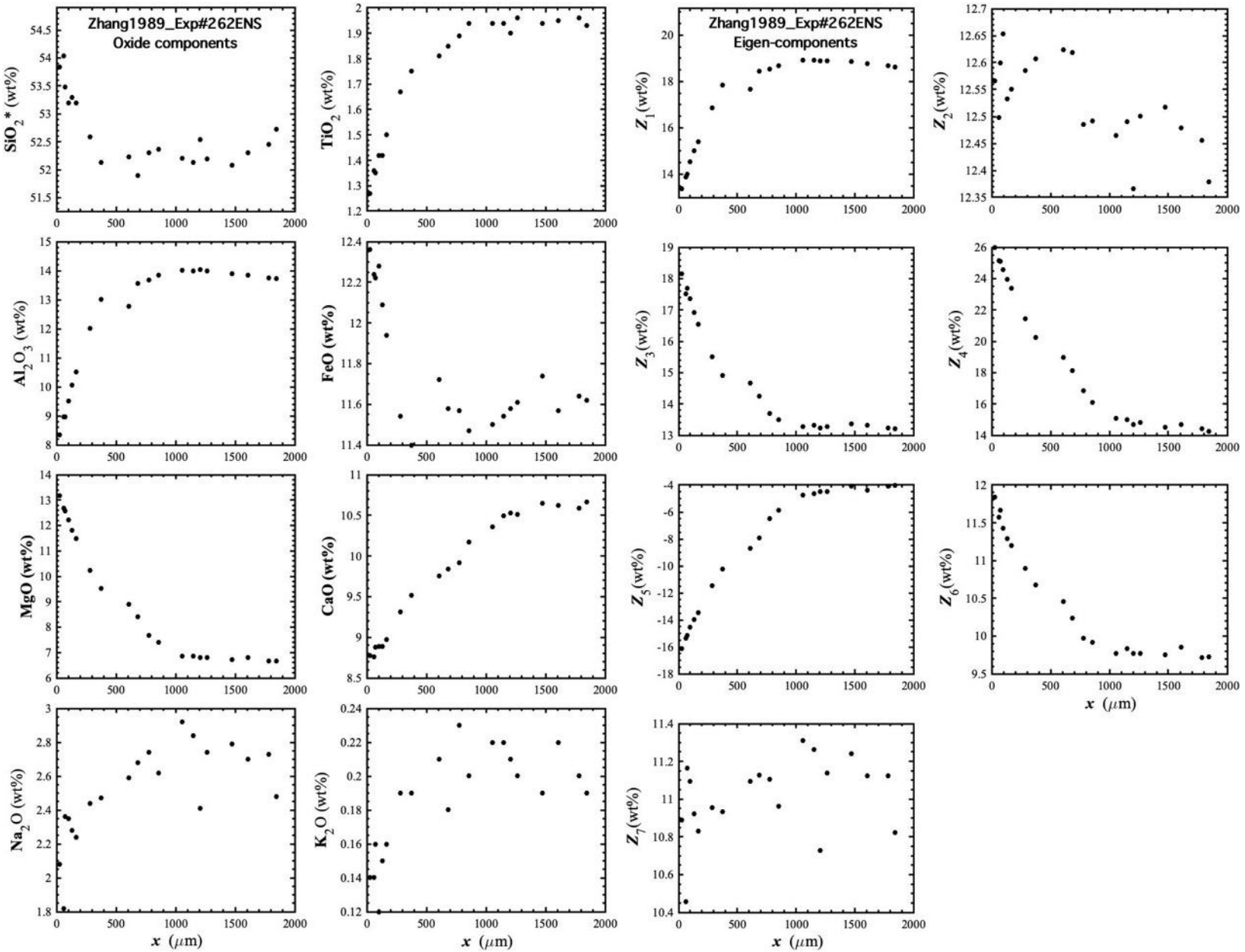

Figure 28. Concentration profiles of oxide components in wt% (left panel) and eigen-components (right panel) of Zhang1989_Exp#262ENS, which is an enstatite dissolution experiment in andesite (Zhang et al., 1989).

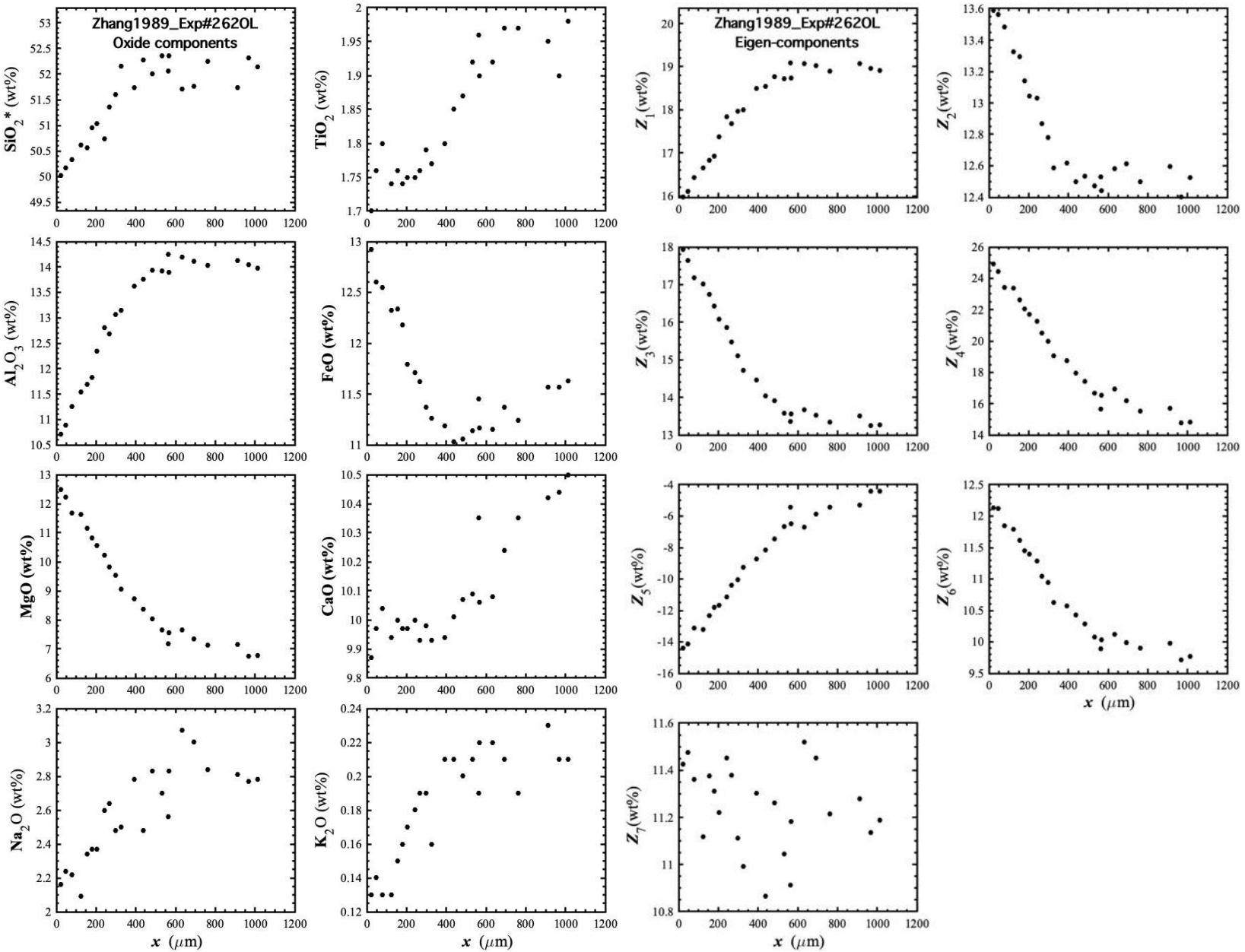

Figure 29. Concentration profiles of oxide components in wt% (left panel) and eigen-components (right panel) of Zhang1989_Exp#262OL, which is an olivine dissolution experiment in andesite (Zhang et al., 1989).

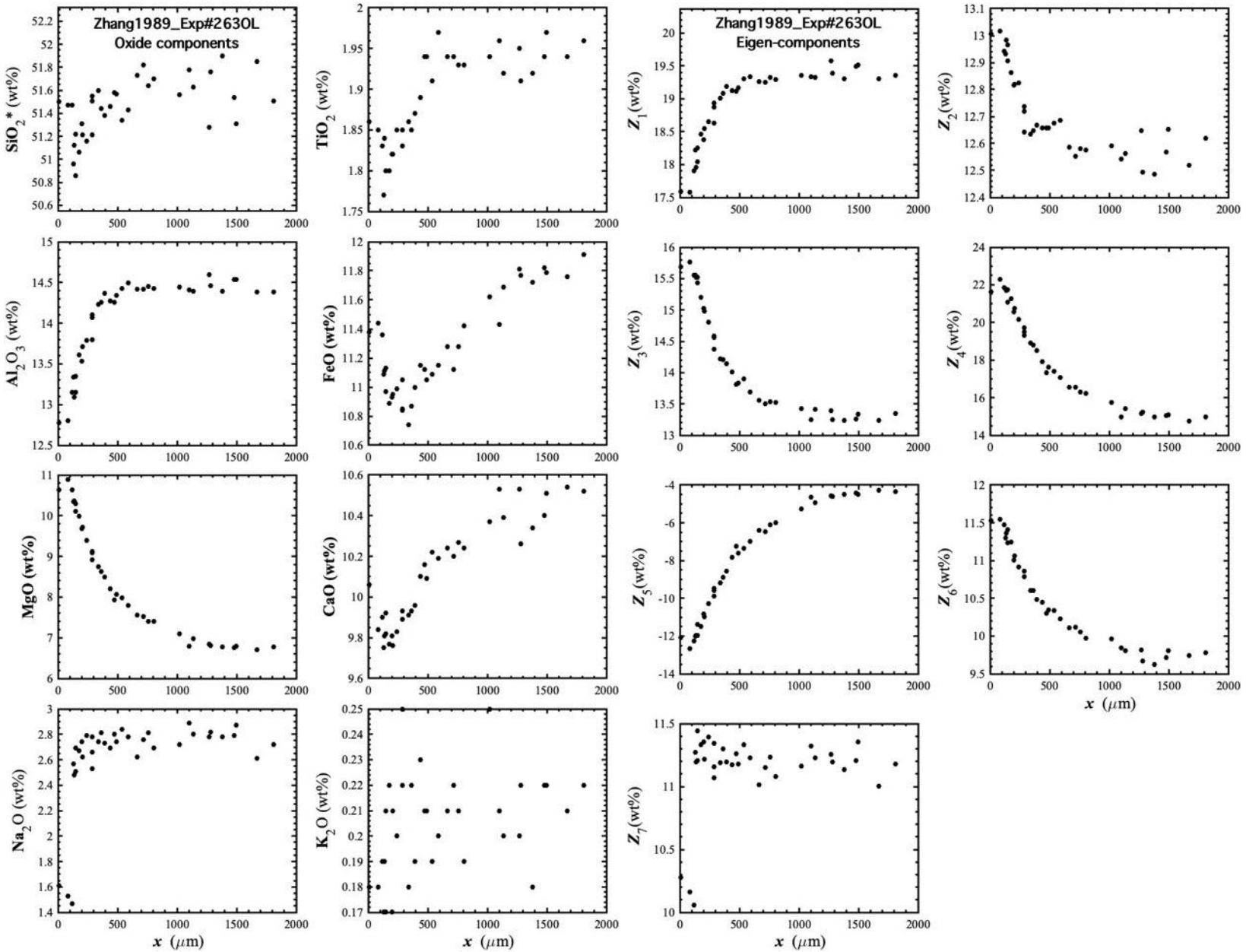

Figure 30. Concentration profiles of oxide components in wt% (left panel) and eigen-components (right panel) of Zhang1989_Exp#263OL, which is an olivine dissolution experiment in andesite (Zhang et al., 1989).

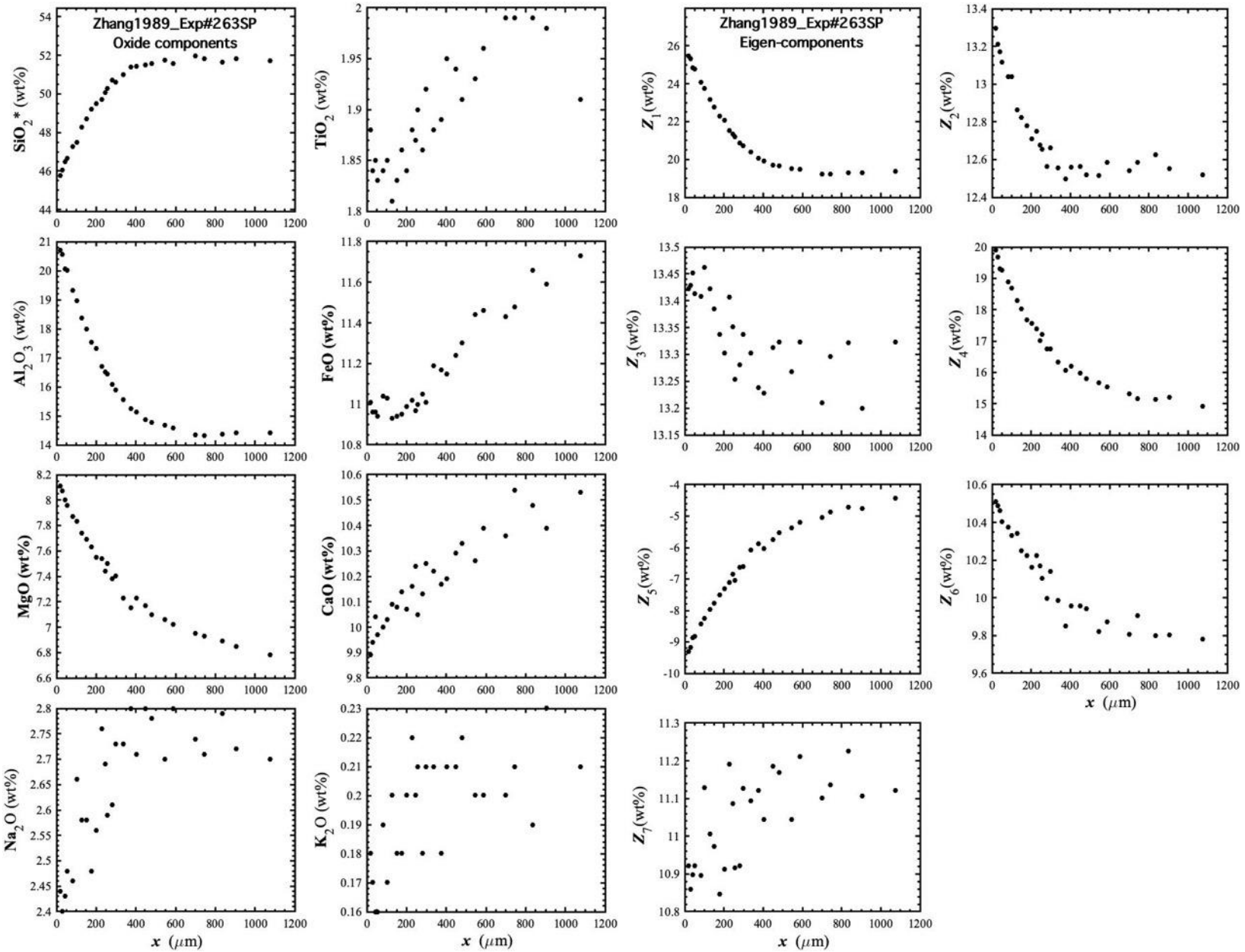

Figure 31. Concentration profiles of oxide components in wt% (left panel) and eigen-components (right panel) of Zhang1989_Exp#263SP, which is a spinel dissolution experiment in andesite (Zhang et al., 1989).

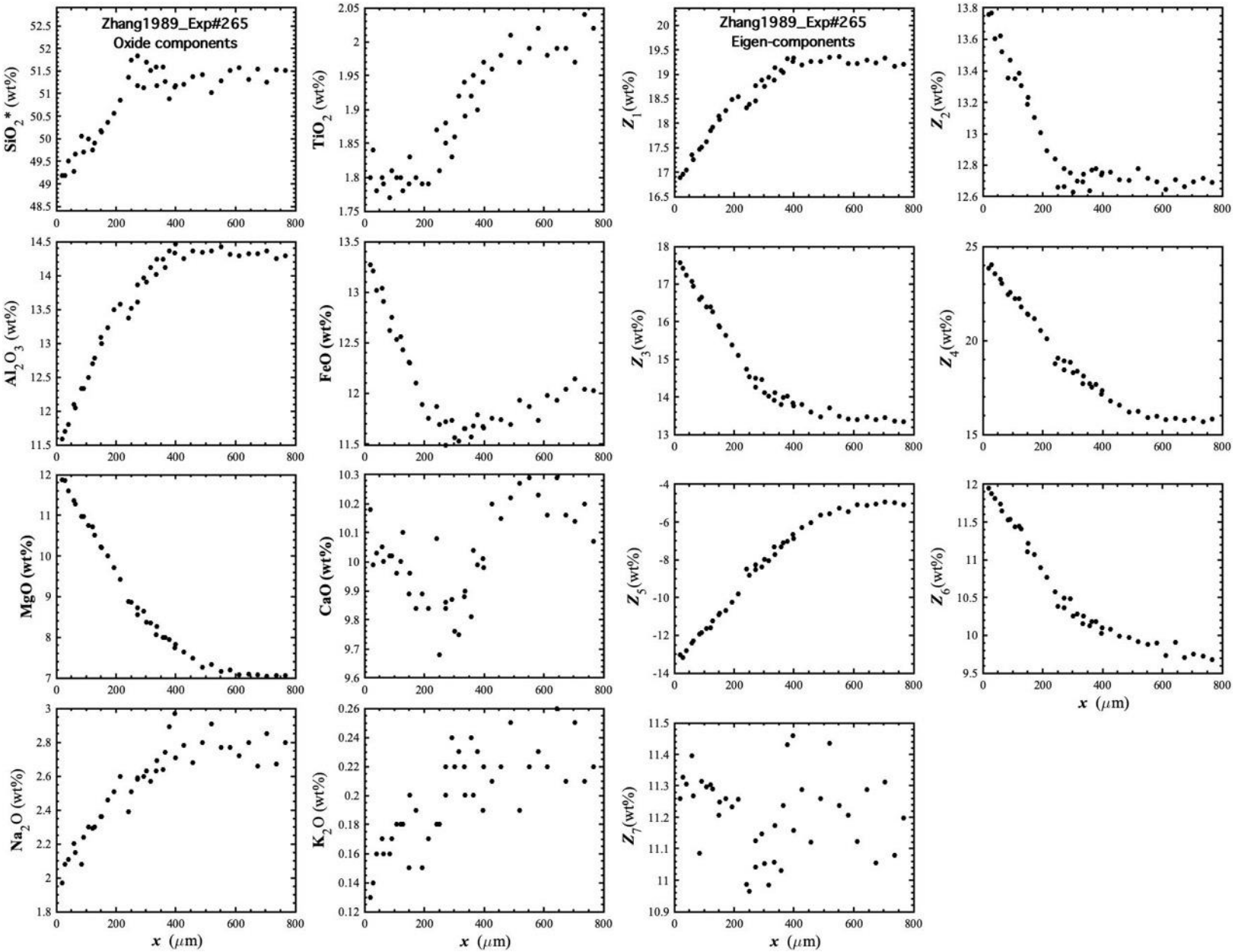

Figure 32. Concentration profiles of oxide components in wt% (left panel) and eigen-components (right panel) of Zhang1989_Exp#265, which is an olivine dissolution experiment in andesite (Zhang et al., 1989).

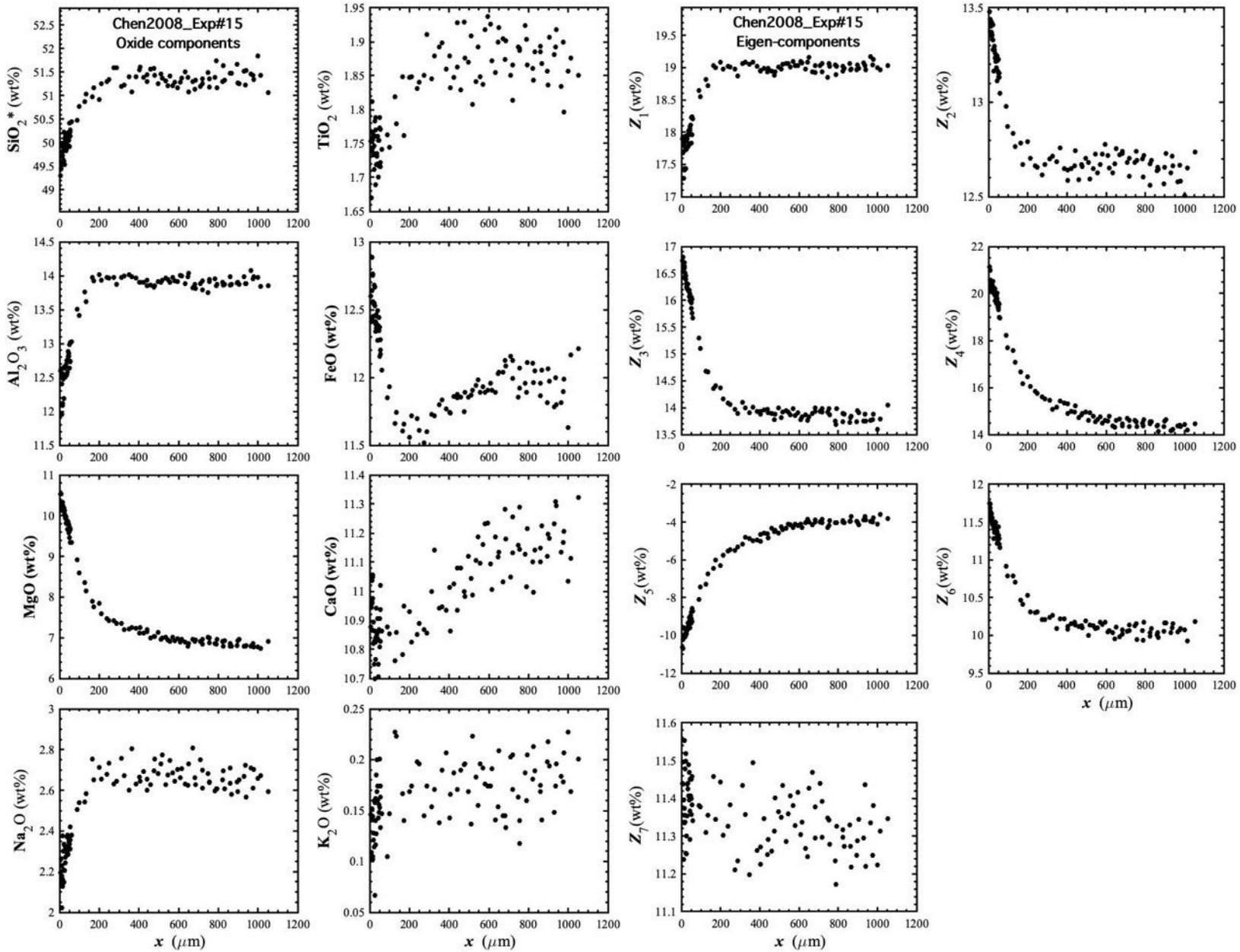

Figure 33. Concentration profiles of oxide components in wt% (left panel) and eigen-components (right panel) of Chen2008_Exp#15, which is an olivine dissolution experiment in basalt (Chen and Zhang, 2008).

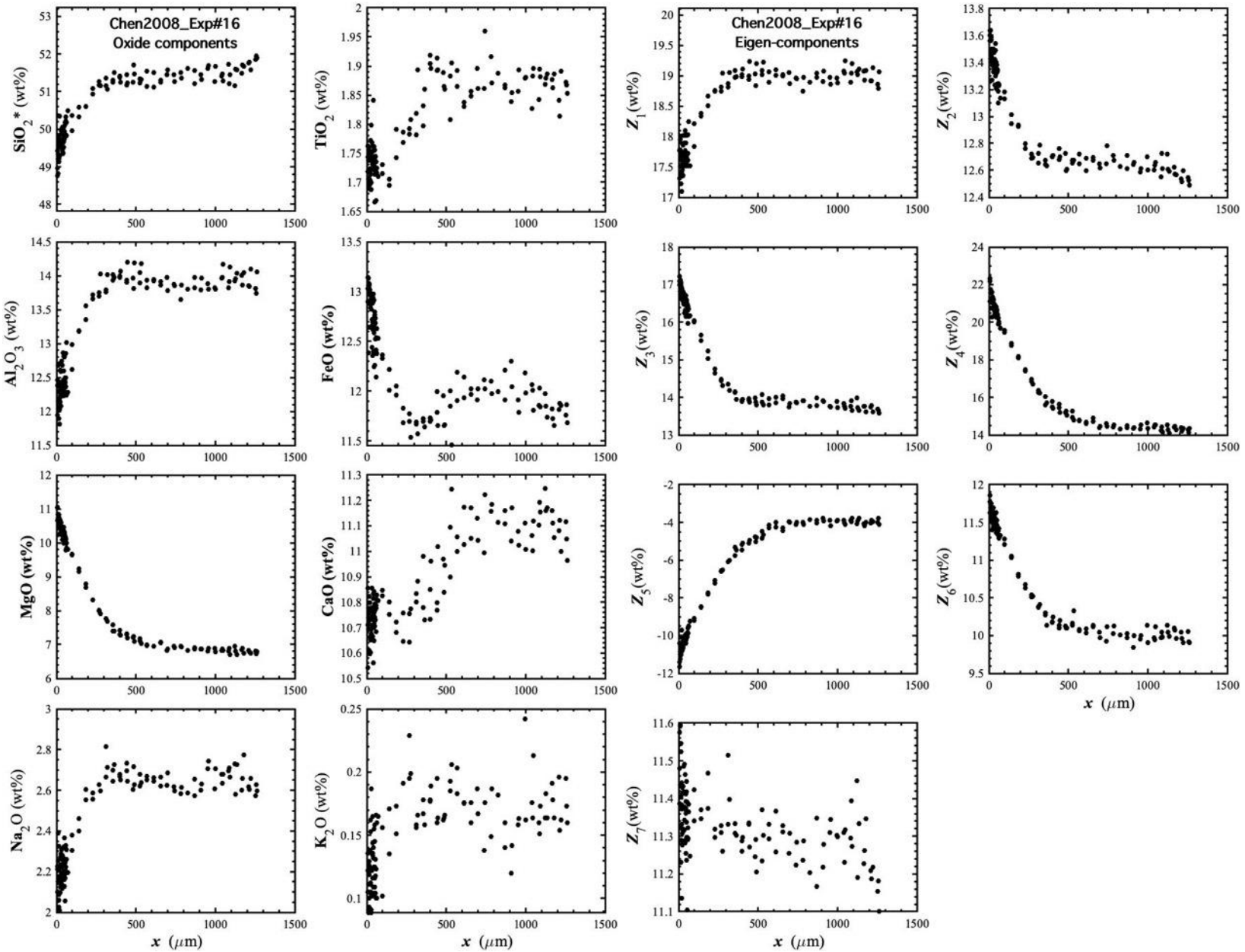

Figure 34. Concentration profiles of oxide components in wt% (left panel) and eigen-components (right panel) of Chen2008_Exp#16, which is an olivine dissolution experiment in basalt (Chen and Zhang, 2008).

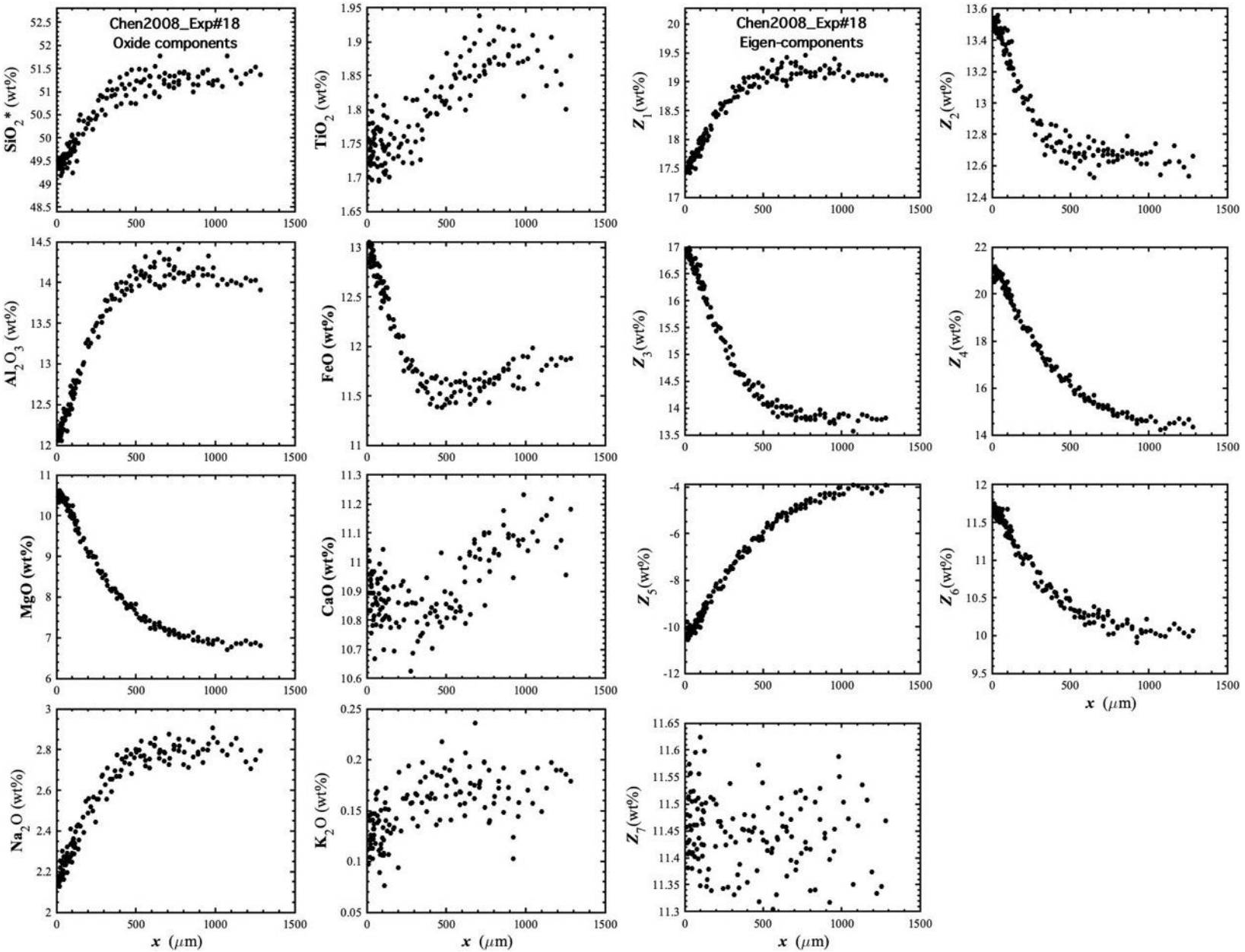

Figure 35. Concentration profiles of oxide components in wt% (left panel) and eigen-components (right panel) of Chen2008_Exp#18, which is an olivine dissolution experiment in basalt (Chen and Zhang, 2008).

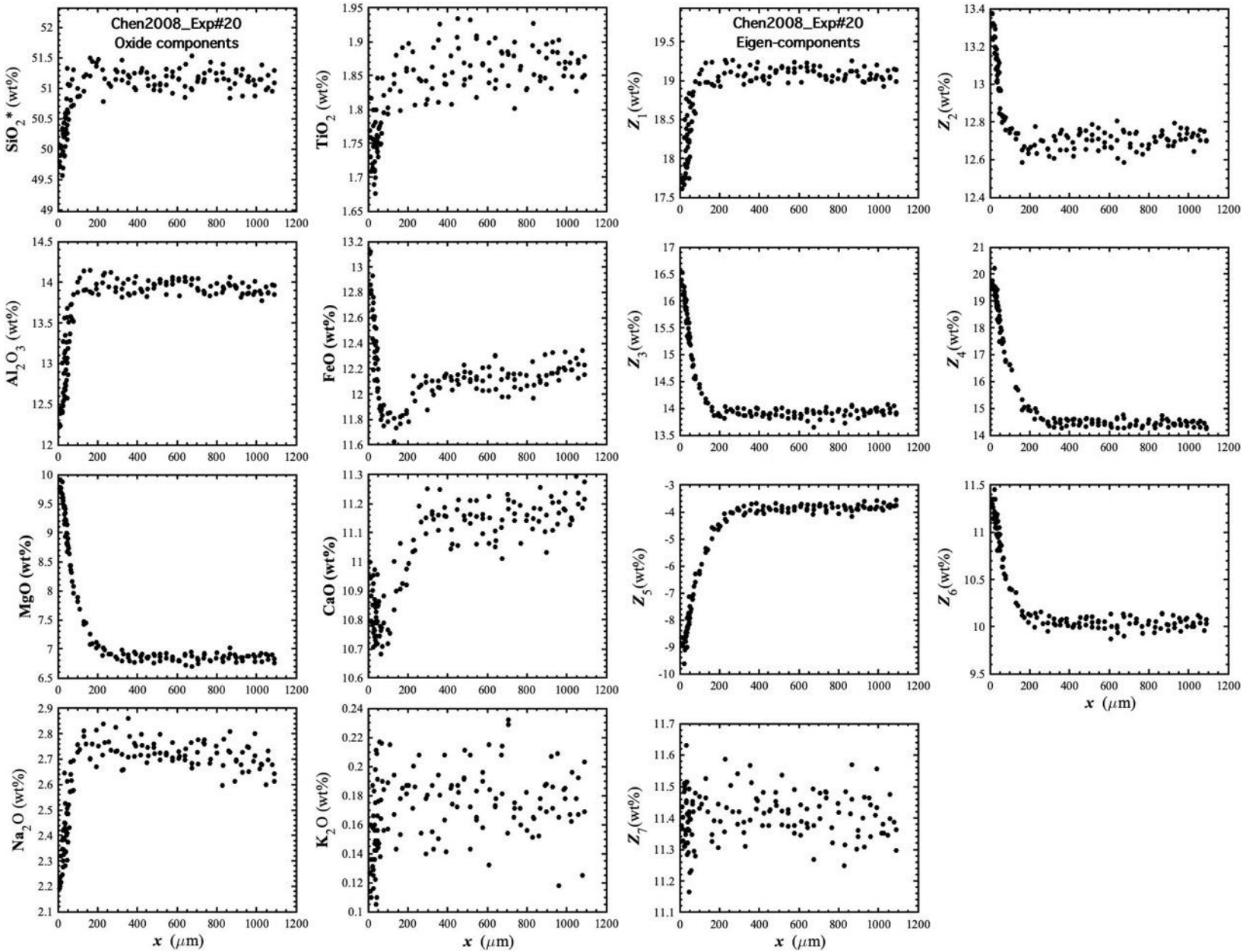

Figure 36. Concentration profiles of oxide components in wt% (left panel) and eigen-components (right panel) of Chen2008_Exp#20, which is an olivine dissolution experiment in basalt (Chen and Zhang, 2008).

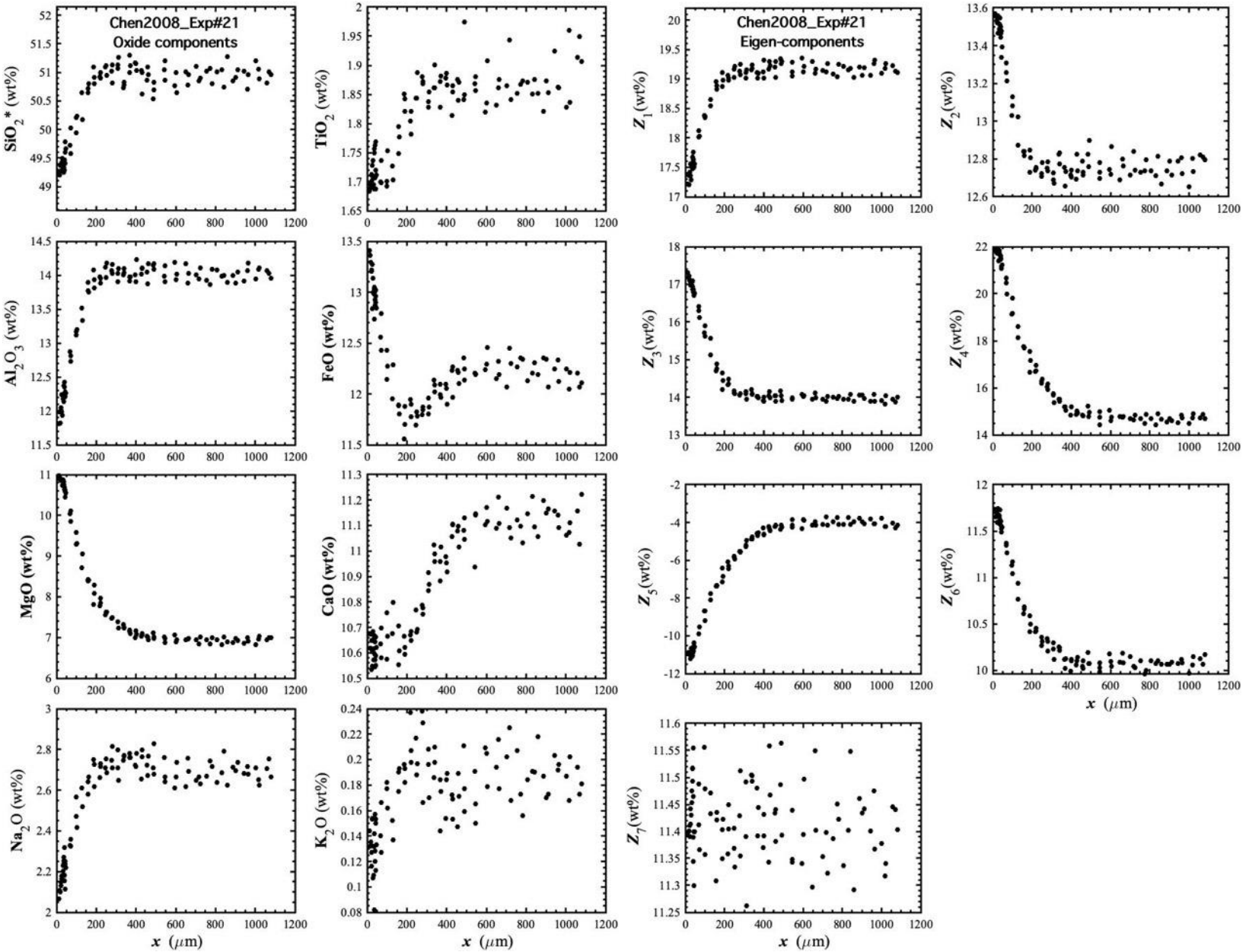

Figure 37. Concentration profiles of oxide components in wt% (left panel) and eigen-components (right panel) of Chen2008_Exp#21, which is an olivine dissolution experiment in basalt (Chen and Zhang, 2008).

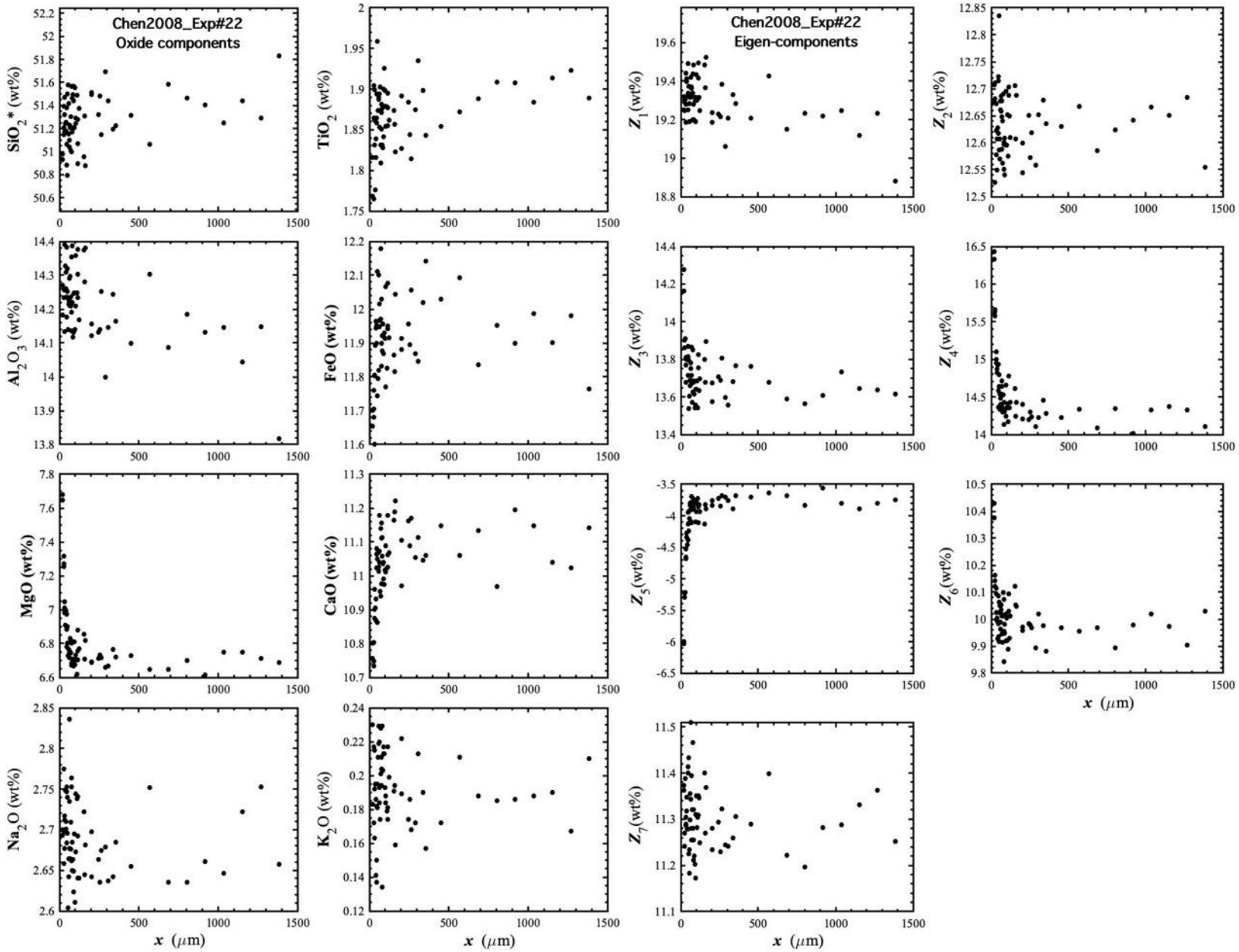

Figure 38. Concentration profiles of oxide components in wt% (left panel) and eigen-components (right panel) of Chen2008_Exp#22, which is an olivine dissolution experiment in basalt (Chen and Zhang, 2008).

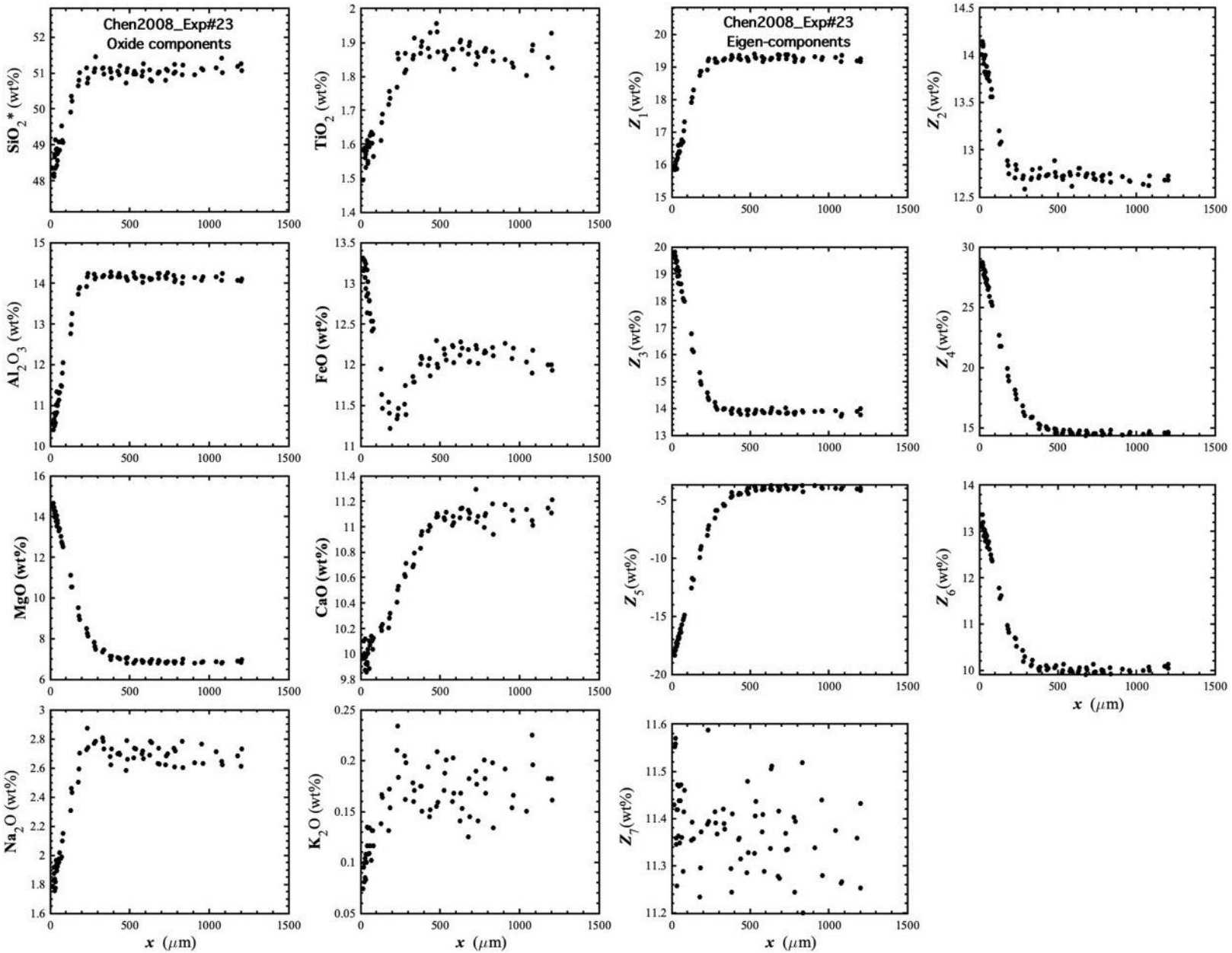

Figure 39. Concentration profiles of oxide components in wt% (left panel) and eigen-components (right panel) of Chen2008_Exp#23, which is an olivine dissolution experiment in basalt (Chen and Zhang, 2008).

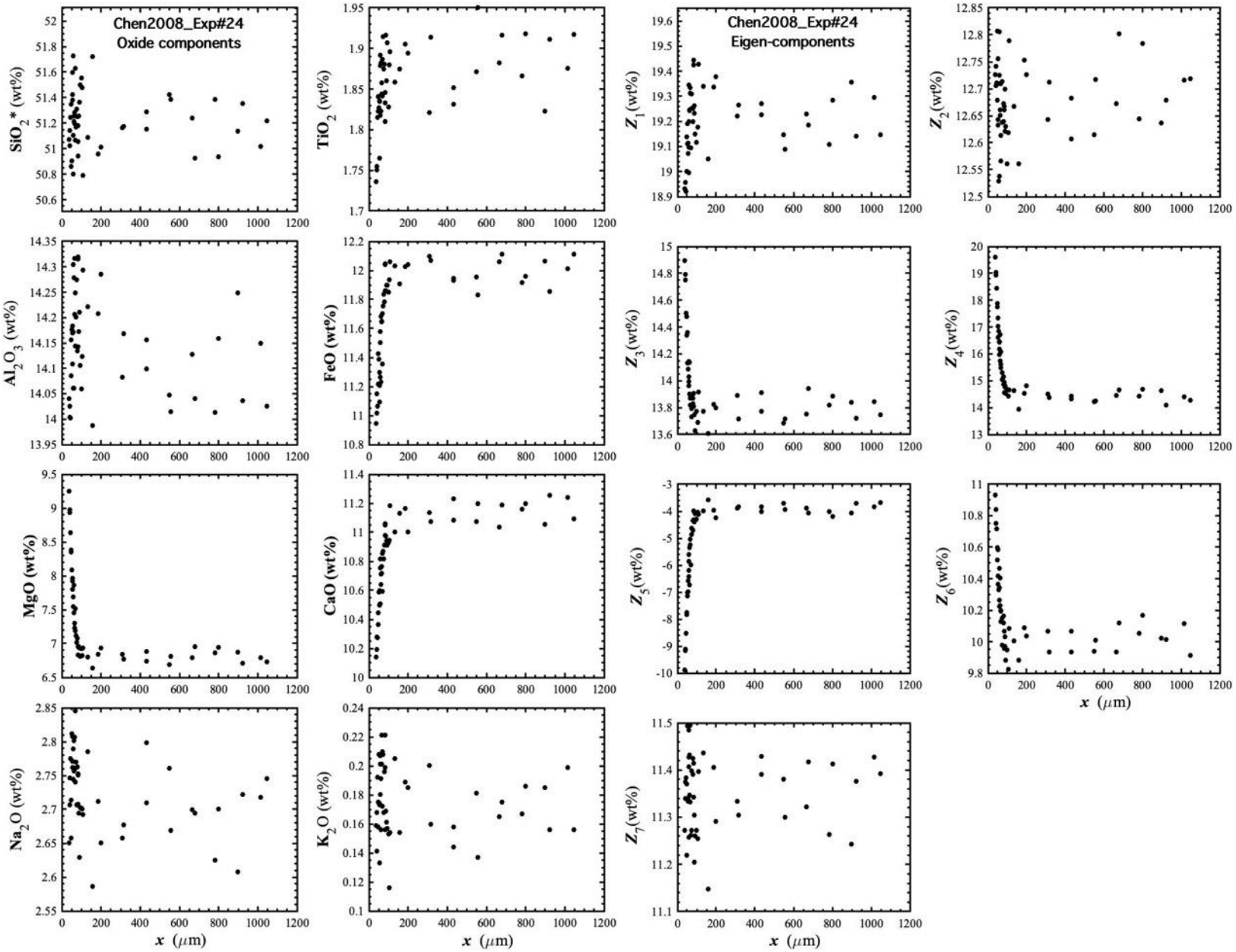

Figure 40. Concentration profiles of oxide components in wt% (left panel) and eigen-components (right panel) of Chen2008_Exp#24, which is an olivine dissolution experiment in basalt (Chen and Zhang, 2008).

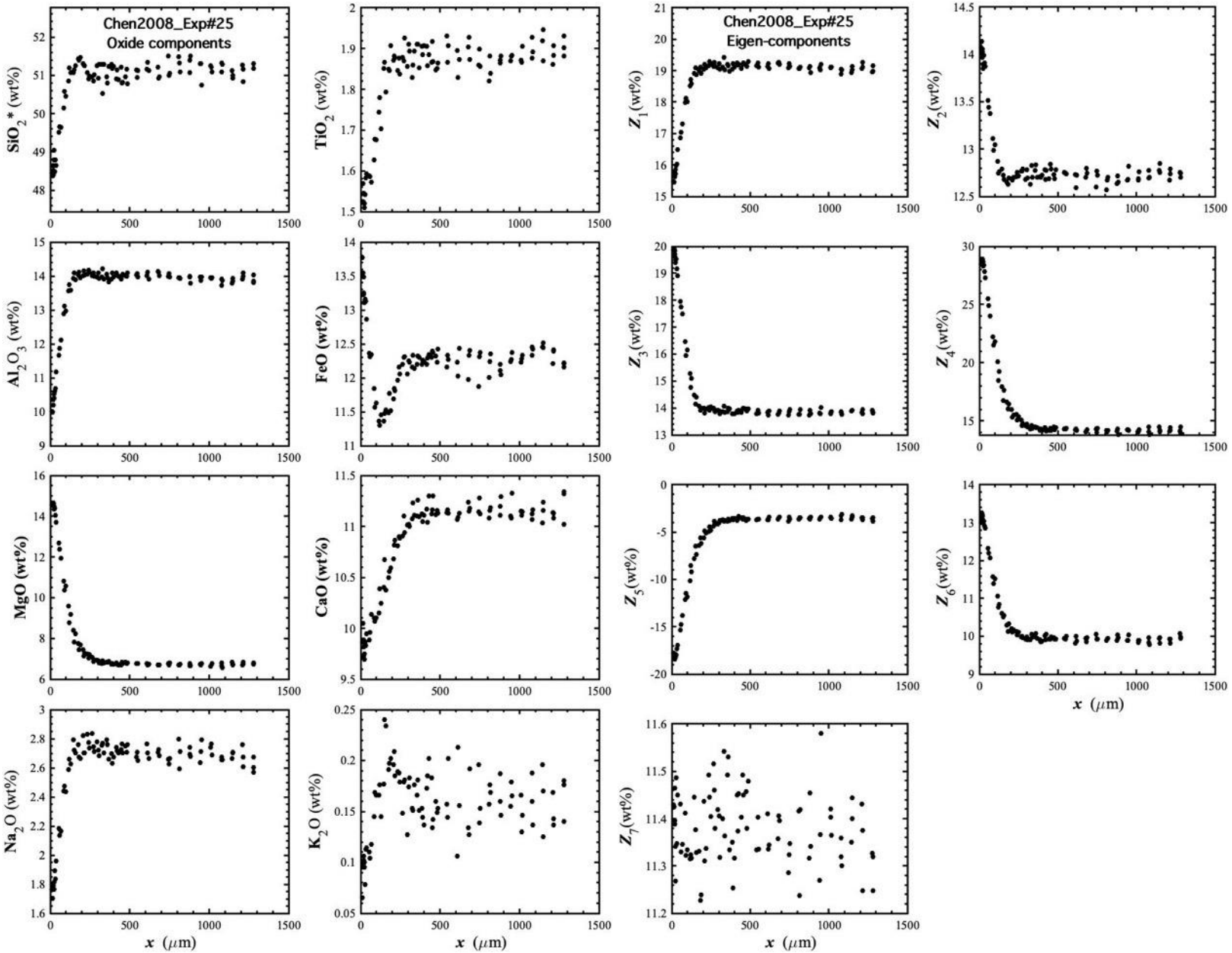

Figure 41. Concentration profiles of oxide components in wt% (left panel) and eigen-components (right panel) of Chen2008_Exp#25, which is an olivine dissolution experiment in basalt (Chen and Zhang, 2008).

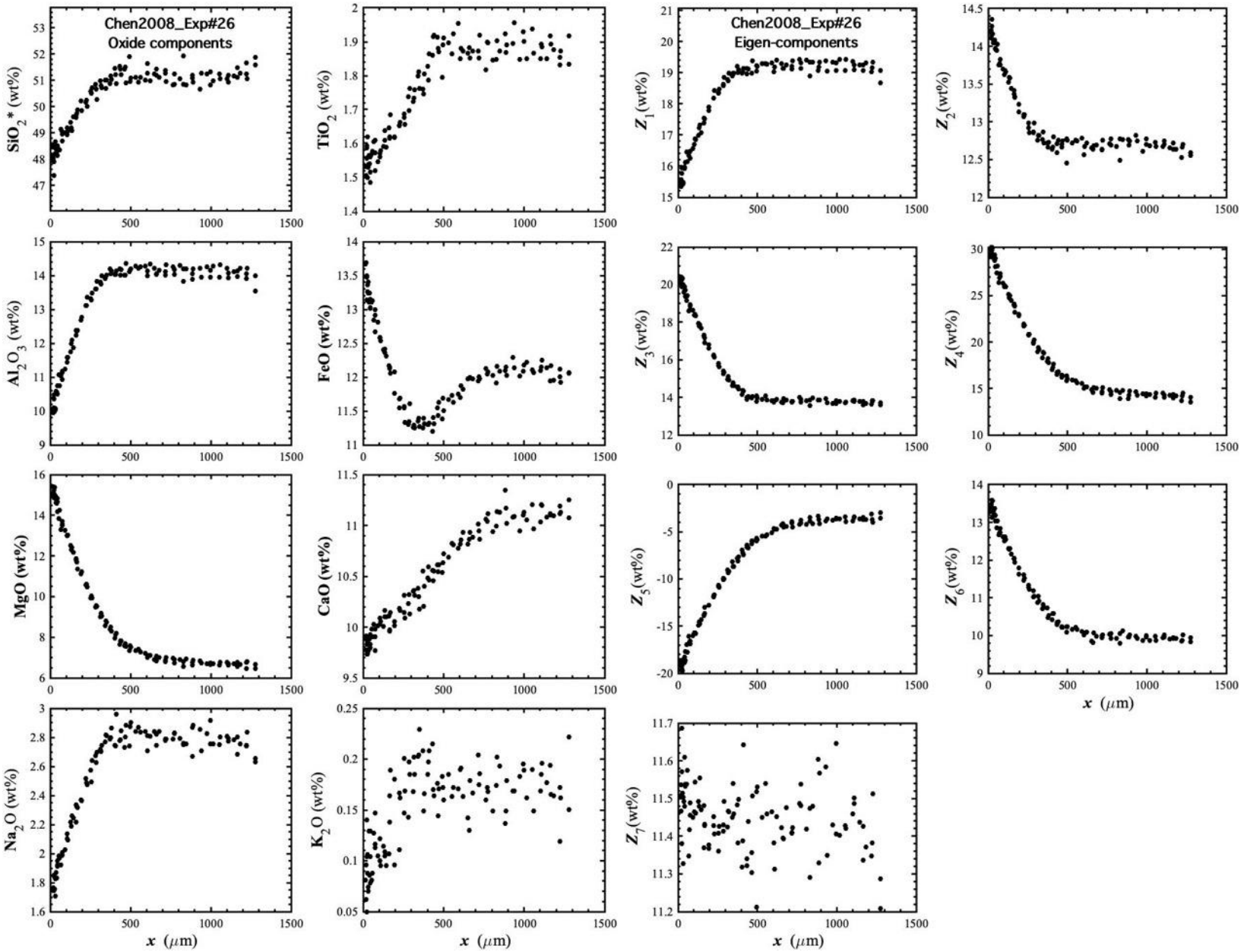

Figure 42. Concentration profiles of oxide components in wt% (left panel) and eigen-components (right panel) of Chen2008_Exp#26, which is an olivine dissolution experiment in basalt (Chen and Zhang, 2008).

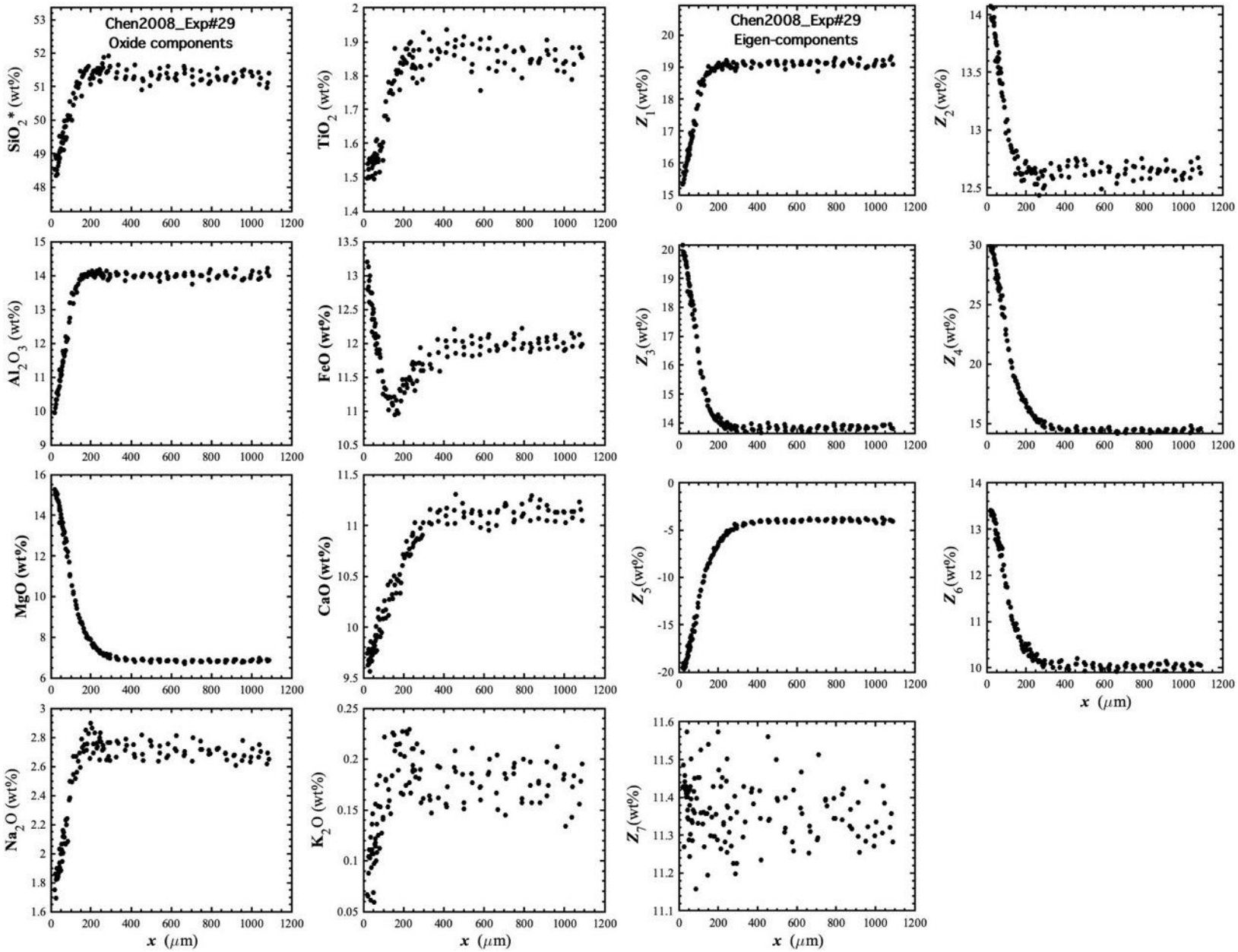

Figure 43. Concentration profiles of oxide components in wt% (left panel) and eigen-components (right panel) of Chen2008_Exp#29, which is an olivine dissolution experiment in basalt (Chen and Zhang, 2008).

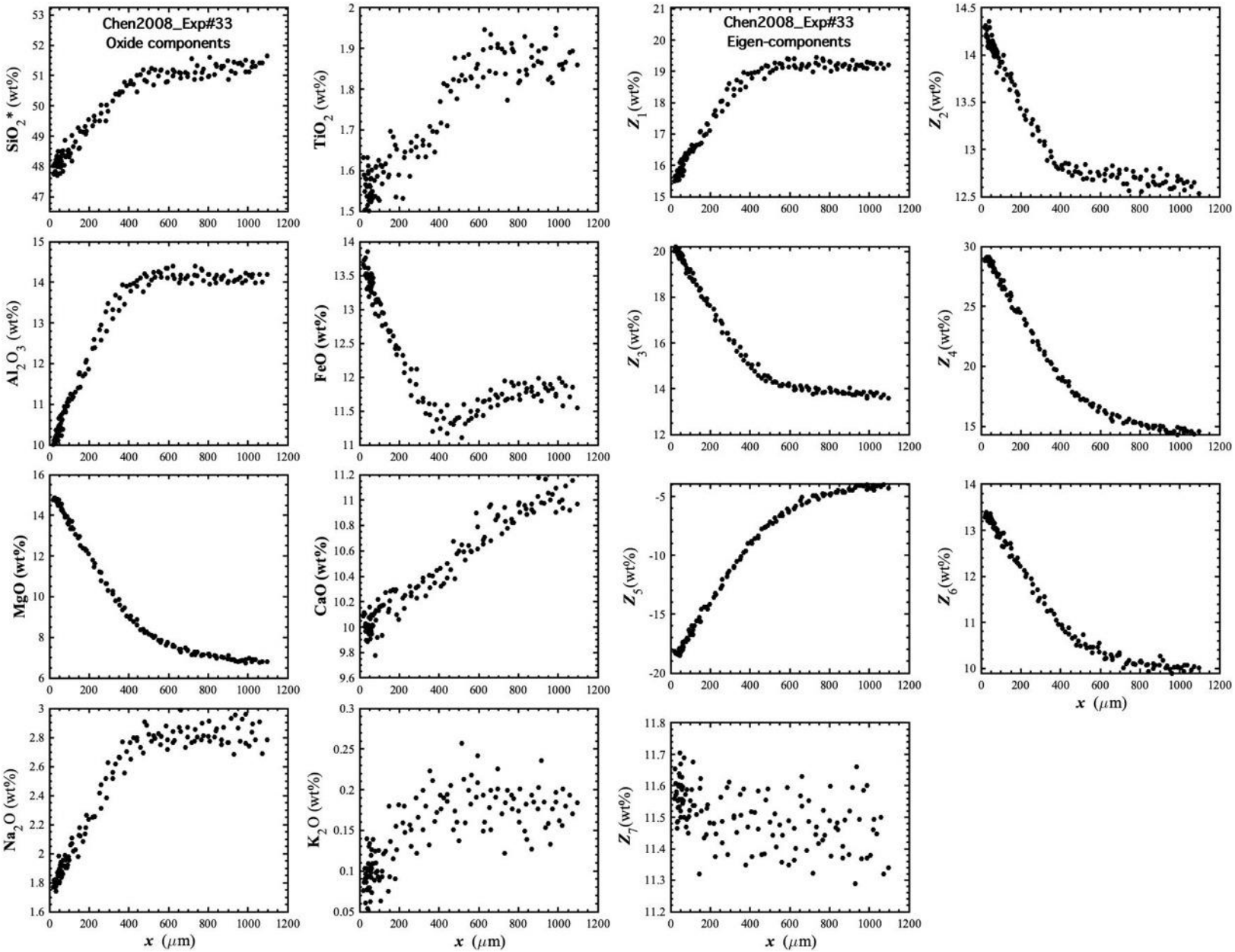

Figure 44. Concentration profiles of oxide components in wt% (left panel) and eigen-components (right panel) of Chen2008_Exp#33, which is an olivine dissolution experiment in basalt (Chen and Zhang, 2008).

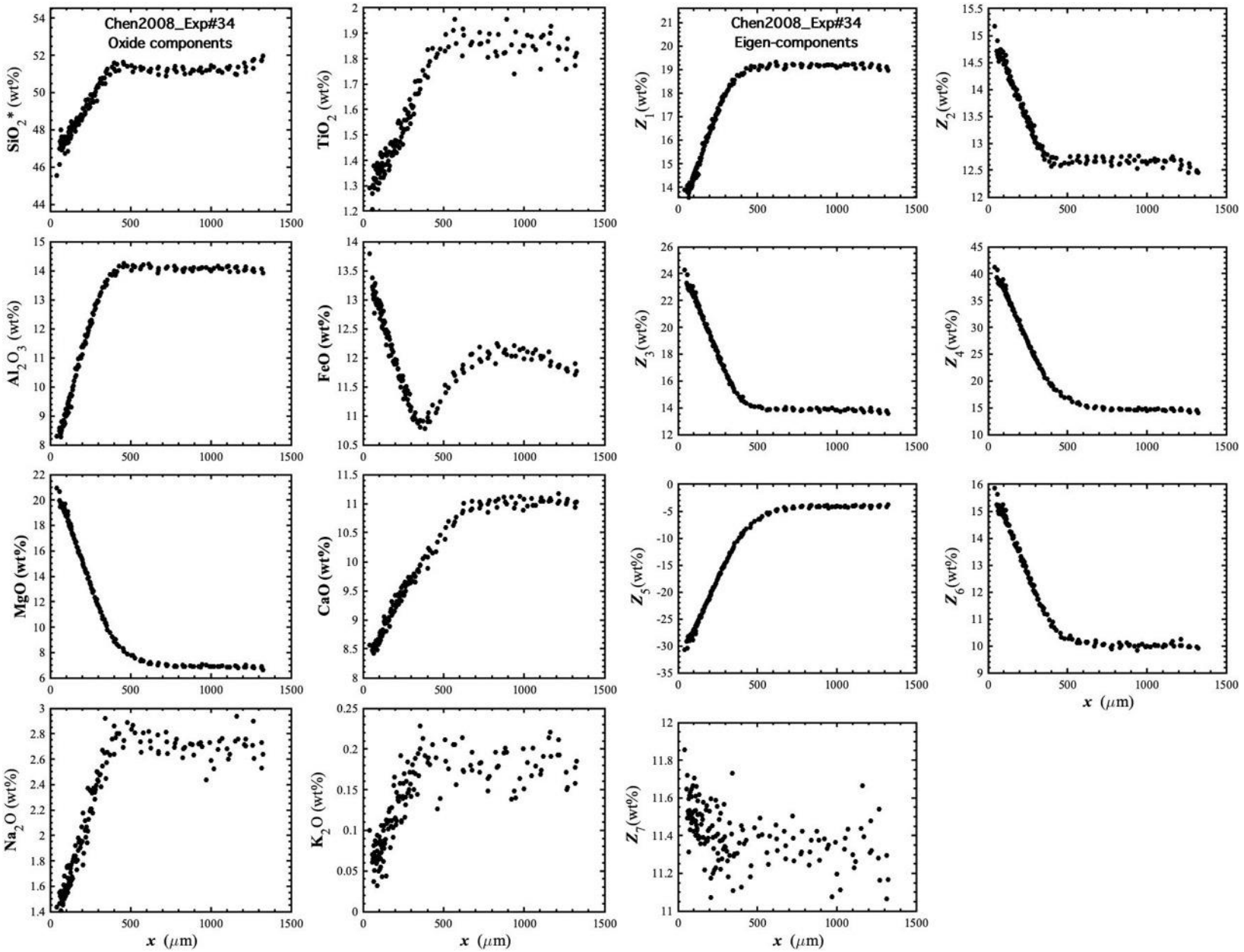

Figure 45. Concentration profiles of oxide components in wt% (left panel) and eigen-components (right panel) of Chen2008_Exp#34, which is an olivine dissolution experiment in basalt (Chen and Zhang, 2008).

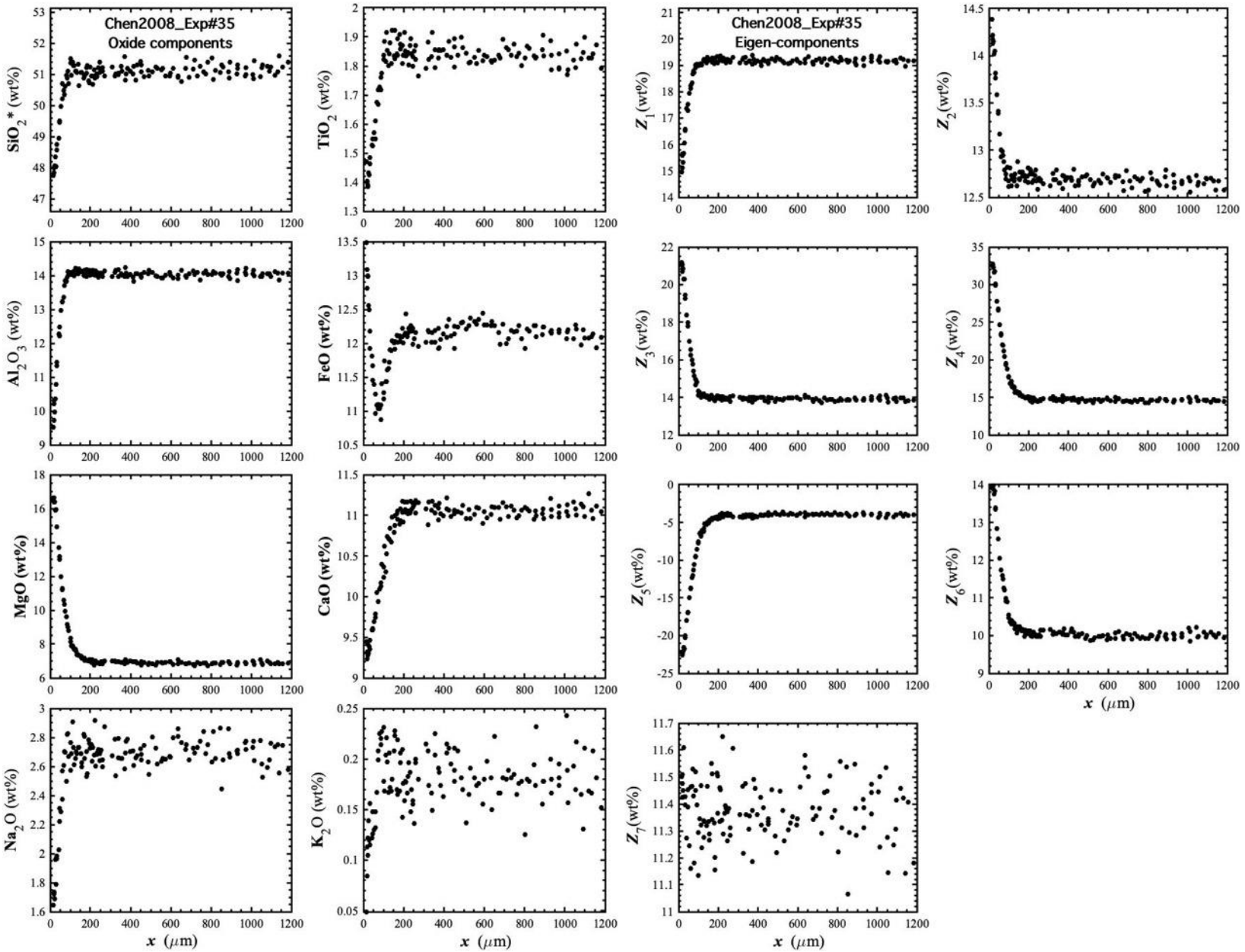

Figure 46. Concentration profiles of oxide components in wt% (left panel) and eigen-components (right panel) of Chen2008_Exp#35, which is an olivine dissolution experiment in basalt (Chen and Zhang, 2008).

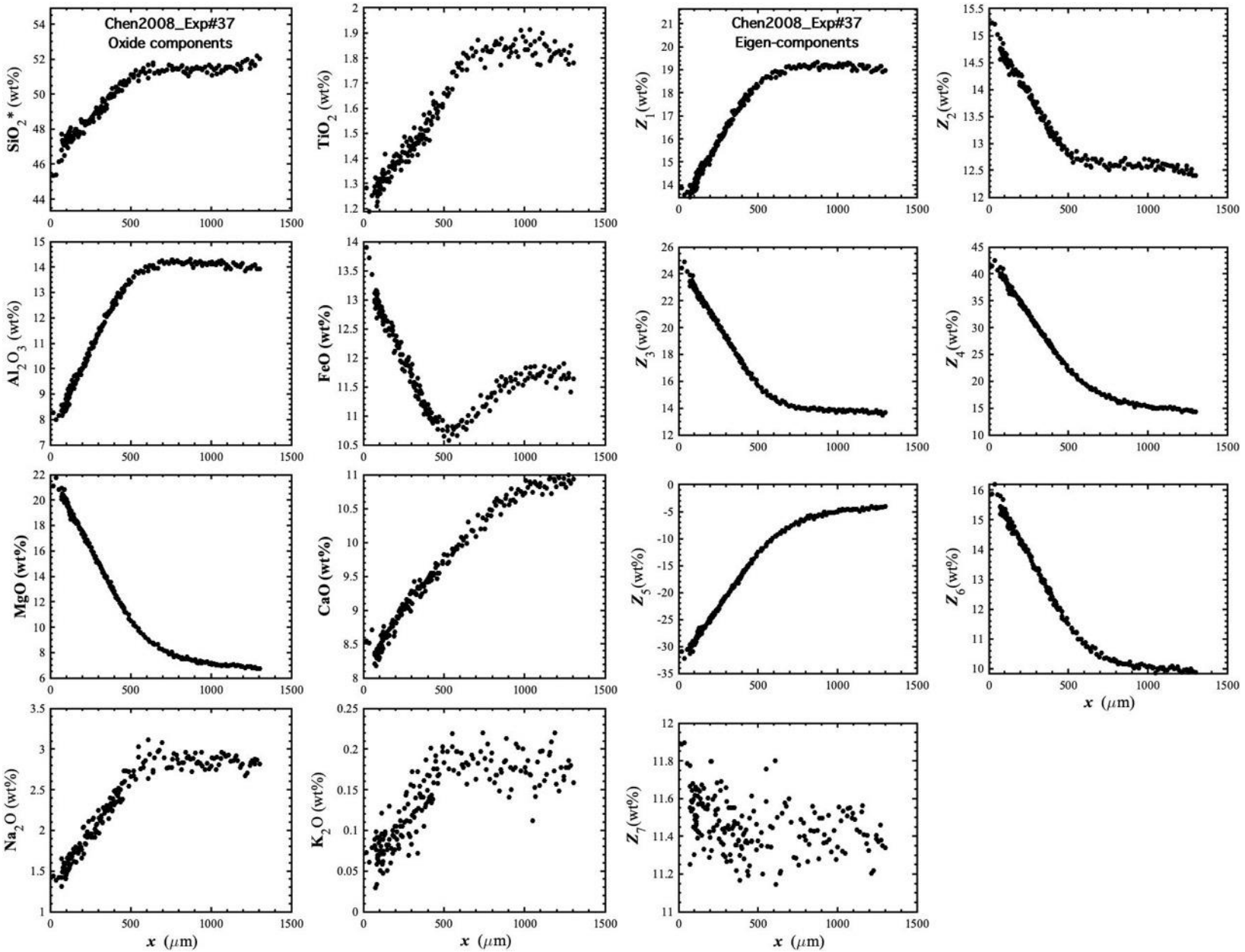

Figure 47. Concentration profiles of oxide components in wt% (left panel) and eigen-components (right panel) of Chen2008_Exp#37, which is an olivine dissolution experiment in basalt (Chen and Zhang, 2008).

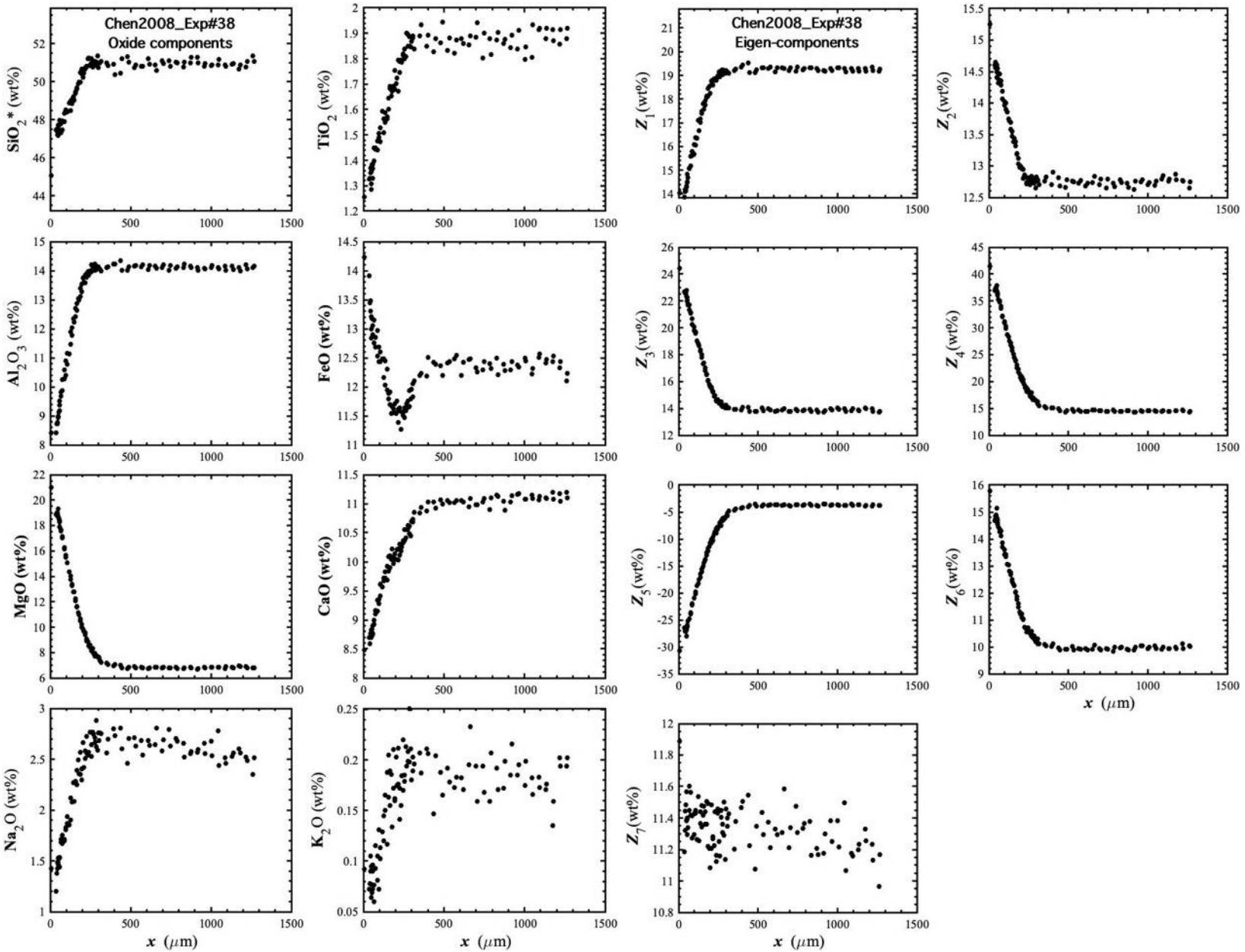

Figure 48. Concentration profiles of oxide components in wt% (left panel) and eigen-components (right panel) of Chen2008_Exp#38, which is an olivine dissolution experiment in basalt (Chen and Zhang, 2008).

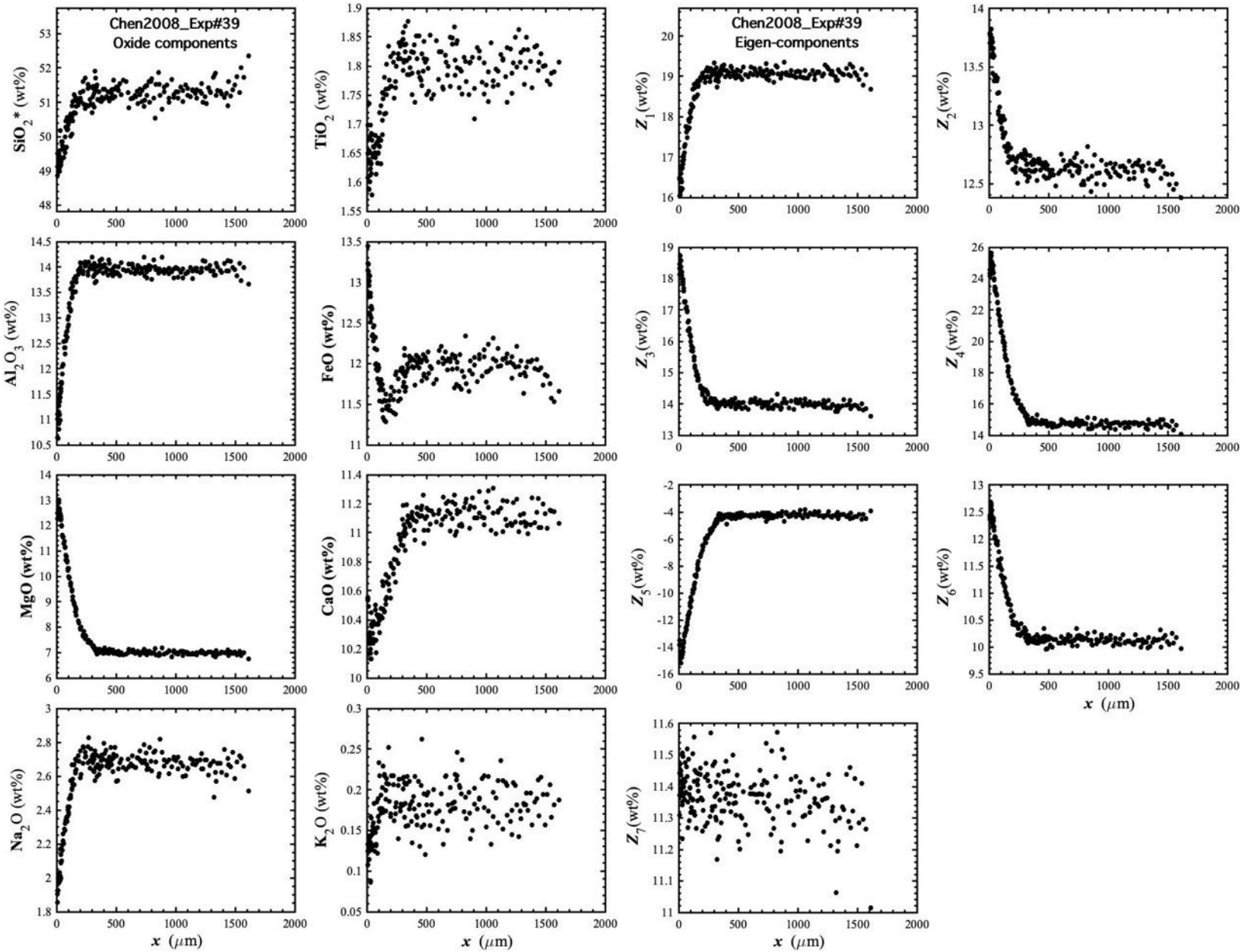

Figure 49. Concentration profiles of oxide components in wt% (left panel) and eigen-components (right panel) of Chen2008_Exp#39, which is an olivine dissolution experiment in basalt (Chen and Zhang, 2008).

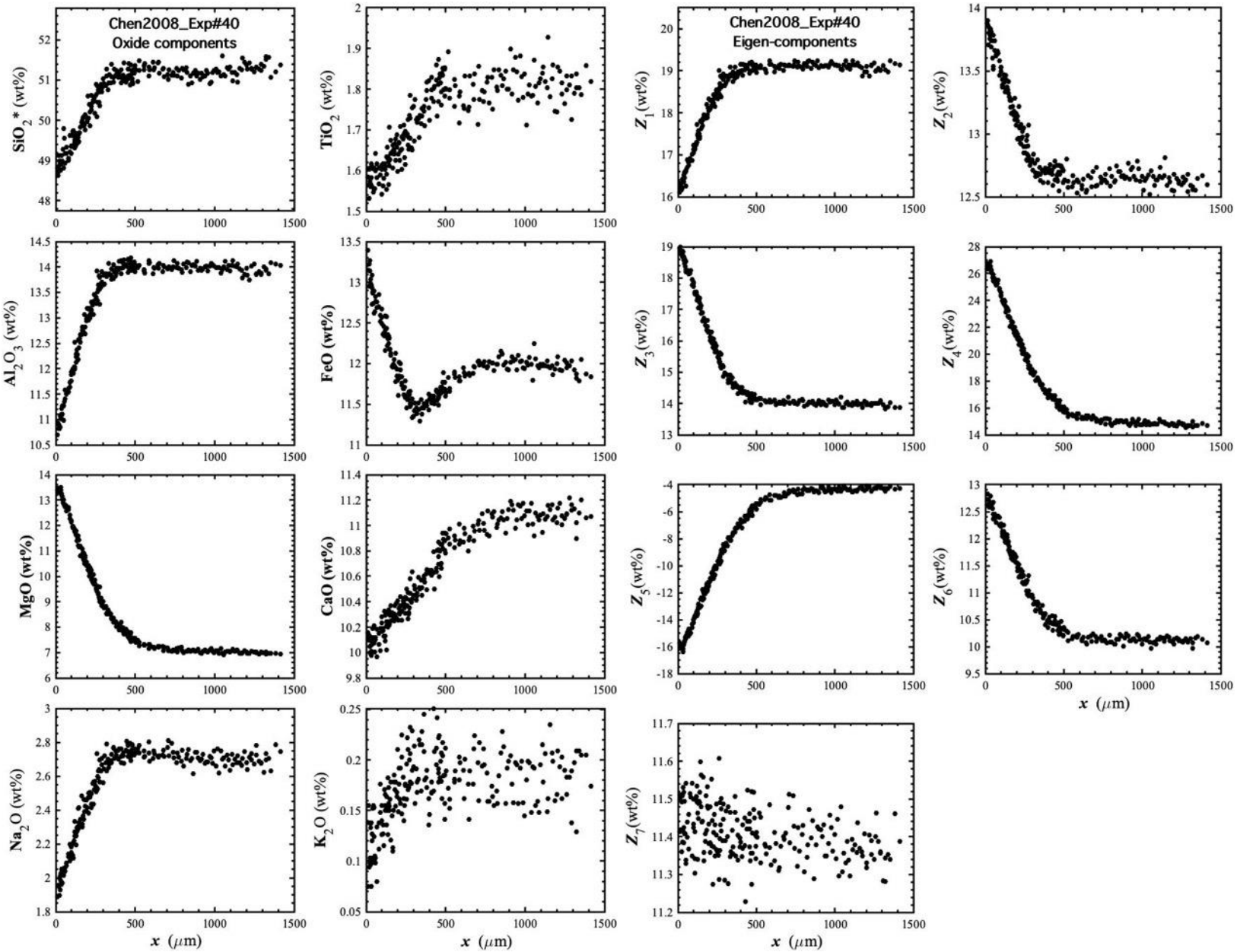

Figure 50. Concentration profiles of oxide components in wt% (left panel) and eigen-components (right panel) of Chen2008_Exp#40, which is an olivine dissolution experiment in basalt (Chen and Zhang, 2008).

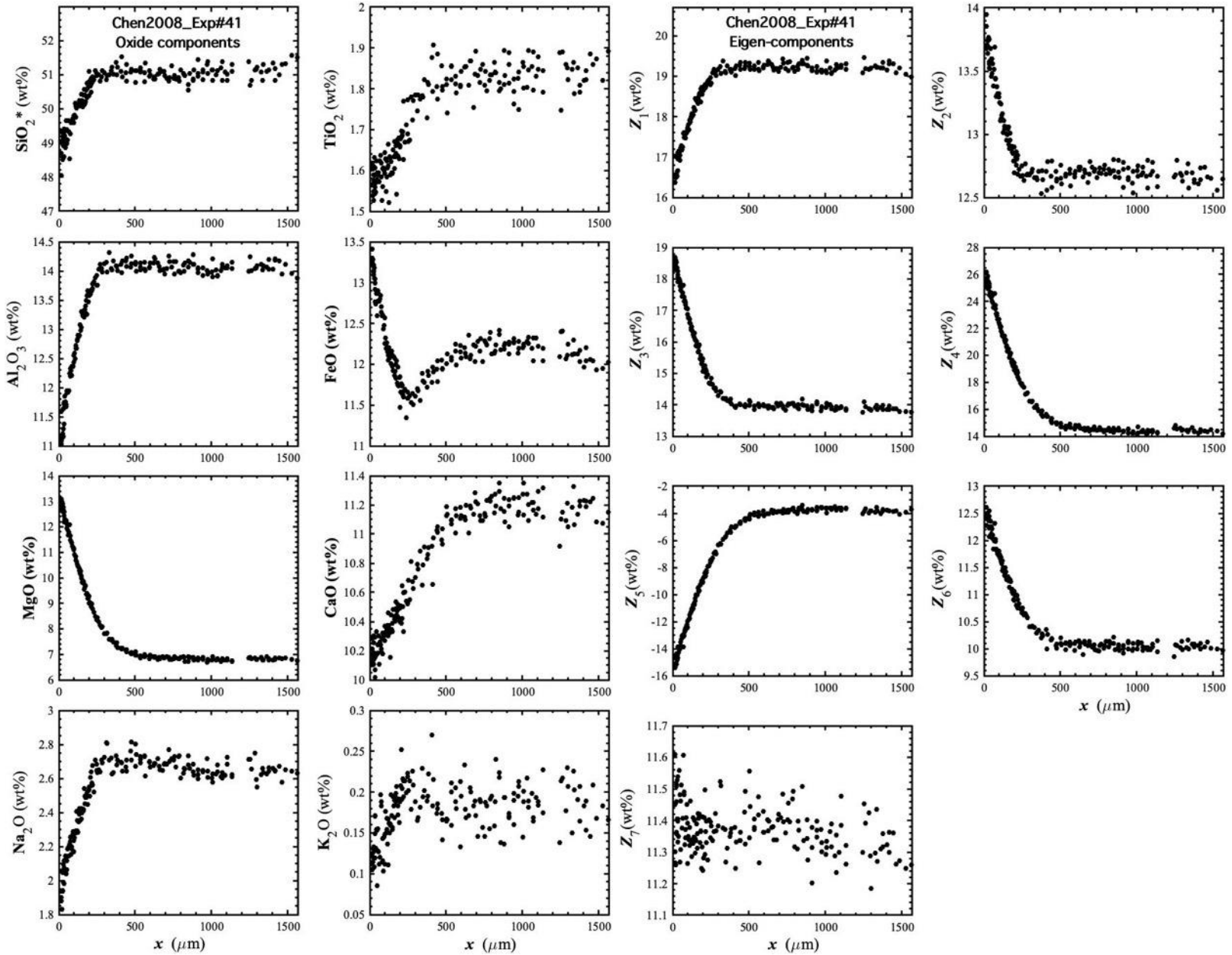

Figure 51. Concentration profiles of oxide components in wt% (left panel) and eigen-components (right panel) of Chen2008_Exp#41, which is an olivine dissolution experiment in basalt (Chen and Zhang, 2008).

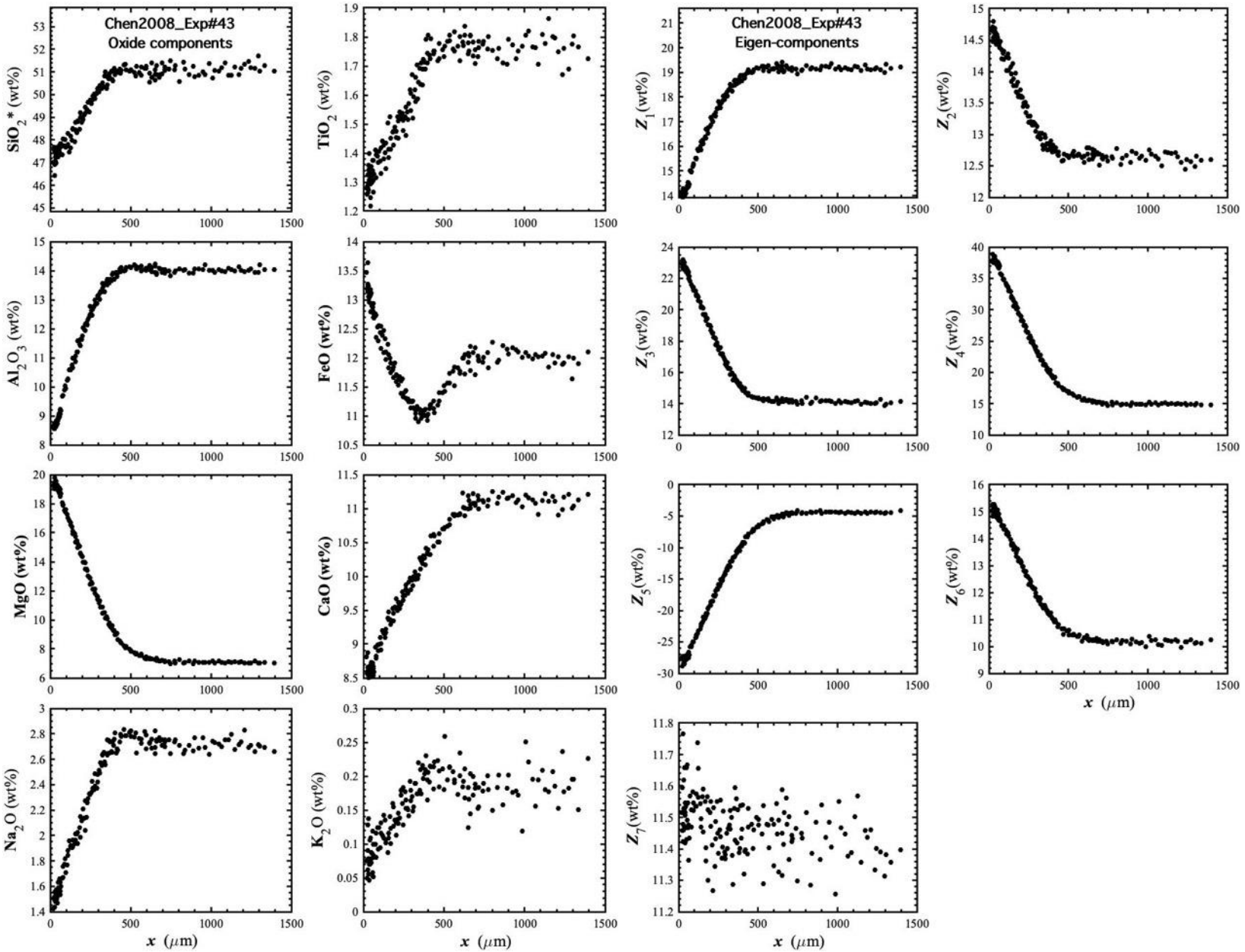

Figure 52. Concentration profiles of oxide components in wt% (left panel) and eigen-components (right panel) of Chen2008_Exp#43, which is an olivine dissolution experiment in basalt (Chen and Zhang, 2008).

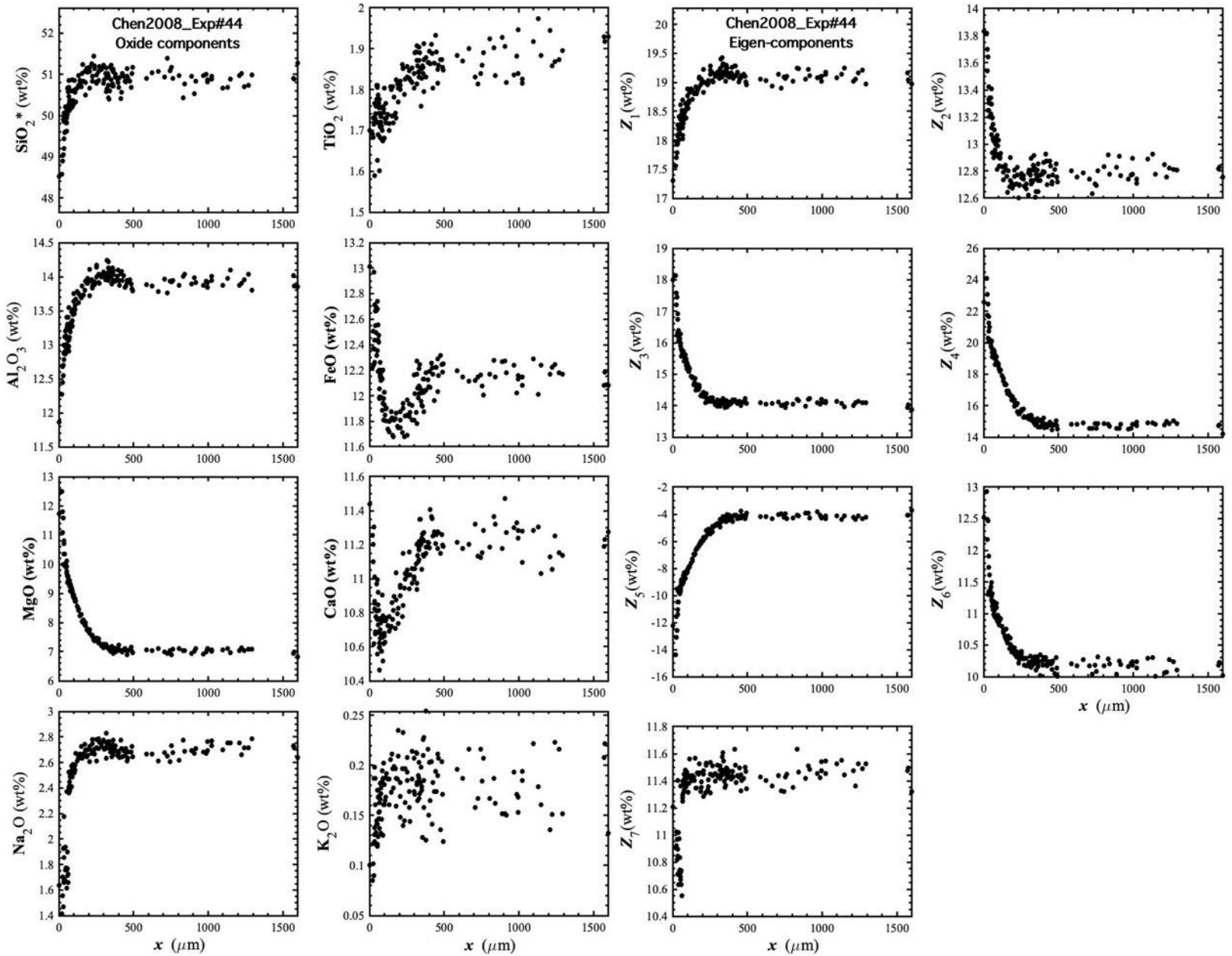

Figure 53. Concentration profiles of oxide components in wt% (left panel) and eigen-components (right panel) of Chen2008_Exp#44, which is an olivine dissolution experiment in basalt (Chen and Zhang, 2008).

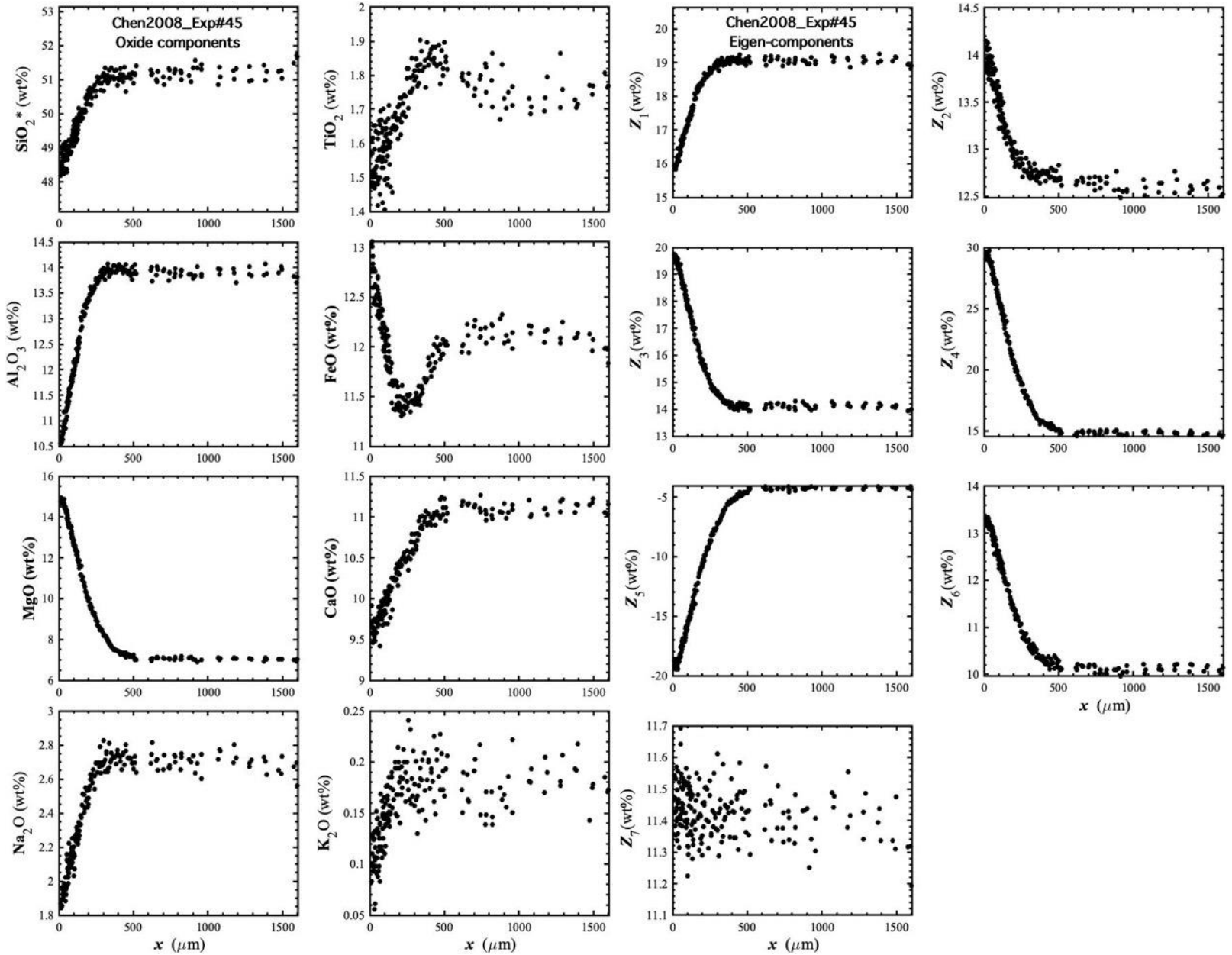

Figure 54. Concentration profiles of oxide components in wt% (left panel) and eigen-components (right panel) of Chen2008_Exp#45, which is an olivine dissolution experiment in basalt (Chen and Zhang, 2008).

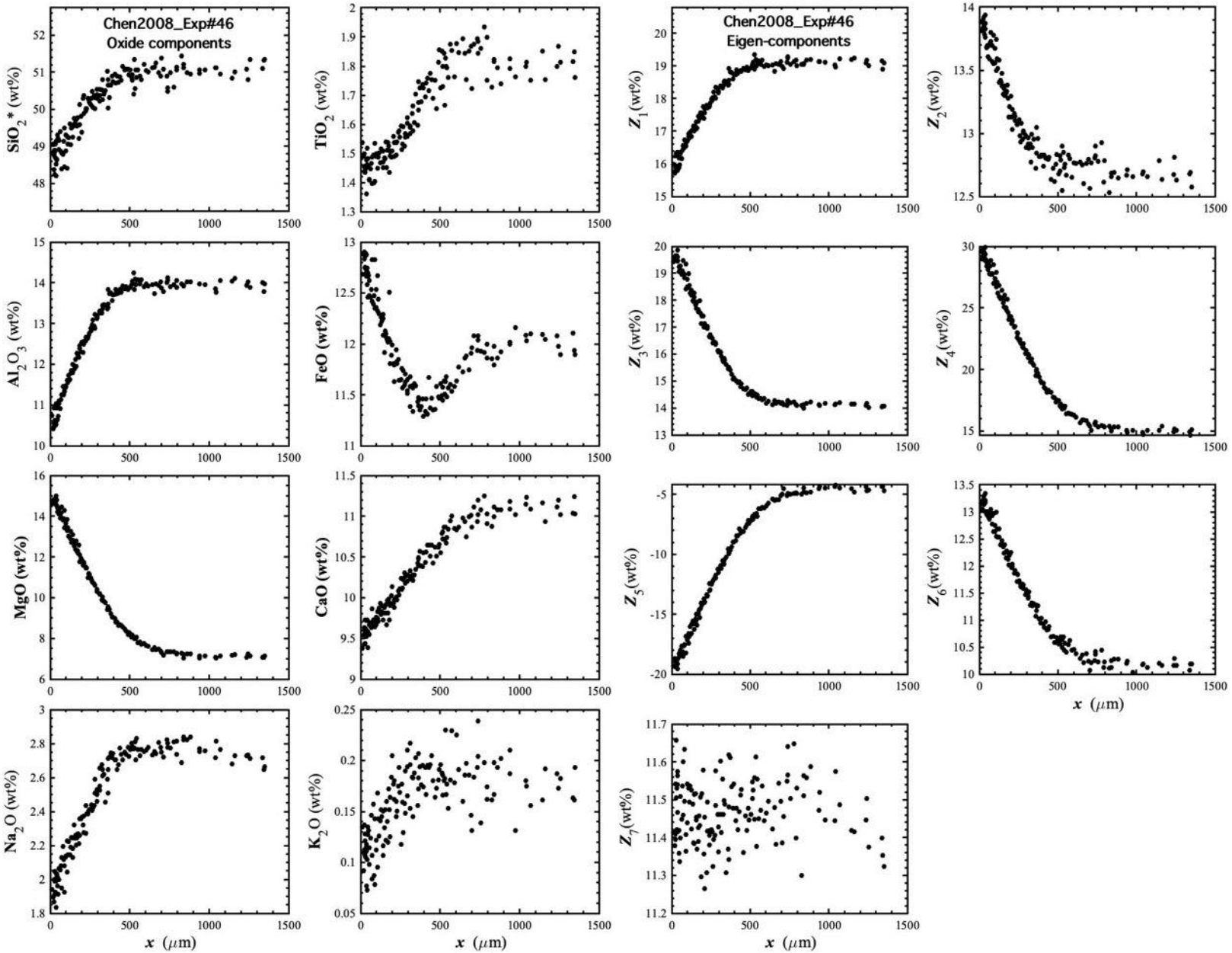

Figure 55. Concentration profiles of oxide components in wt% (left panel) and eigen-components (right panel) of Chen2008_Exp#46, which is an olivine dissolution experiment in basalt (Chen and Zhang, 2008).

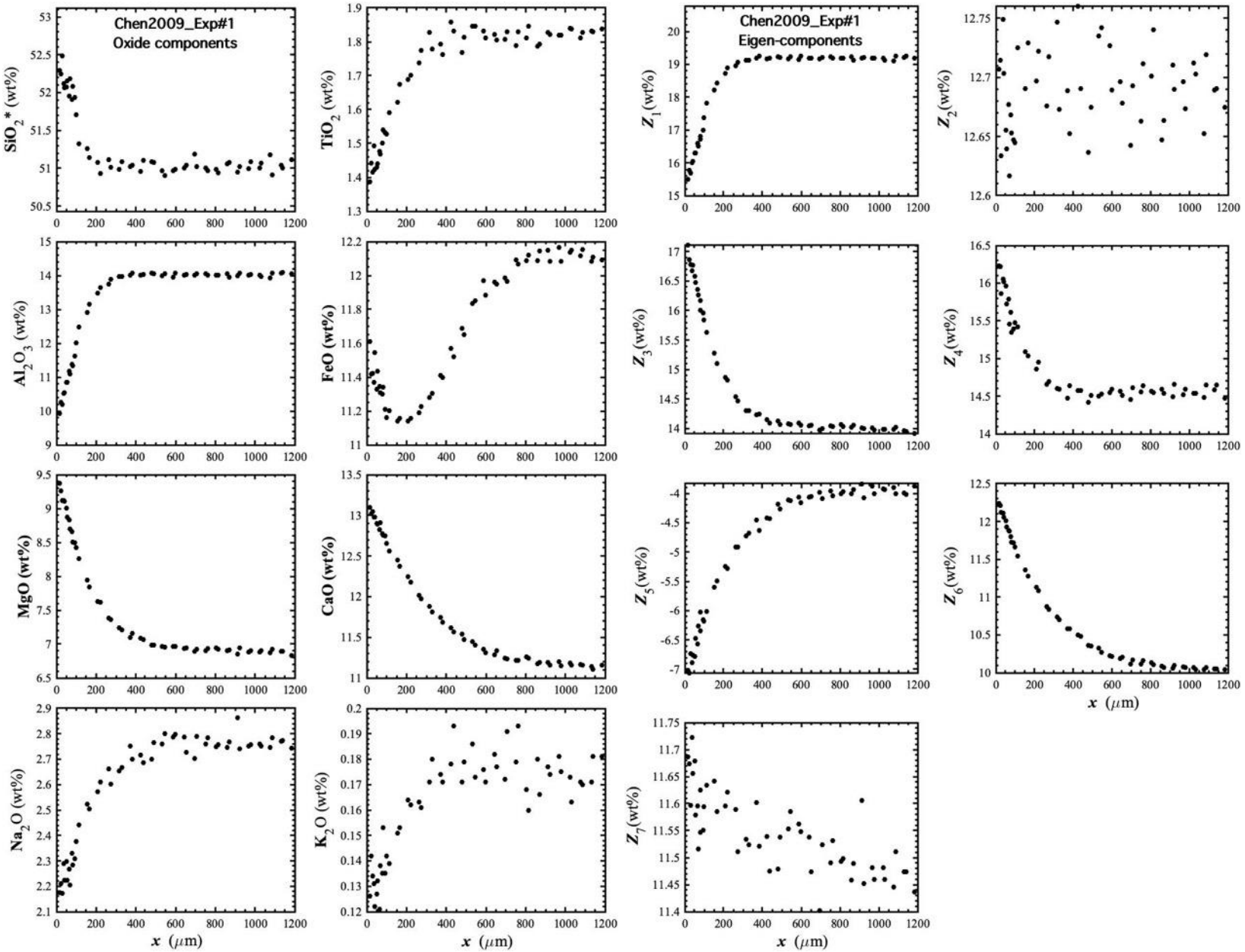

Figure 56. Concentration profiles of oxide components in wt% (left panel) and eigen-components (right panel) of Chen2009_Exp#1, which is a diopside dissolution experiment in basalt (Chen and Zhang, 2009).

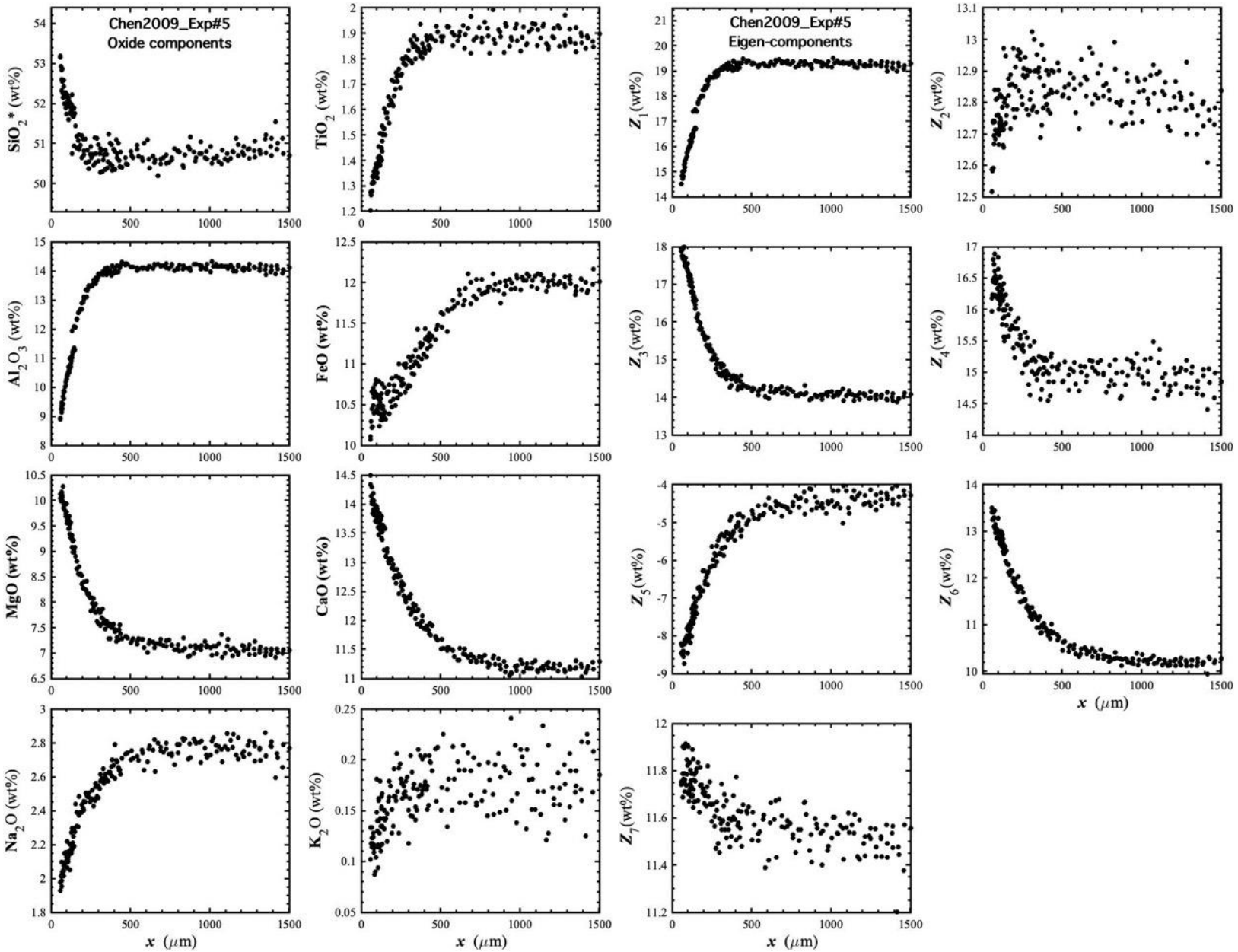

Figure 57. Concentration profiles of oxide components in wt% (left panel) and eigen-components (right panel) of Chen2009_Exp#5, which is a diopside dissolution experiment in basalt (Chen and Zhang, 2009).

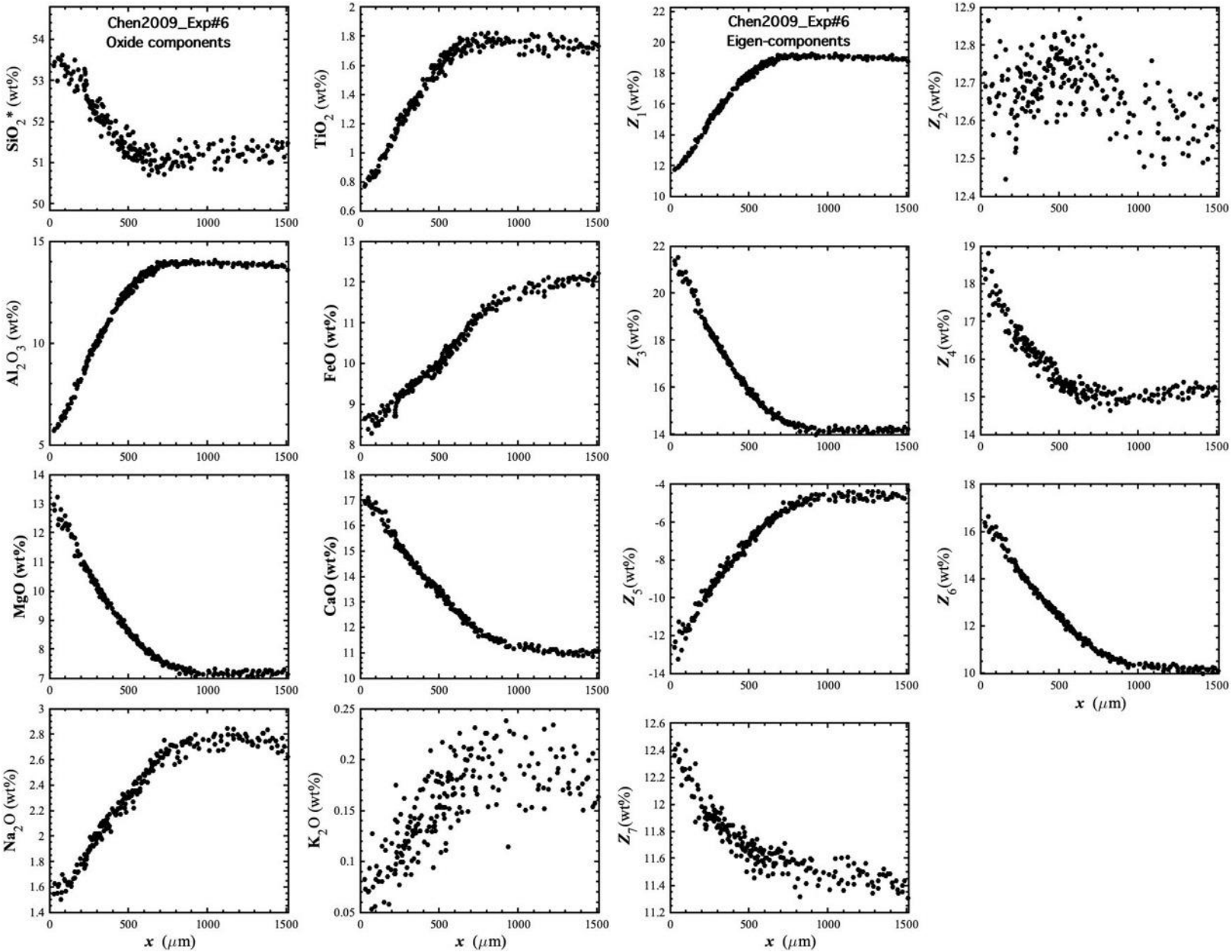

Figure 58. Concentration profiles of oxide components in wt% (left panel) and eigen-components (right panel) of Chen2009_Exp#6, which is a diopside dissolution experiment in basalt (Chen and Zhang, 2009).

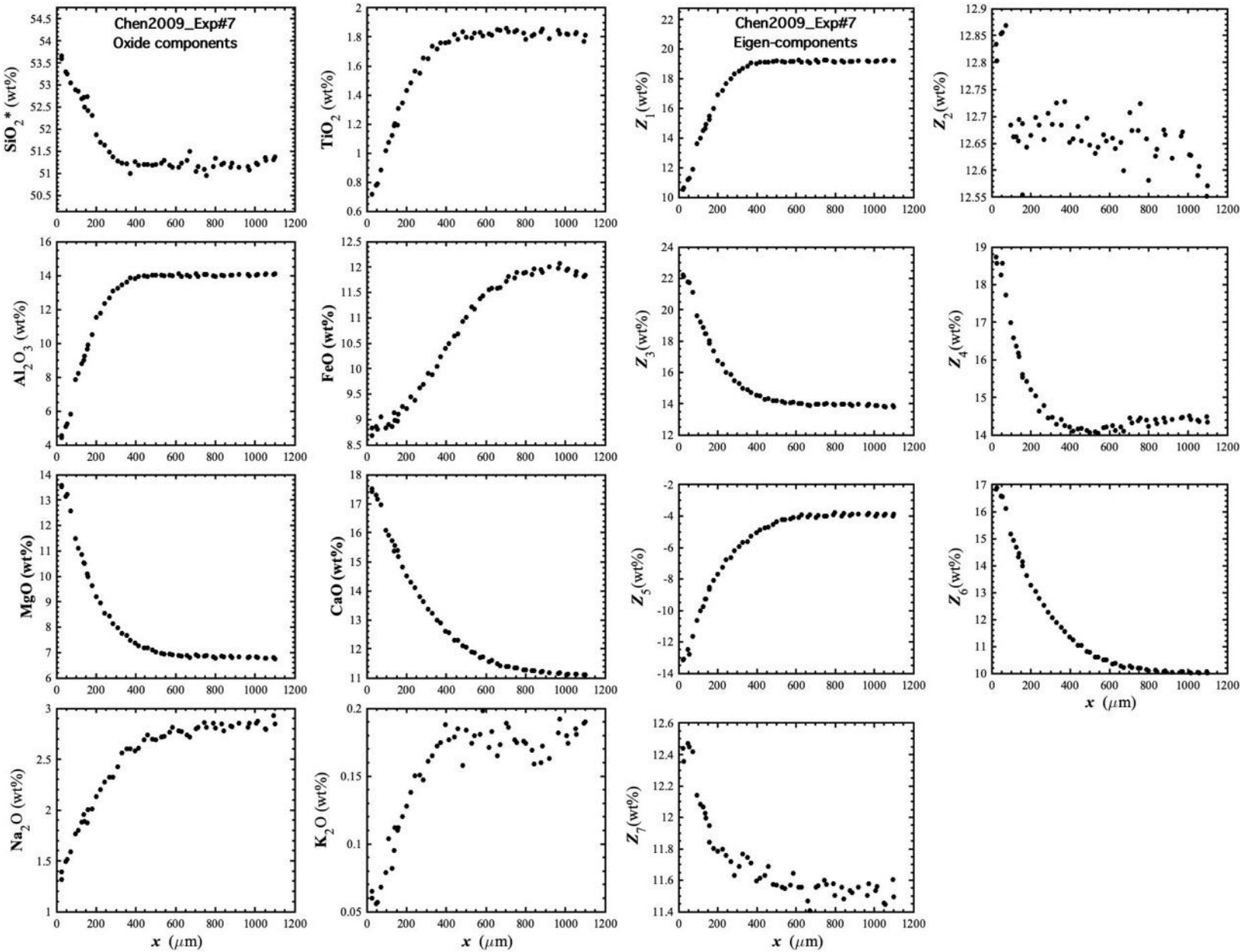

Figure 59. Concentration profiles of oxide components in wt% (left panel) and eigen-components (right panel) of Chen2009_Exp#7, which is a diopside dissolution experiment in basalt (Chen and Zhang, 2009).

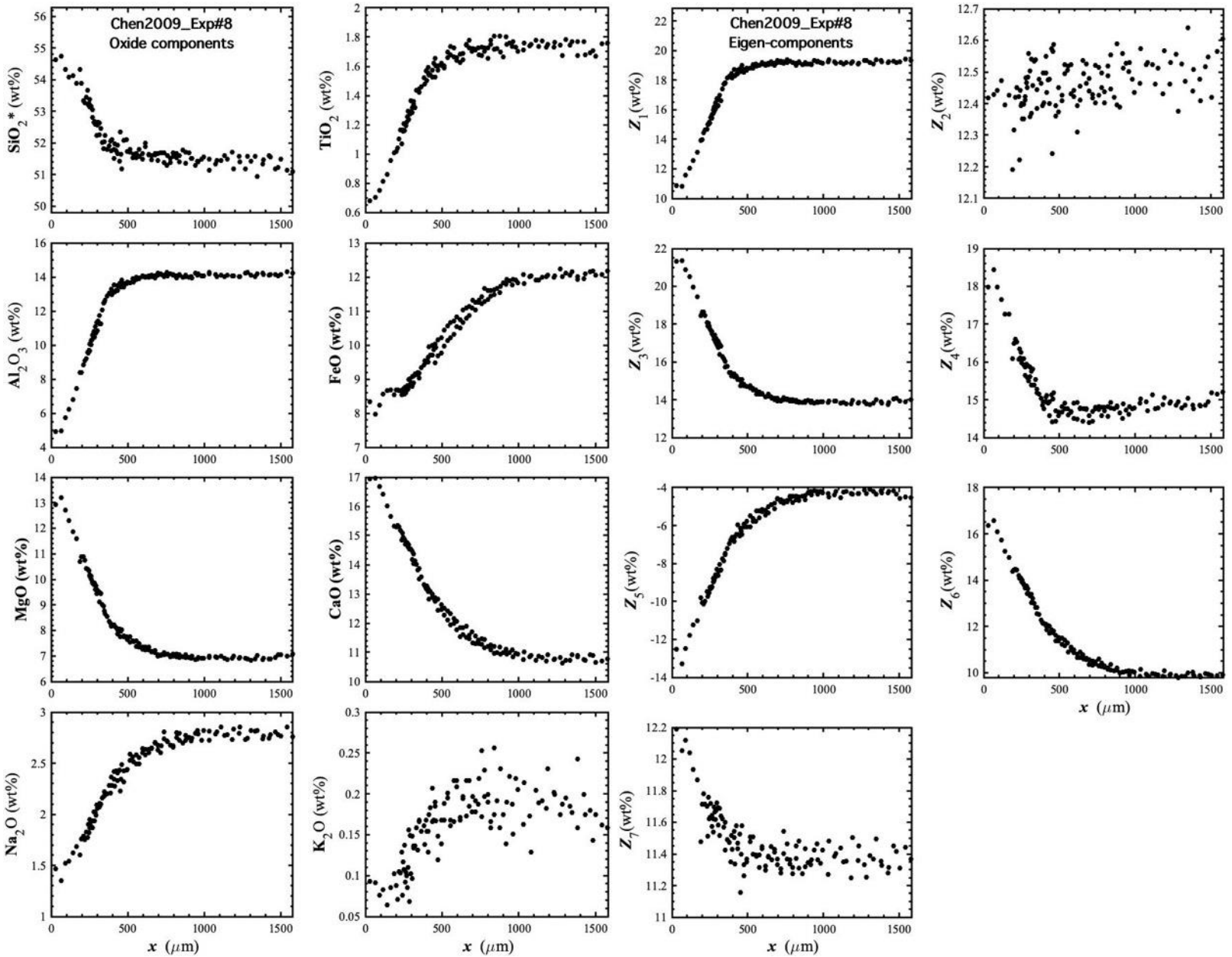

Figure 60. Concentration profiles of oxide components in wt% (left panel) and eigen-components (right panel) of Chen2009_Exp#8, which is a diopside dissolution experiment in basalt (Chen and Zhang, 2009).

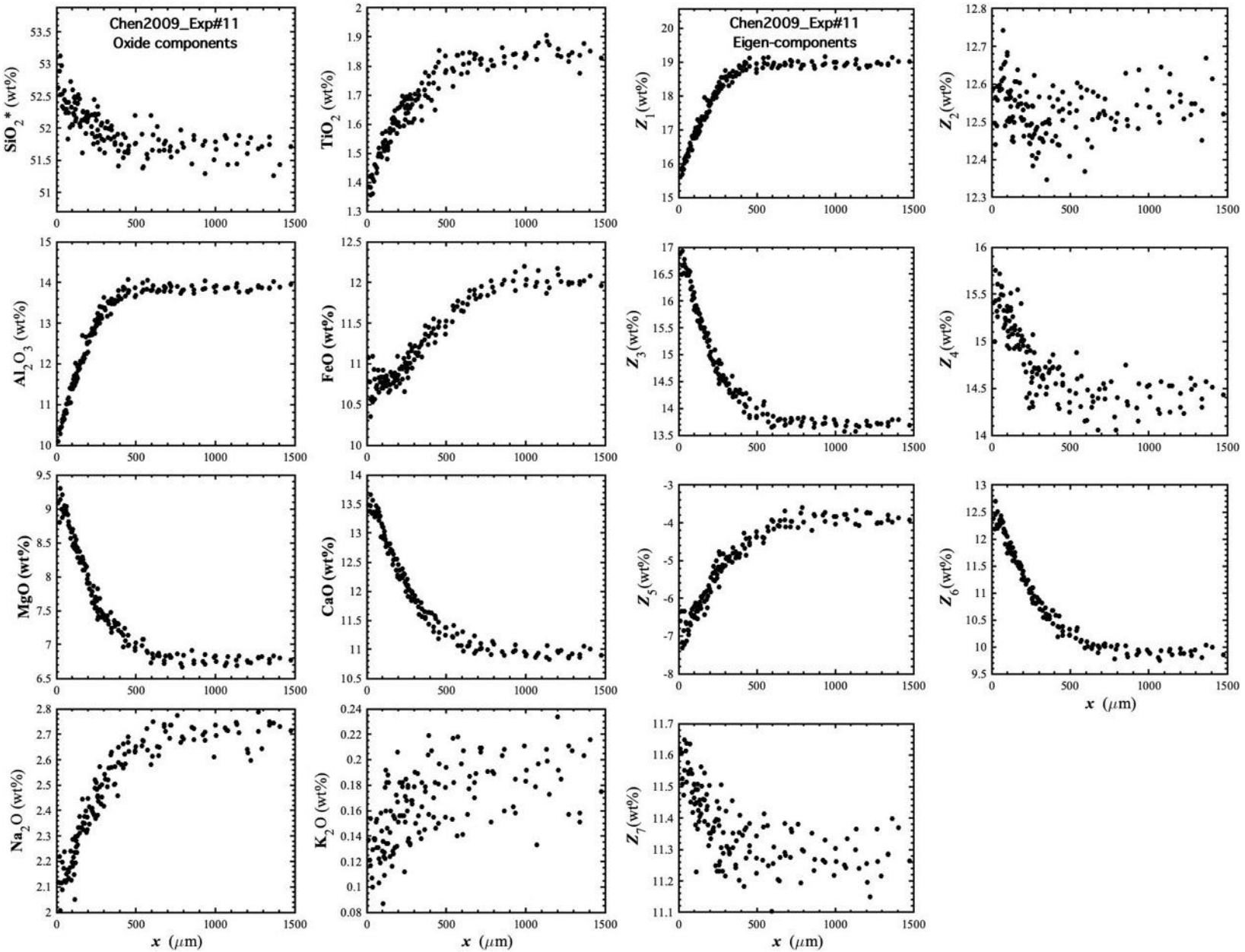

Figure 61. Concentration profiles of oxide components in wt% (left panel) and eigen-components (right panel) of Chen2009_Exp#11, which is a diopside dissolution experiment in basalt (Chen and Zhang, 2009).

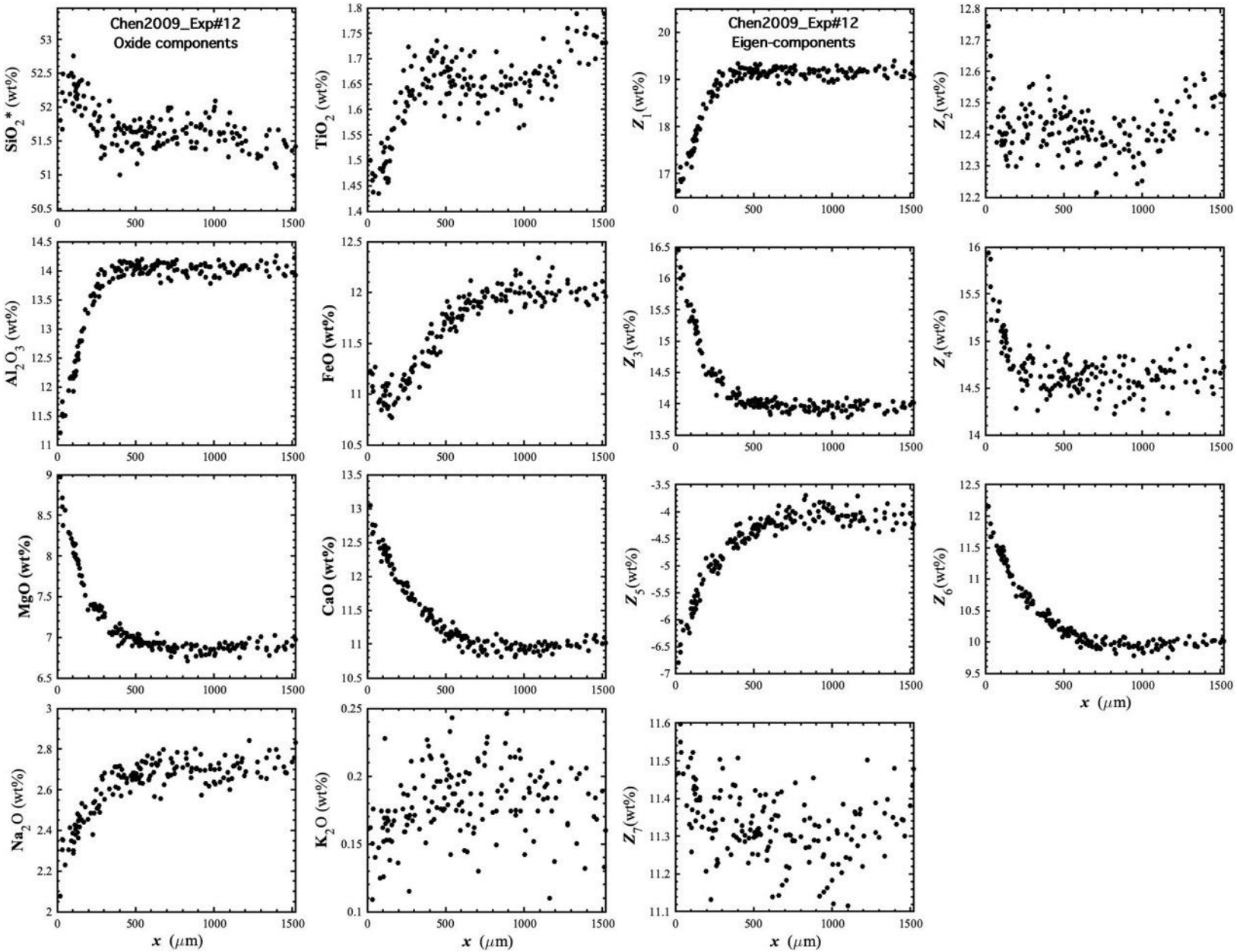

Figure 62. Concentration profiles of oxide components in wt% (left panel) and eigen-components (right panel) of Chen2009_Exp#12, which is a diopside dissolution experiment in basalt (Chen and Zhang, 2009).

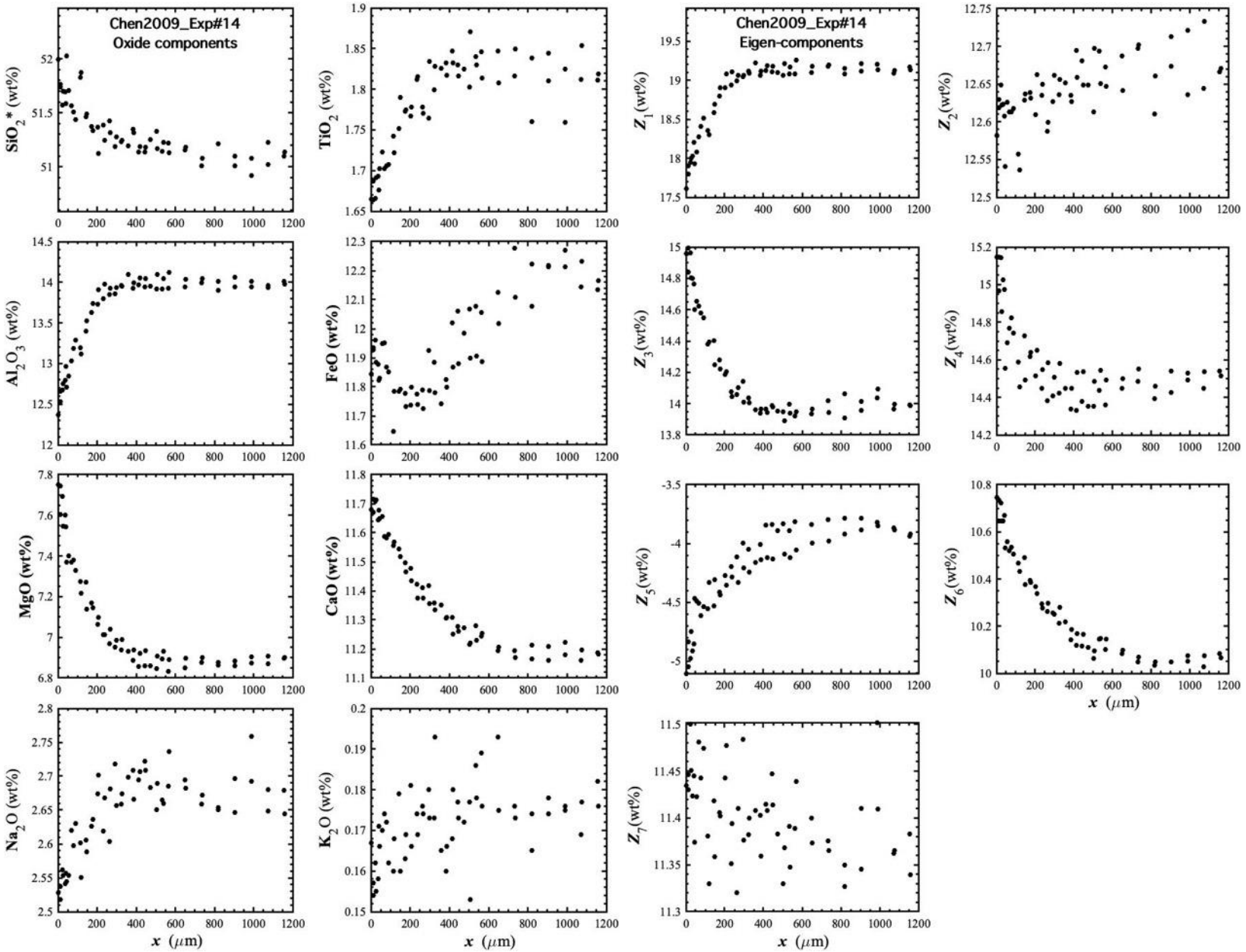

Figure 63. Concentration profiles of oxide components in wt% (left panel) and eigen-components (right panel) of Chen2009_Exp#14, which is a diopside dissolution experiment in basalt (Chen and Zhang, 2009).

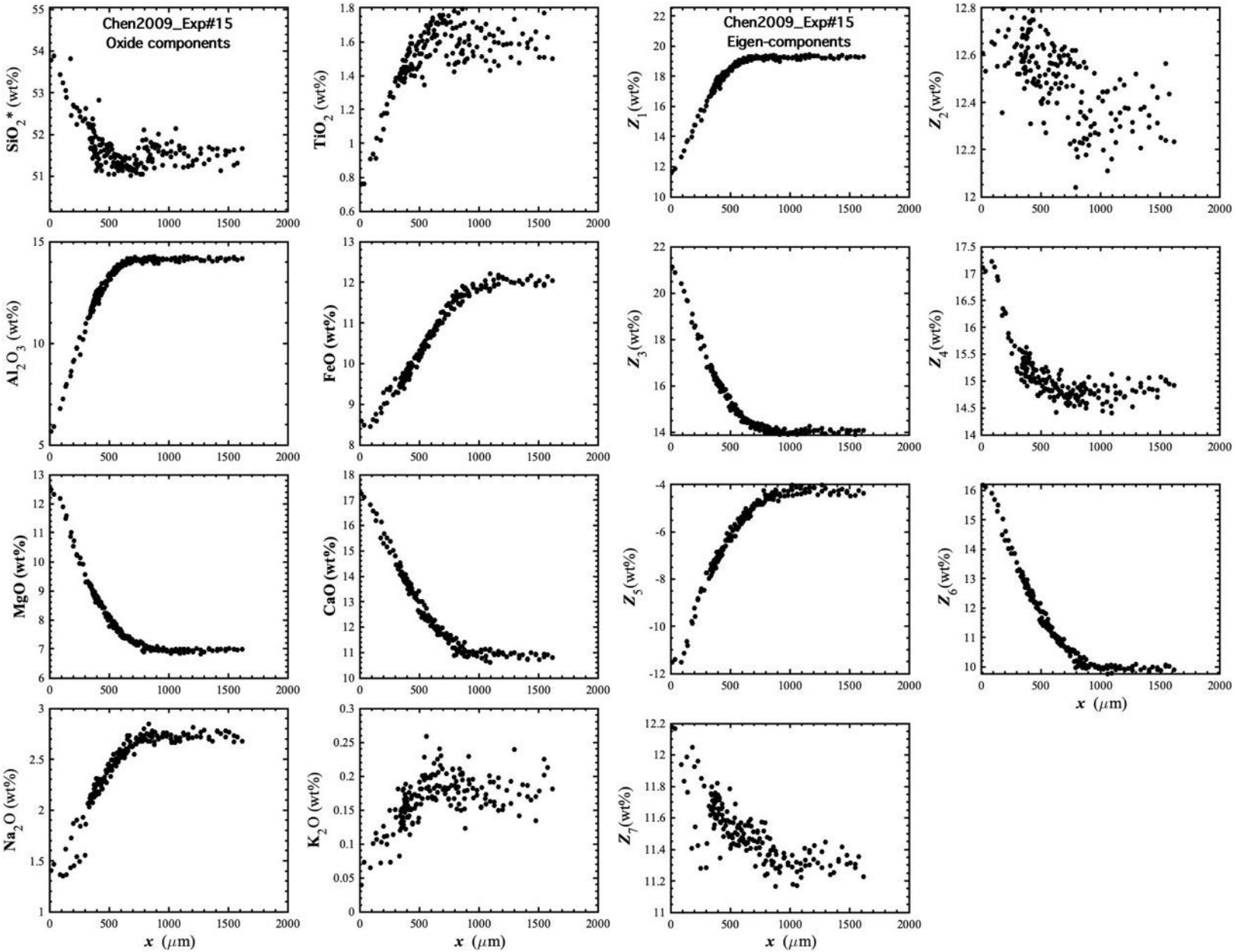

Figure 64. Concentration profiles of oxide components in wt% (left panel) and eigen-components (right panel) of Chen2009_Exp#15, which is a diopside dissolution experiment in basalt (Chen and Zhang, 2009).

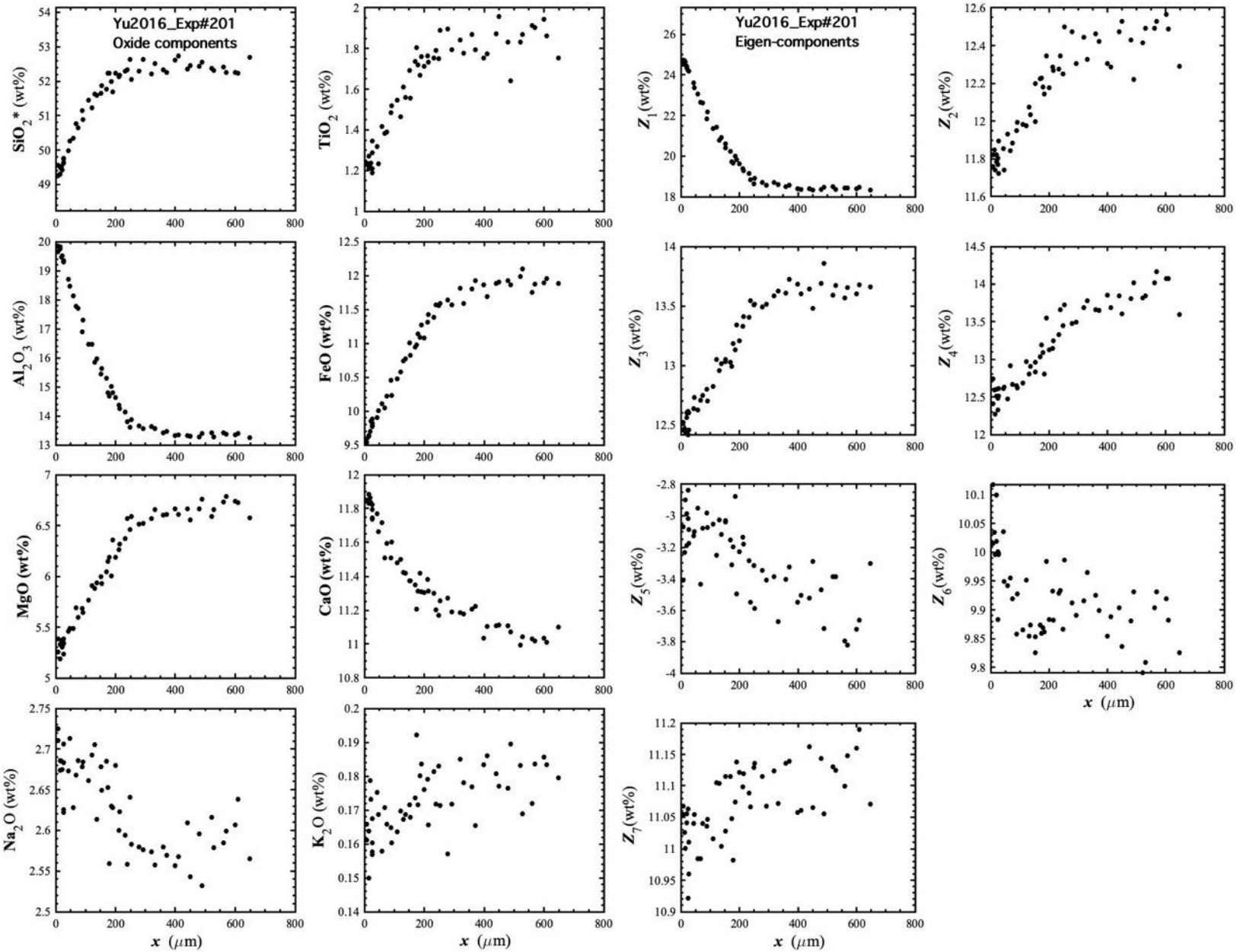

Figure 65. Concentration profiles of oxide components in wt% (left panel) and eigen-components (right panel) of Yu2016_Exp#201, which is a plagioclase dissolution experiment in basalt (Yu et al., 2016).

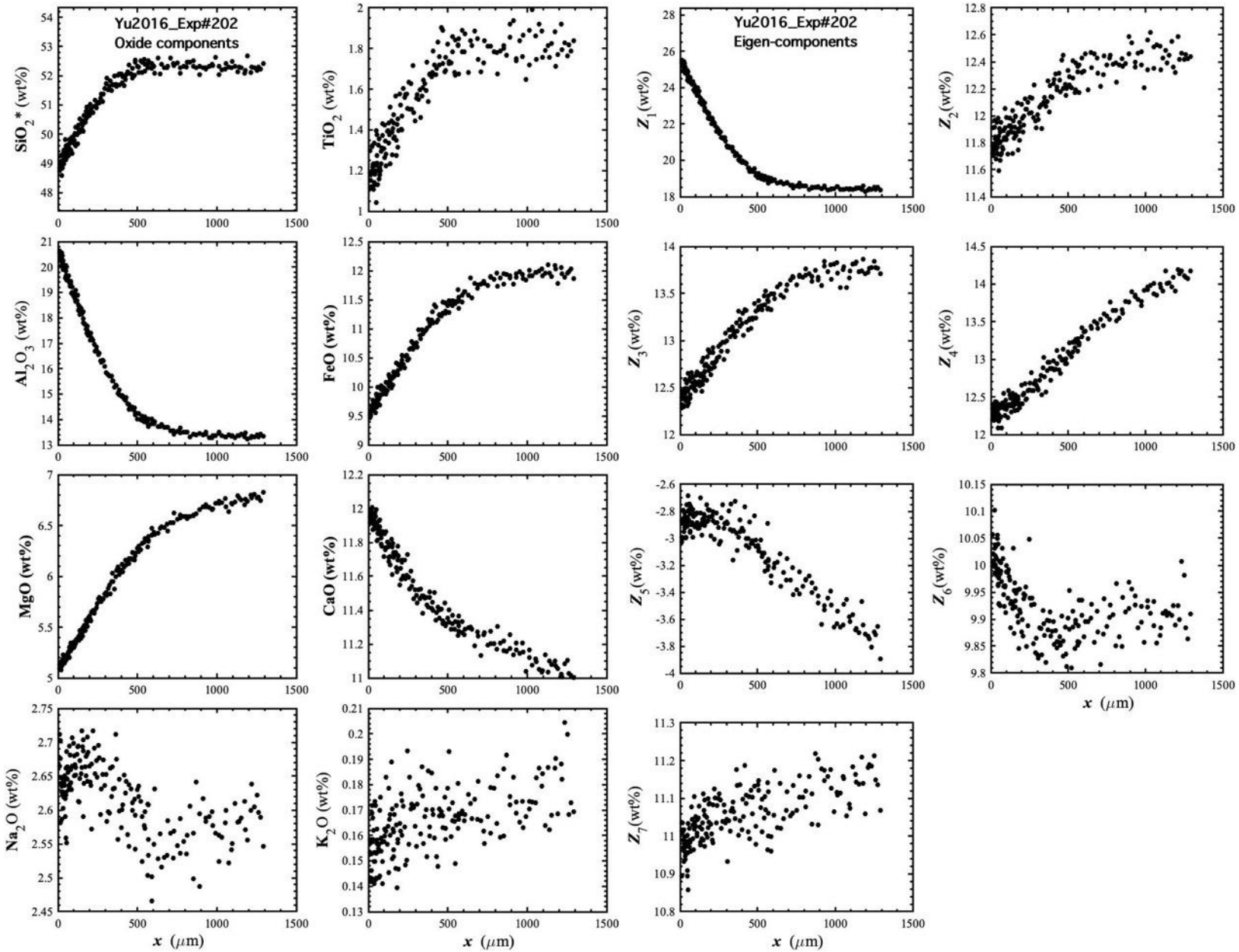

Figure 66. Concentration profiles of oxide components in wt% (left panel) and eigen-components (right panel) of Yu2016_Exp#202, which is a plagioclase dissolution experiment in basalt (Yu et al., 2016).

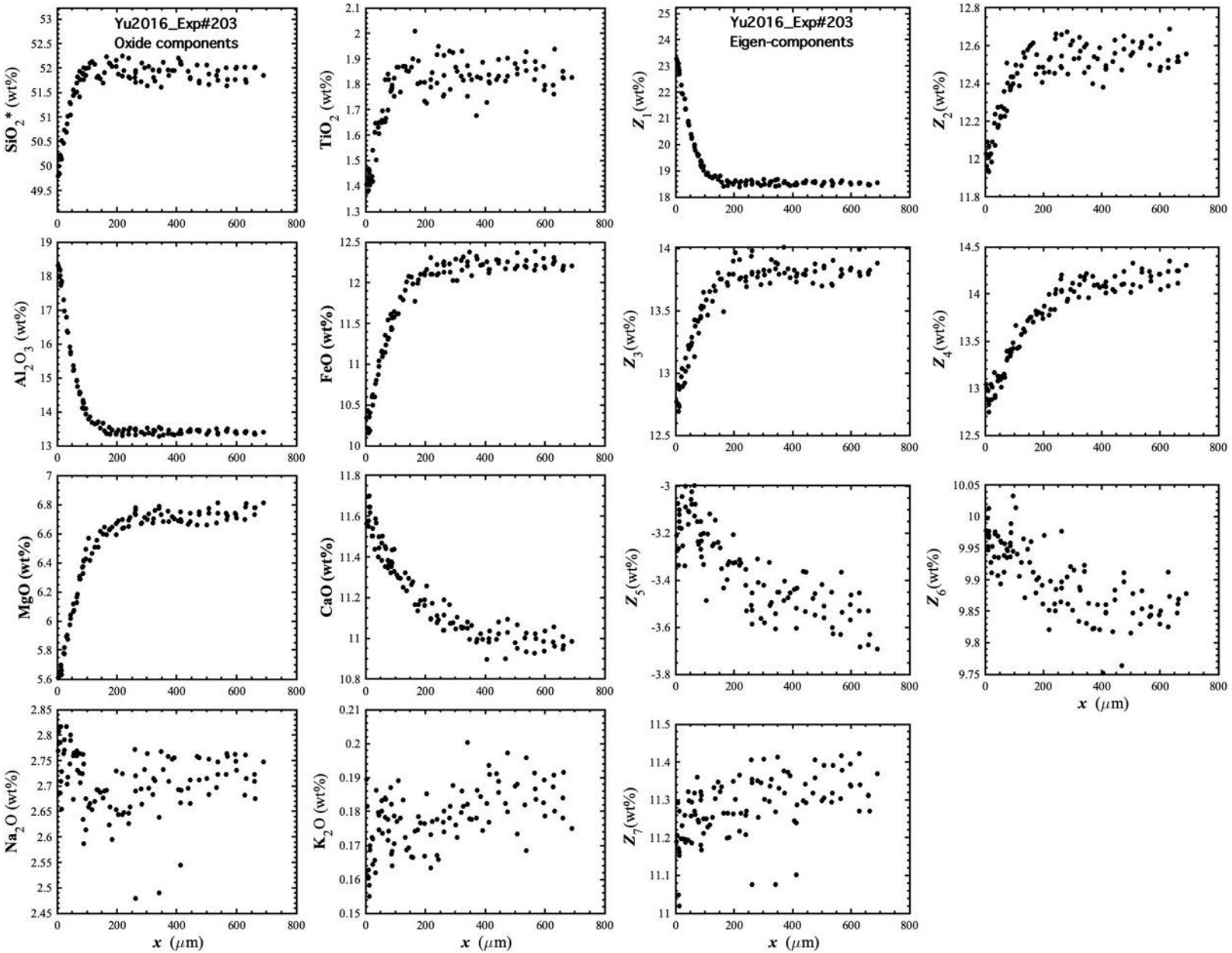

Figure 67. Concentration profiles of oxide components in wt% (left panel) and eigen-components (right panel) of Yu2016_Exp#203, which is a plagioclase dissolution experiment in basalt (Yu et al., 2016).

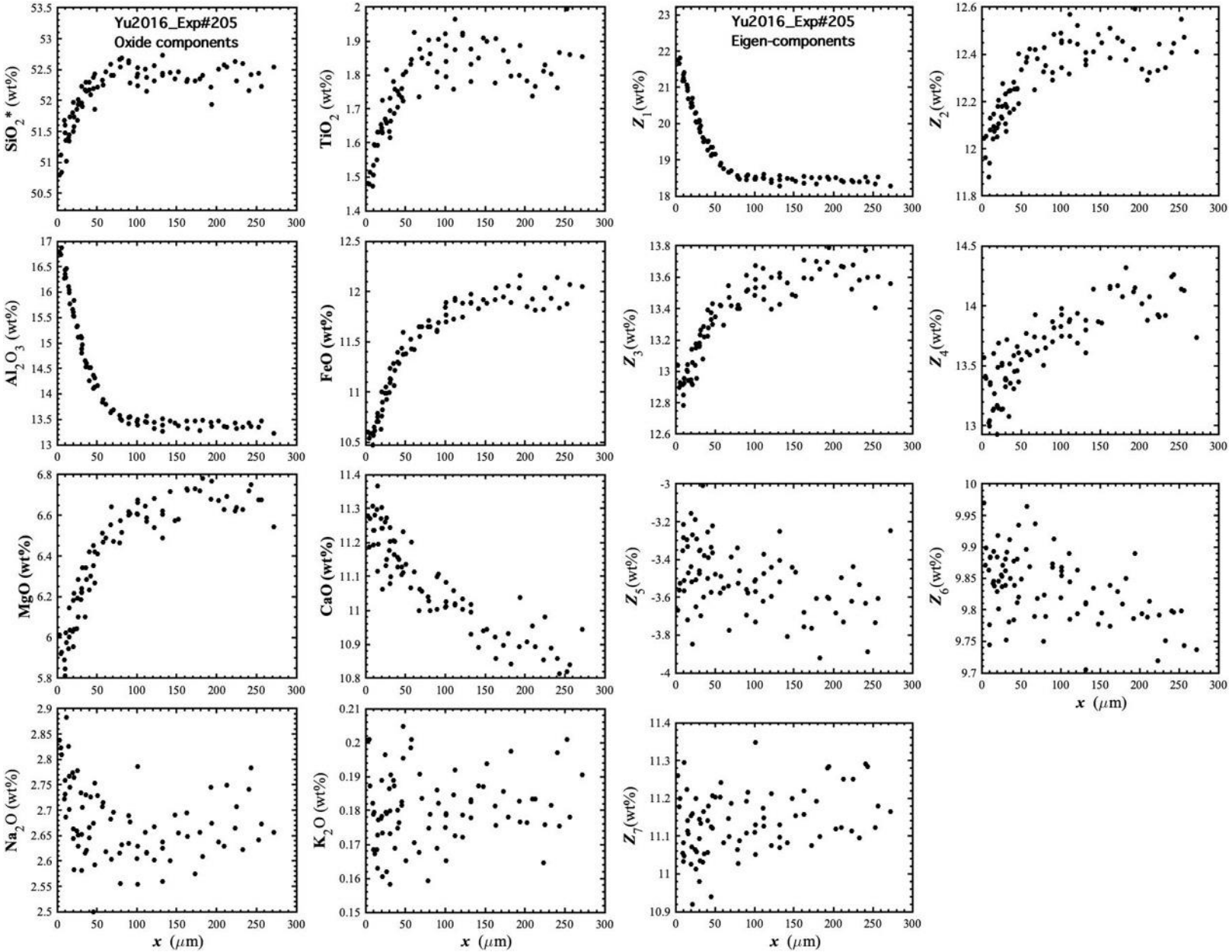

Figure 68. Concentration profiles of oxide components in wt% (left panel) and eigen-components (right panel) of Yu2016_Exp#205, which is a plagioclase dissolution experiment in basalt (Yu et al., 2016).

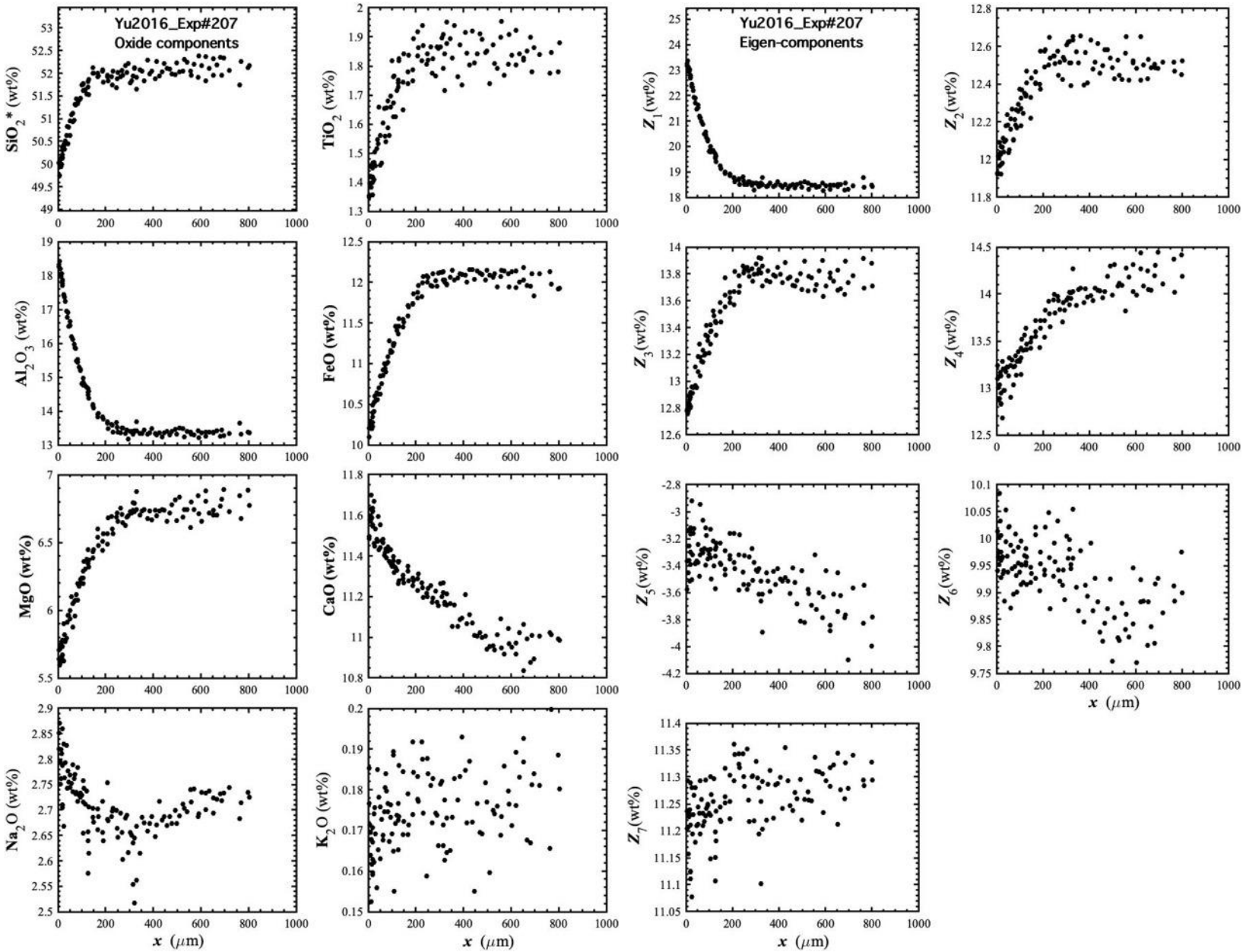

Figure 69. Concentration profiles of oxide components in wt% (left panel) and eigen-components (right panel) of Yu2016_Exp#207, which is a plagioclase dissolution experiment in basalt (Yu et al., 2016).

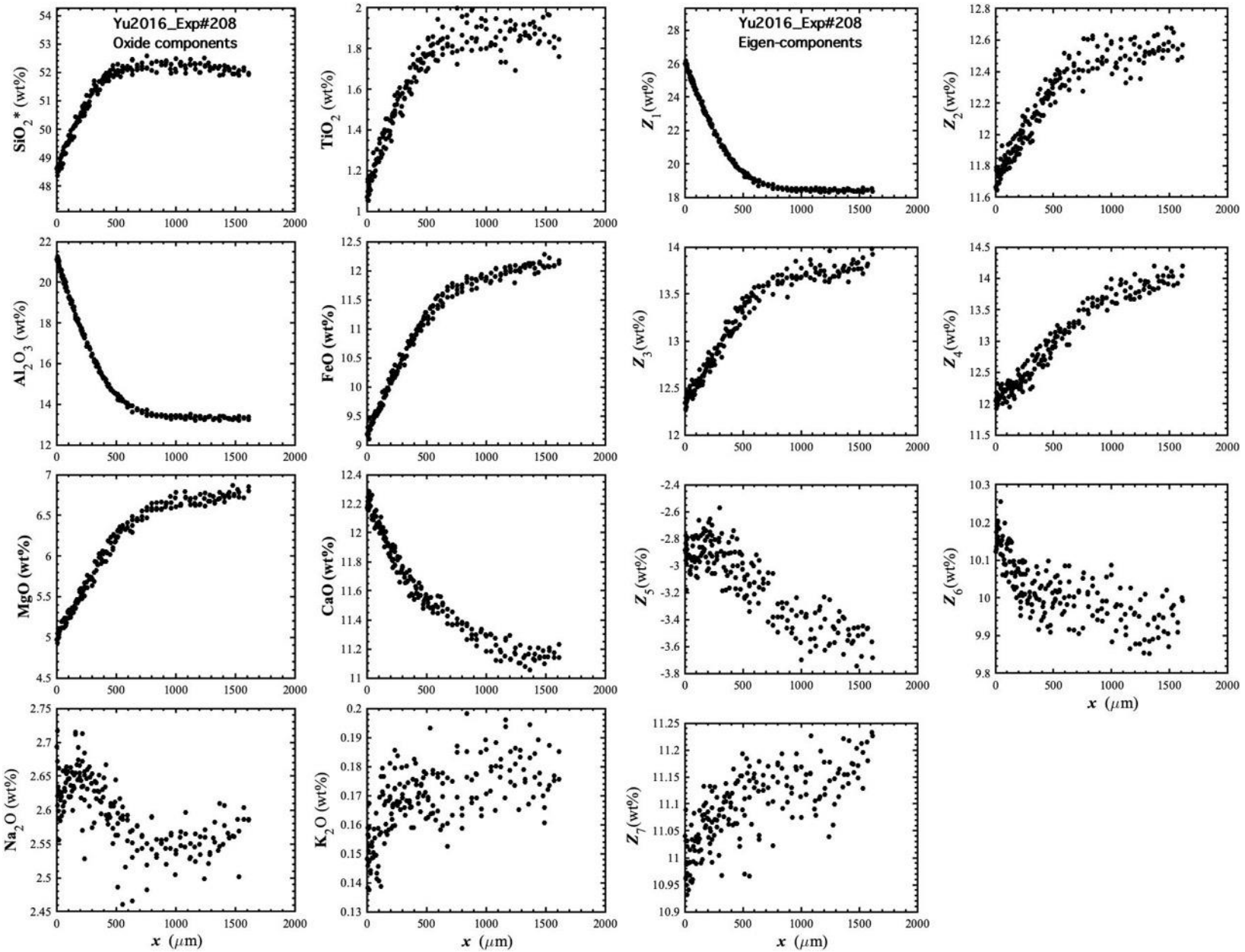

Figure 70. Concentration profiles of oxide components in wt% (left panel) and eigen-components (right panel) of Yu2016_Exp#208, which is a plagioclase dissolution experiment in basalt (Yu et al., 2016).

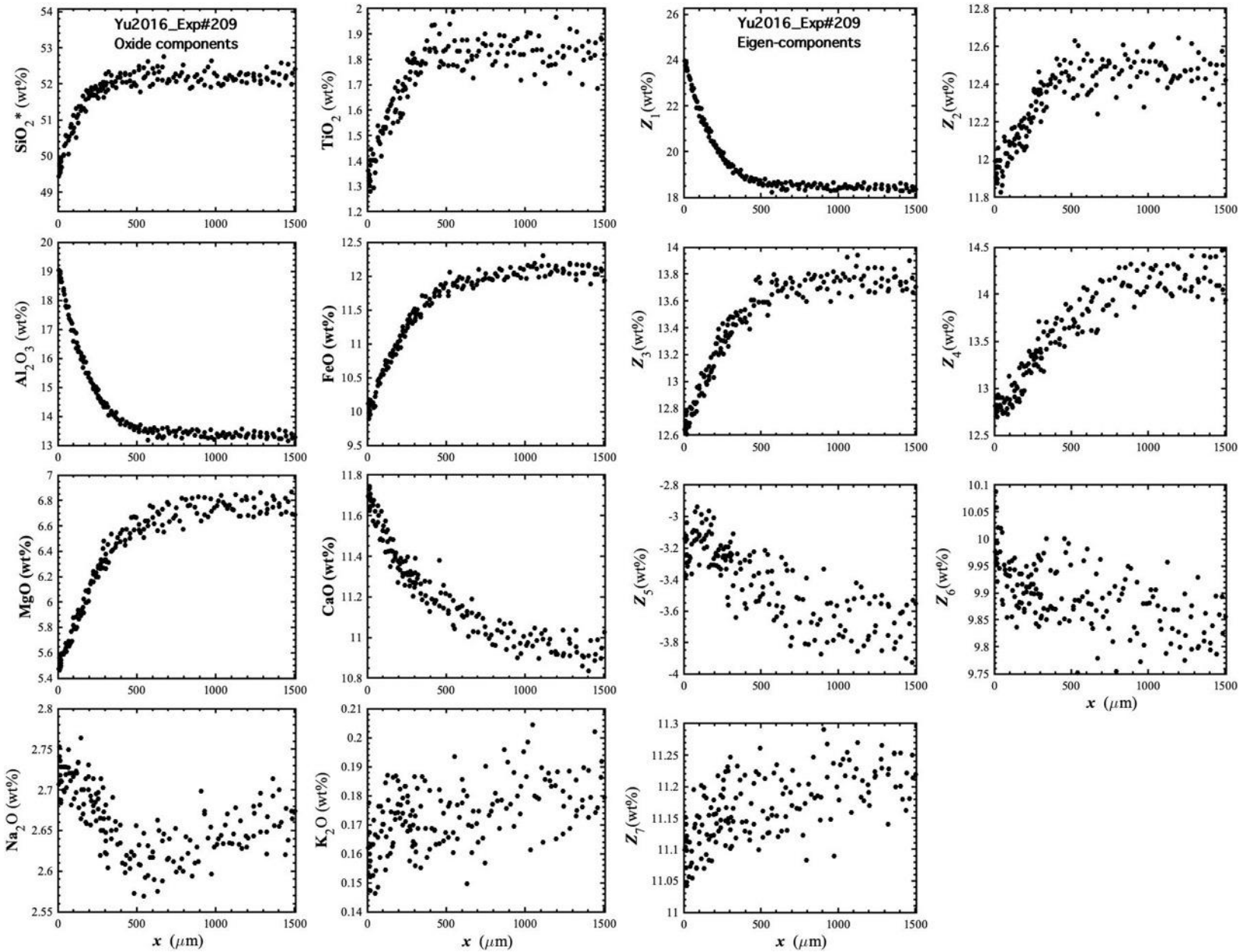

Figure 71. Concentration profiles of oxide components in wt% (left panel) and eigen-components (right panel) of Yu2016_Exp#209, which is a plagioclase dissolution experiment in basalt (Yu et al., 2016).

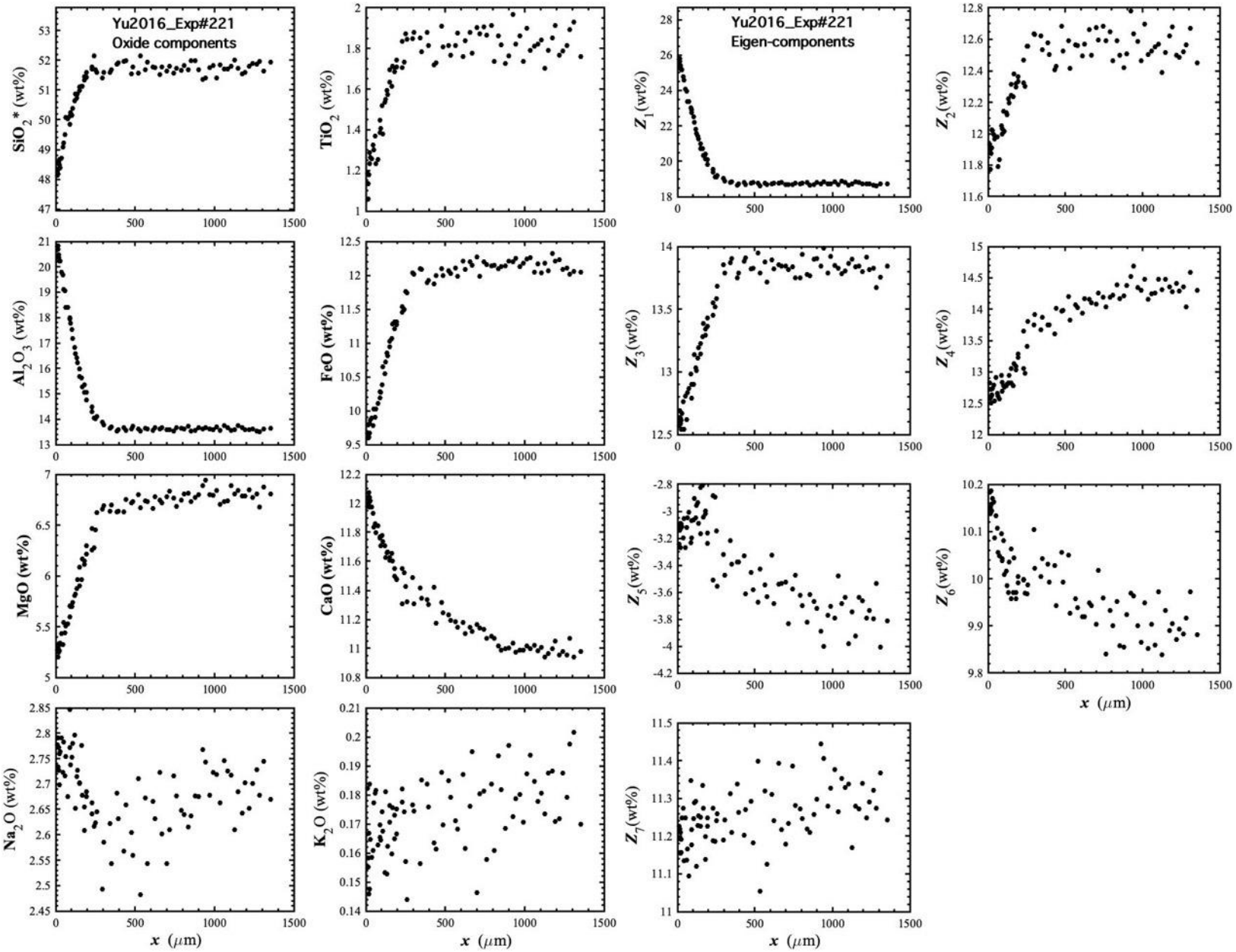

Figure 72. Concentration profiles of oxide components in wt% (left panel) and eigen-components (right panel) of Yu2016_Exp#221, which is a plagioclase dissolution experiment in basalt (Yu et al., 2016).

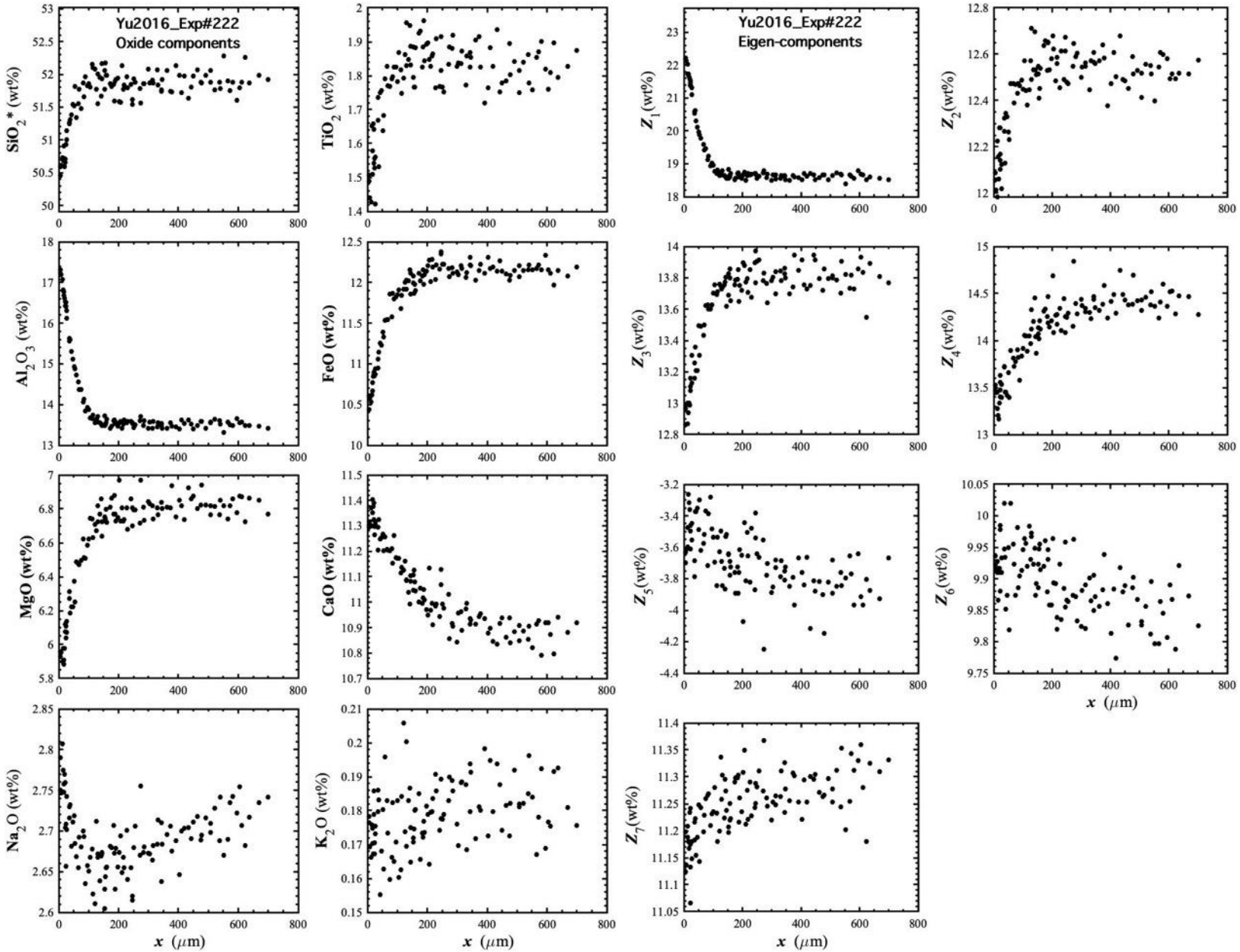

Figure 73. Concentration profiles of oxide components in wt% (left panel) and eigen-components (right panel) of Yu2016_Exp#222, which is a plagioclase dissolution experiment in basalt (Yu et al., 2016).

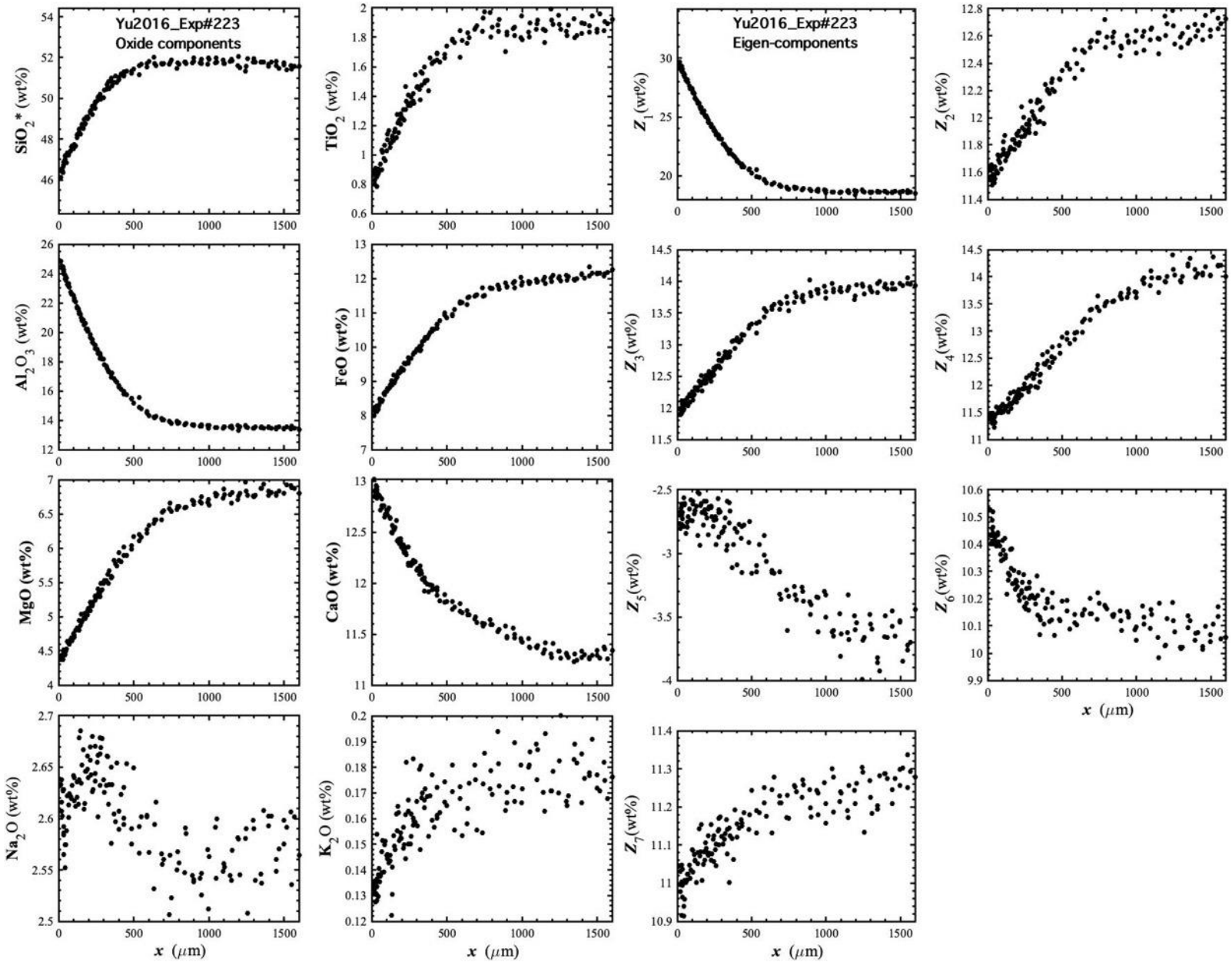

Figure 74. Concentration profiles of oxide components in wt% (left panel) and eigen-components (right panel) of Yu2016_Exp#223, which is a plagioclase dissolution experiment in basalt (Yu et al., 2016).

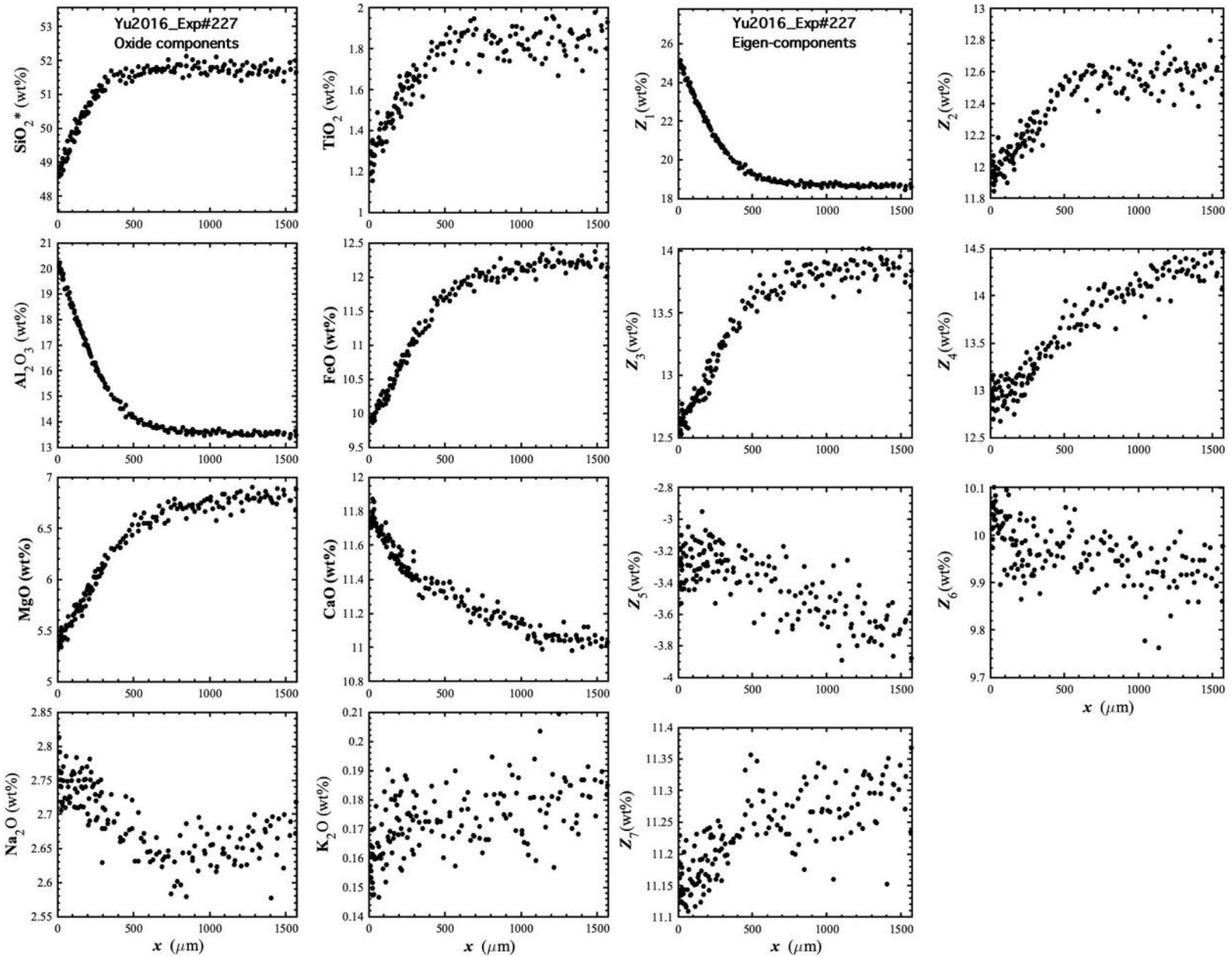

Figure 75. Concentration profiles of oxide components in wt% (left panel) and eigen-components (right panel) of Yu2016_Exp#227, which is a plagioclase dissolution experiment in basalt (Yu et al., 2016).

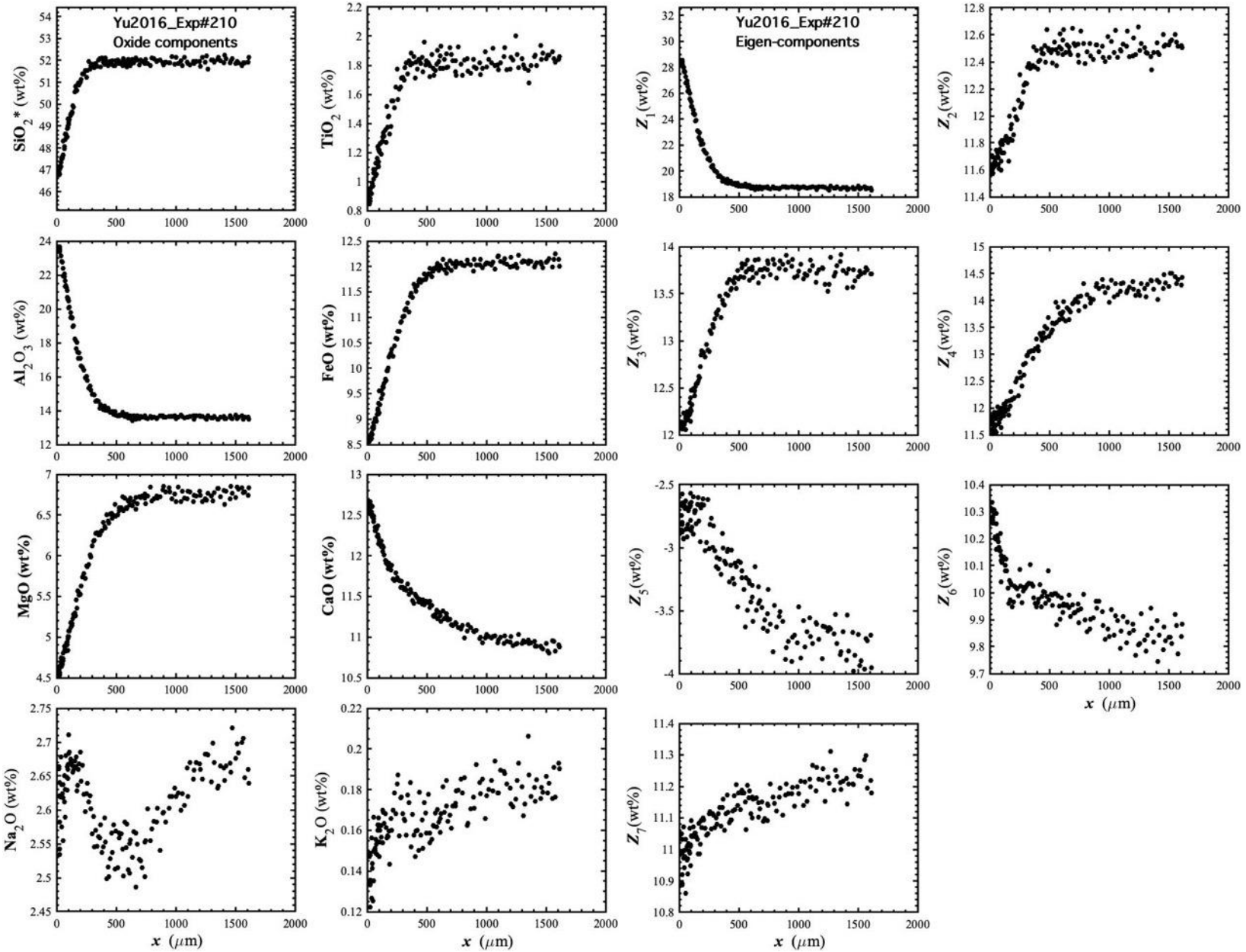

Figure 76. Concentration profiles of oxide components in wt% (left panel) and eigen-components (right panel) of Yu2016_Exp#210, which is a plagioclase dissolution experiment in basalt (Yu et al., 2016).

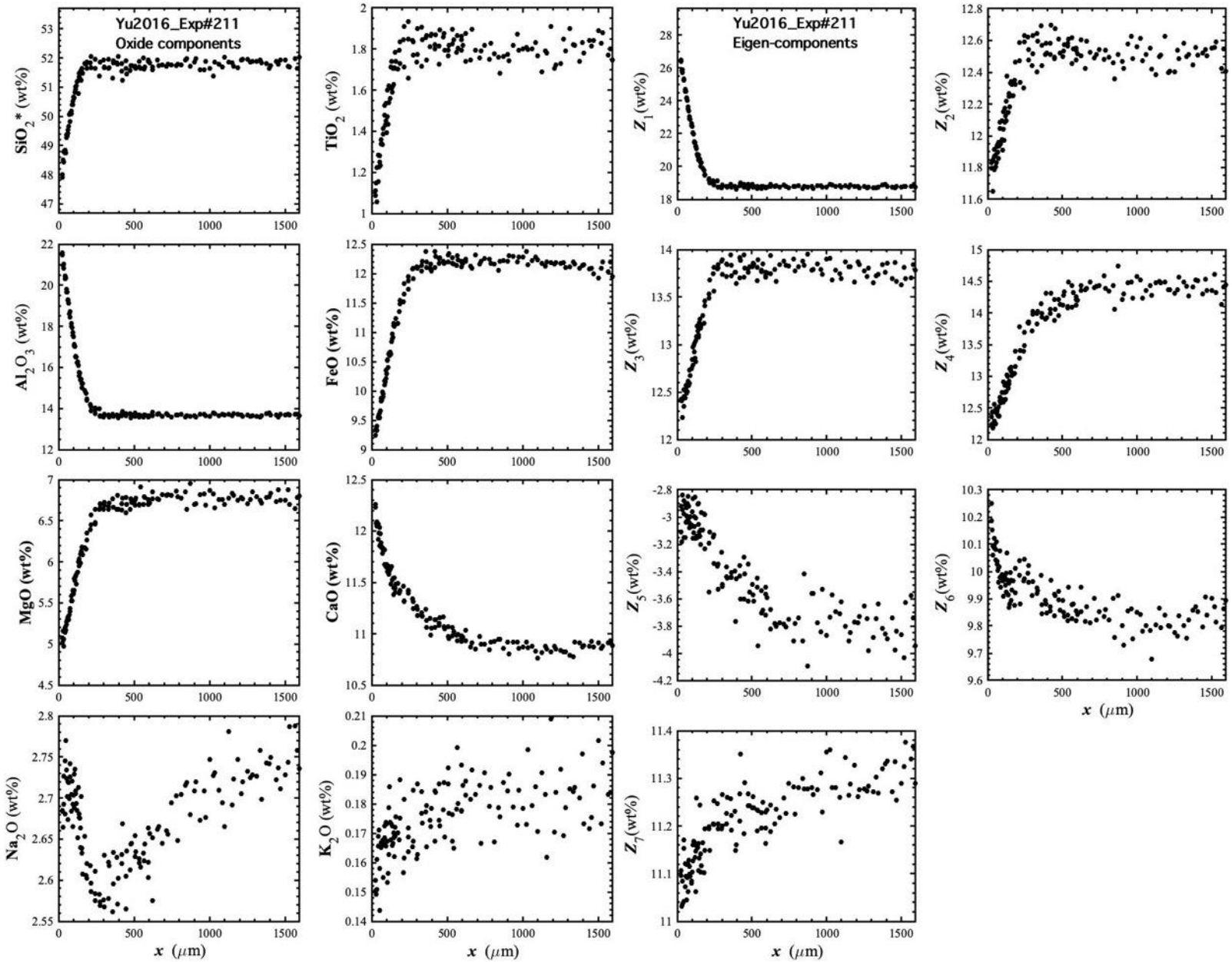

Figure 77. Concentration profiles of oxide components in wt% (left panel) and eigen-components (right panel) of Yu2016_Exp#211, which is a plagioclase dissolution experiment in basalt (Yu et al., 2016).

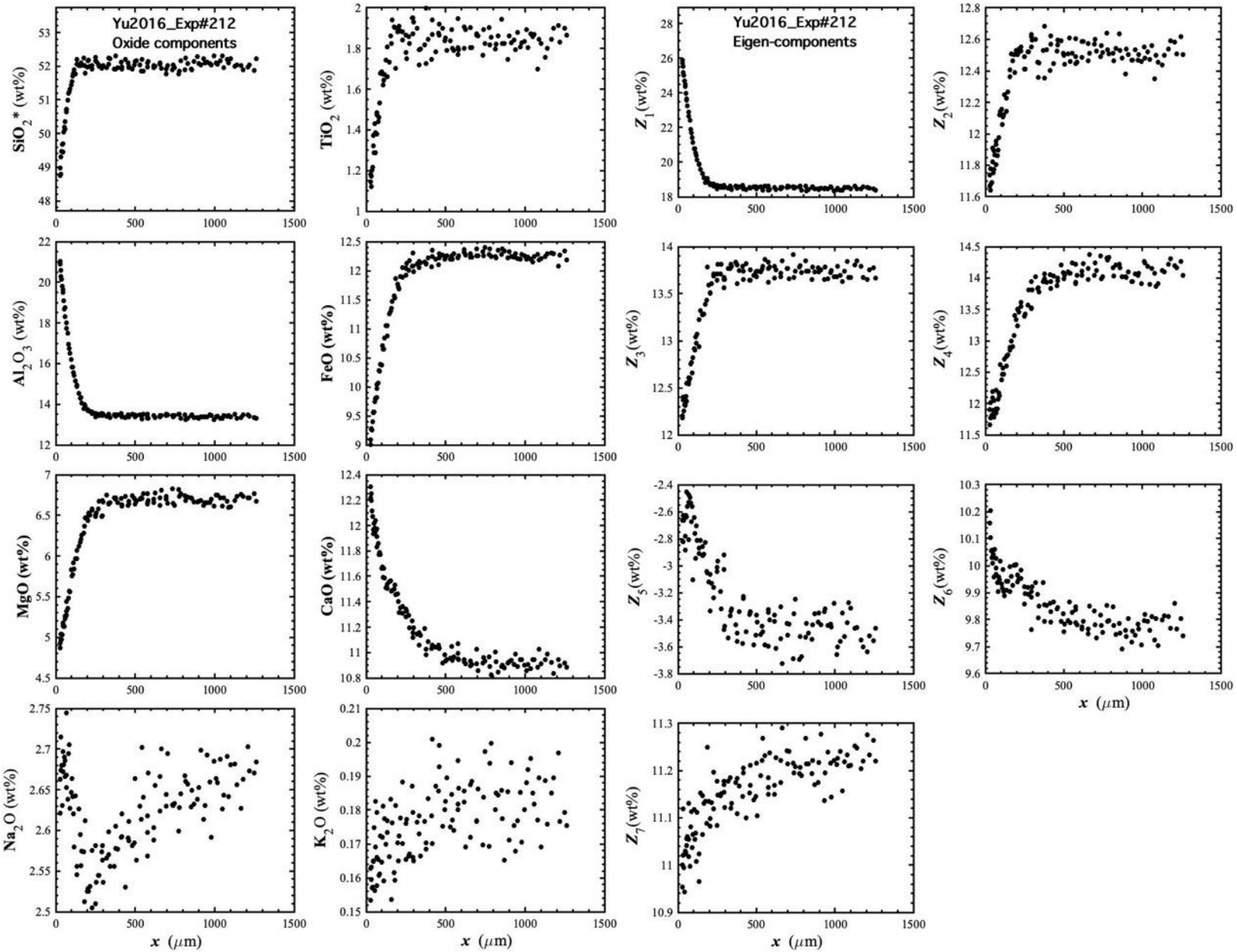

Figure 78. Concentration profiles of oxide components in wt% (left panel) and eigen-components (right panel) of Yu2016_Exp#212, which is a plagioclase dissolution experiment in basalt (Yu et al., 2016).

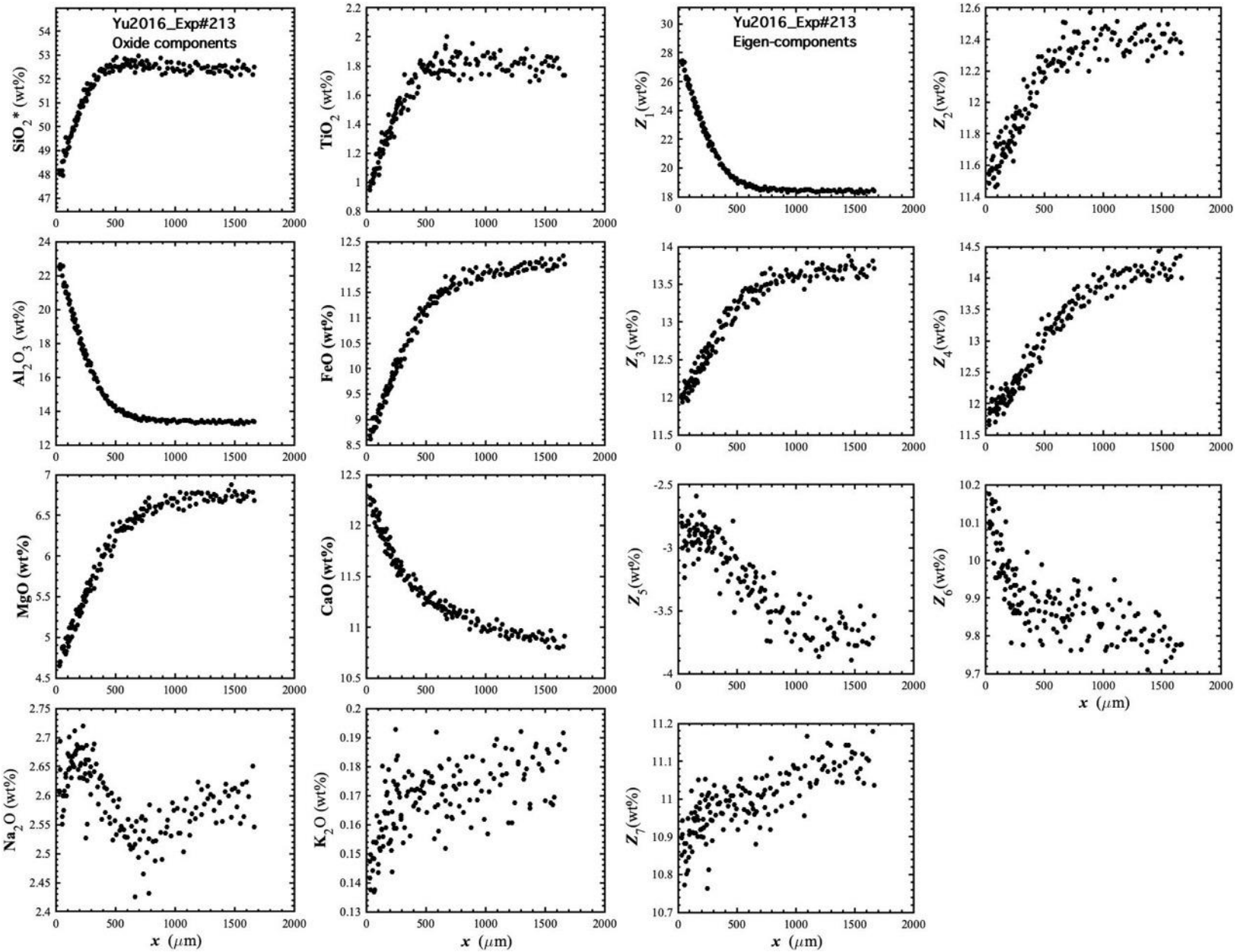

Figure 79. Concentration profiles of oxide components in wt% (left panel) and eigen-components (right panel) of Yu2016_Exp#213, which is a plagioclase dissolution experiment in basalt (Yu et al., 2016).

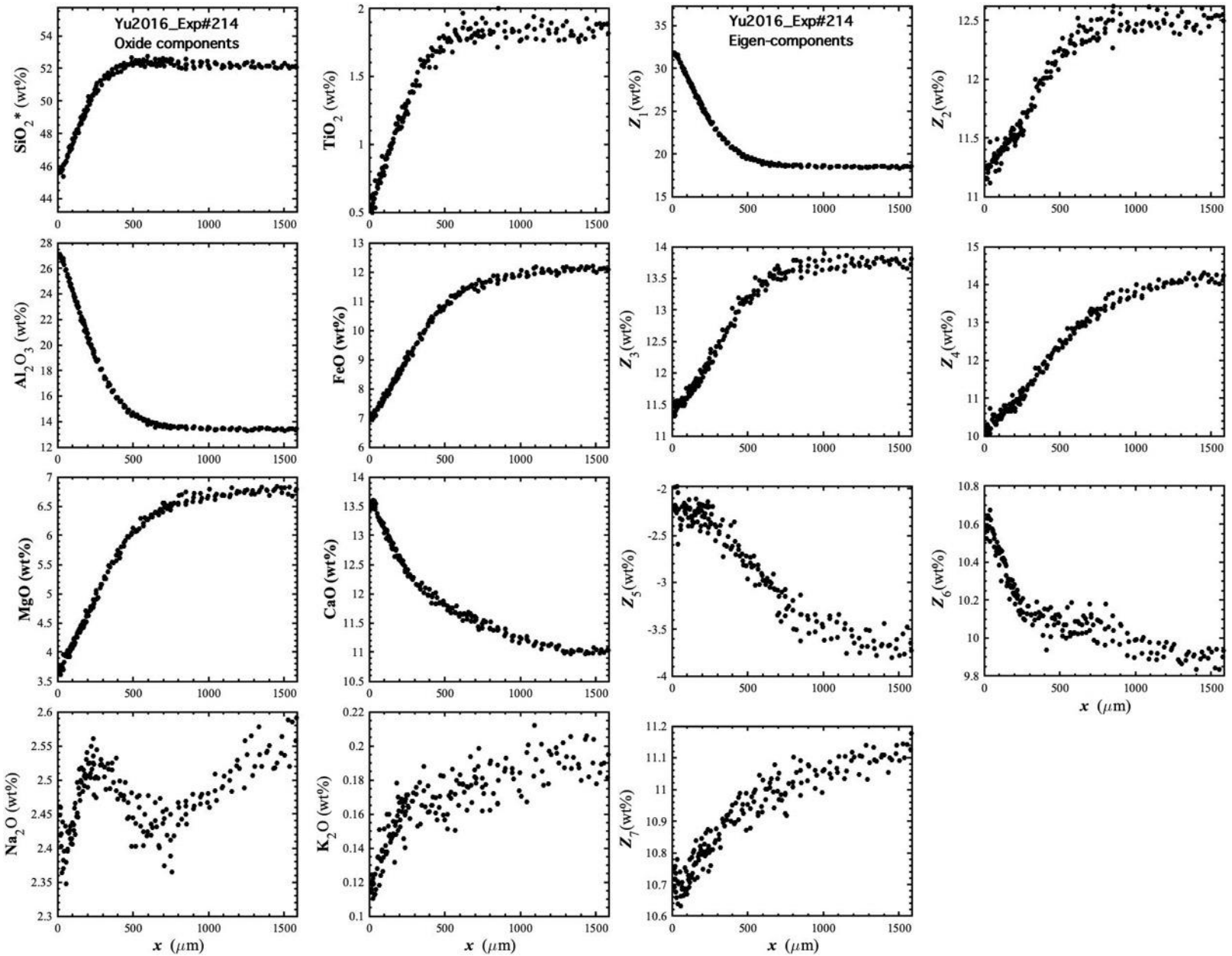

Figure 80. Concentration profiles of oxide components in wt% (left panel) and eigen-components (right panel) of Yu2016_Exp#214, which is a plagioclase dissolution experiment in basalt (Yu et al., 2016).

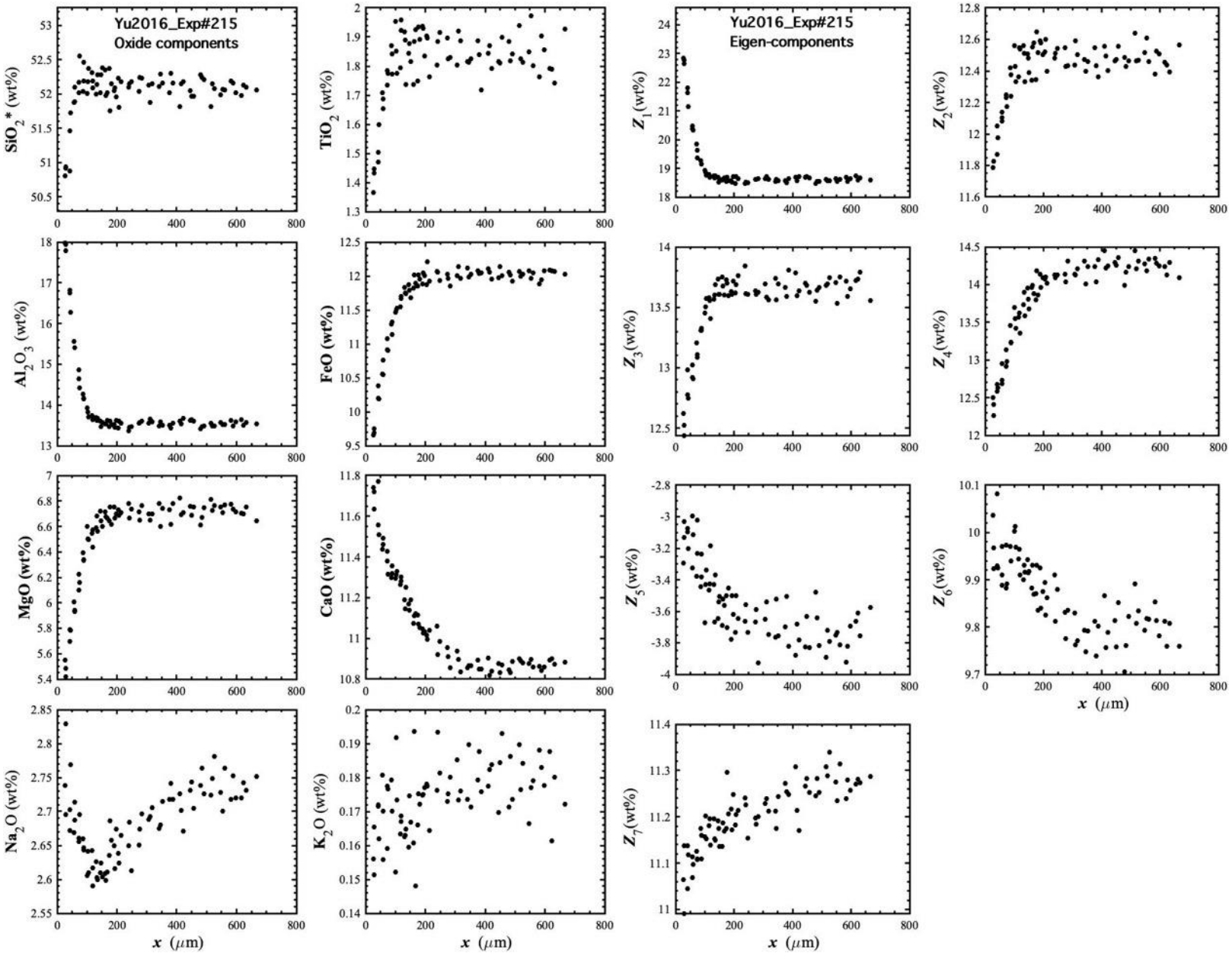

Figure 81. Concentration profiles of oxide components in wt% (left panel) and eigen-components (right panel) of Yu2016_Exp#215, which is a plagioclase dissolution experiment in basalt (Yu et al., 2016).

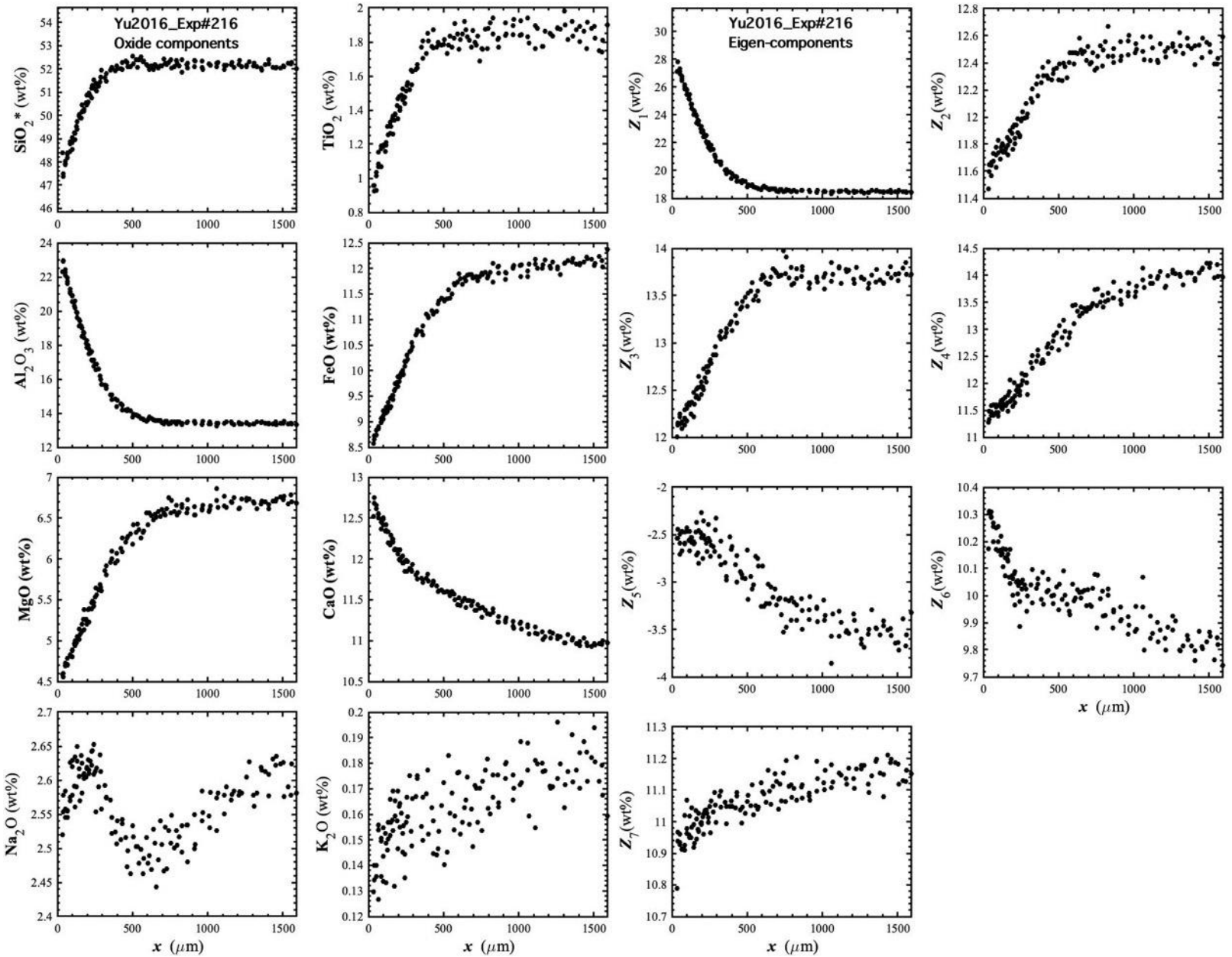

Figure 82. Concentration profiles of oxide components in wt% (left panel) and eigen-components (right panel) of Yu2016_Exp#216, which is a plagioclase dissolution experiment in basalt (Yu et al., 2016).

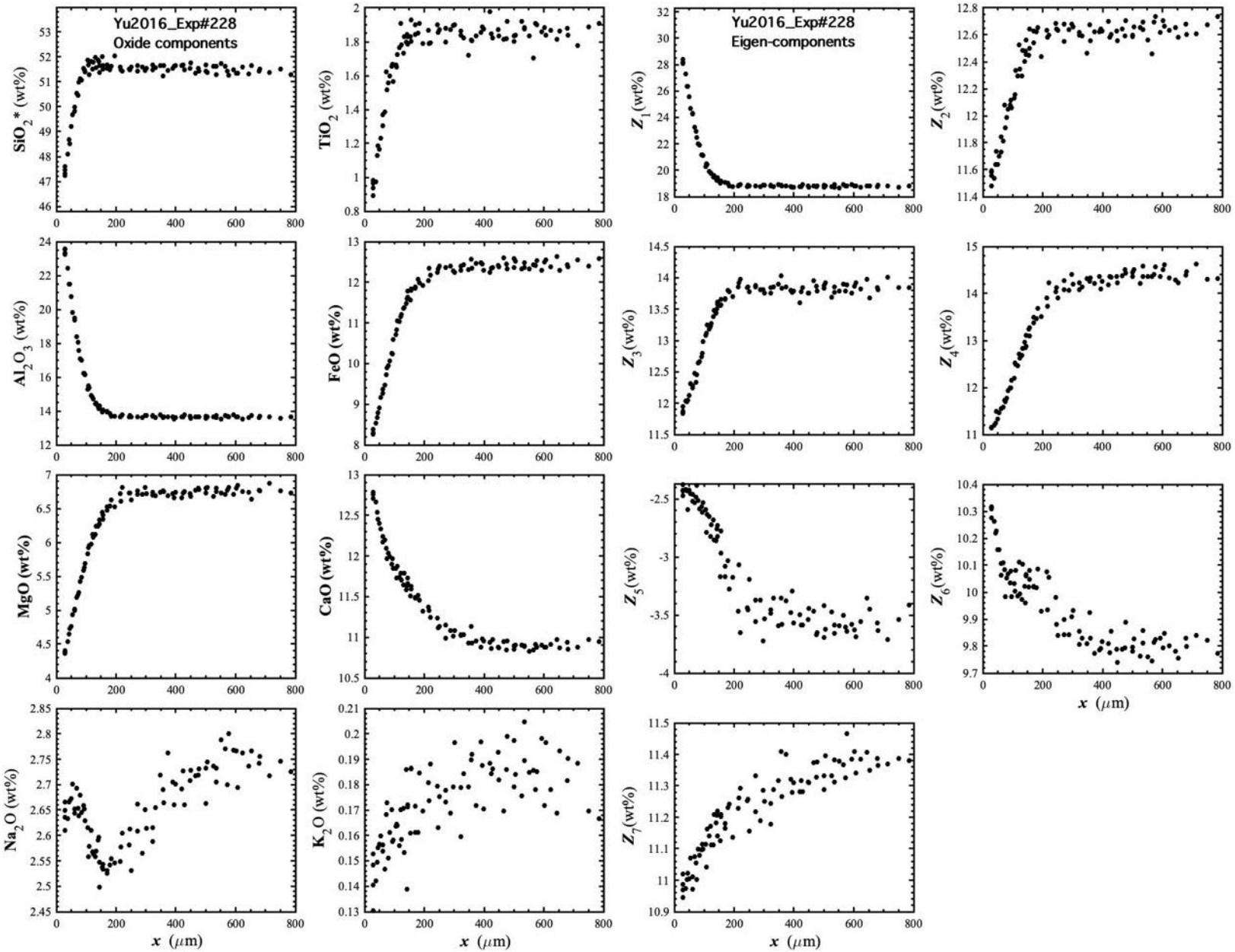

Figure 83. Concentration profiles of oxide components in wt% (left panel) and eigen-components (right panel) of Yu2016_Exp#228, which is a plagioclase dissolution experiment in basalt (Yu et al., 2016).

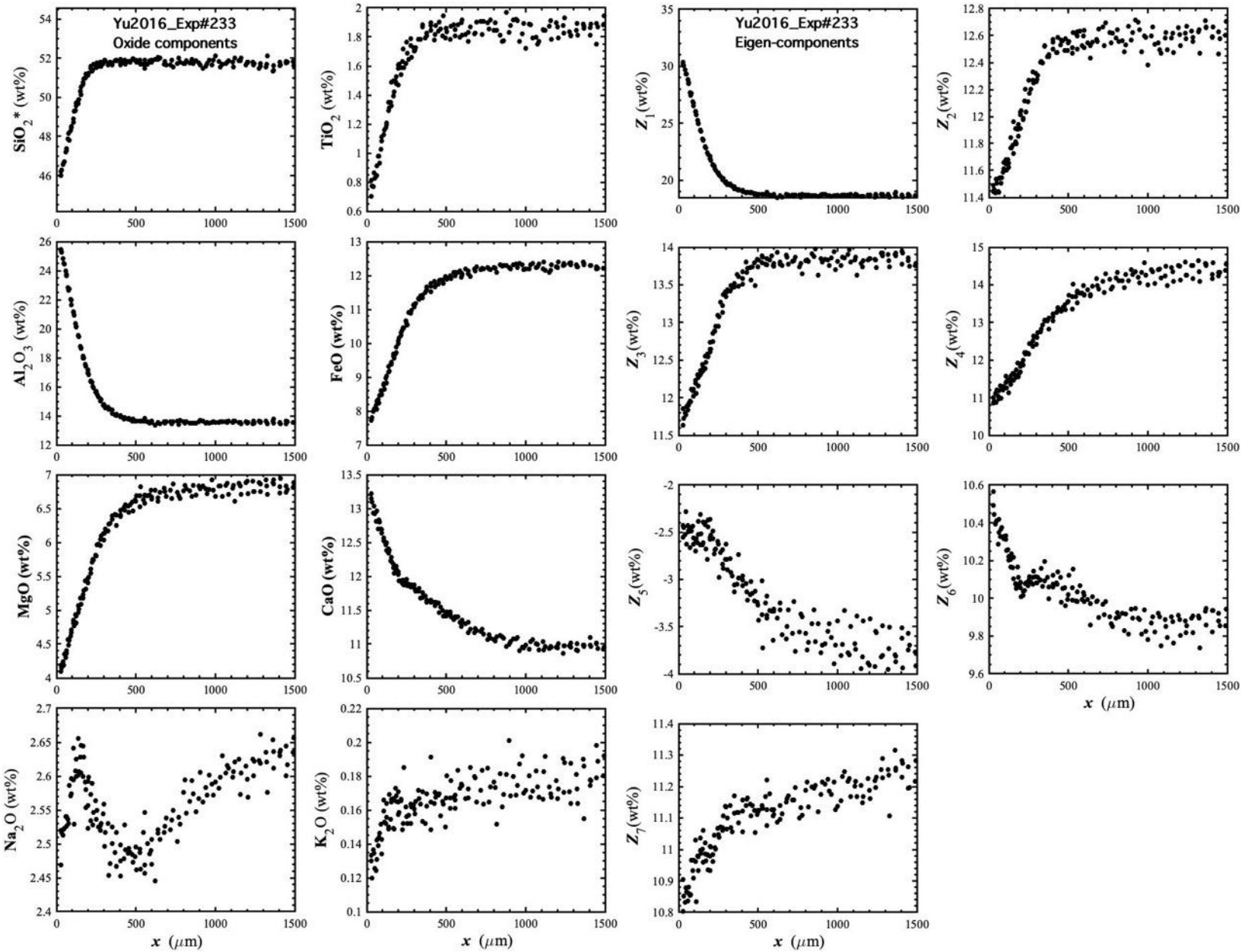

Figure 84. Concentration profiles of oxide components in wt% (left panel) and eigen-components (right panel) of Yu2016_Exp#233, which is a plagioclase dissolution experiment in basalt (Yu et al., 2016).

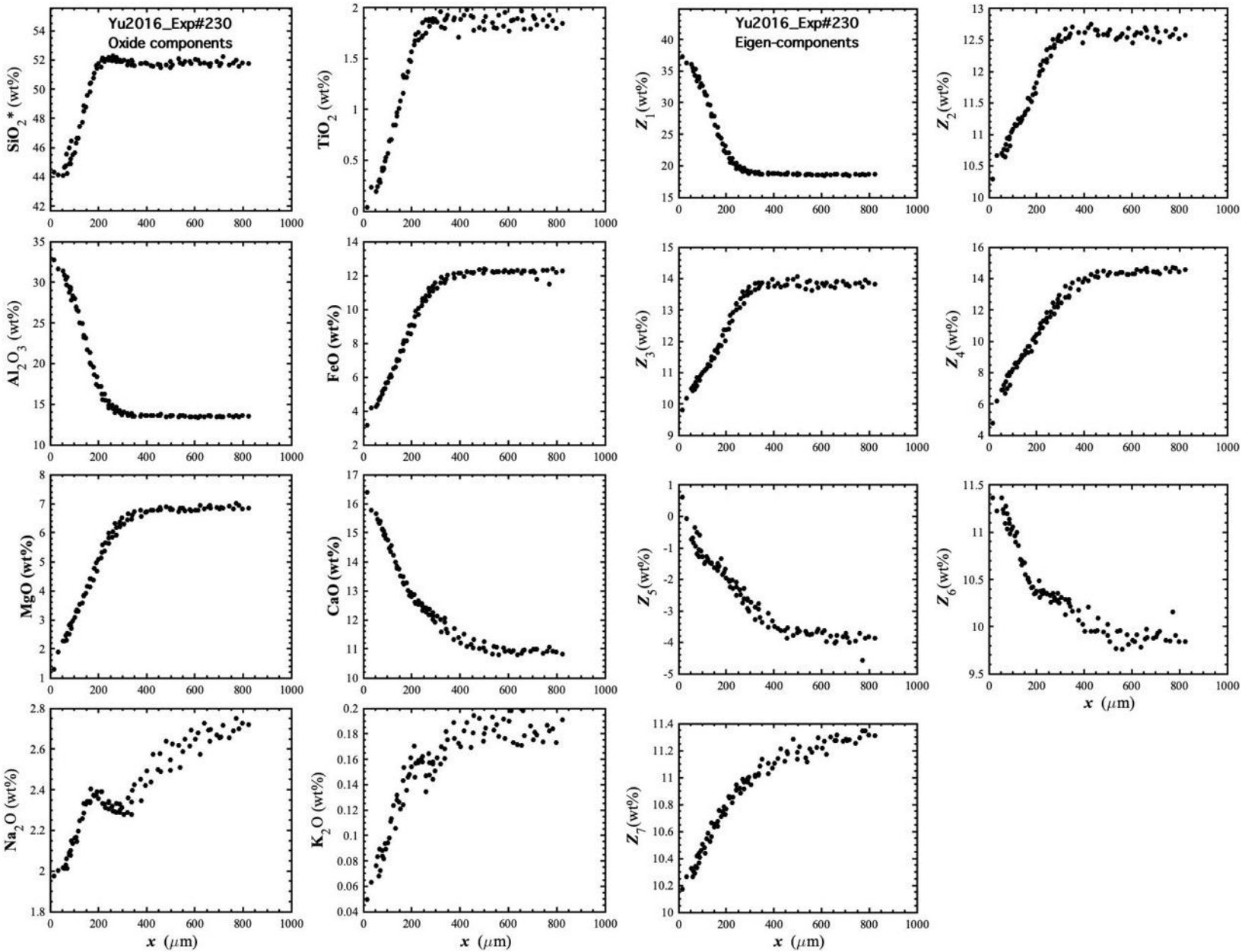

Figure 85. Concentration profiles of oxide components in wt% (left panel) and eigen-components (right panel) of Yu2016_Exp#230, which is a plagioclase dissolution experiment in basalt (Yu et al., 2016).

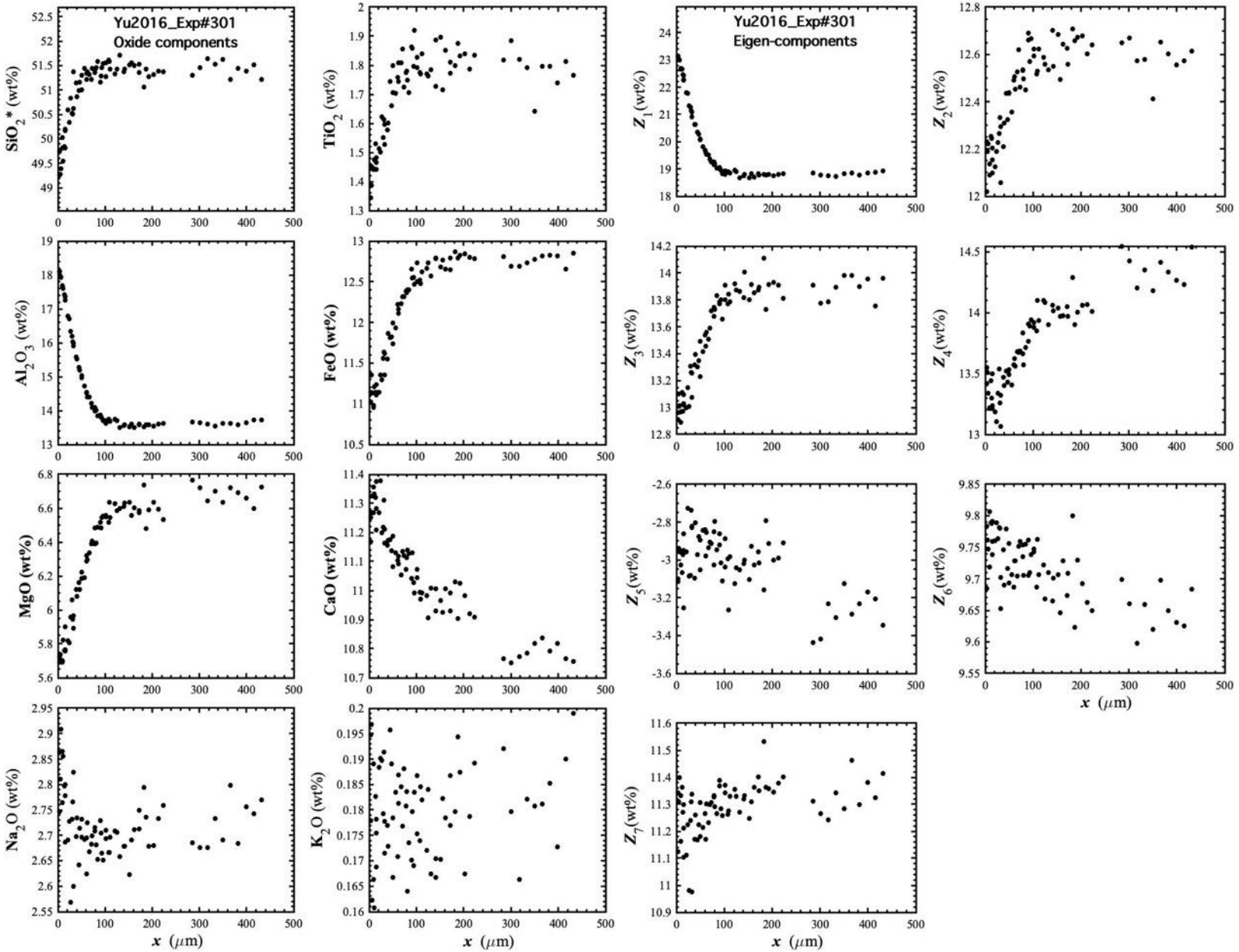

Figure 86. Concentration profiles of oxide components in wt% (left panel) and eigen-components (right panel) of Yu2016_Exp#301, which is a plagioclase dissolution experiment in basalt (Yu et al., 2016).

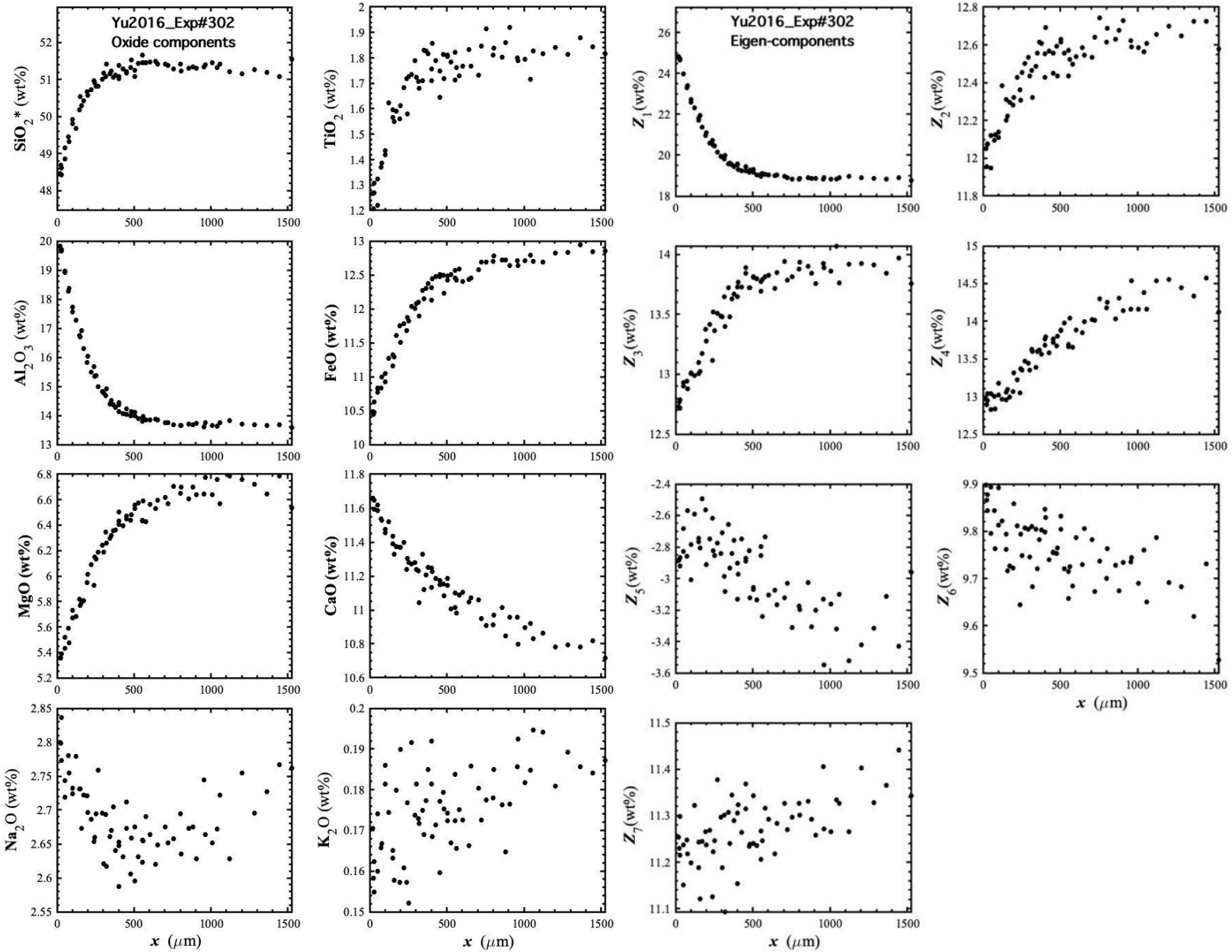

Figure 87. Concentration profiles of oxide components in wt% (left panel) and eigen-components (right panel) of Yu2016_Exp#302, which is a plagioclase dissolution experiment in basalt (Yu et al., 2016).

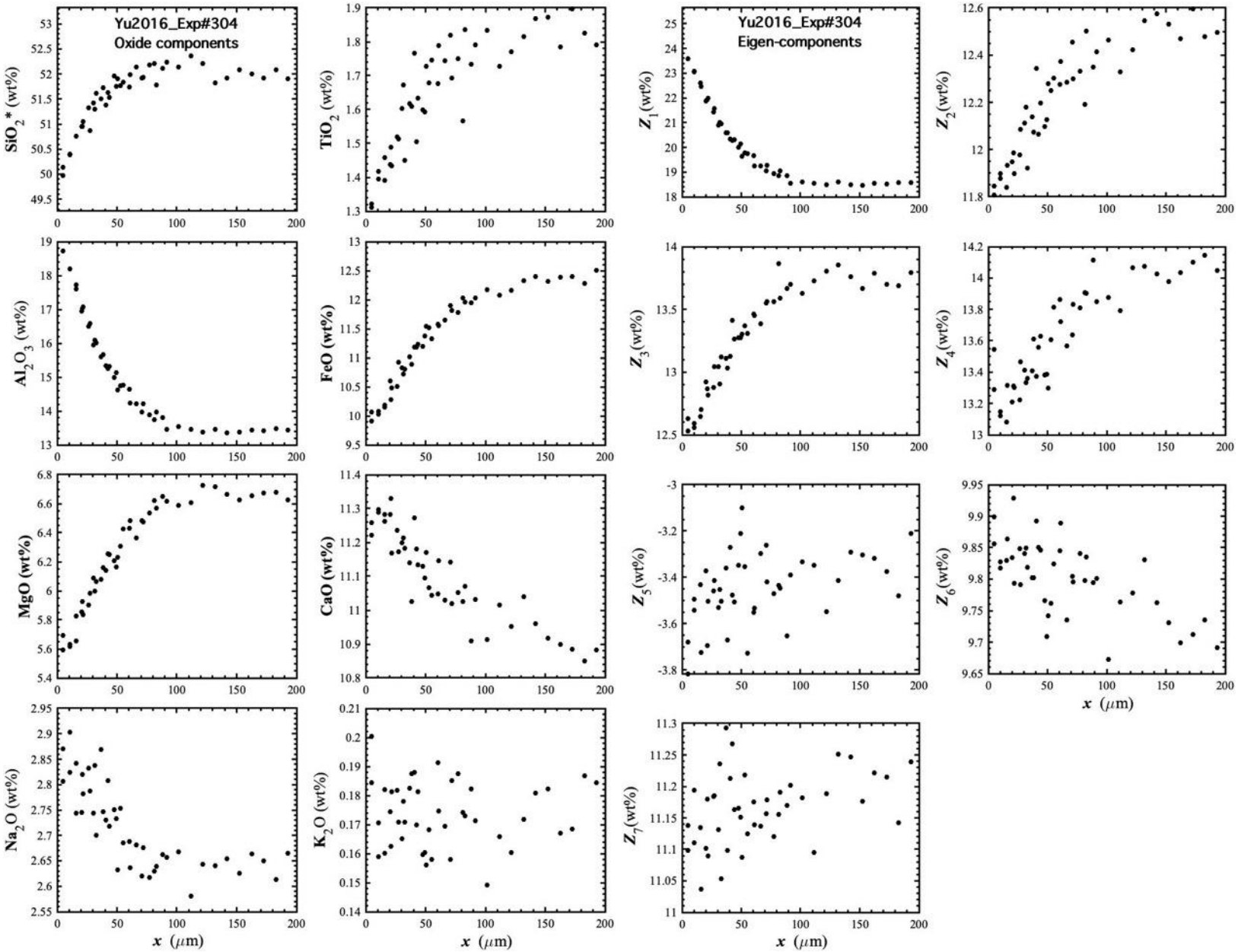

Figure 88. Concentration profiles of oxide components in wt% (left panel) and eigen-components (right panel) of Yu2016_Exp#304, which is a plagioclase dissolution experiment in basalt (Yu et al., 2016).

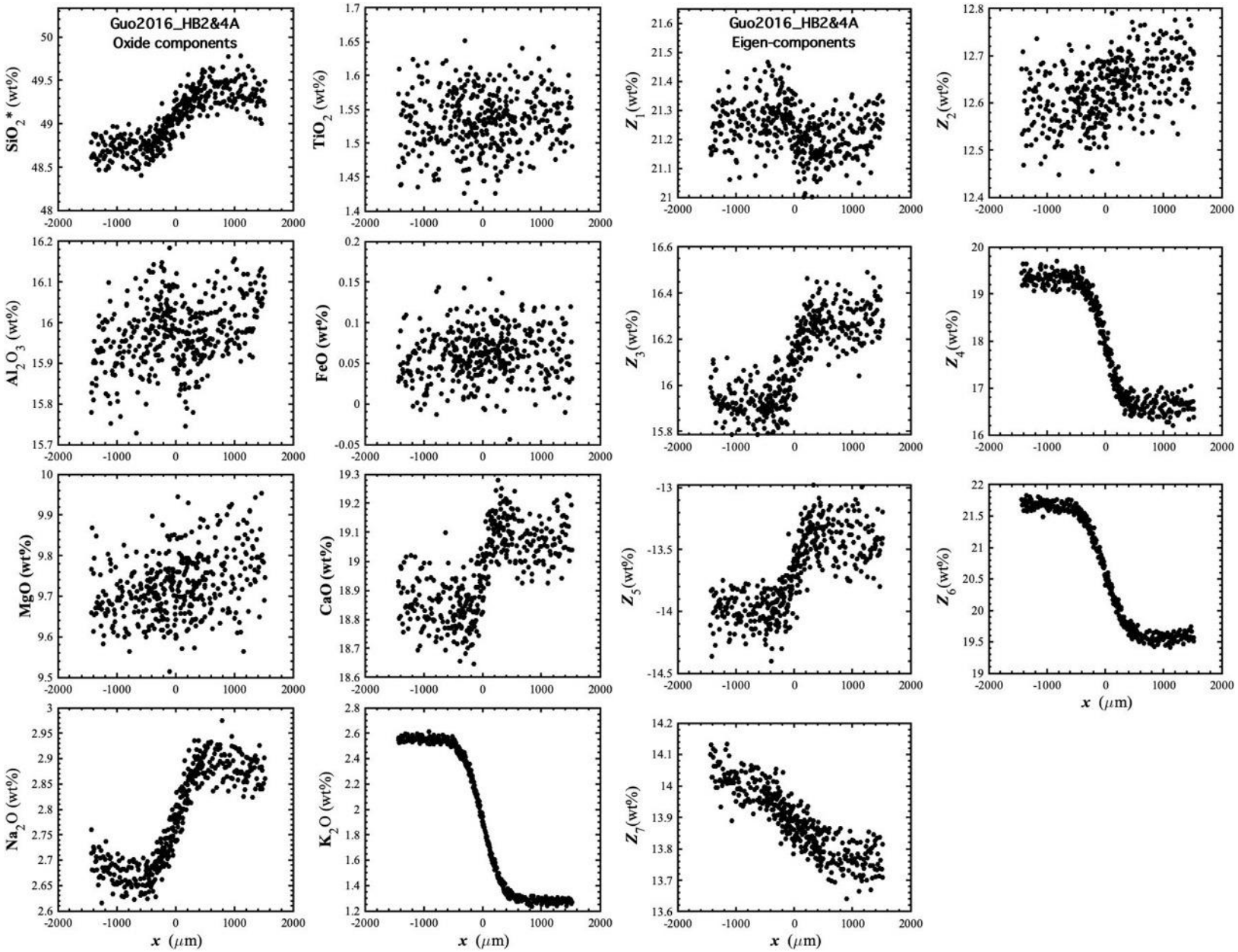

Figure 89. Concentration profiles of oxide components in wt% (left panel) and eigen-components (right panel) of Guo2016_HB2&4A, which is a diffusion couple experiment in haplo-basalt (Guo and Zhang, 2016).

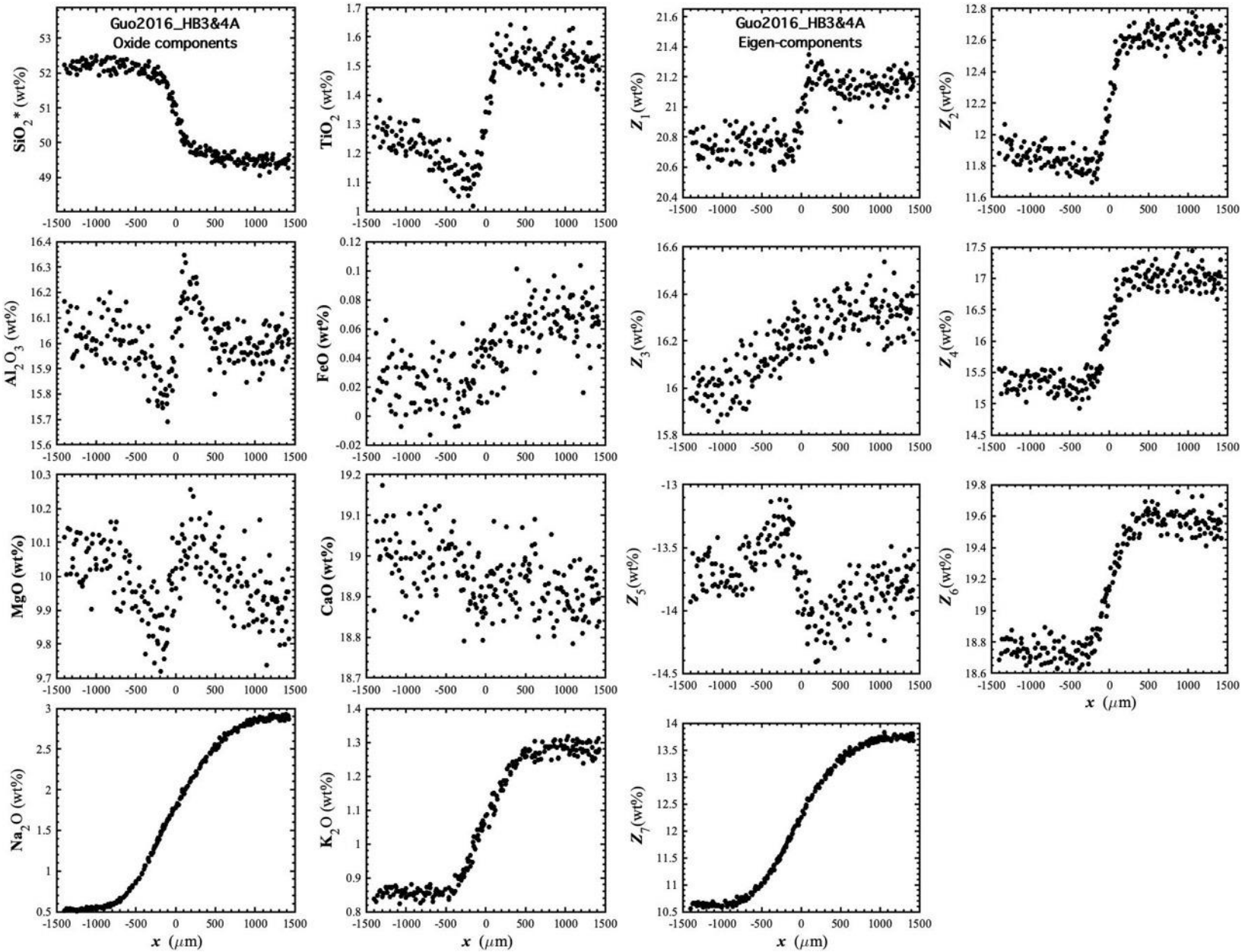

Figure 90. Concentration profiles of oxide components in wt% (left panel) and eigen-components (right panel) of Guo2016_HB3&4A, which is a diffusion couple experiment in haplo-basalt (Guo and Zhang, 2016).

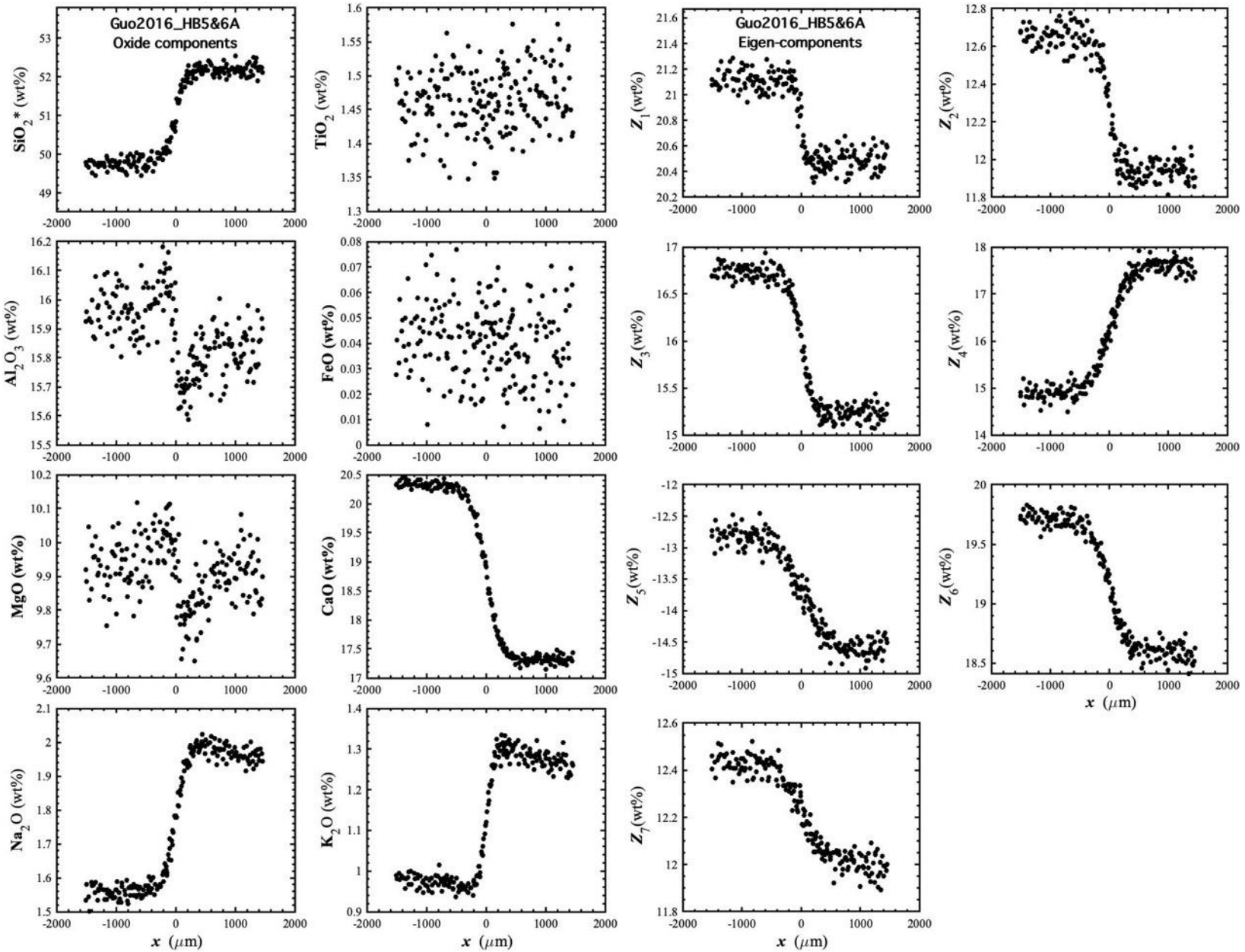

Figure 91. Concentration profiles of oxide components in wt% (left panel) and eigen-components (right panel) of Guo2016_HB5&6A, which is a diffusion couple experiment in haplo-basalt (Guo and Zhang, 2016).

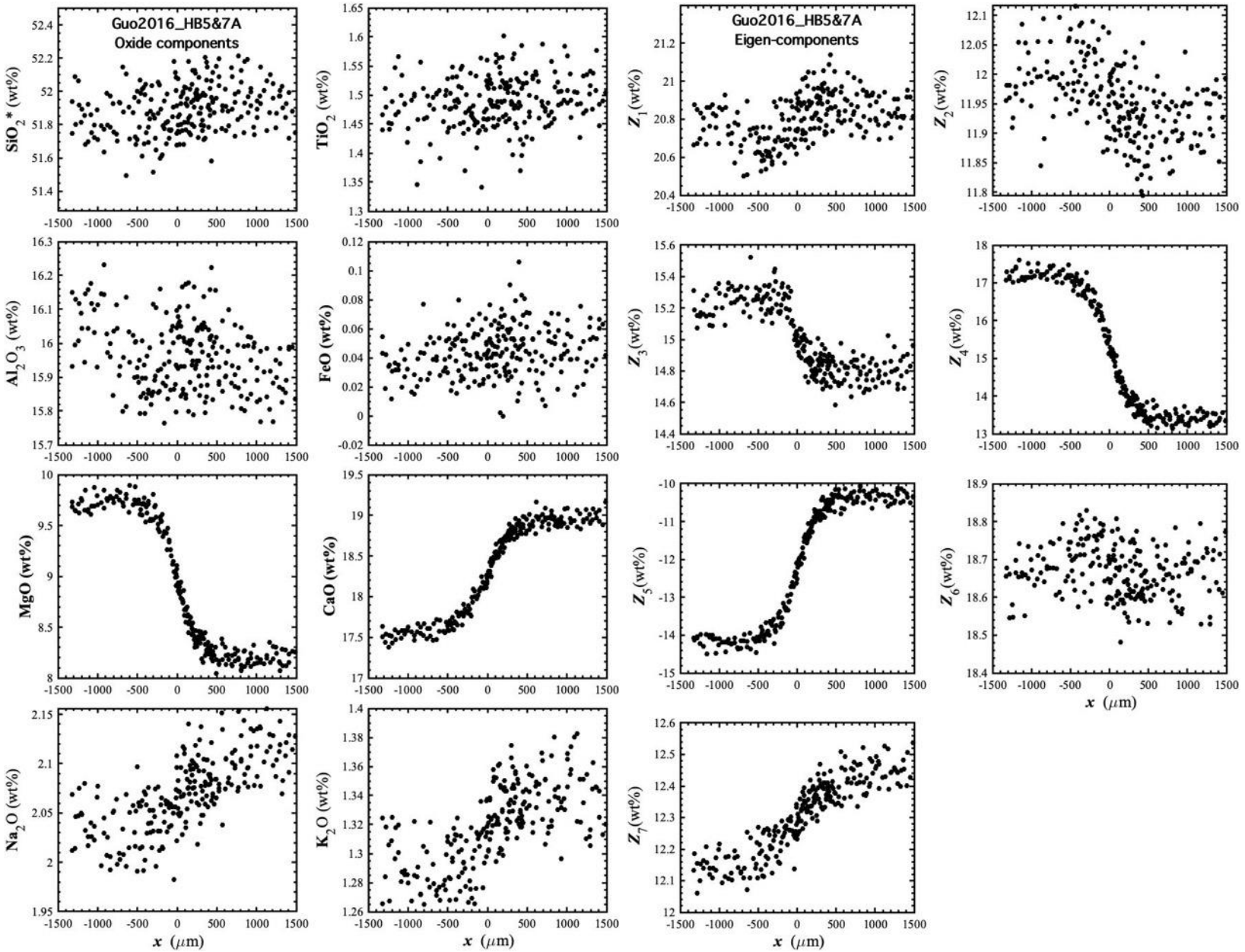

Figure 92. Concentration profiles of oxide components in wt% (left panel) and eigen-components (right panel) of Guo2016_HB5&7A, which is a diffusion couple experiment in haplo-basalt (Guo and Zhang, 2016).

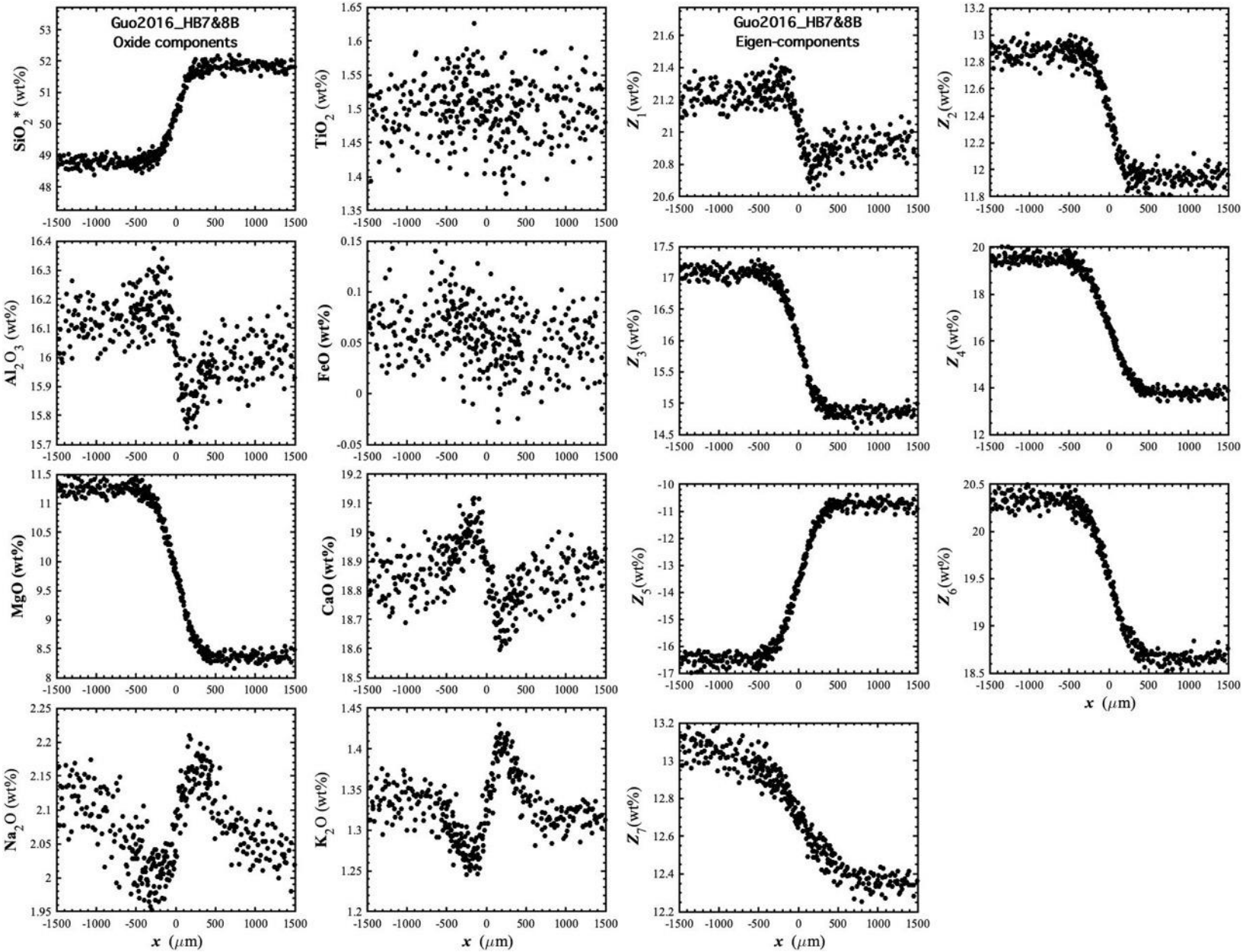

Figure 93. Concentration profiles of oxide components in wt% (left panel) and eigen-components (right panel) of Guo2016_HB7&8B, which is a diffusion couple experiment in haplo-basalt (Guo and Zhang, 2016).

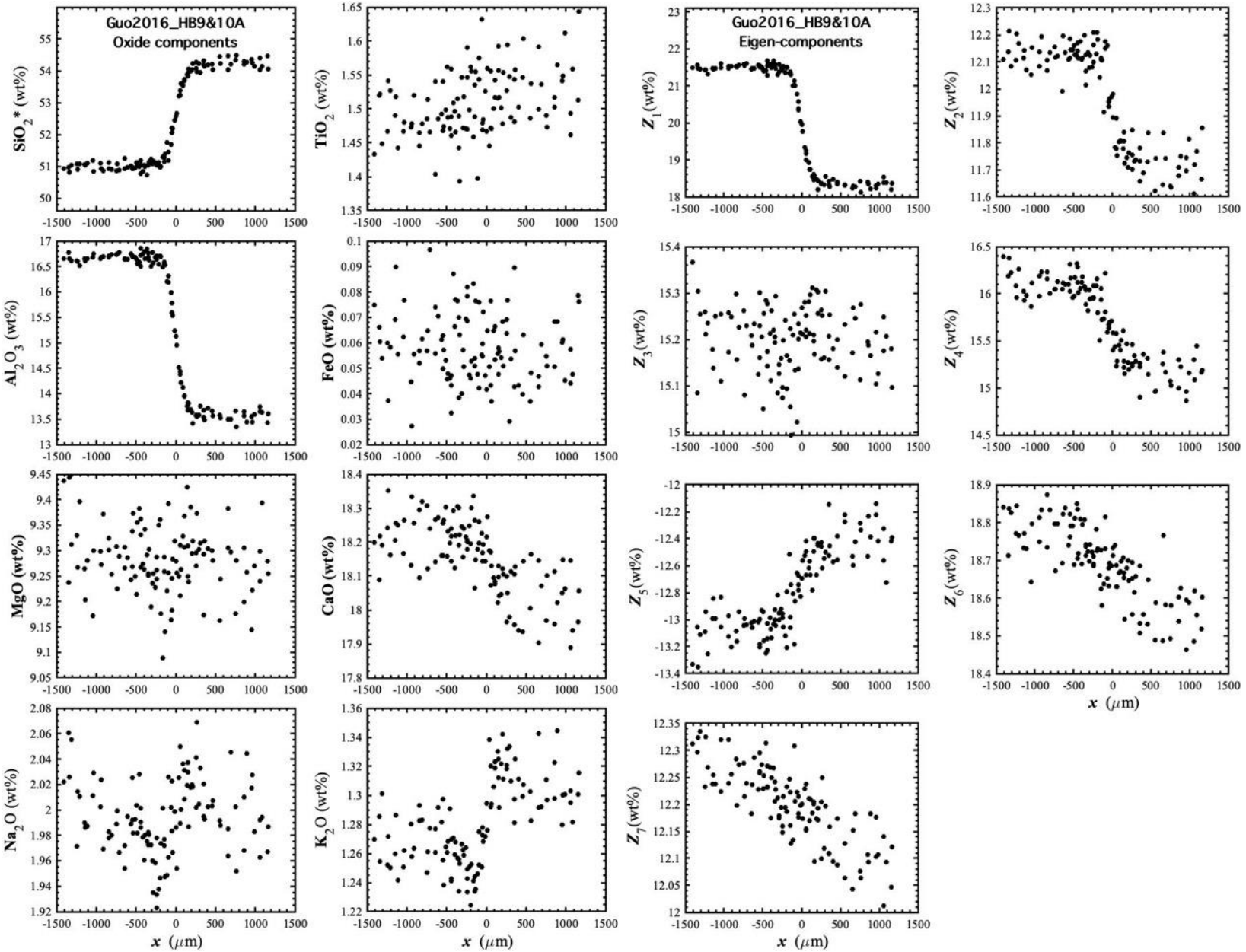

Figure 94. Concentration profiles of oxide components in wt% (left panel) and eigen-components (right panel) of Guo2016_HB9&10A, which is a diffusion couple experiment in haplo-basalt (Guo and Zhang, 2016).

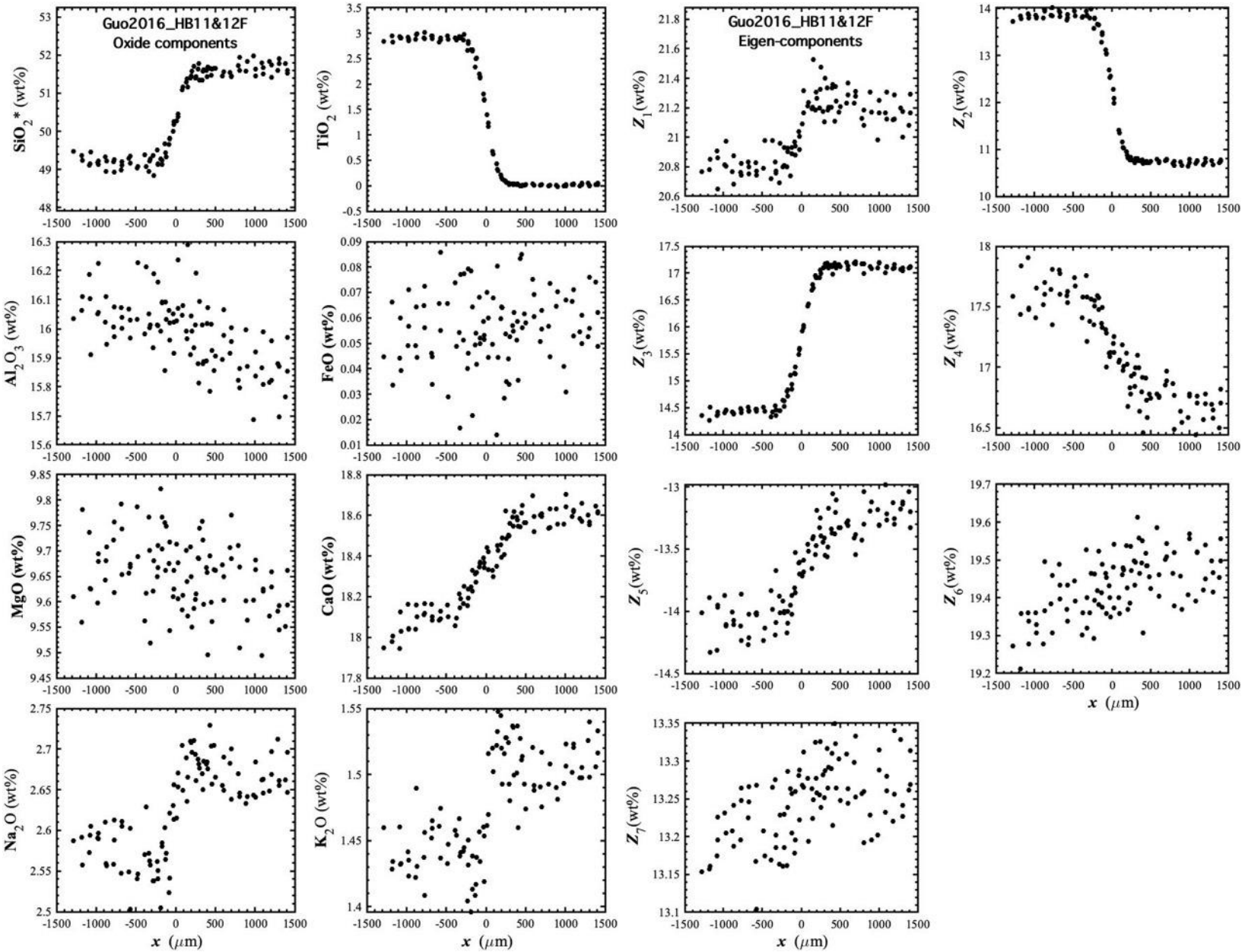

Figure 95. Concentration profiles of oxide components in wt% (left panel) and eigen-components (right panel) of Guo2016_HB11&12F, which is a diffusion couple experiment in haplo-basalt (Guo and Zhang, 2016).

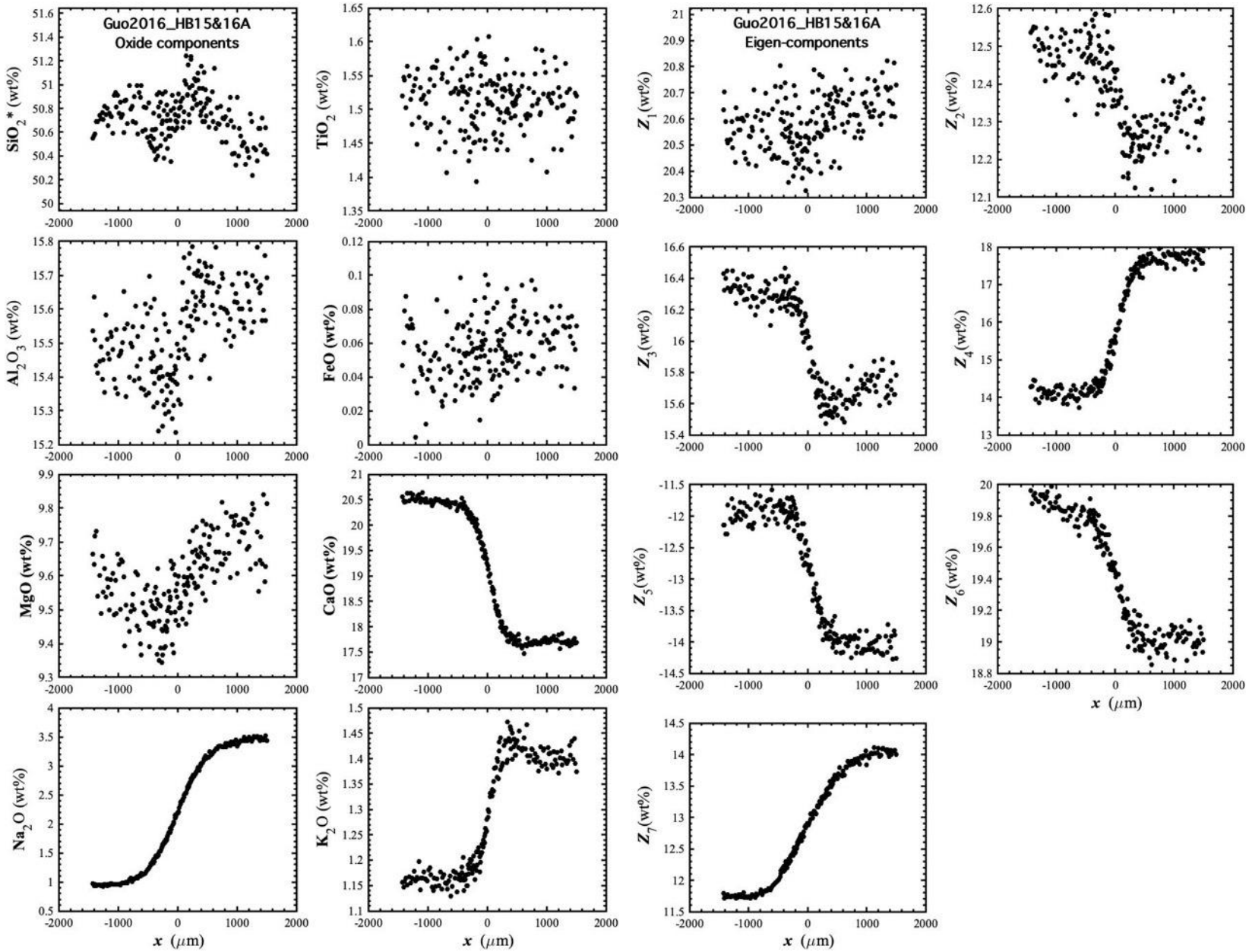

Figure 96. Concentration profiles of oxide components in wt% (left panel) and eigen-components (right panel) of Guo2016_HB15&16A, which is a diffusion couple experiment in haplo-basalt (Guo and Zhang, 2016).

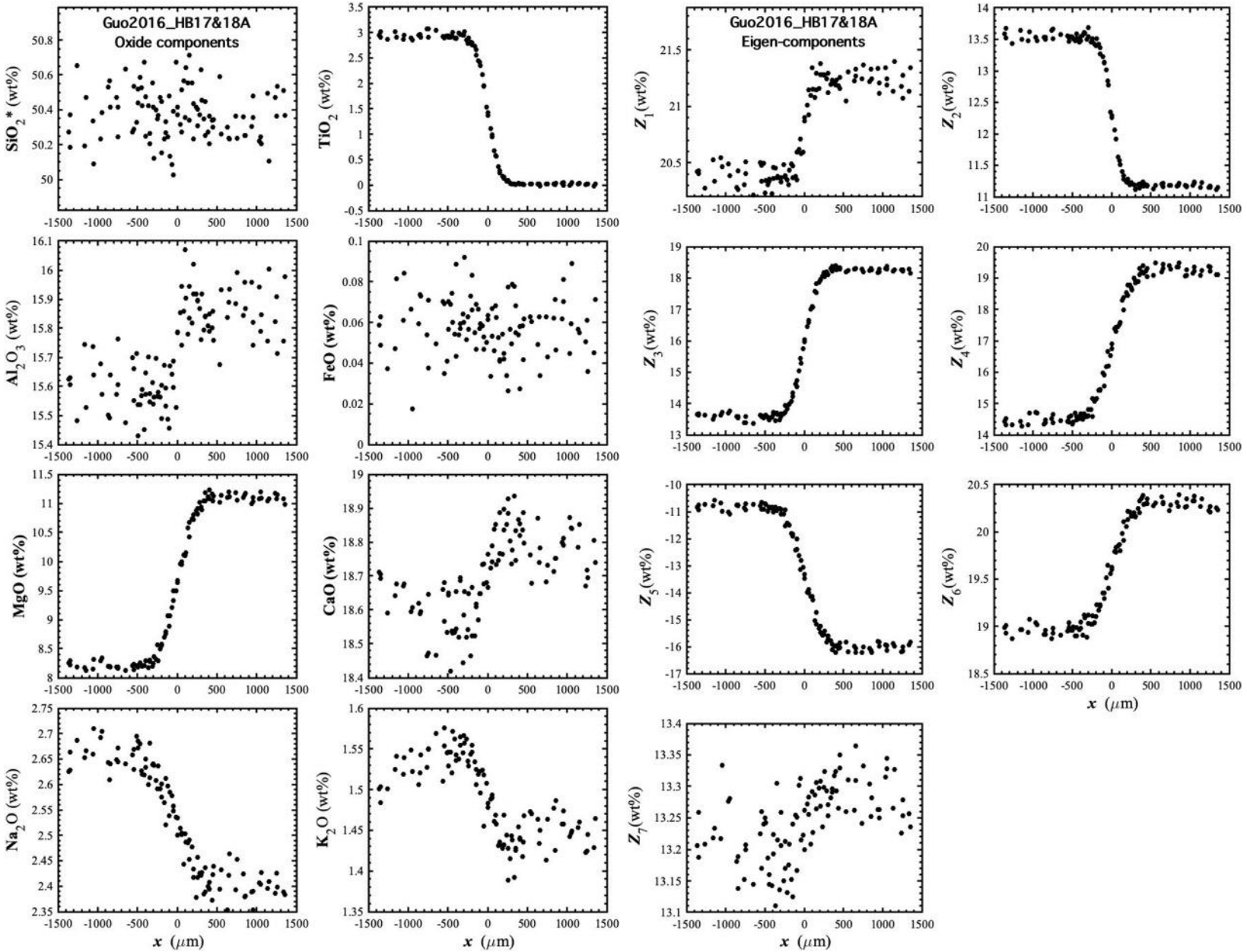

Figure 97. Concentration profiles of oxide components in wt% (left panel) and eigen-components (right panel) of Guo2016_HB17&18A, which is a diffusion couple experiment in haplo-basalt (Guo and Zhang, 2016).

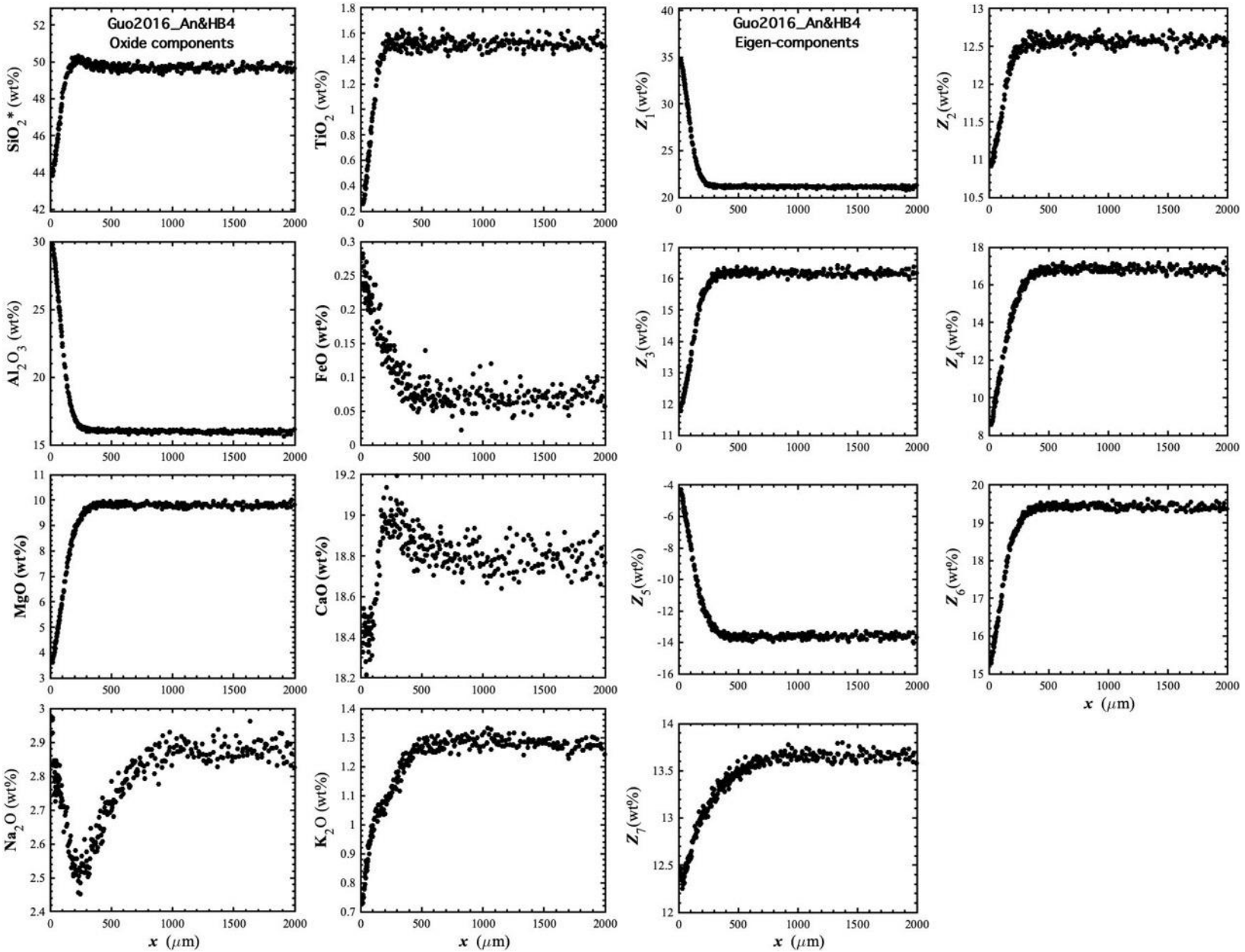

Figure 98. Concentration profiles of oxide components in wt% (left panel) and eigen-components (right panel) of Guo2016_An&HB4, which is an anorthite dissolution experiment in haplo-basalt (Guo and Zhang, 2016).

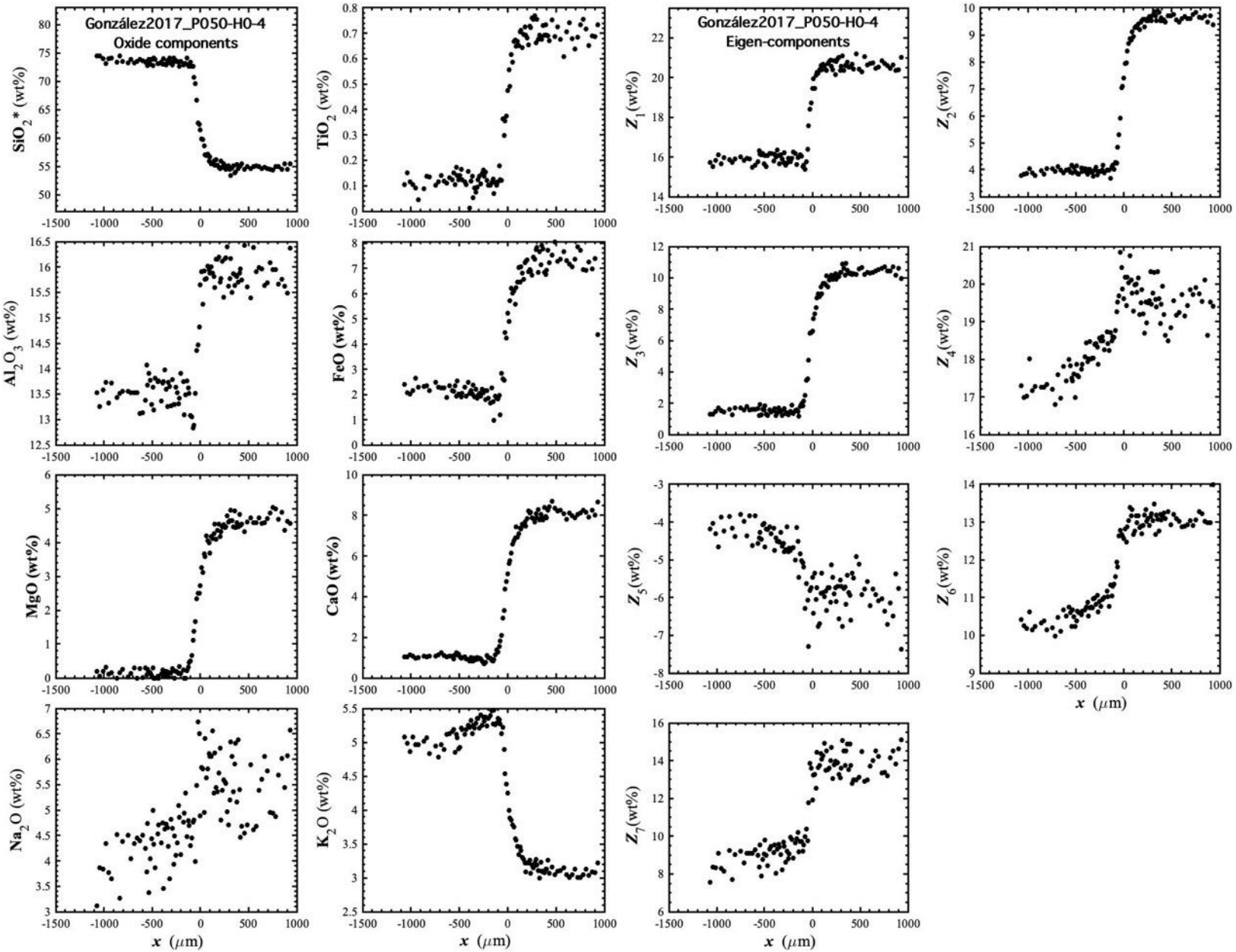

Figure 99. Concentration profiles of oxide components in wt% (left panel) and eigen-components (right panel) of González2017_P050-H0-4, which is a diffusion couple experiment between natural shoshonite and a high-K rhyolite (González -Garcia et al., 2017).

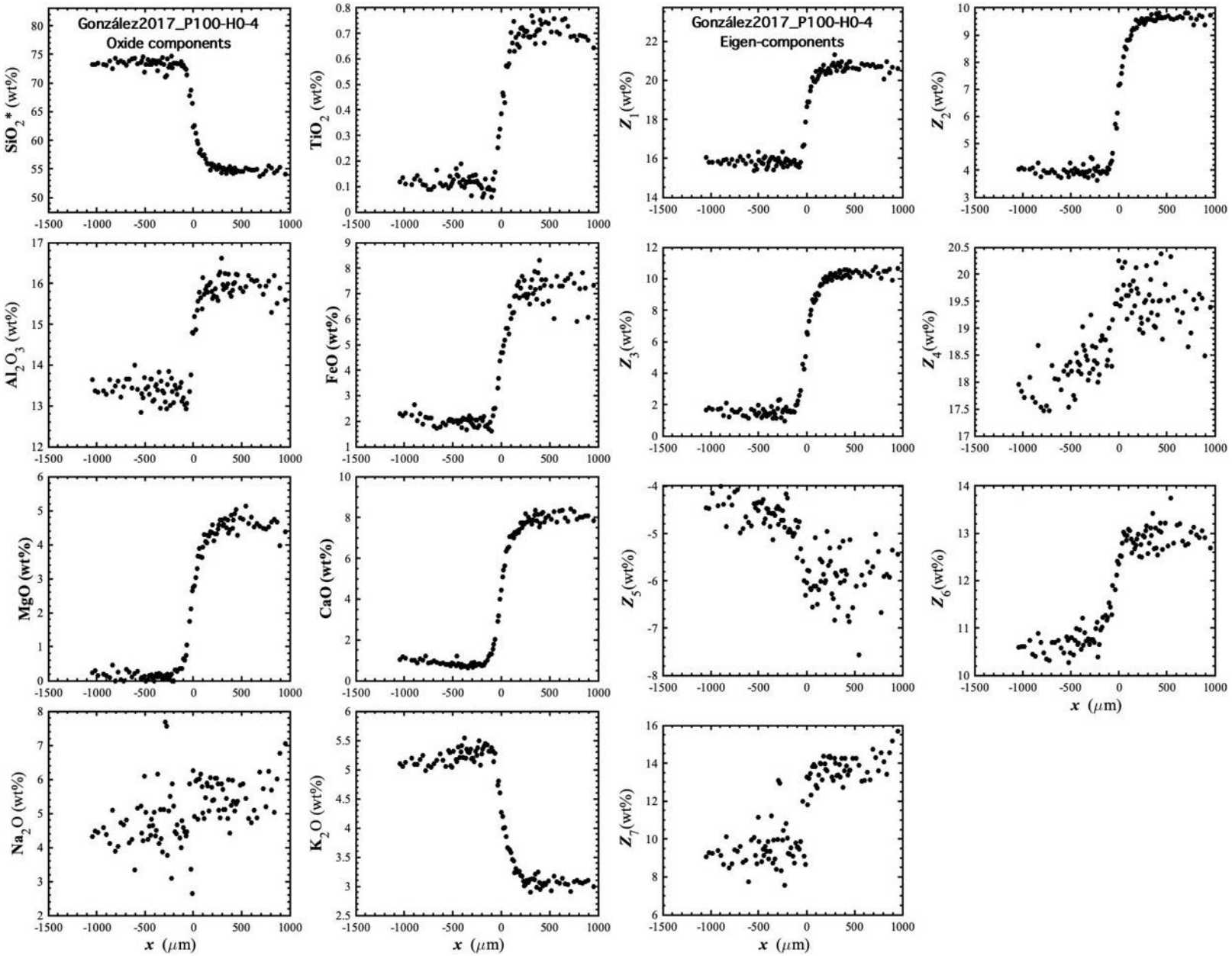

Figure 100. Concentration profiles of oxide components in wt% (left panel) and eigen-components (right panel) of González2017_P100-H0-4, which is a diffusion couple experiment between natural shoshonite and a high-K rhyolite (González -Garcia et al., 2017).

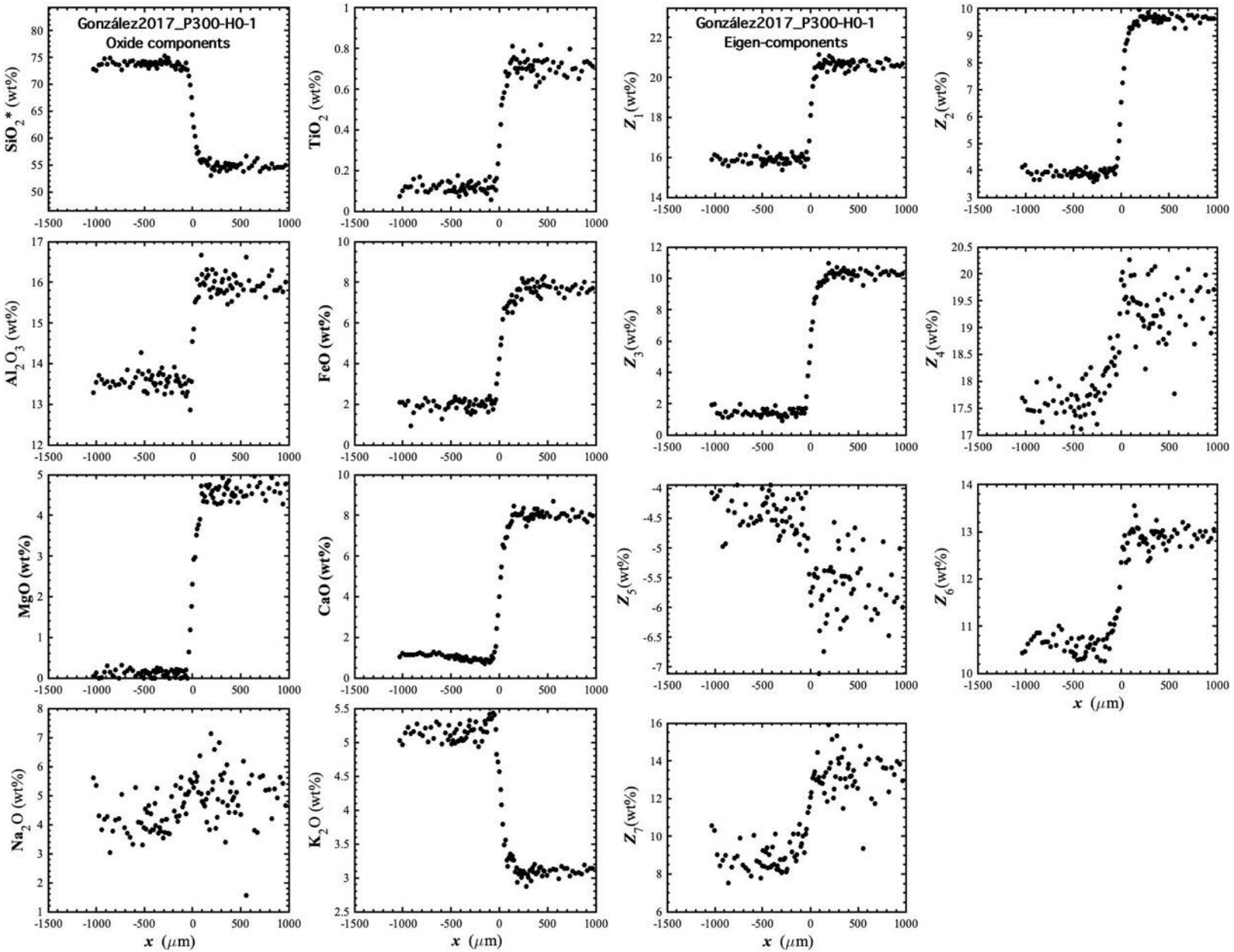

Figure 101. Concentration profiles of oxide components in wt% (left panel) and eigen-components (right panel) of González2017_P300-H0-1, which is a diffusion couple experiment between natural shoshonite and a high-K rhyolite (González -Garcia et al., 2017).

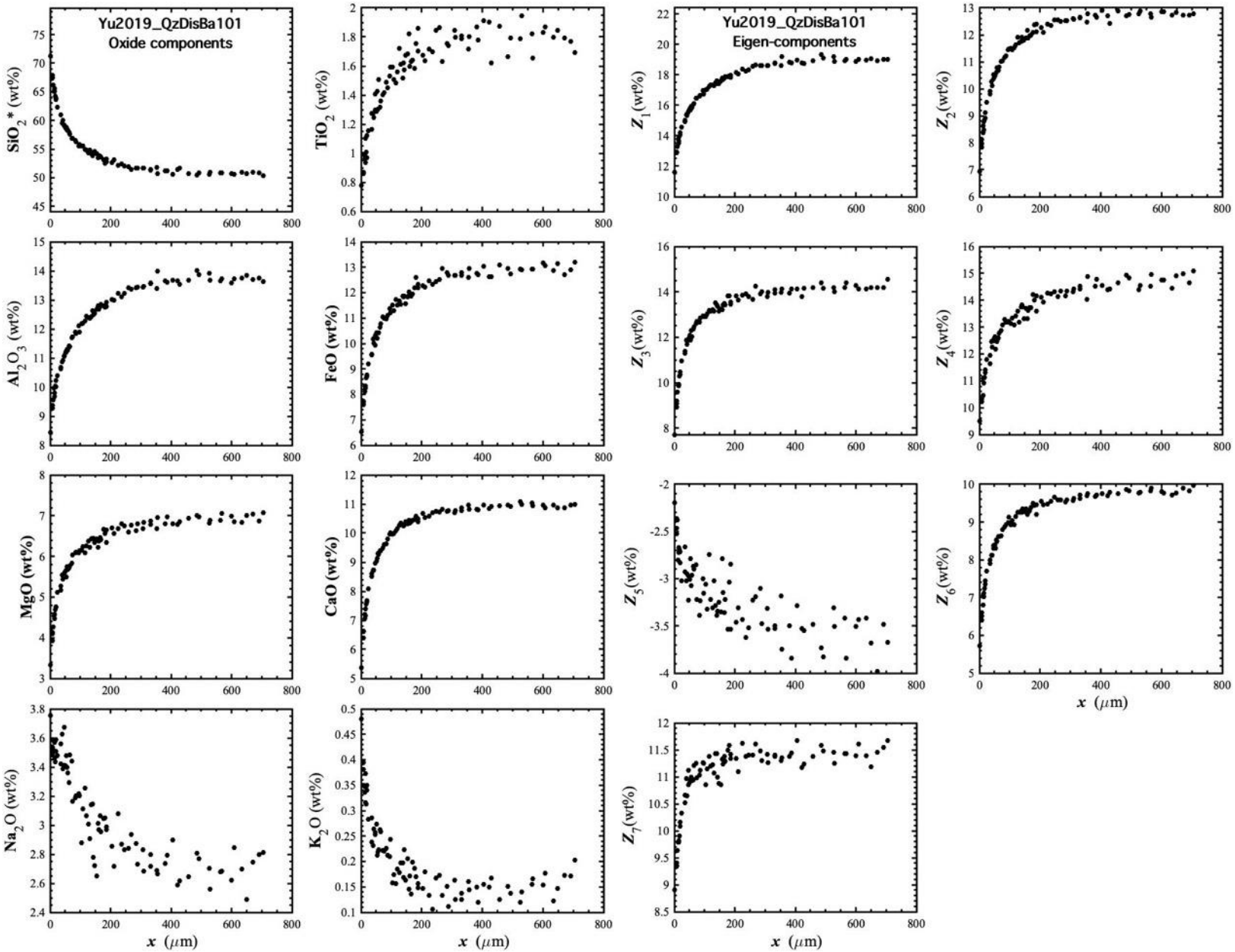

Figure 102. Concentration profiles of oxide components in wt% (left panel) and eigen-components (right panel) of Yu2019_QzDisBa#101, which is a quartz dissolution experiment in basalt (Yu et al., 2019).

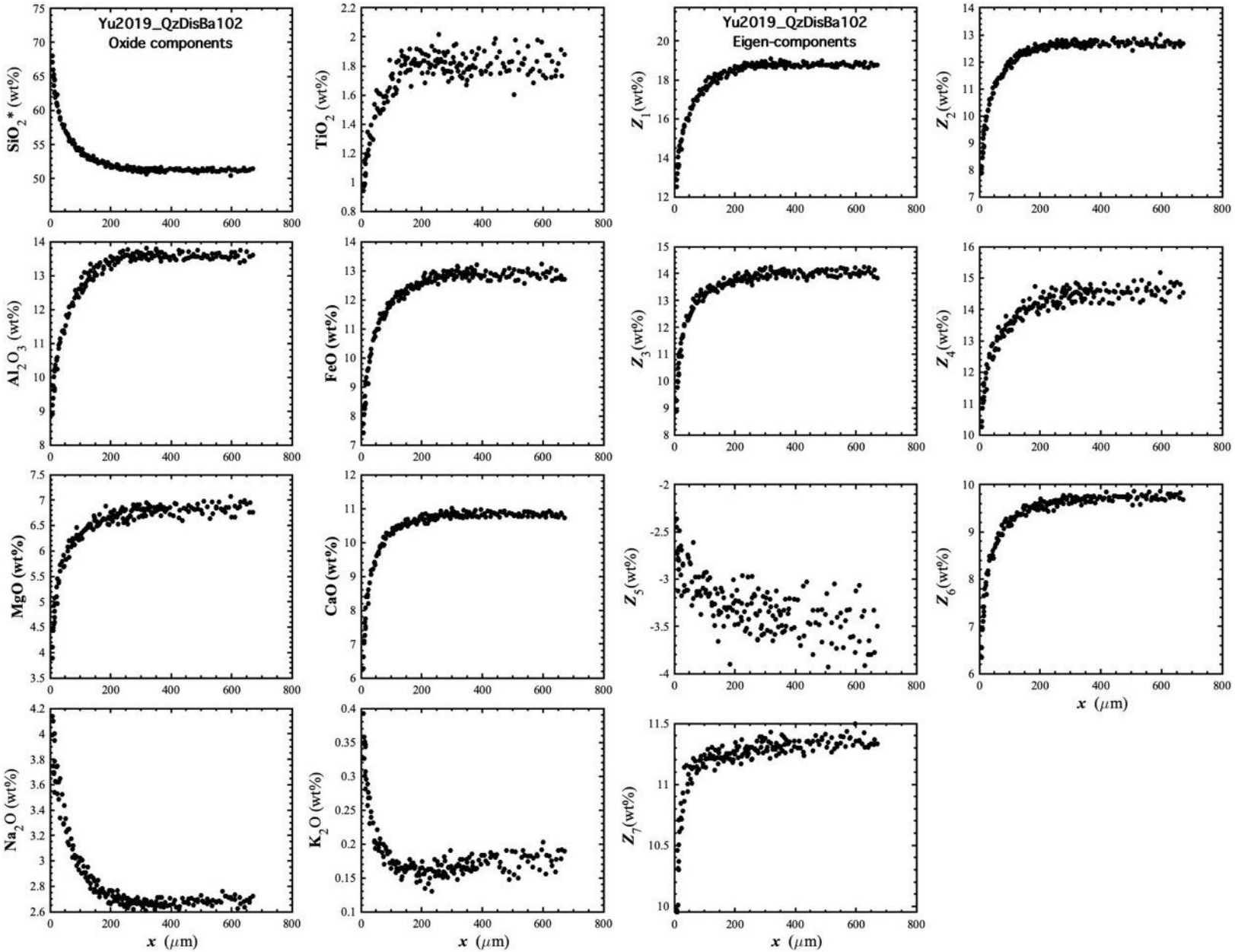

Figure 103. Concentration profiles of oxide components in wt% (left panel) and eigen-components (right panel) of Yu2019_QzDisBa#102, which is a quartz dissolution experiment in basalt (Yu et al., 2019).

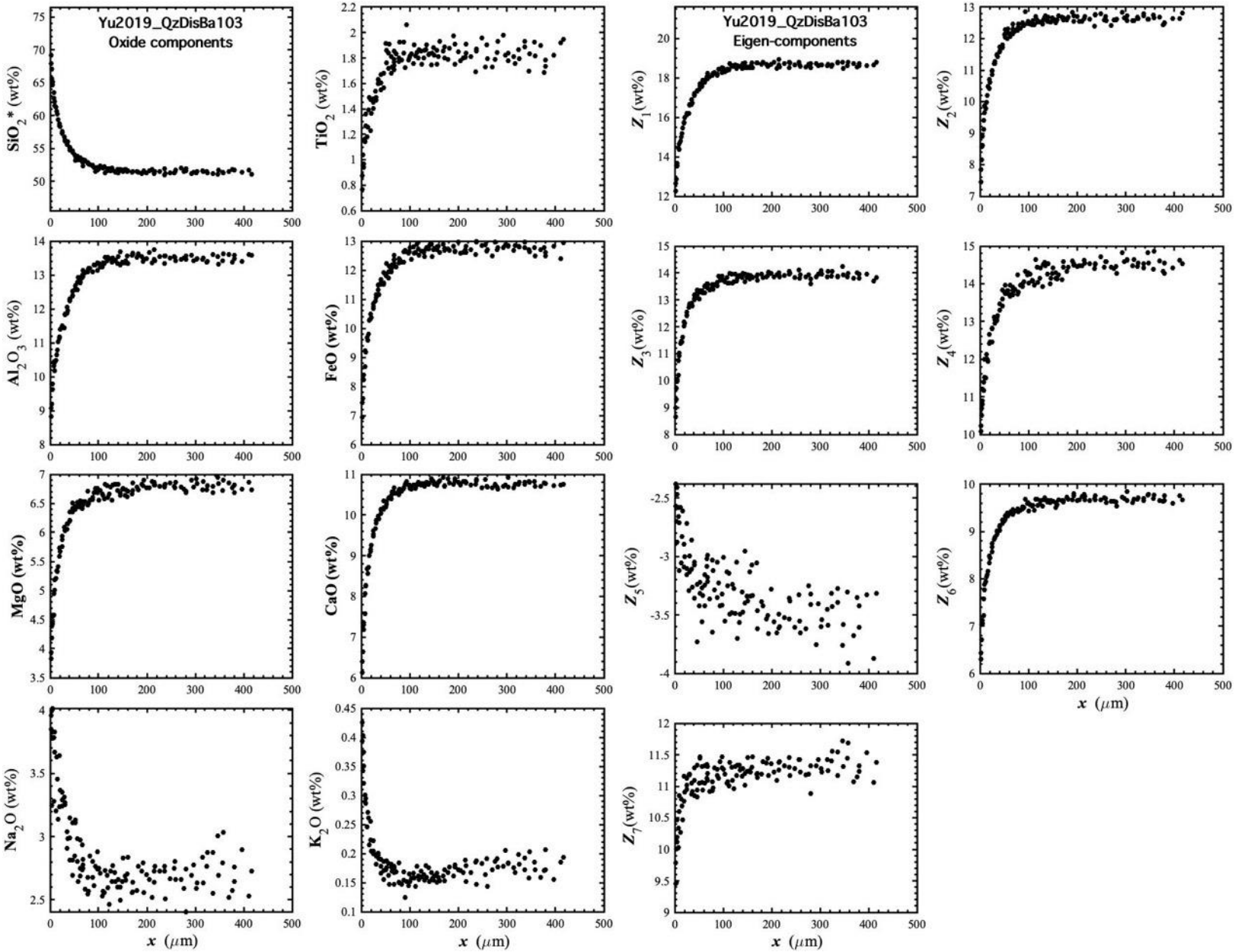

Figure 104. Concentration profiles of oxide components in wt% (left panel) and eigen-components (right panel) of Yu2019_QzDisBa#103, which is a quartz dissolution experiment in basalt (Yu et al., 2019).

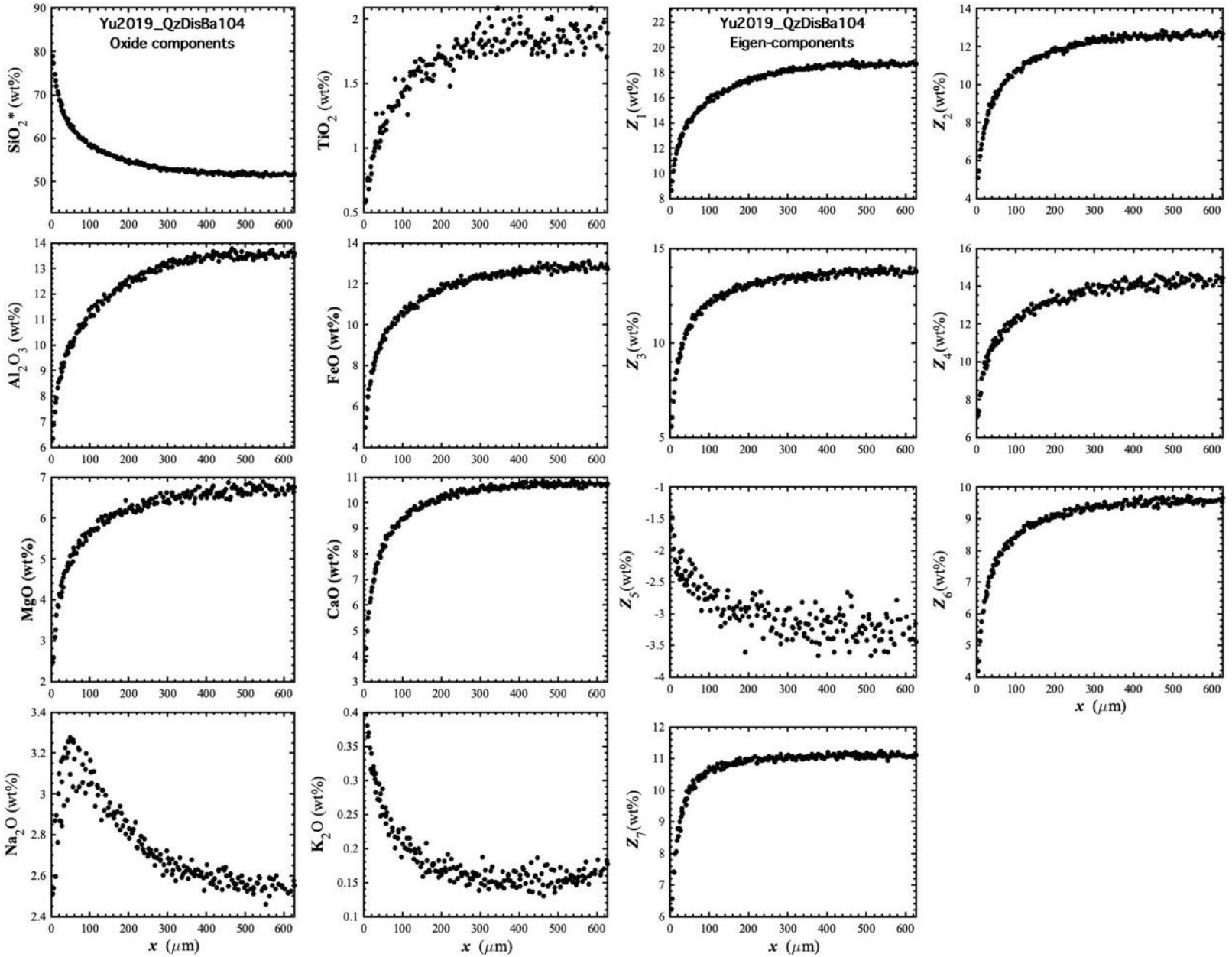

Figure 105. Concentration profiles of oxide components in wt% (left panel) and eigen-components (right panel) of Yu2019_QzDisBa#104, which is a quartz dissolution experiment in basalt (Yu et al., 2019).

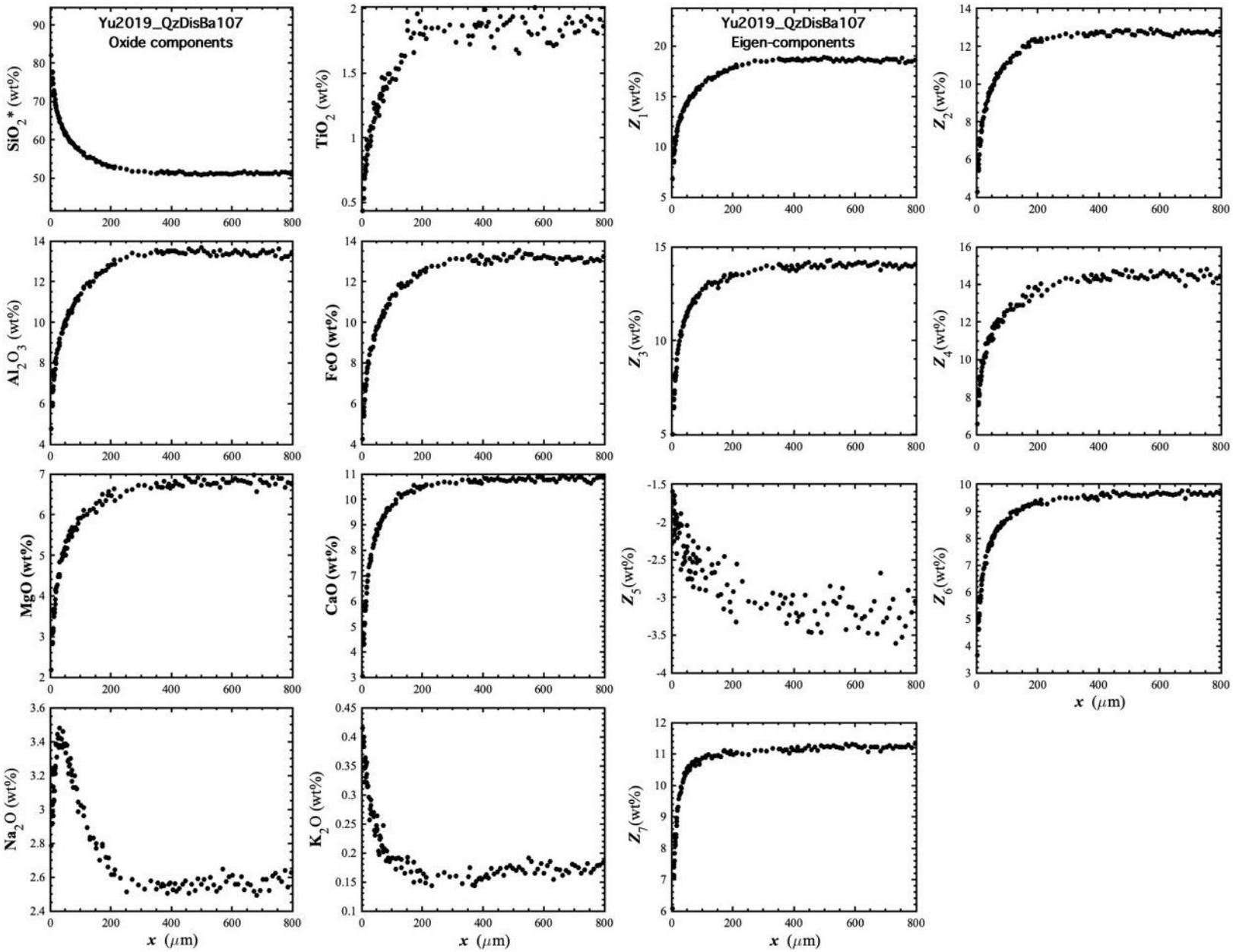

Figure 106. Concentration profiles of oxide components in wt% (left panel) and eigen-components (right panel) of Yu2019_QzDisBa#107, which is a quartz dissolution experiment in basalt (Yu et al., 2019).

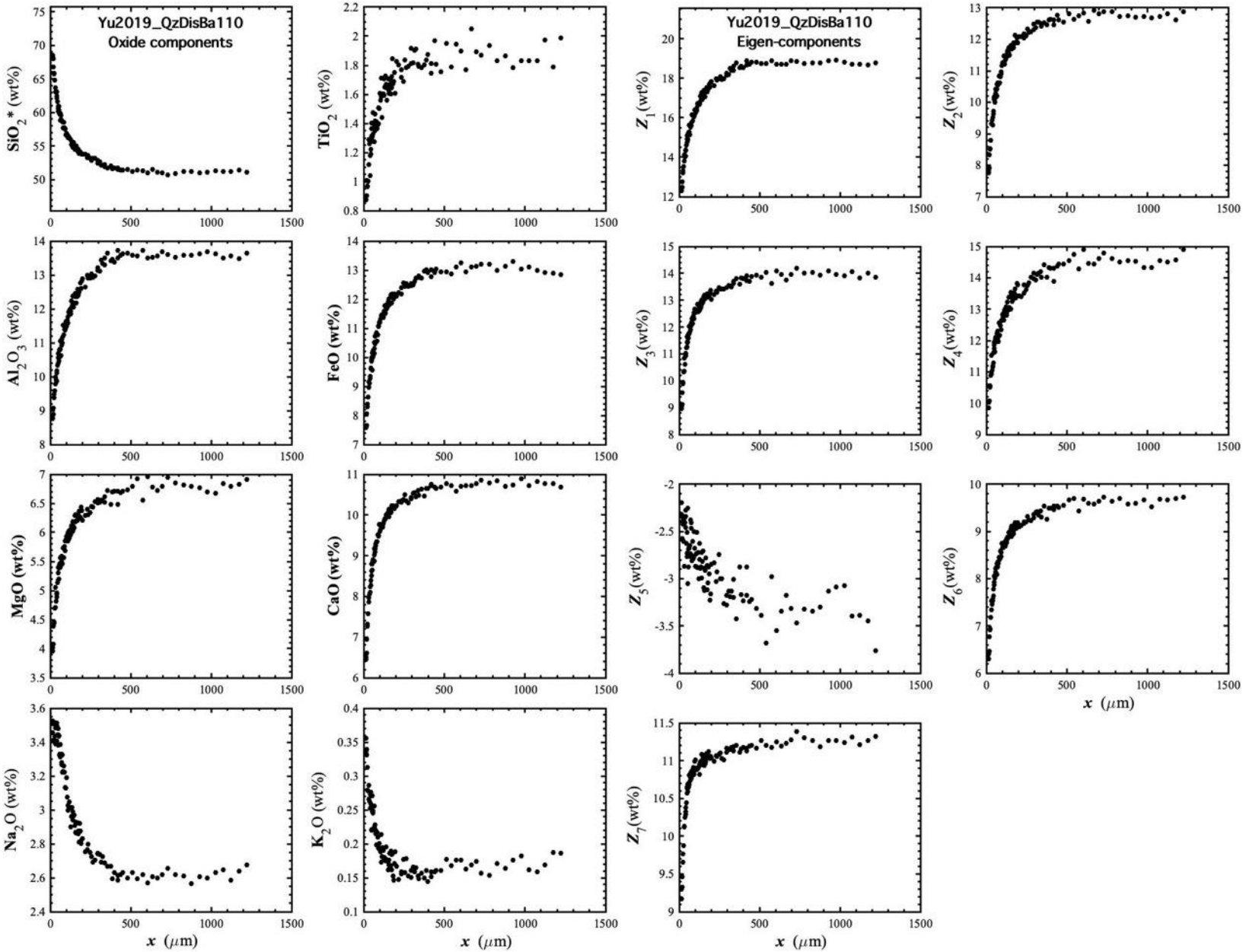

Figure 107. Concentration profiles of oxide components in wt% (left panel) and eigen-components (right panel) of Yu2019_QzDisBa#110, which is a quartz dissolution experiment in basalt (Yu et al., 2019).

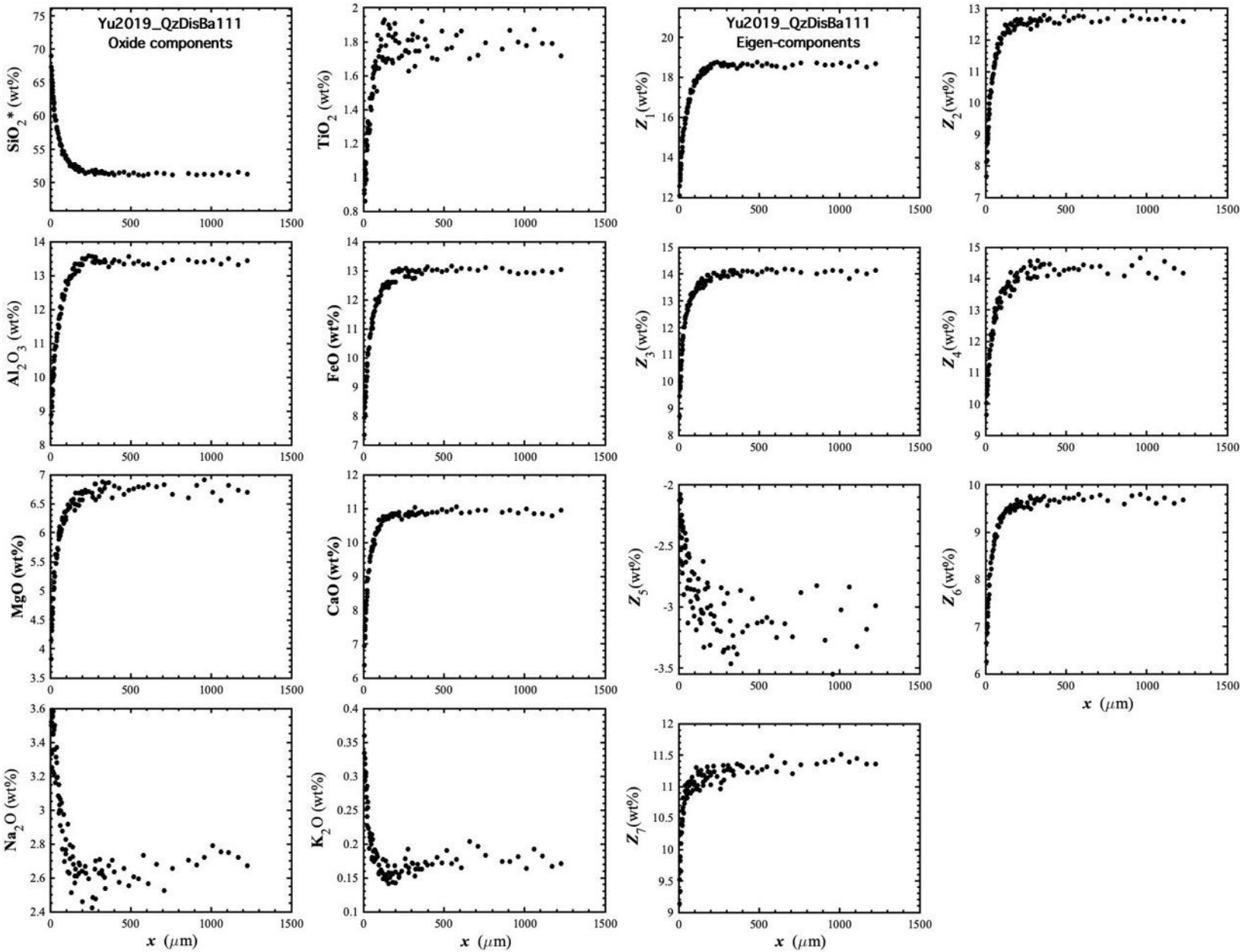

Figure 108. Concentration profiles of oxide components in wt% (left panel) and eigen-components (right panel) of Yu2019_QzDisBa#111, which is a quartz dissolution experiment in basalt (Yu et al., 2019).

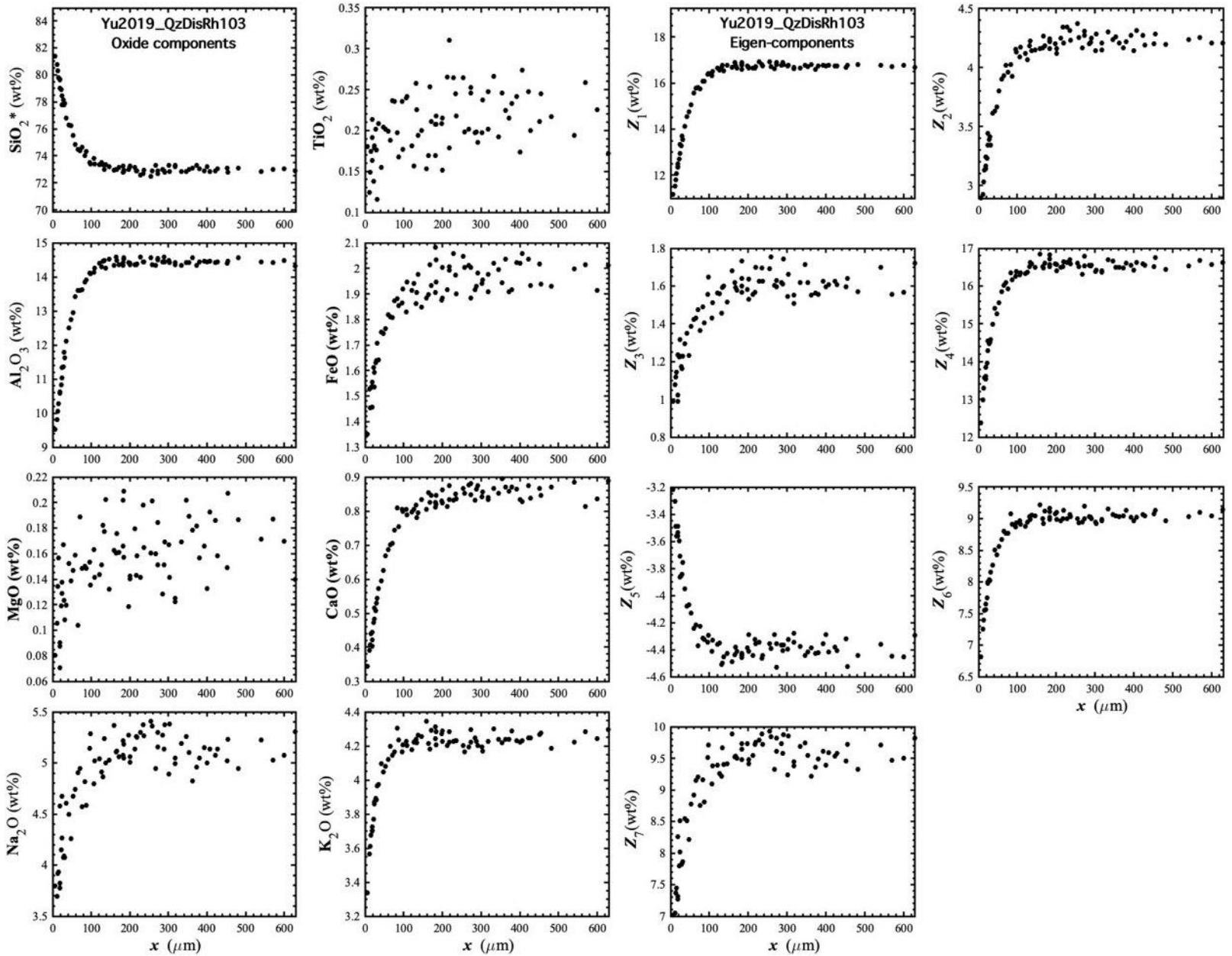

Figure 109. Concentration profiles of oxide components in wt% (left panel) and eigen-components (right panel) of Yu2019_QzDisRh#103, which is a quartz dissolution experiment in rhyolite (Yu et al., 2019).

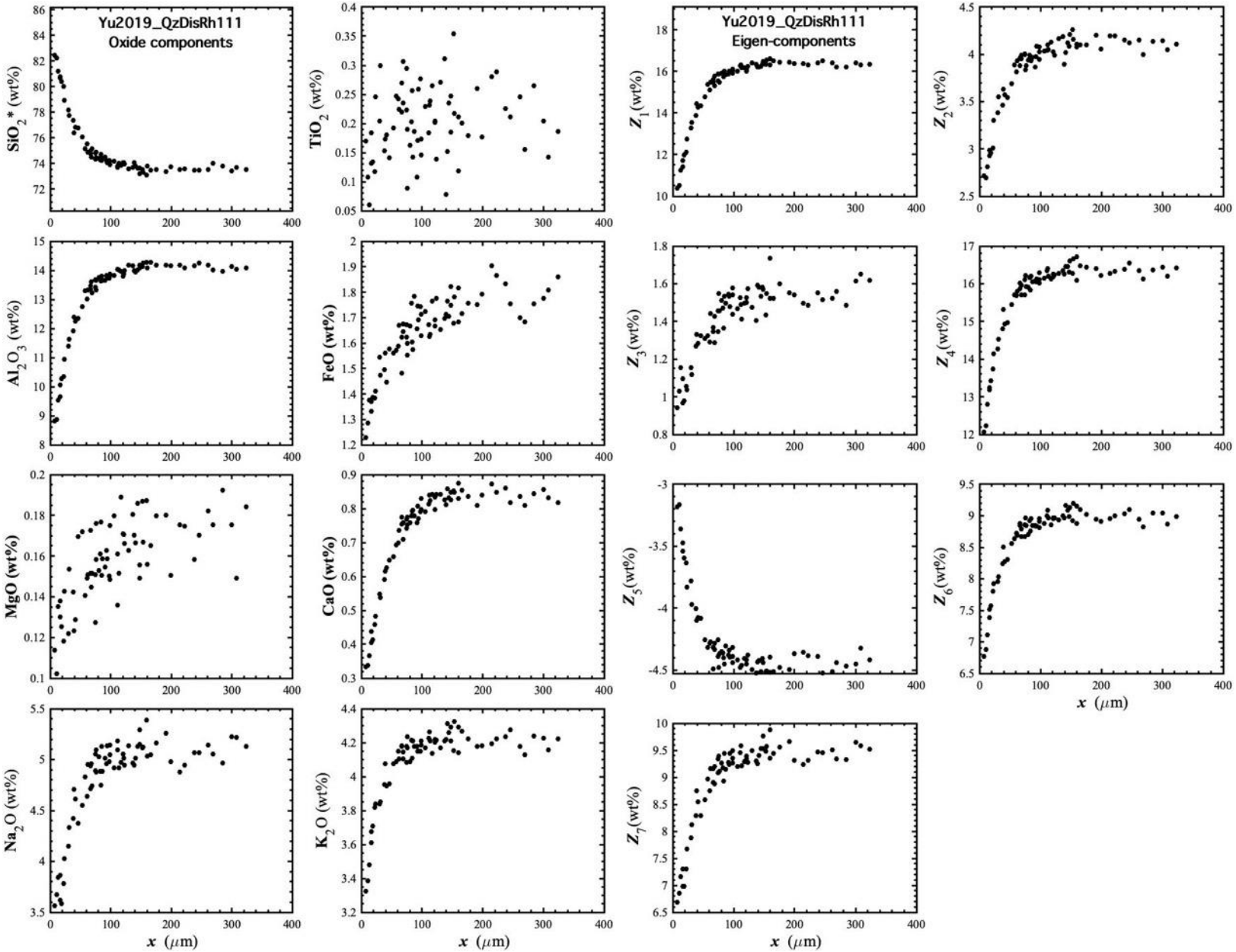

Figure 110. Concentration profiles of oxide components in wt% (left panel) and eigen-components (right panel) of Yu2019_QzDisRh#111, which is a quartz dissolution experiment in rhyolite (Yu et al., 2019).

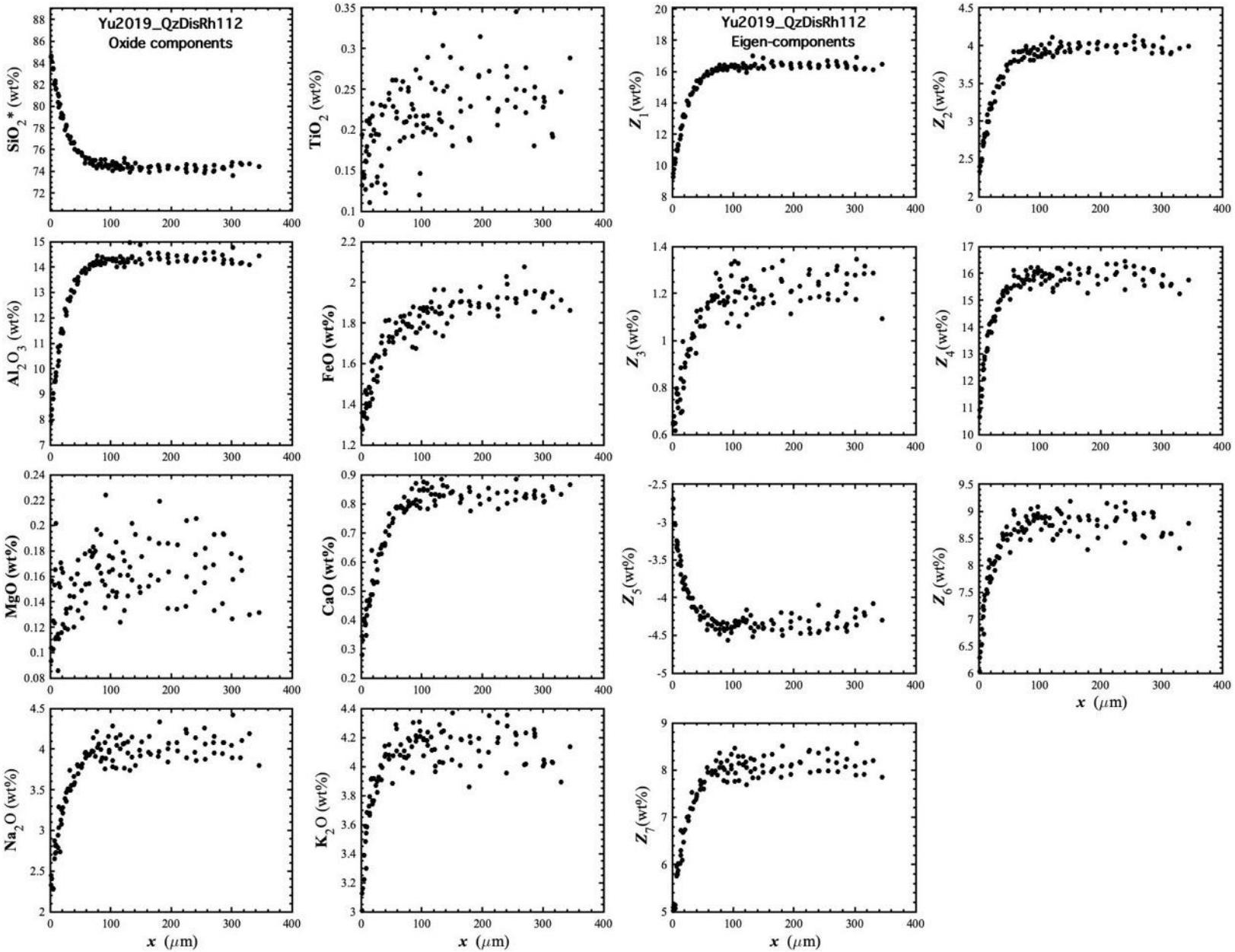

Figure 111. Concentration profiles of oxide components in wt% (left panel) and eigen-components (right panel) of Yu2019_QzDisRh#112, which is a quartz dissolution experiment in rhyolite (Yu et al., 2019).

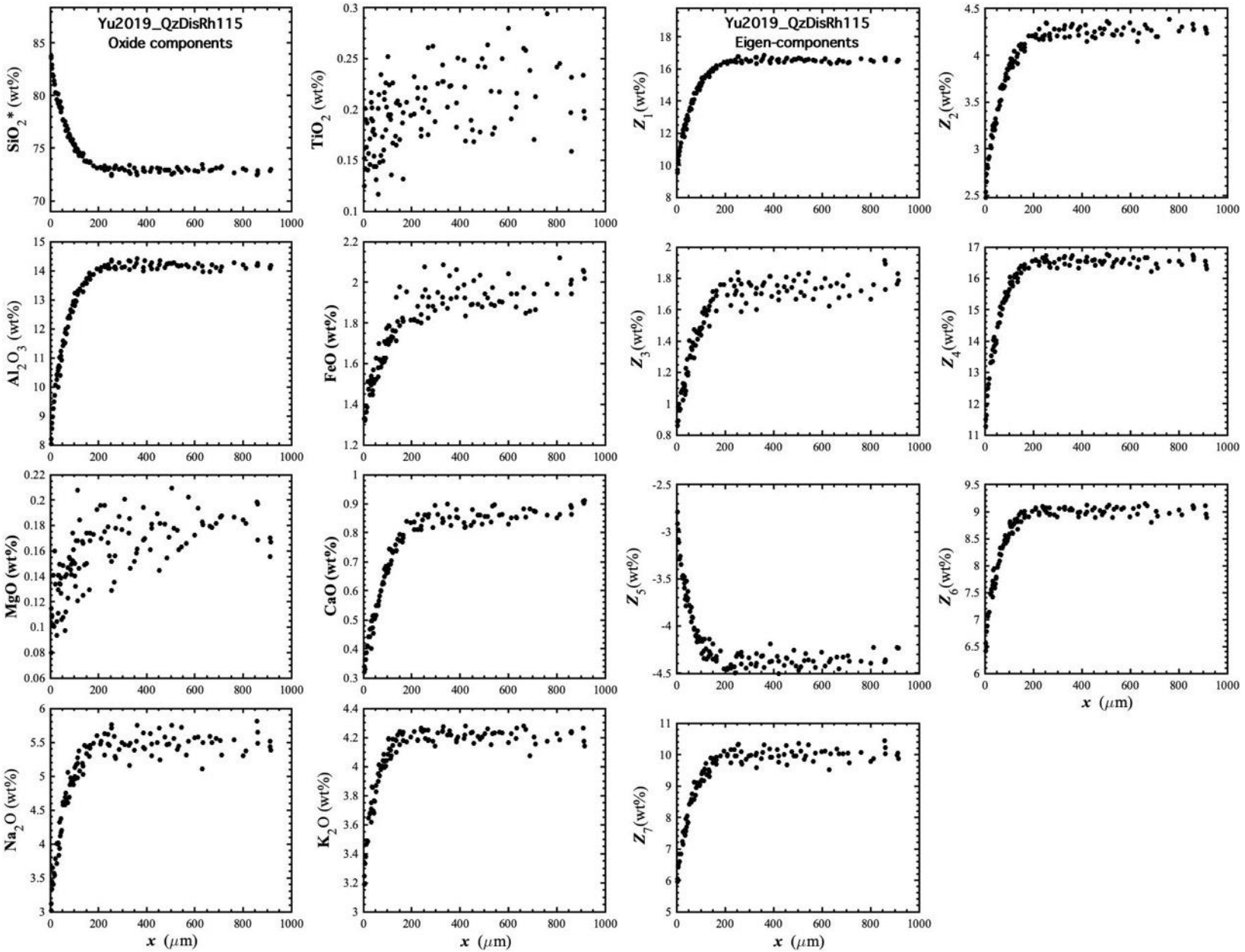

Figure 112. Concentration profiles of oxide components in wt% (left panel) and eigen-components (right panel) of Yu2019_QzDisRh#115, which is a quartz dissolution experiment in rhyolite (Yu et al., 2019).

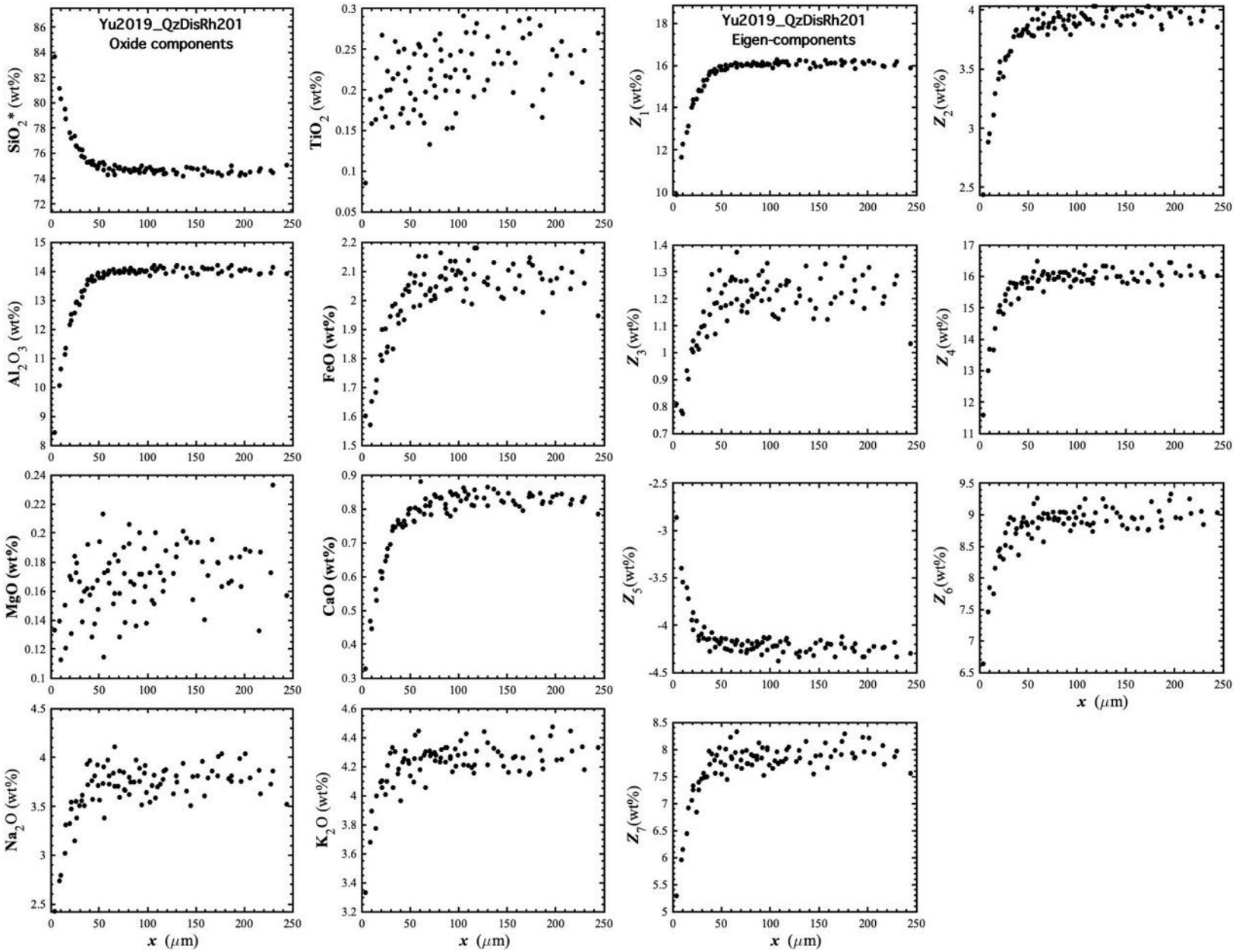

Figure 113. Concentration profiles of oxide components in wt% (left panel) and eigen-components (right panel) of Yu2019_QzDisRh#201, which is a quartz dissolution experiment in rhyolite (Yu et al., 2019).

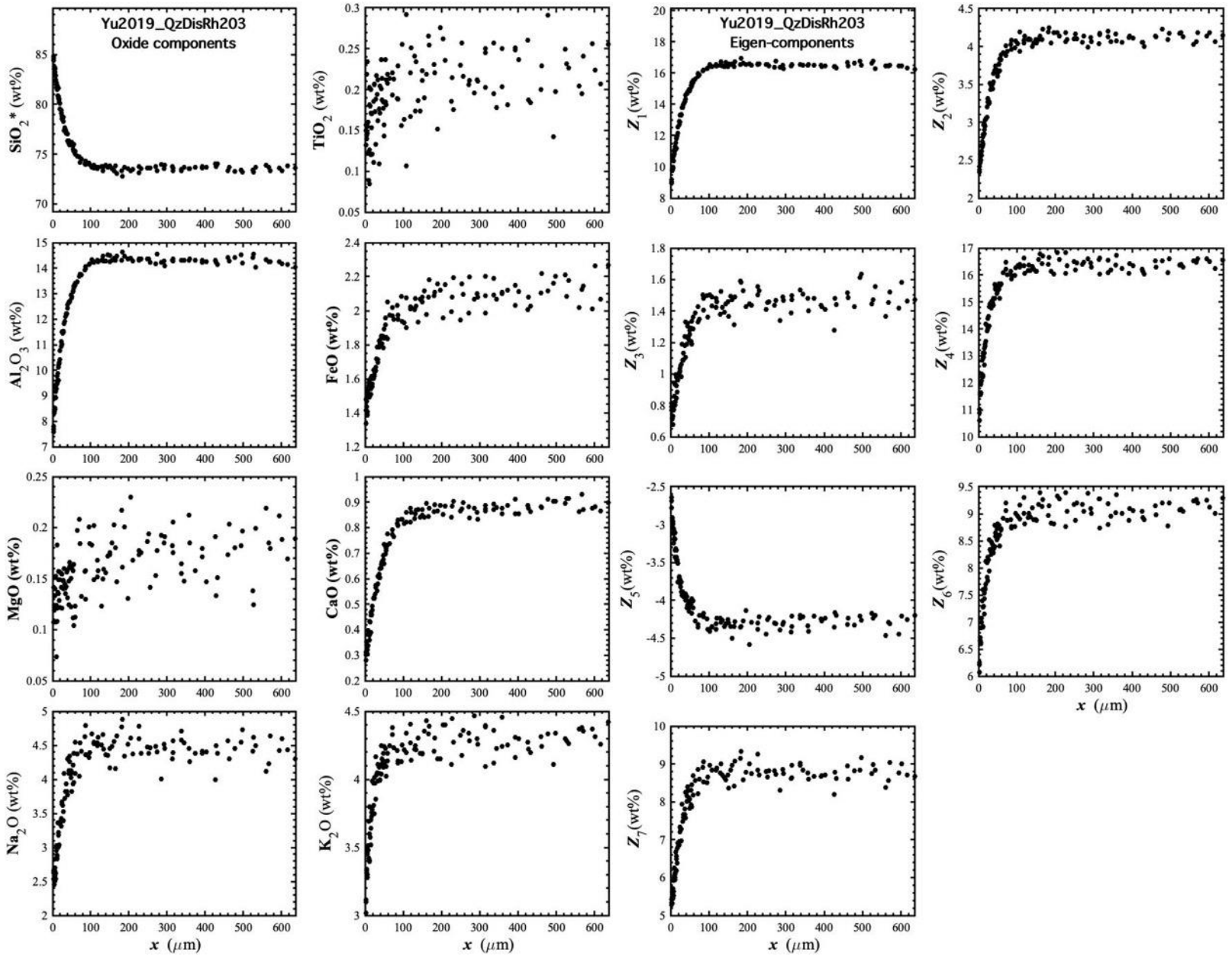

Figure 114. Concentration profiles of oxide components in wt% (left panel) and eigen-components (right panel) of Yu2019_QzDisRh#203, which is a quartz dissolution experiment in rhyolite (Yu et al., 2019).

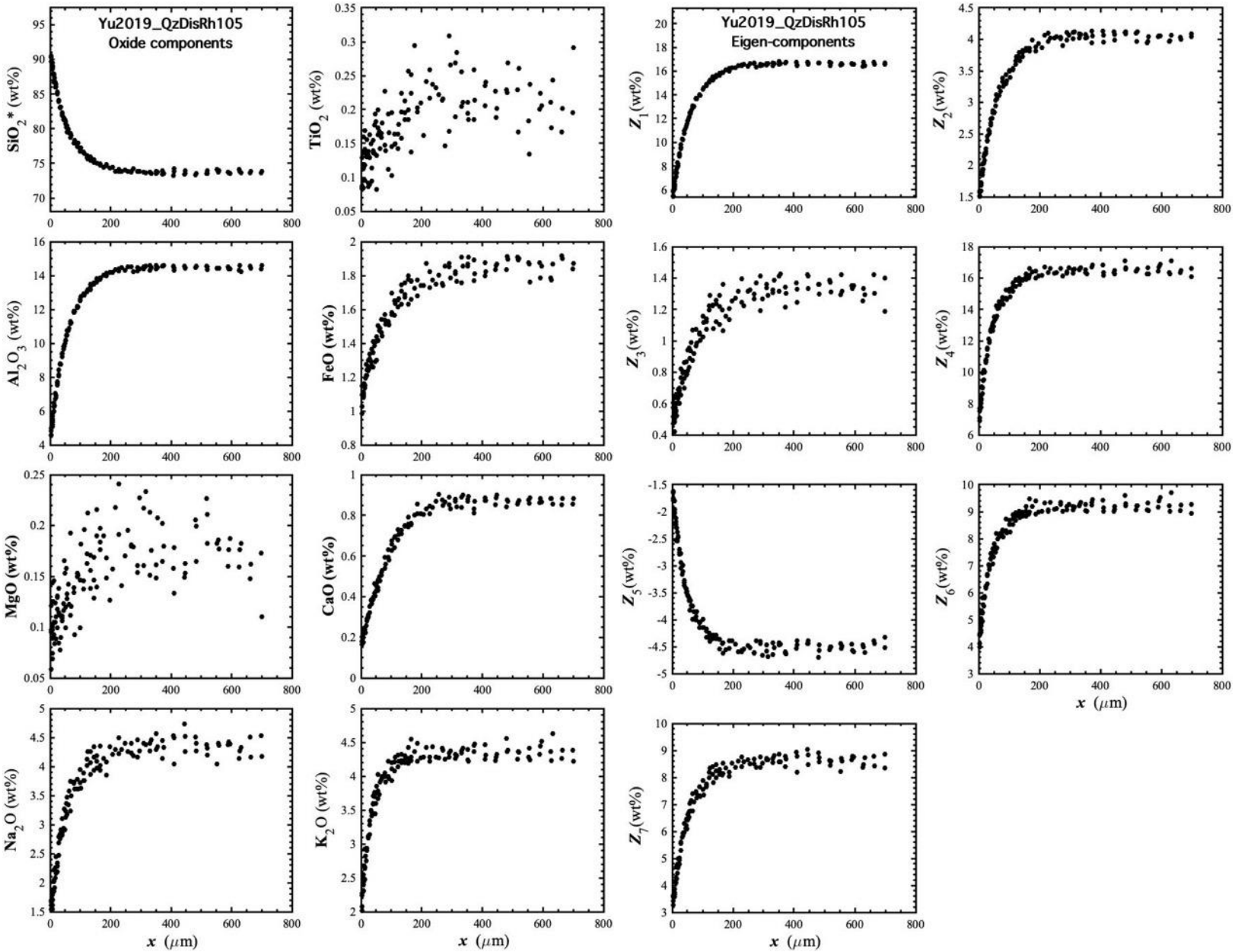

Figure 115. Concentration profiles of oxide components in wt% (left panel) and eigen-components (right panel) of Yu2019_QzDisRh#105, which is a quartz dissolution experiment in rhyolite (Yu et al., 2019).

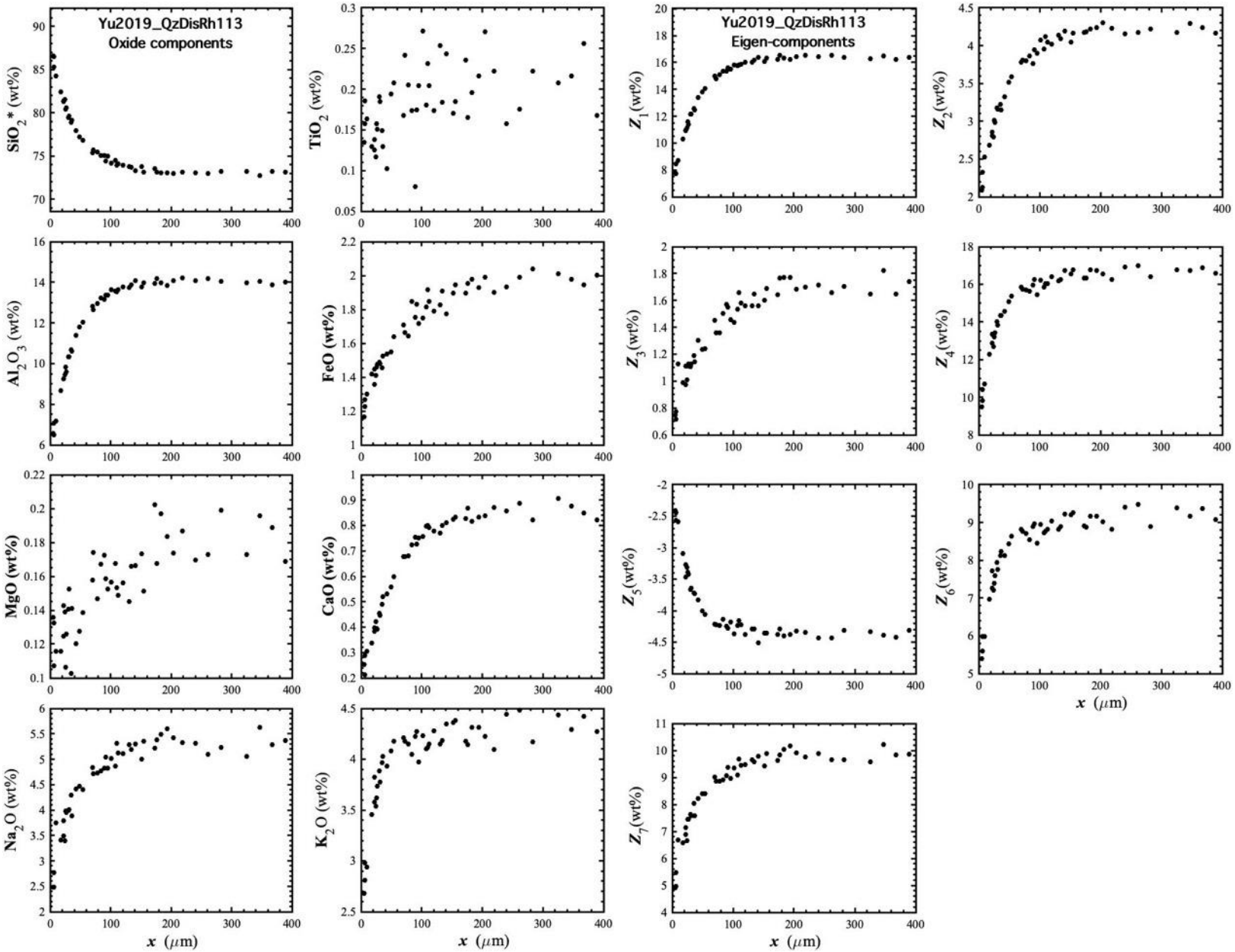

Figure 116. Concentration profiles of oxide components in wt% (left panel) and eigen-components (right panel) of Yu2019_QzDisRh#113, which is a quartz dissolution experiment in rhyolite (Yu et al., 2019).

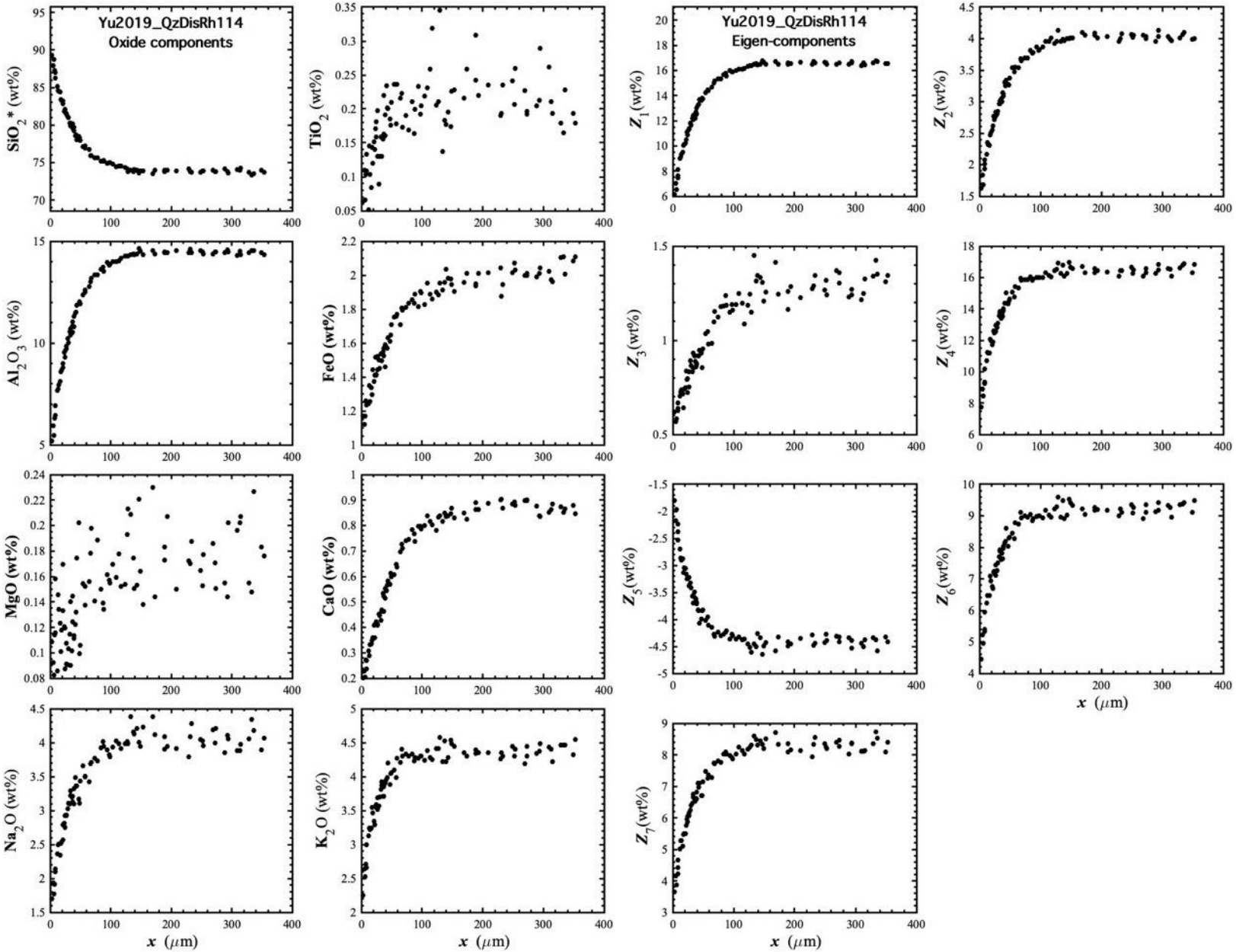

Figure 117. Concentration profiles of oxide components in wt% (left panel) and eigen-components (right panel) of Yu2019_QzDisRh#114, which is a quartz dissolution experiment in rhyolite (Yu et al., 2019).

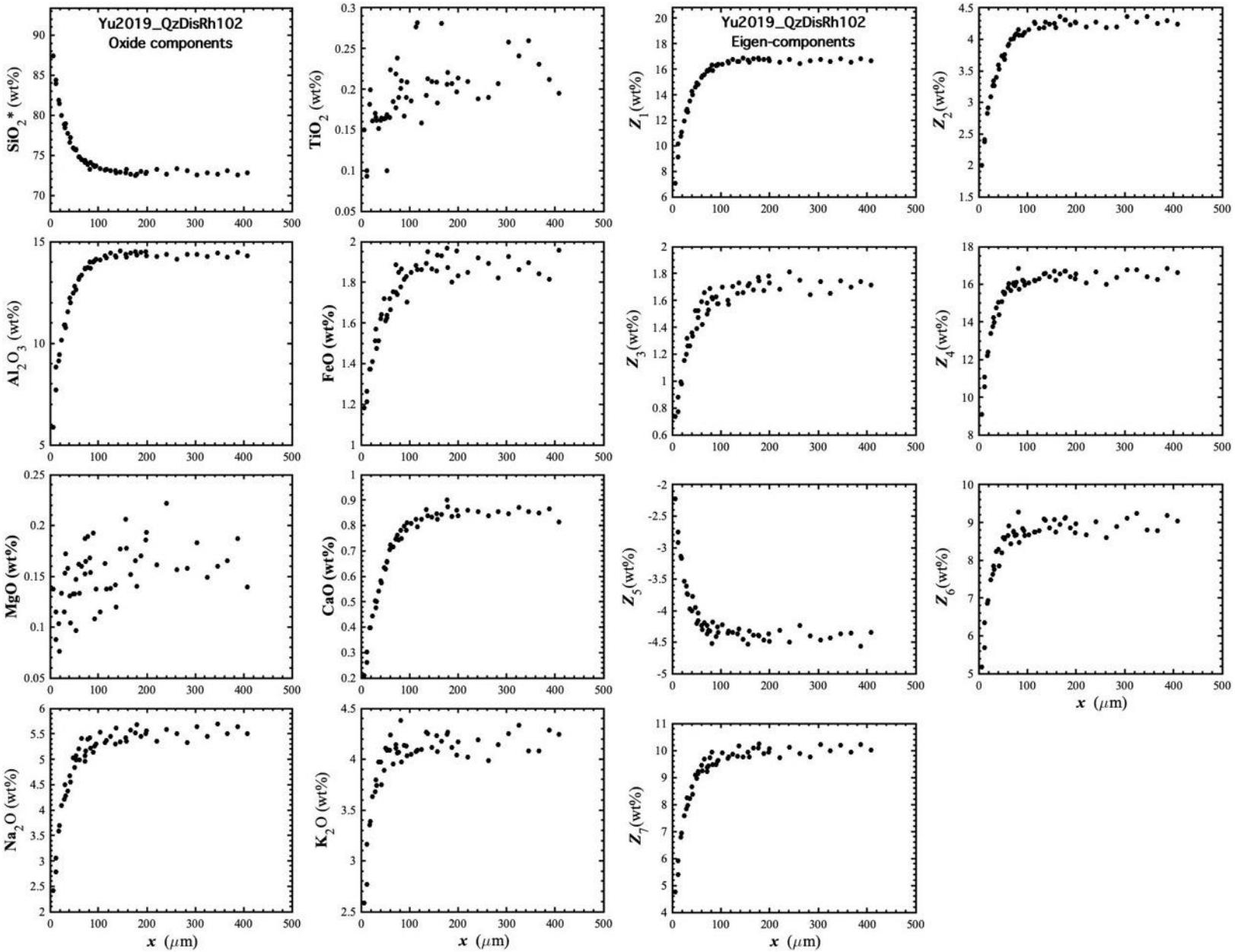

Figure 118. Concentration profiles of oxide components in wt% (left panel) and eigen-components (right panel) of Yu2019_QzDisRh#102, which is a quartz dissolution experiment in rhyolite (Yu et al., 2019).

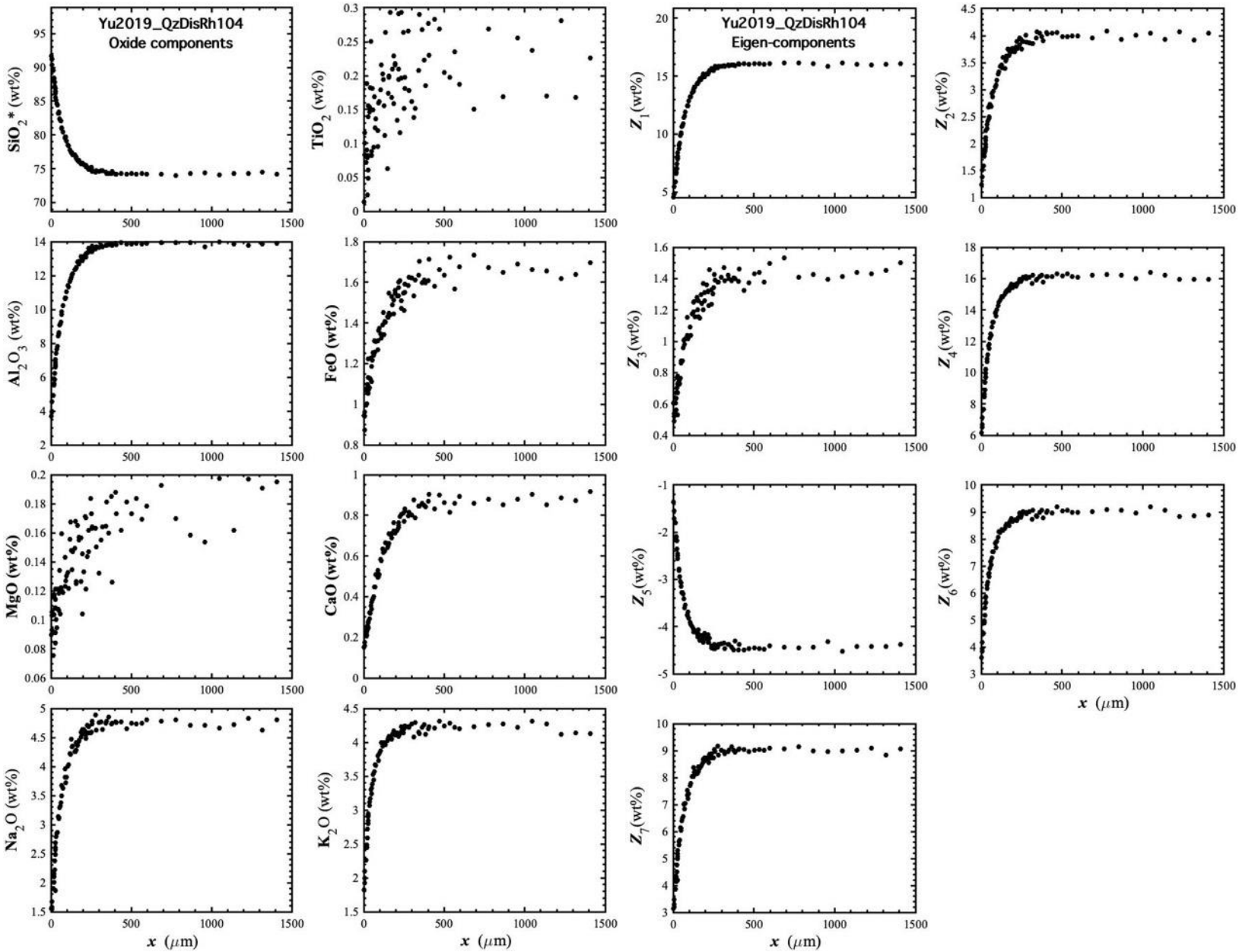

Figure 119. Concentration profiles of oxide components in wt% (left panel) and eigen-components (right panel) of Yu2019_QzDisRh#104, which is a quartz dissolution experiment in rhyolite (Yu et al., 2019).

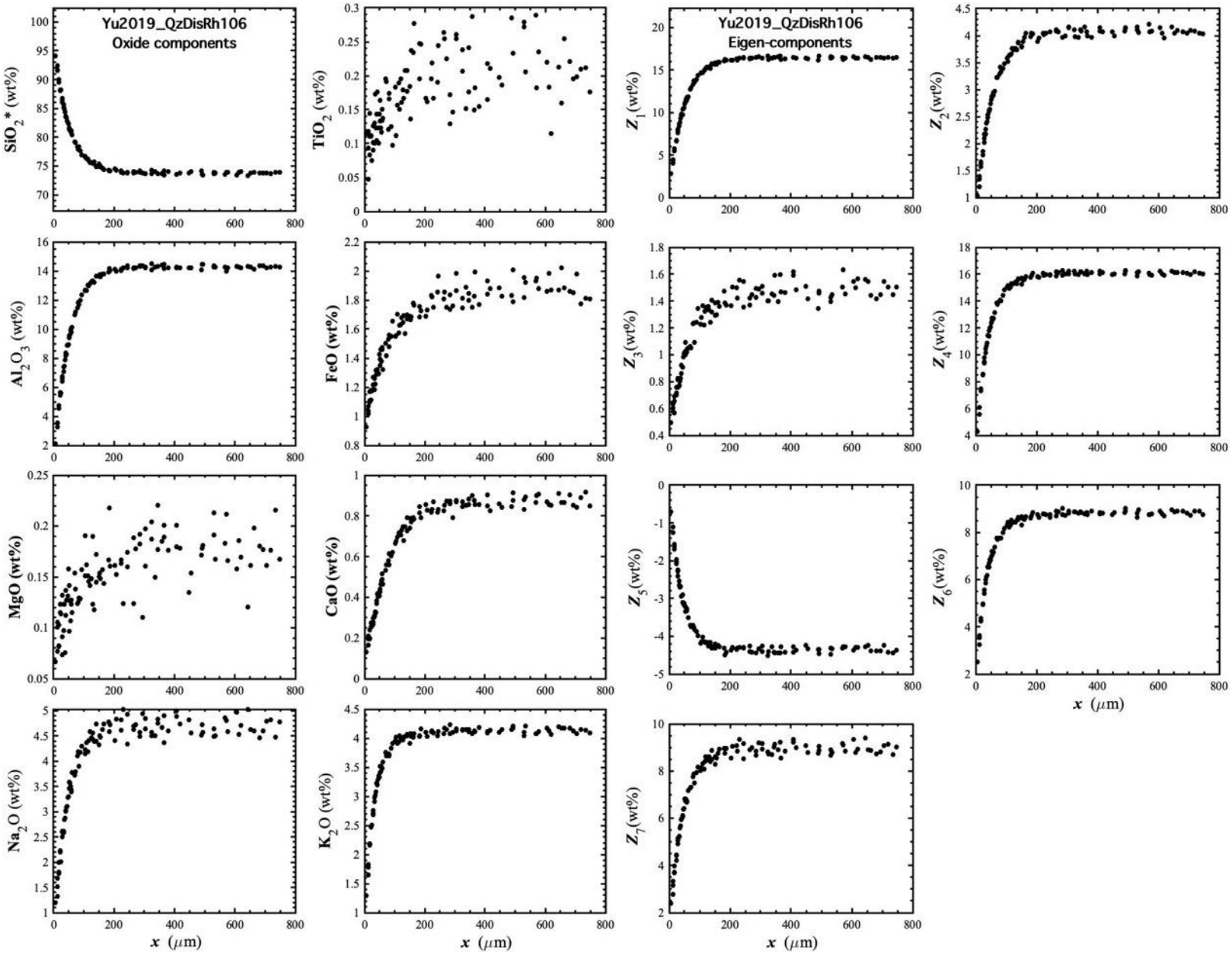

Figure 120. Concentration profiles of oxide components in wt% (left panel) and eigen-components (right panel) of Yu2019_QzDisRh#106, which is a quartz dissolution experiment in rhyolite (Yu et al., 2019).

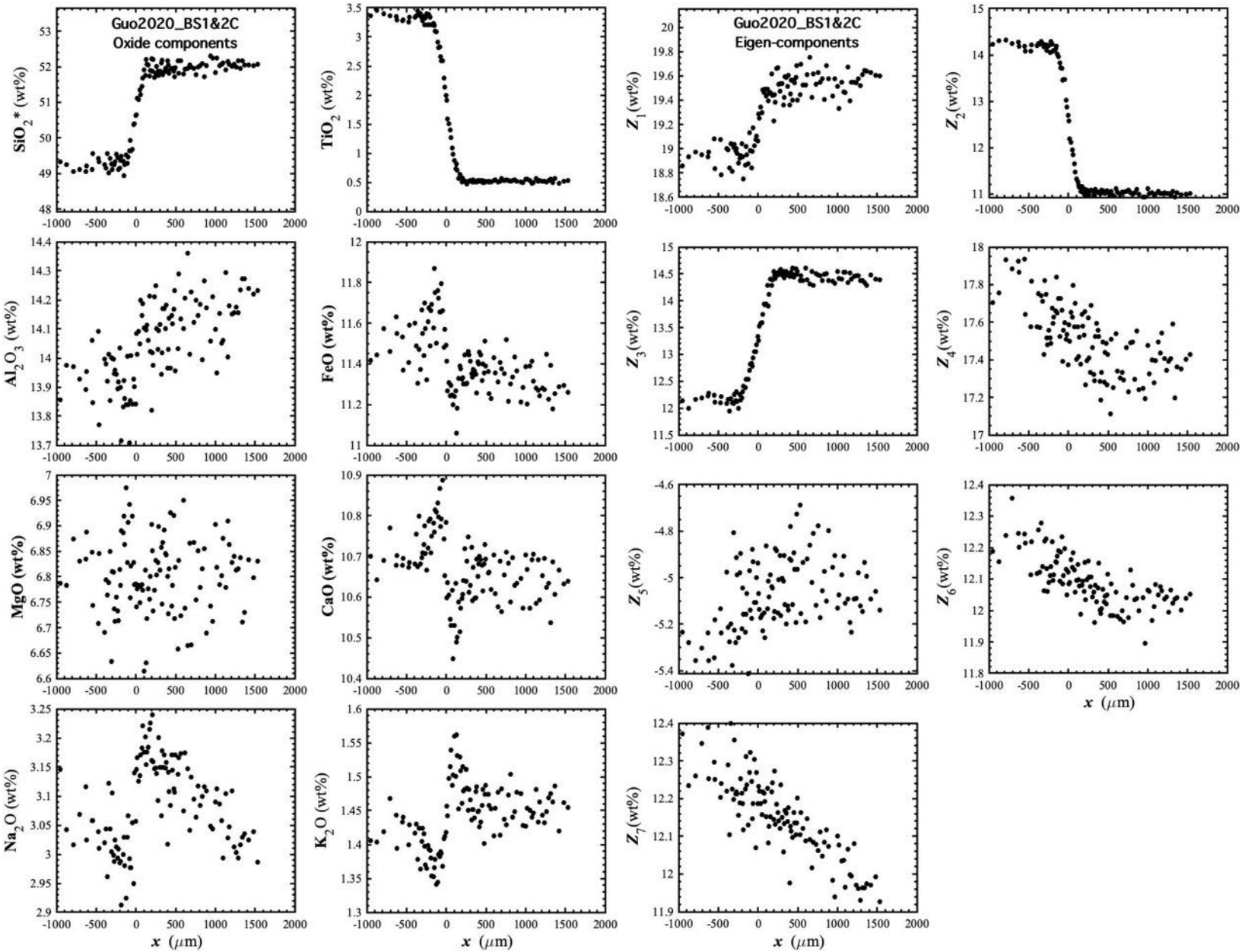

Figure 121. Concentration profiles of oxide components in wt% (left panel) and eigen-components (right panel) of Guo2020_BS1&2C, which is a diffusion couple experiment in basalt (Guo and Zhang, 2020).

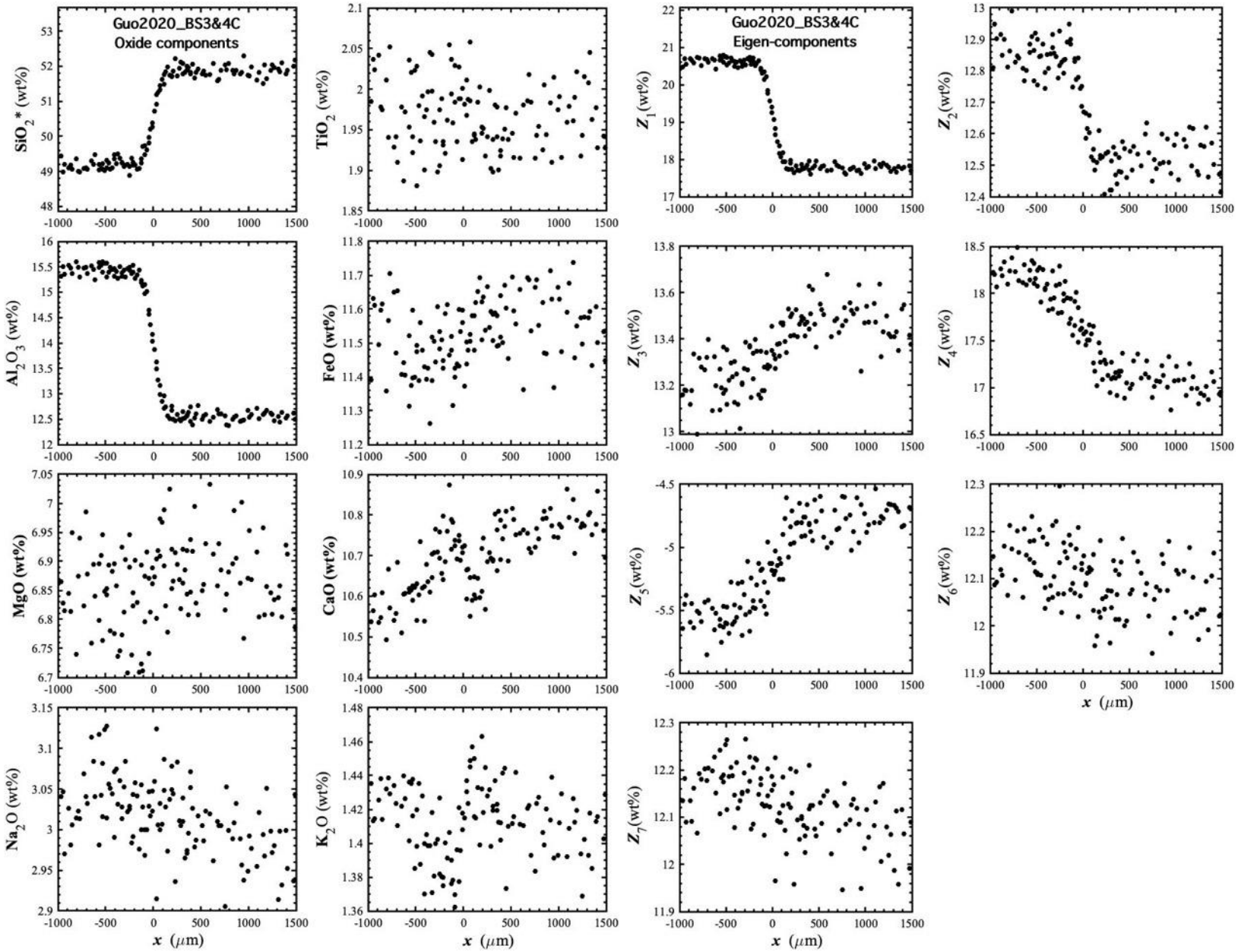

Figure 122. Concentration profiles of oxide components in wt% (left panel) and eigen-components (right panel) of Guo2020_BS3&4C, which is a diffusion couple experiment in basalt (Guo and Zhang, 2020).

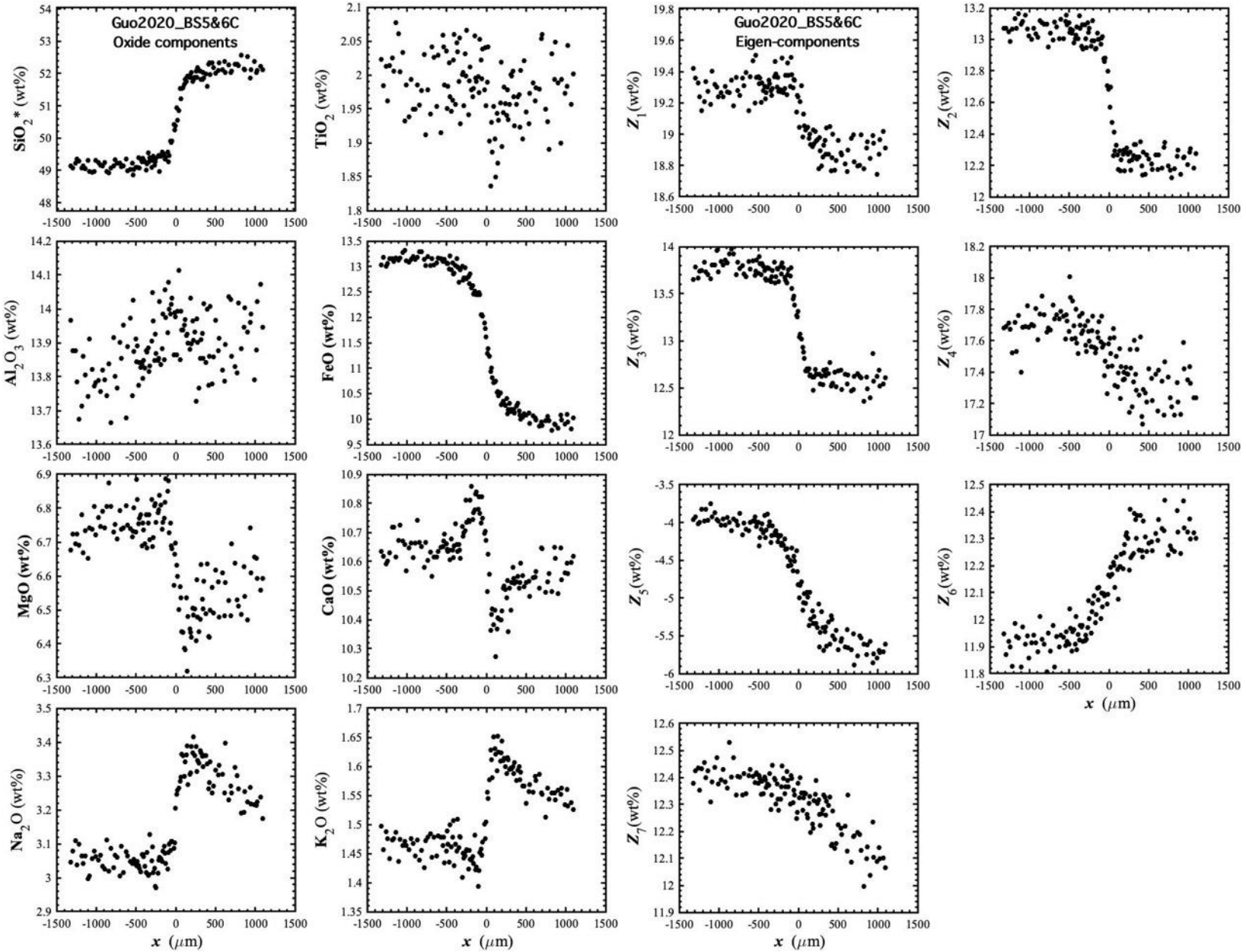

Figure 123. Concentration profiles of oxide components in wt% (left panel) and eigen-components (right panel) of Guo2020_BS5&6C, which is a diffusion couple experiment in basalt (Guo and Zhang, 2020).

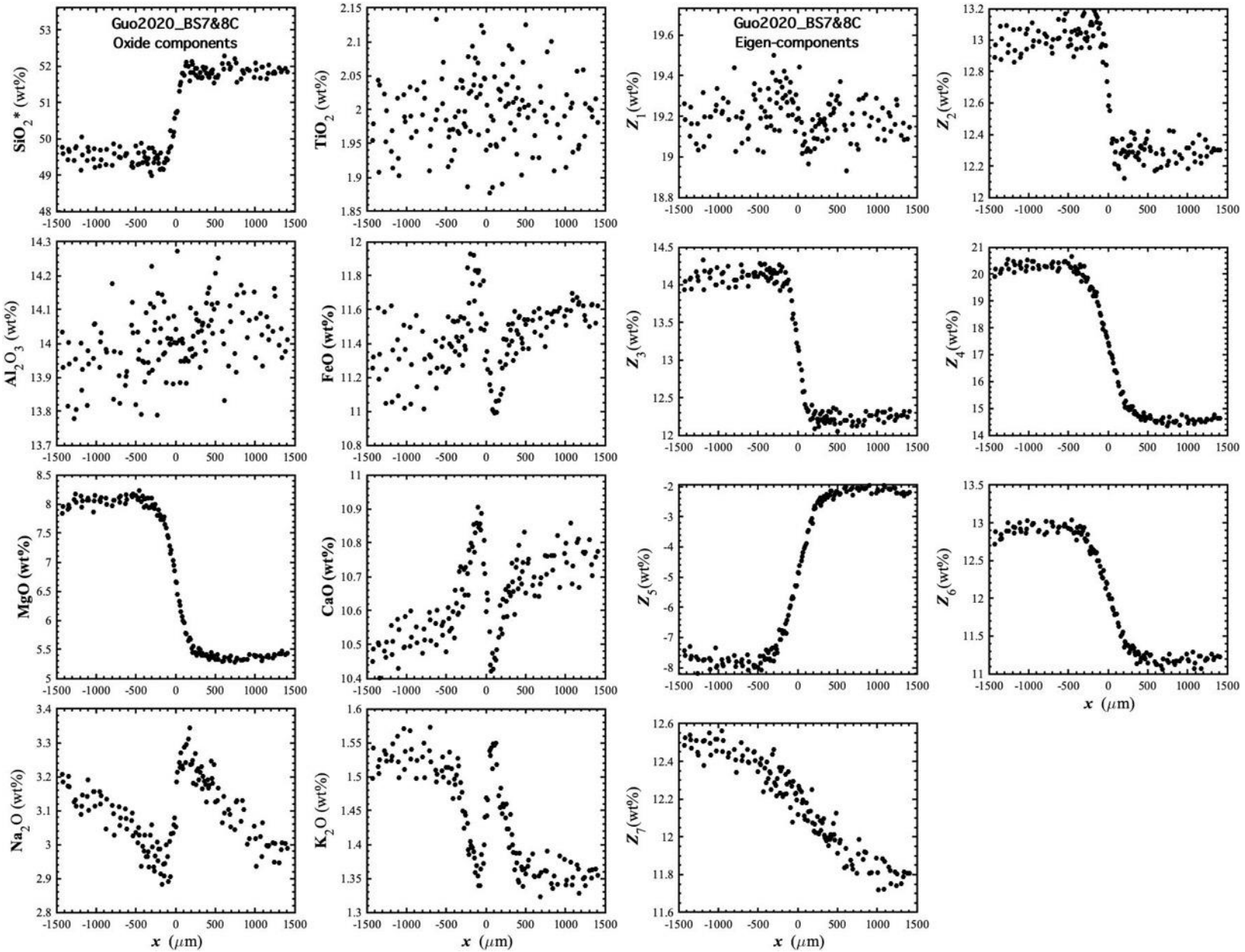

Figure 124. Concentration profiles of oxide components in wt% (left panel) and eigen-components (right panel) of Guo2020_BS7&8C, which is a diffusion couple experiment in basalt (Guo and Zhang, 2020).

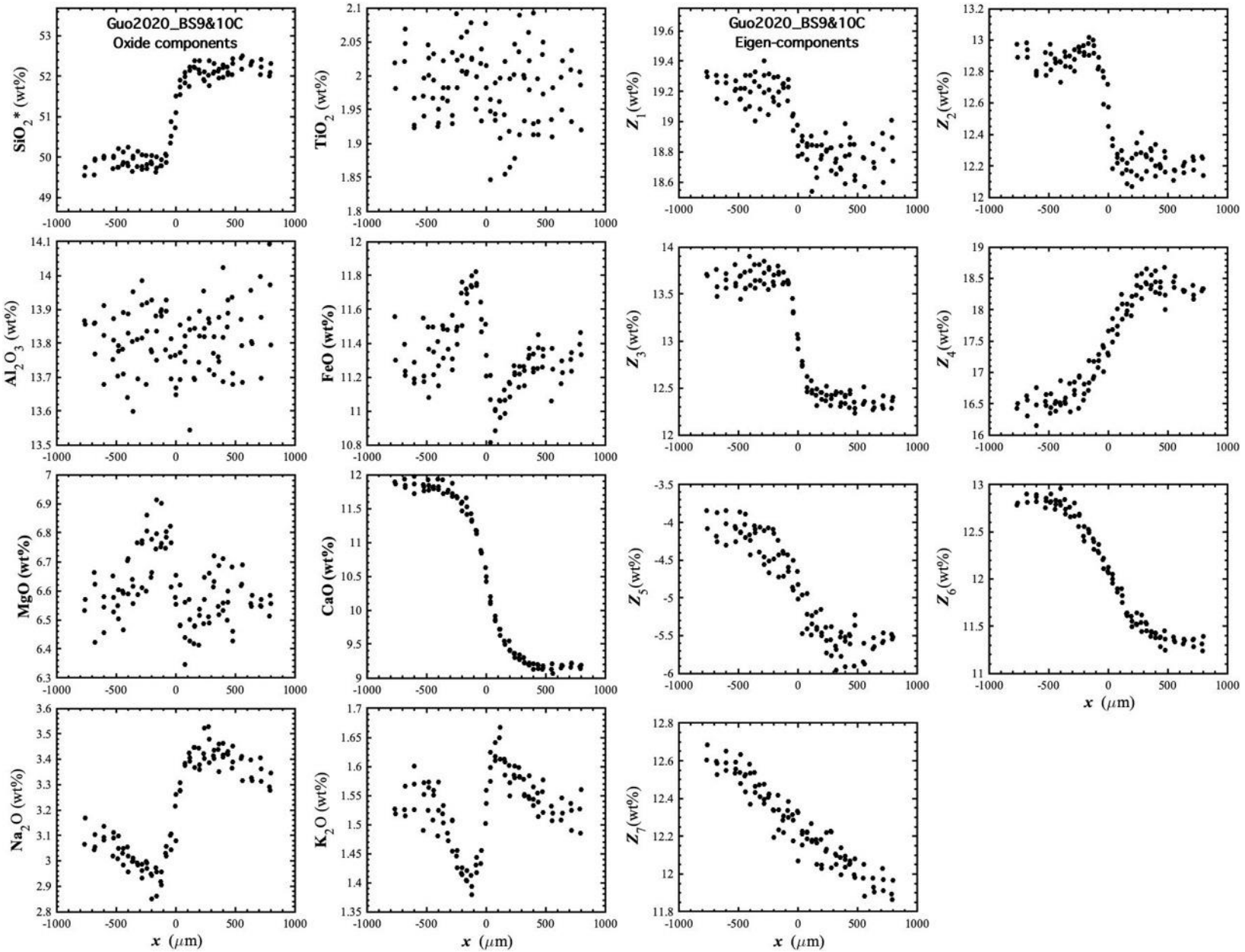

Figure 125. Concentration profiles of oxide components in wt% (left panel) and eigen-components (right panel) of Guo2020_BS9&10C, which is a diffusion couple experiment in basalt (Guo and Zhang, 2020).

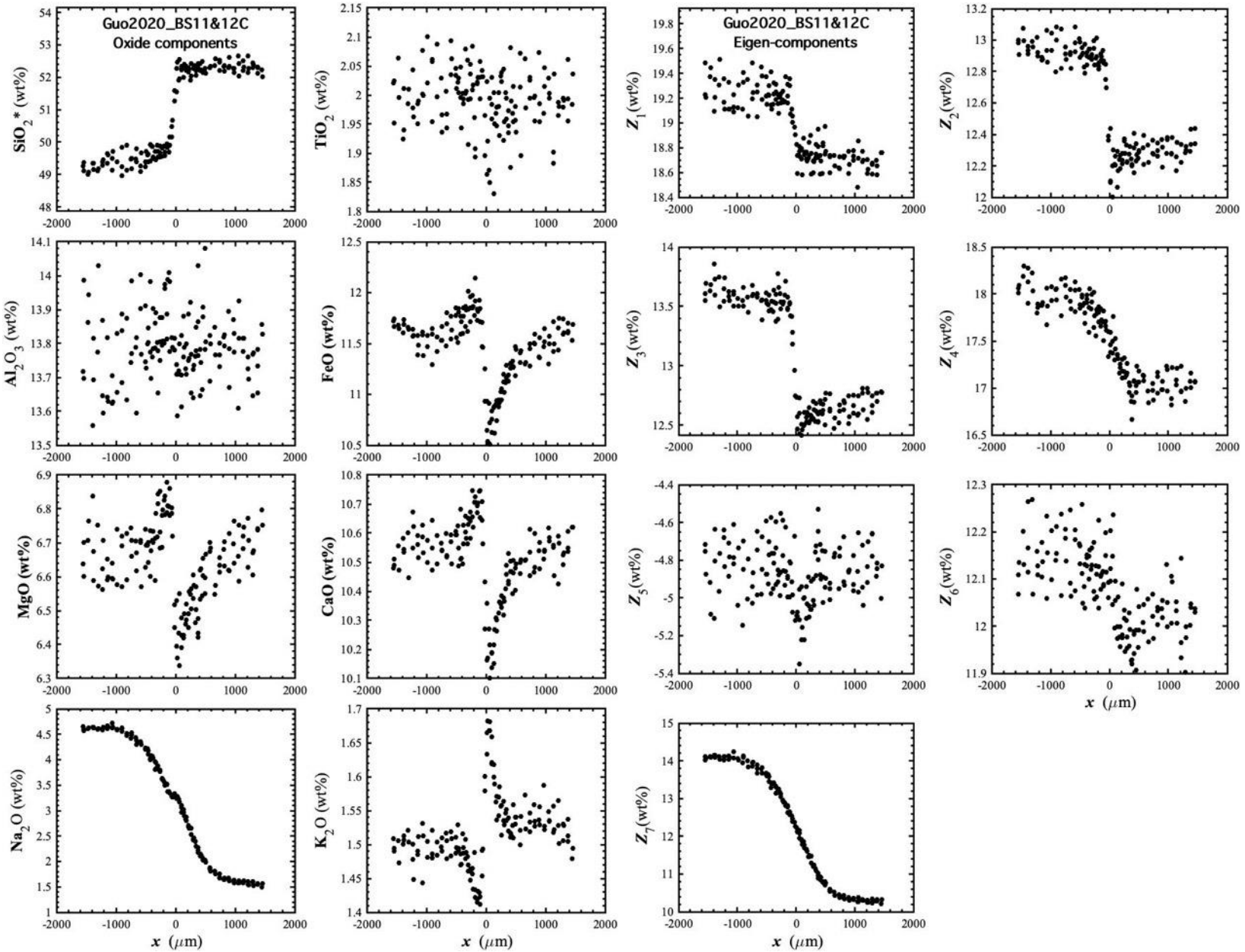

Figure 126. Concentration profiles of oxide components in wt% (left panel) and eigen-components (right panel) of Guo2020_BS11&12C, which is a diffusion couple experiment in basalt (Guo and Zhang, 2020).

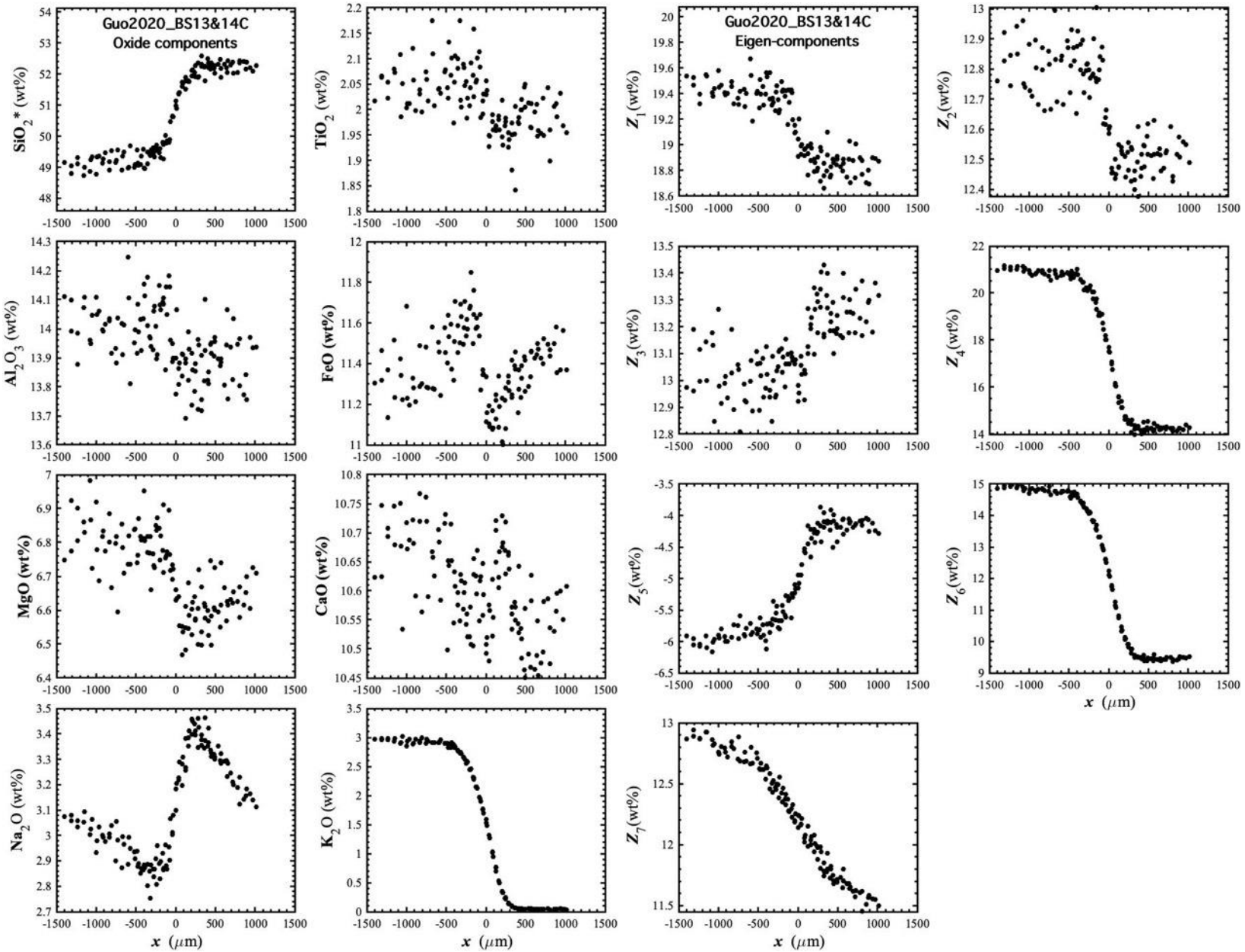

Figure 127. Concentration profiles of oxide components in wt% (left panel) and eigen-components (right panel) of Guo2020_BS13&14C, which is a diffusion couple experiment in basalt (Guo and Zhang, 2020).

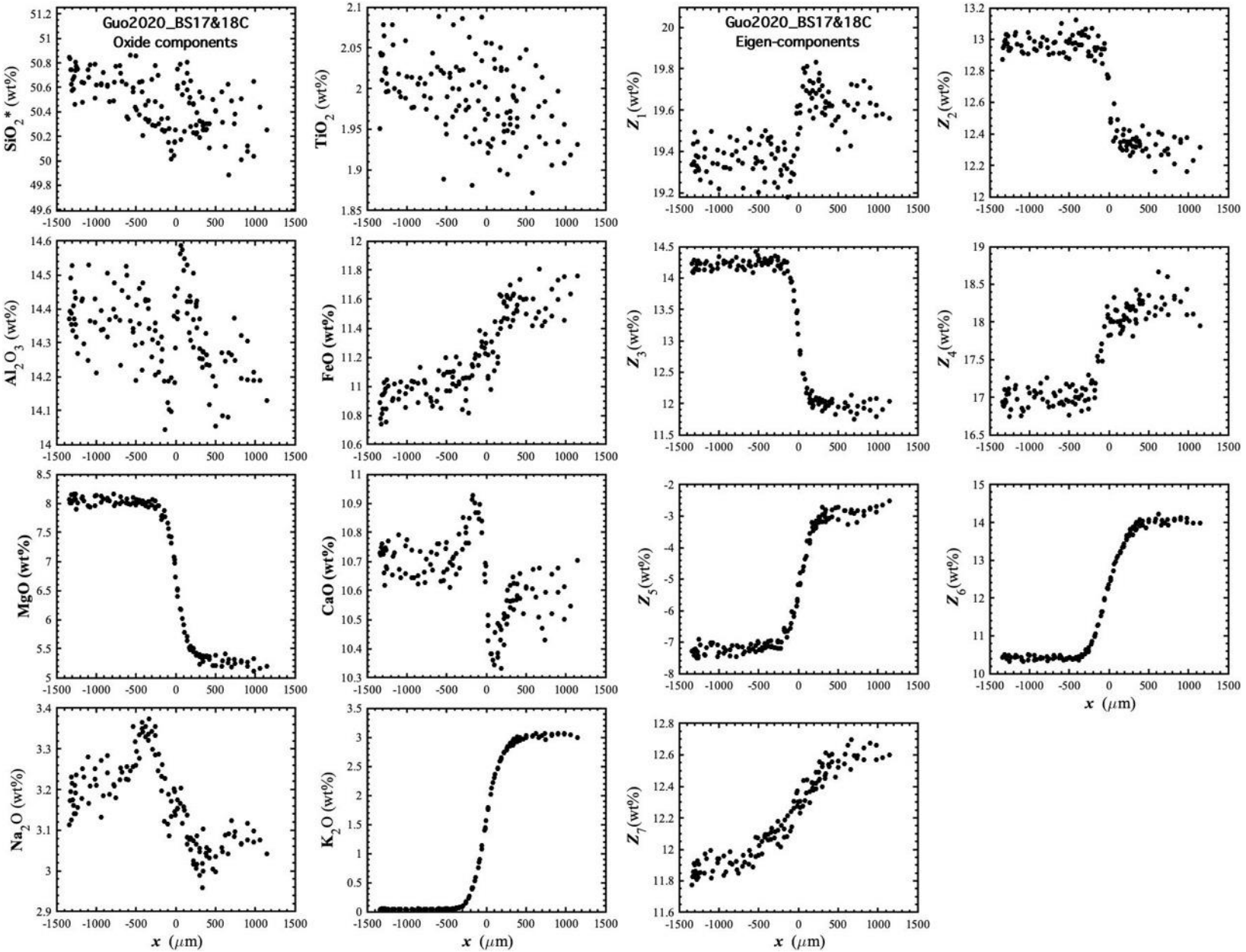

Figure 128. Concentration profiles of oxide components in wt% (left panel) and eigen-components (right panel) of Guo2020_BS17&18C, which is a diffusion couple experiment in basalt (Guo and Zhang, 2020).

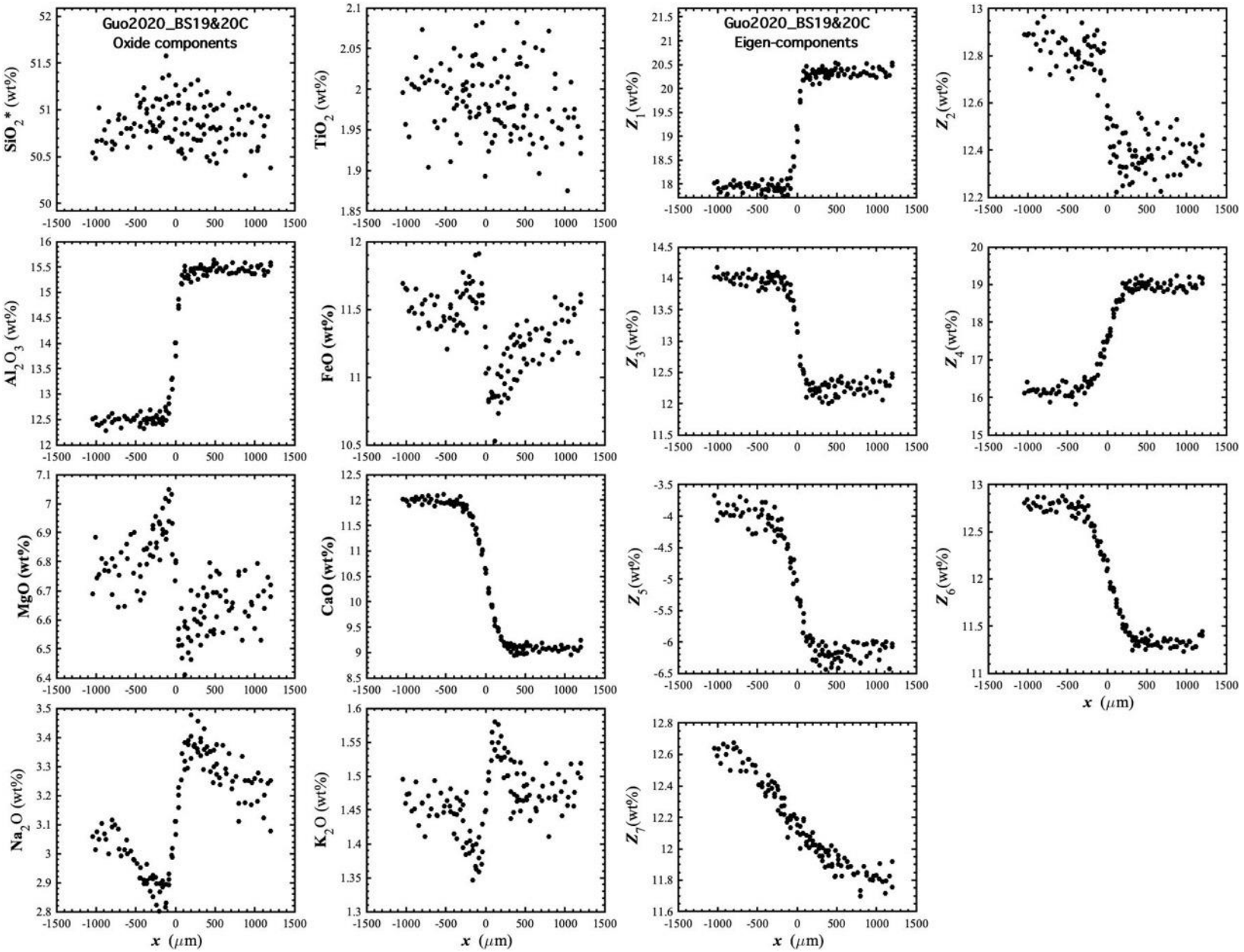

Figure 129. Concentration profiles of oxide components in wt% (left panel) and eigen-components (right panel) of Guo2020_BS19&20C, which is a diffusion couple experiment in basalt (Guo and Zhang, 2020).

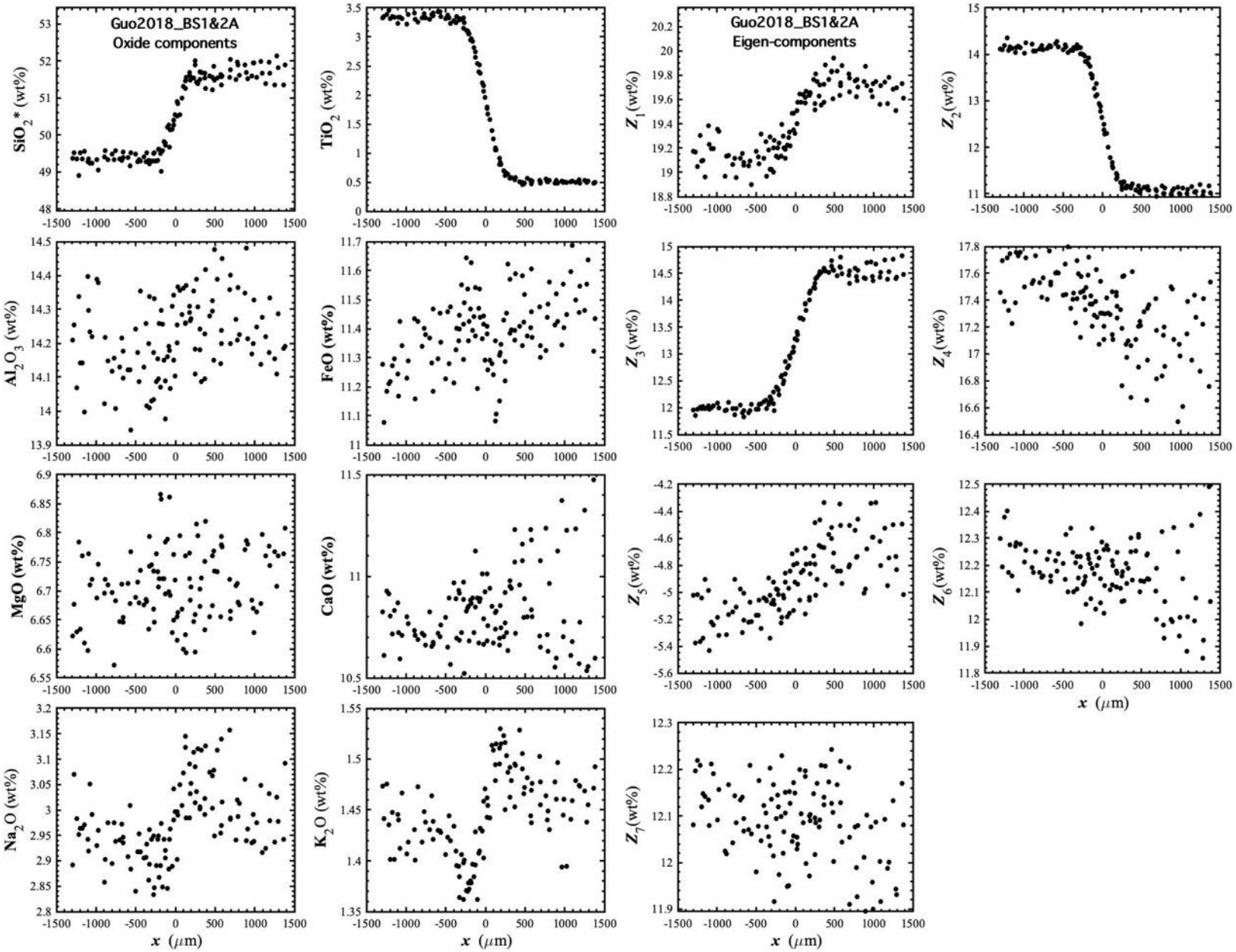

Figure 130. Concentration profiles of oxide components in wt% (left panel) and eigen-components (right panel) of Guo2018_BS1&2A, which is a diffusion couple experiment in basalt (Guo and Zhang, 2018).

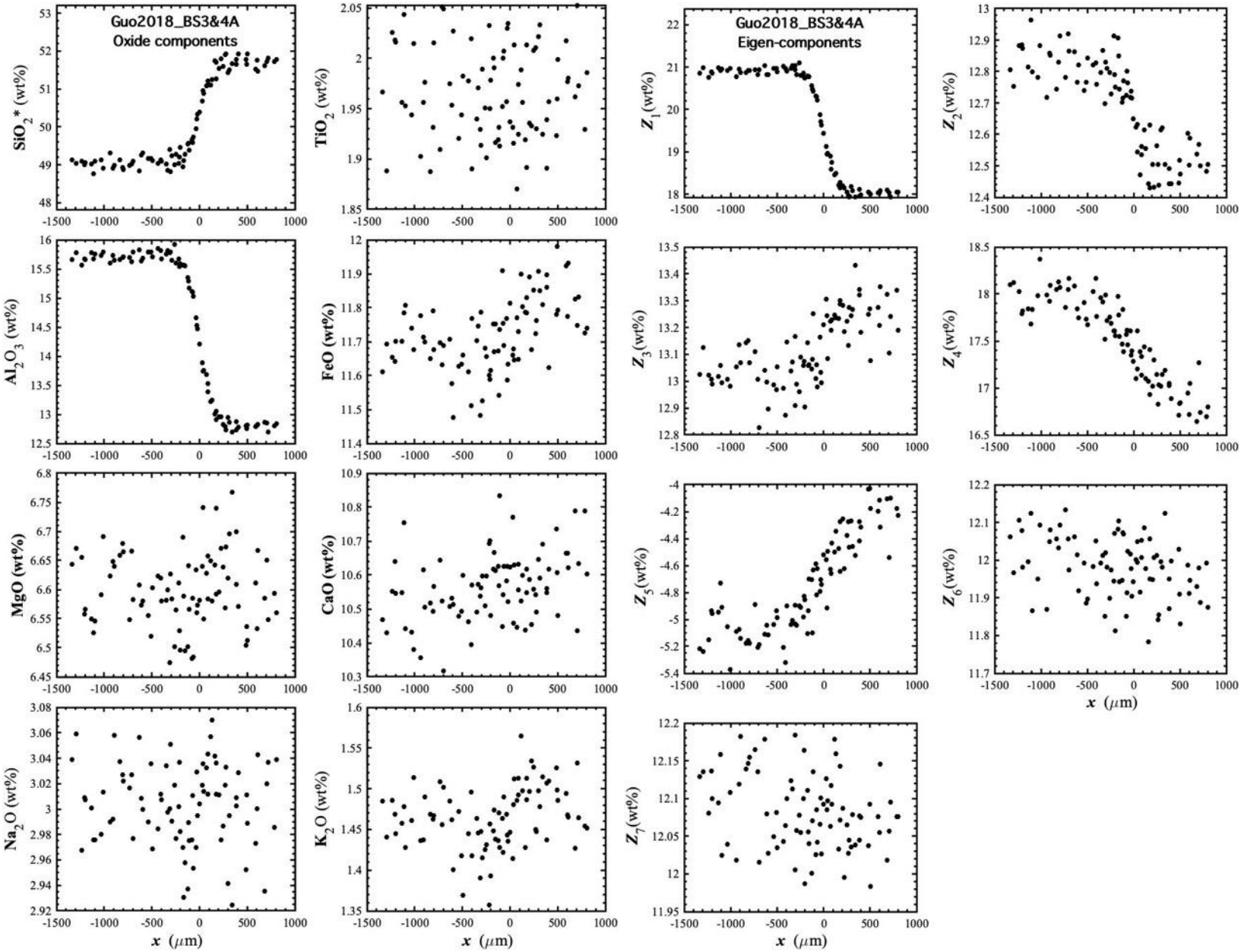

Figure 131. Concentration profiles of oxide components in wt% (left panel) and eigen-components (right panel) of Guo2018_BS3&4A, which is a diffusion couple experiment in basalt (Guo and Zhang, 2018).

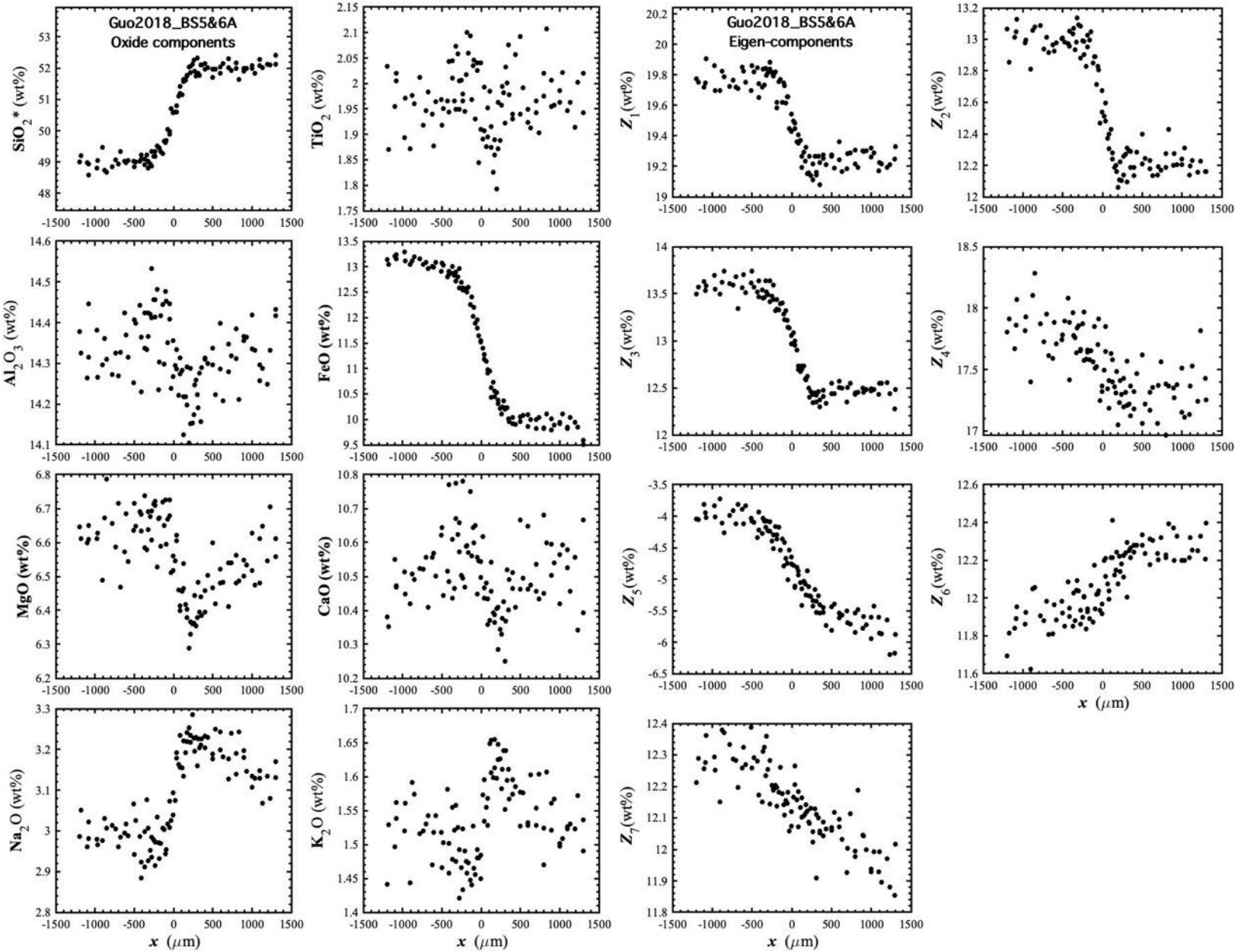

Figure 132. Concentration profiles of oxide components in wt% (left panel) and eigen-components (right panel) of Guo2018_BS5&6A, which is a diffusion couple experiment in basalt (Guo and Zhang, 2018).

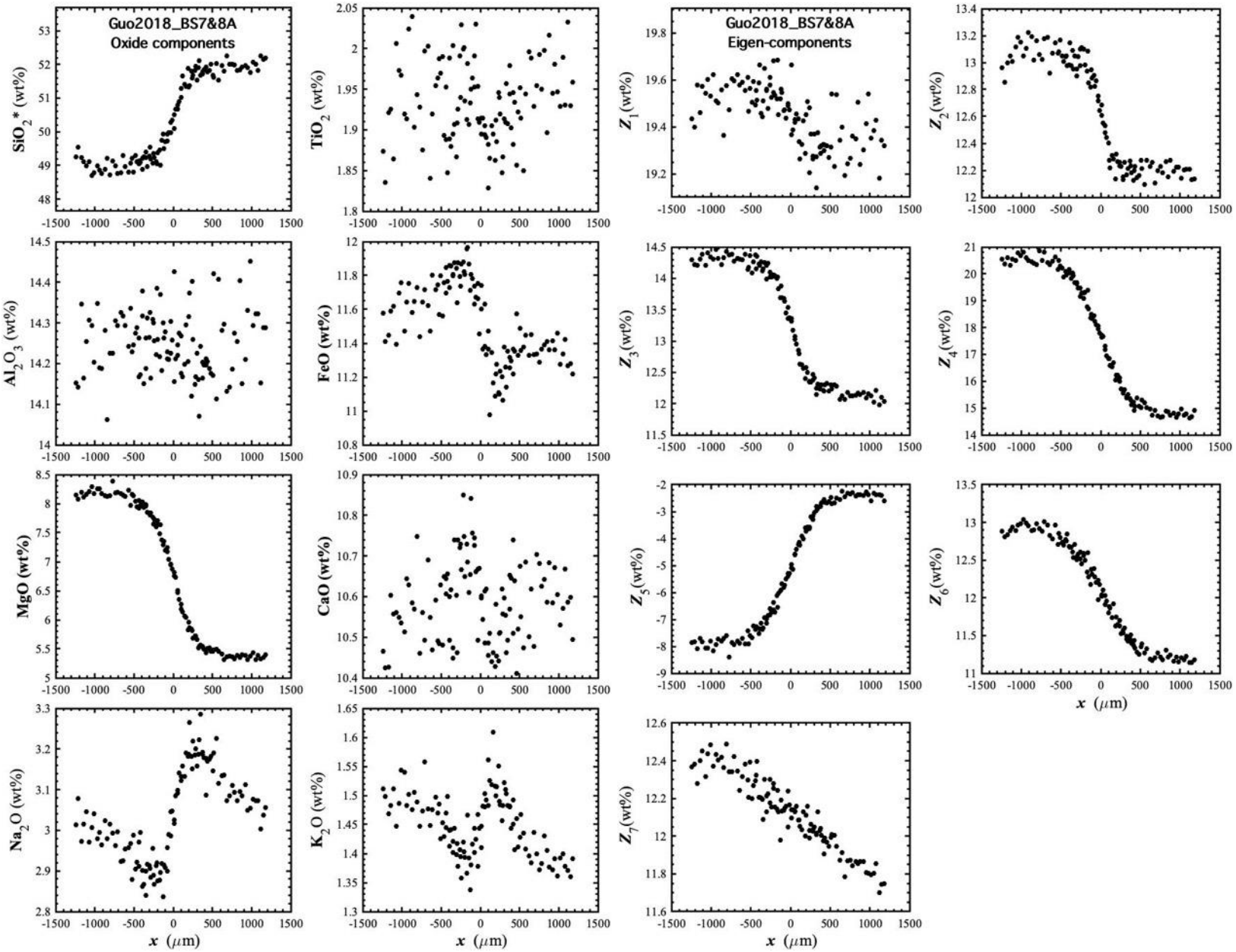

Figure 133. Concentration profiles of oxide components in wt% (left panel) and eigen-components (right panel) of Guo2018_BS7&8A, which is a diffusion couple experiment in basalt (Guo and Zhang, 2018).

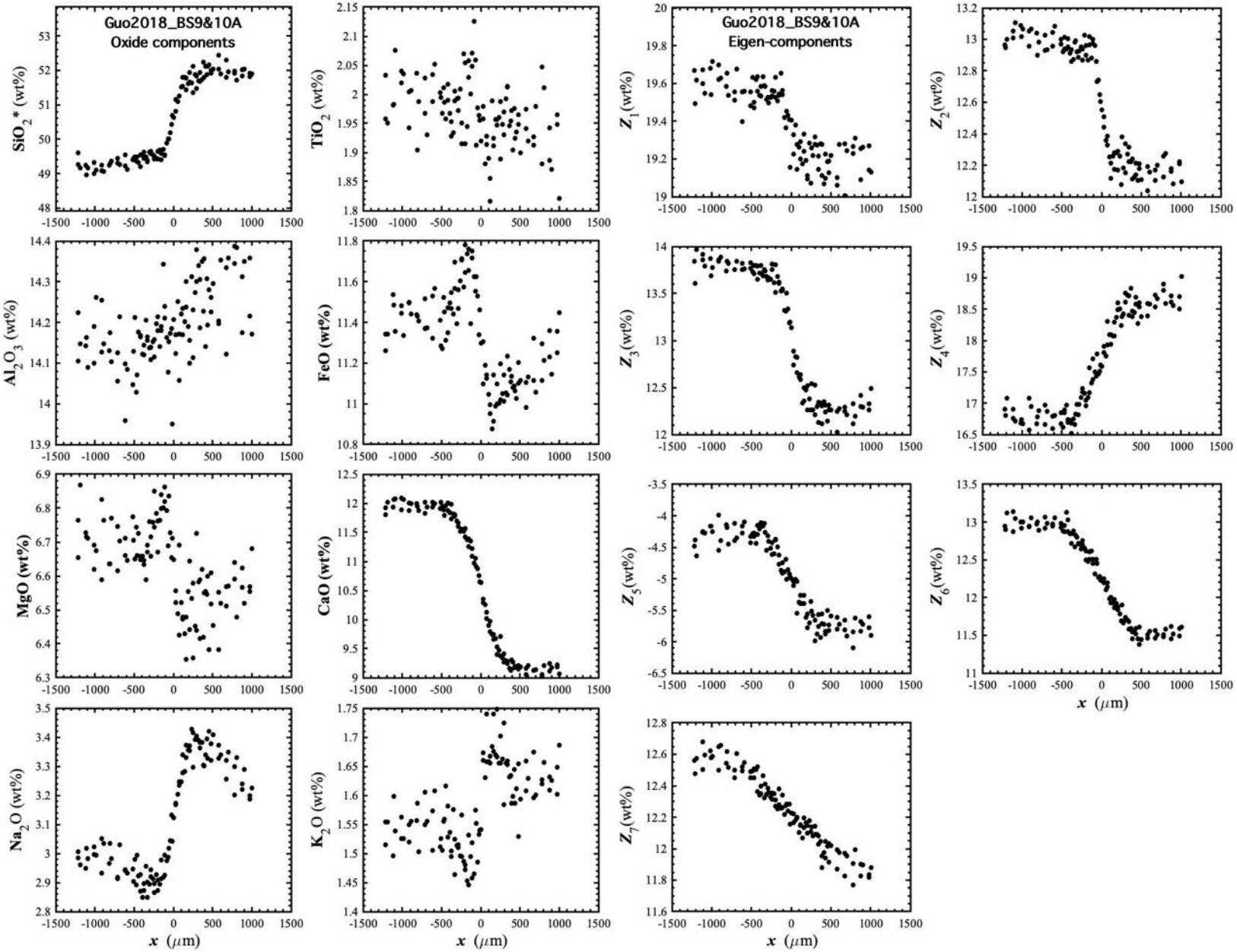

Figure 134. Concentration profiles of oxide components in wt% (left panel) and eigen-components (right panel) of Guo2018_BS9&10A, which is a diffusion couple experiment in basalt (Guo and Zhang, 2018).

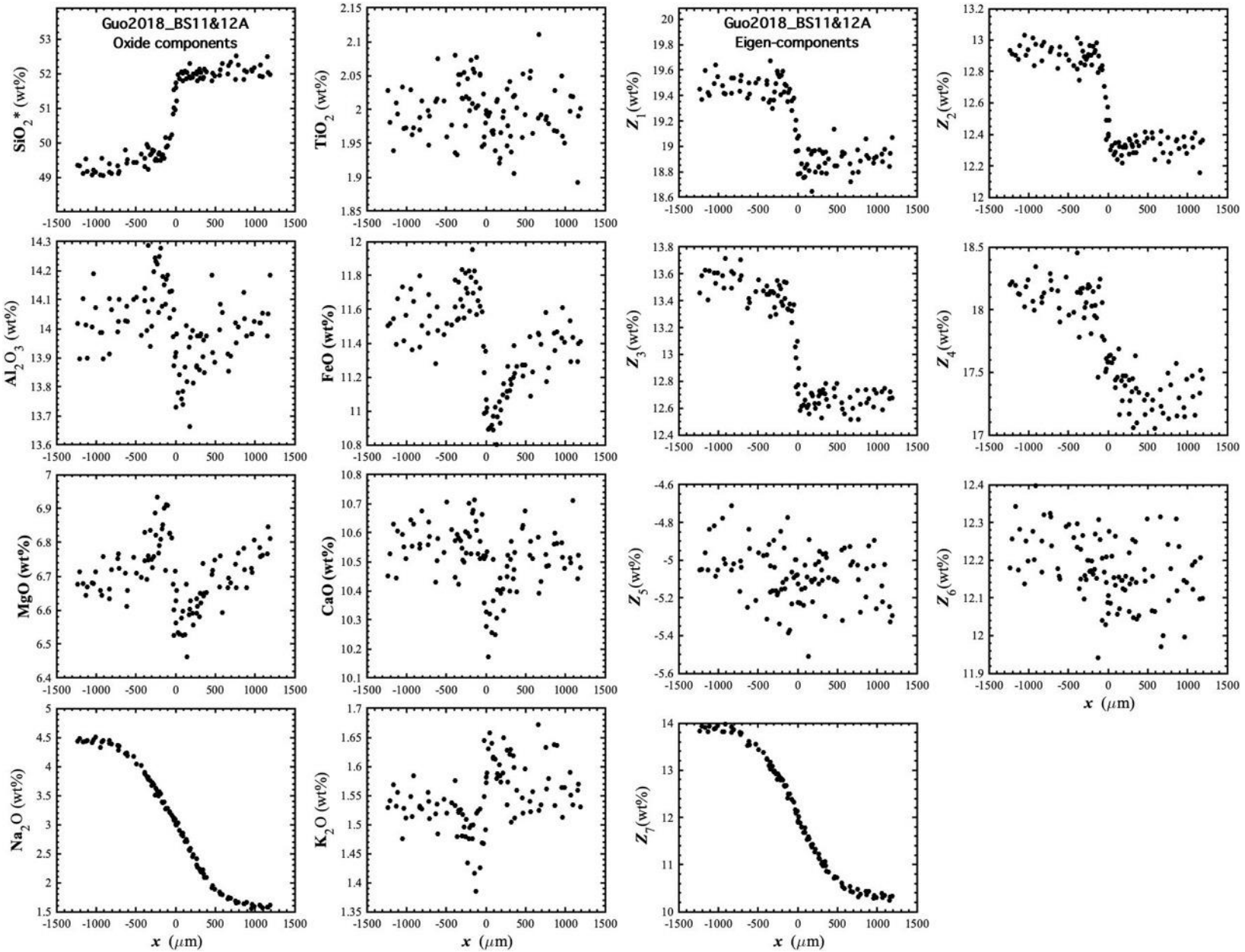

Figure 135. Concentration profiles of oxide components in wt% (left panel) and eigen-components (right panel) of Guo2018_BS11&12A, which is a diffusion couple experiment in basalt (Guo and Zhang, 2018).

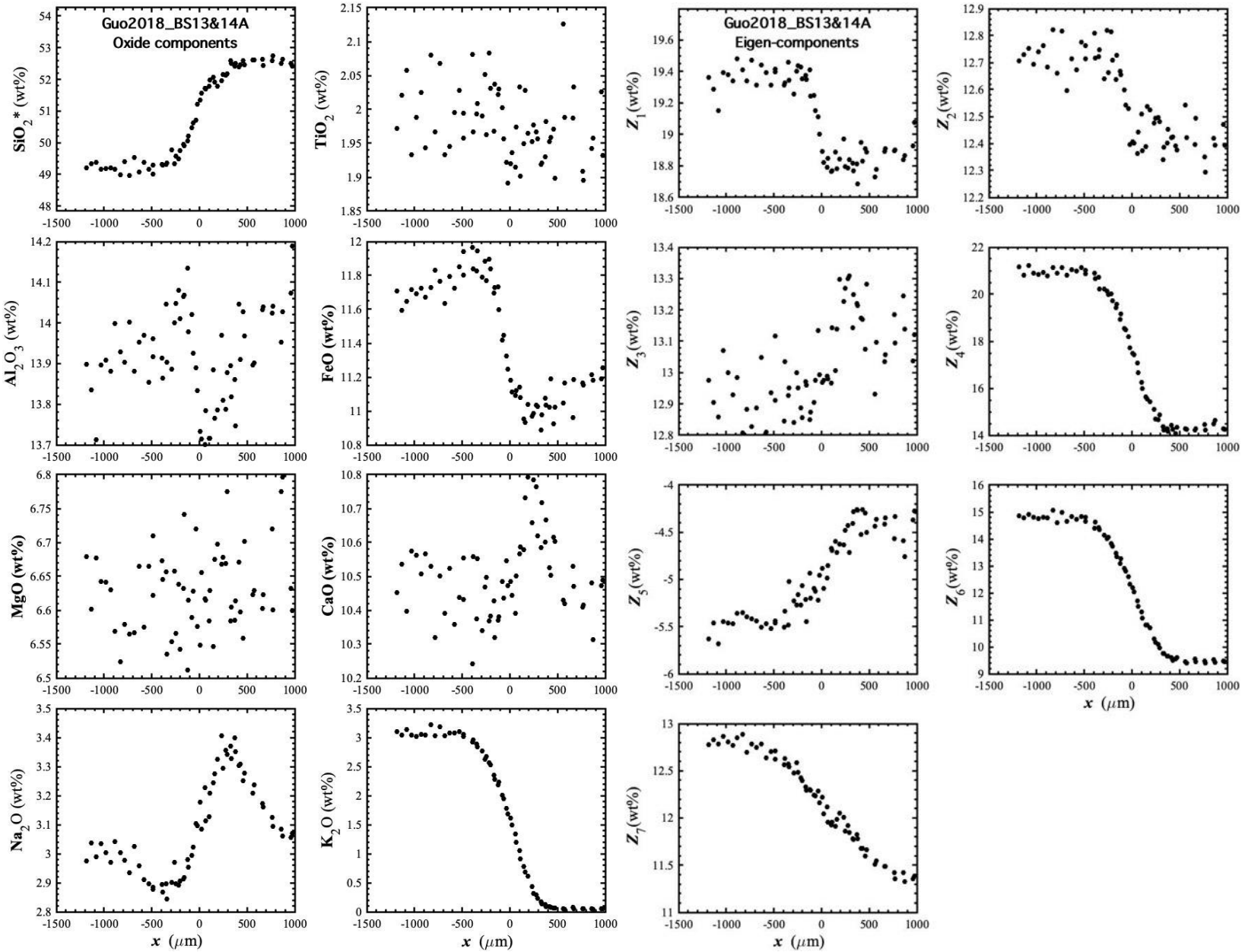

Figure 136. Concentration profiles of oxide components in wt% (left panel) and eigen-components (right panel) of Guo2018_BS13&14A, which is a diffusion couple experiment in basalt (Guo and Zhang, 2018).

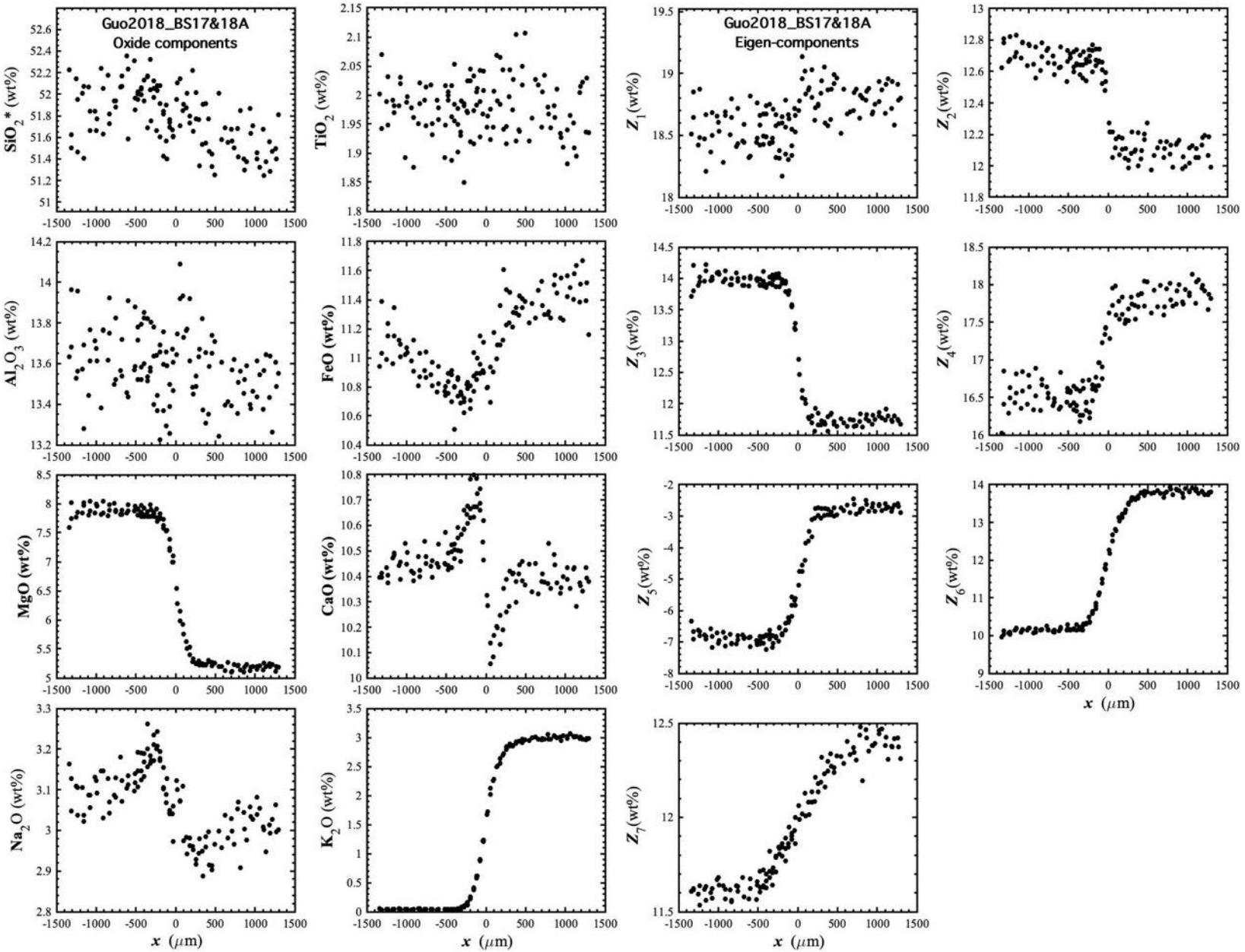

Figure 137. Concentration profiles of oxide components in wt% (left panel) and eigen-components (right panel) of Guo2018_BS17&18A, which is a diffusion couple experiment in basalt (Guo and Zhang, 2018).

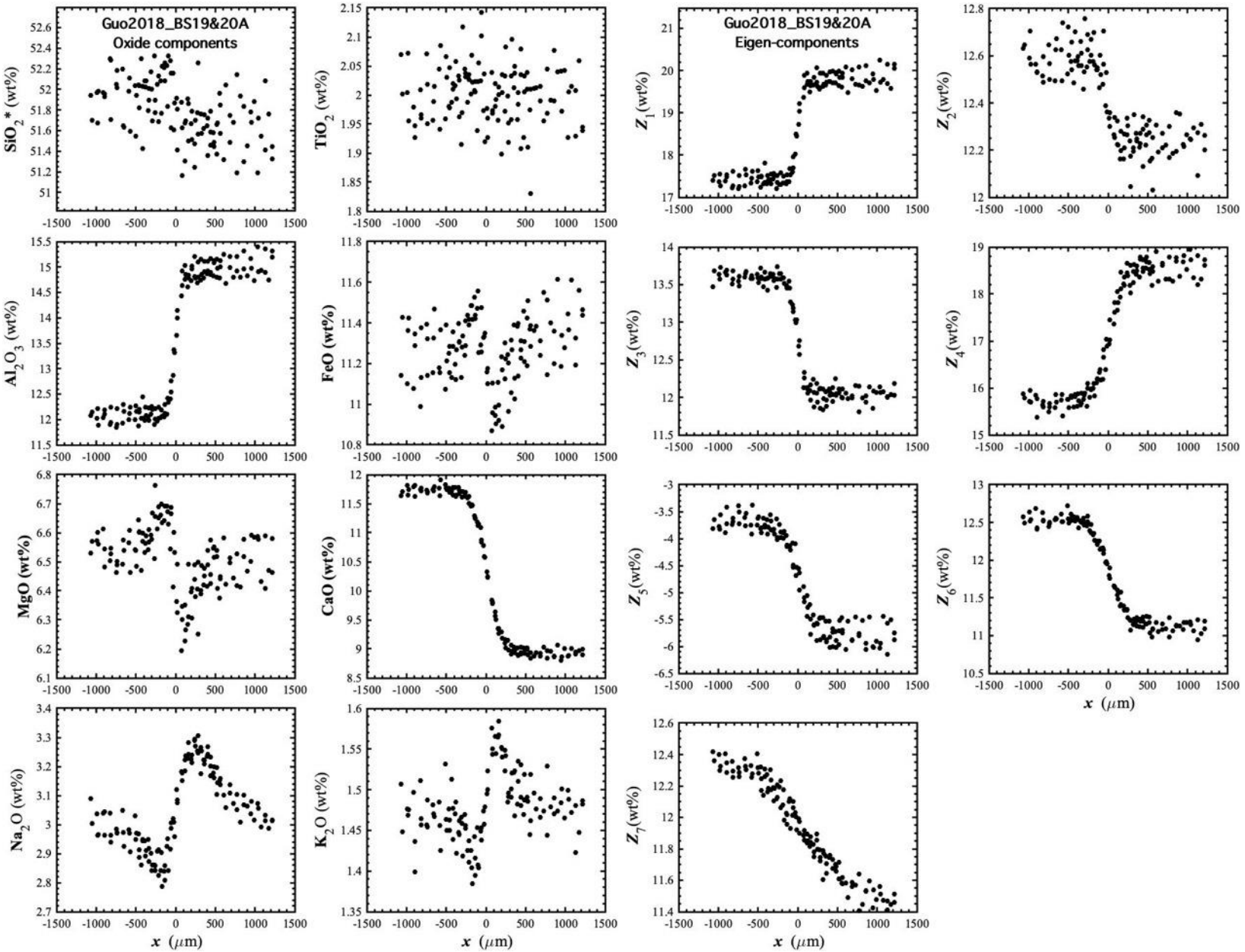

Figure 138. Concentration profiles of oxide components in wt% (left panel) and eigen-components (right panel) of Guo2018_BS19&20A, which is a diffusion couple experiment in basalt (Guo and Zhang, 2018).

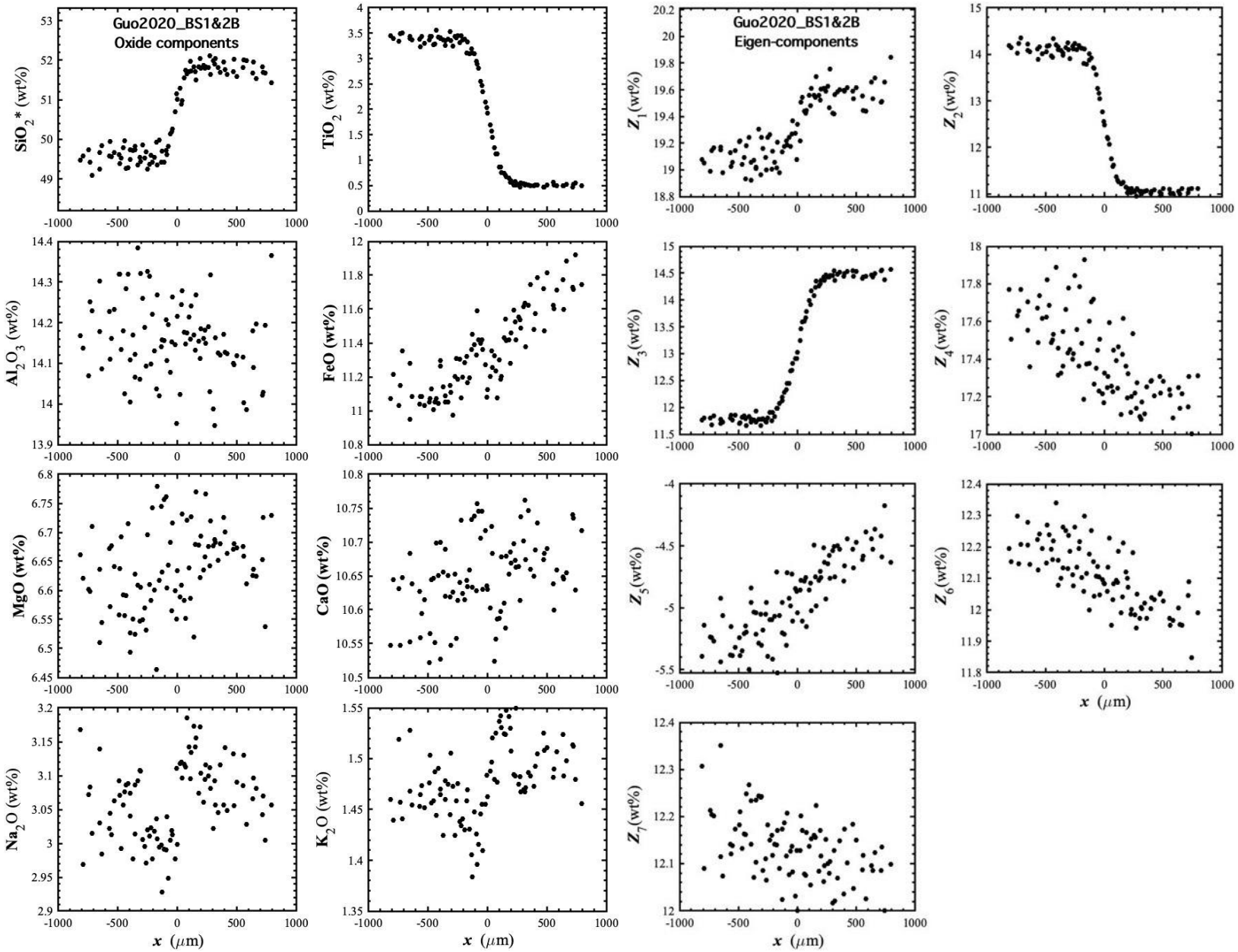

Figure 139. Concentration profiles of oxide components in wt% (left panel) and eigen-components (right panel) of Guo2020_BS1&2B, which is a diffusion couple experiment in basalt (Guo and Zhang, 2020).

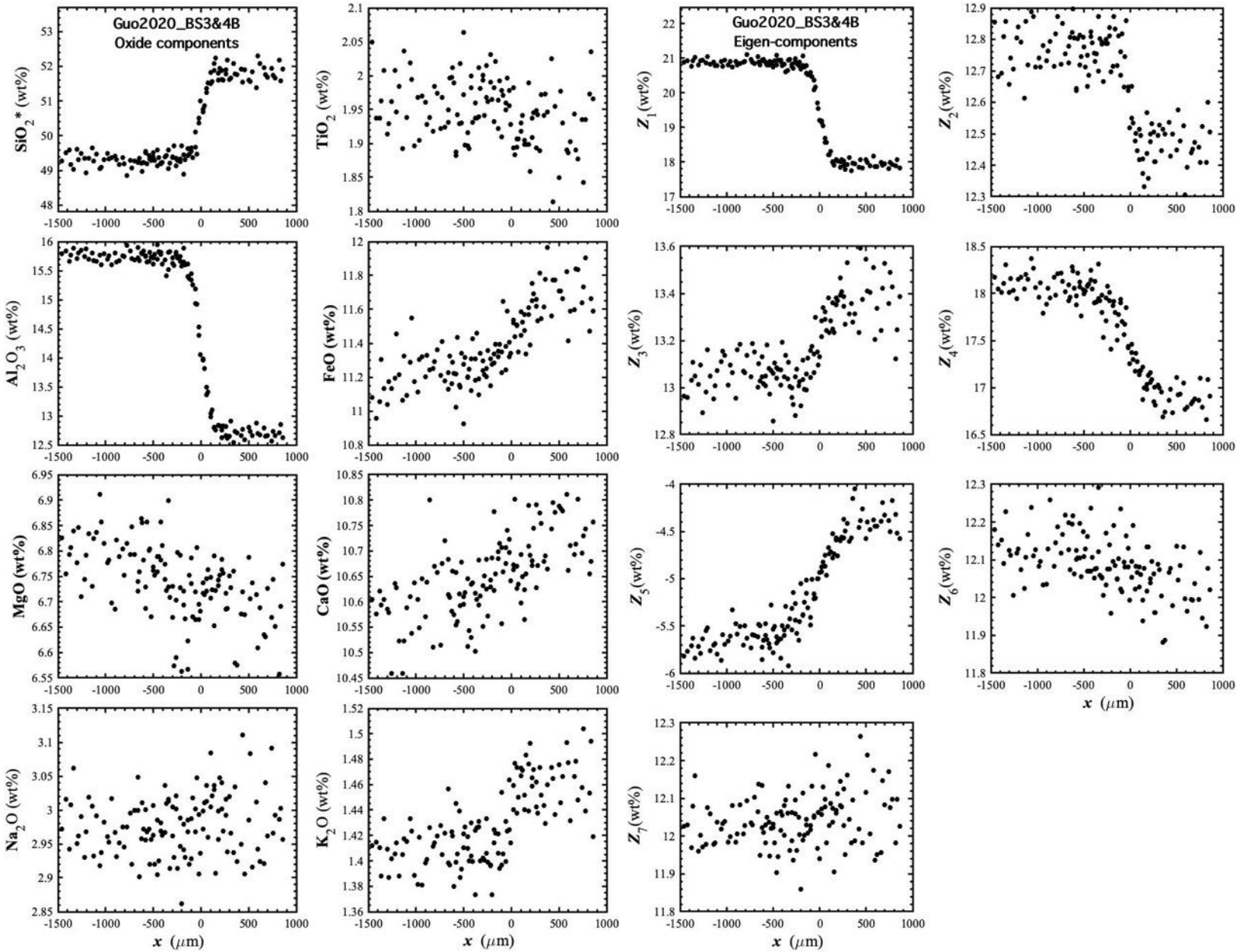

Figure 140. Concentration profiles of oxide components in wt% (left panel) and eigen-components (right panel) of Guo2020_BS3&4B, which is a diffusion couple experiment in basalt (Guo and Zhang, 2020).

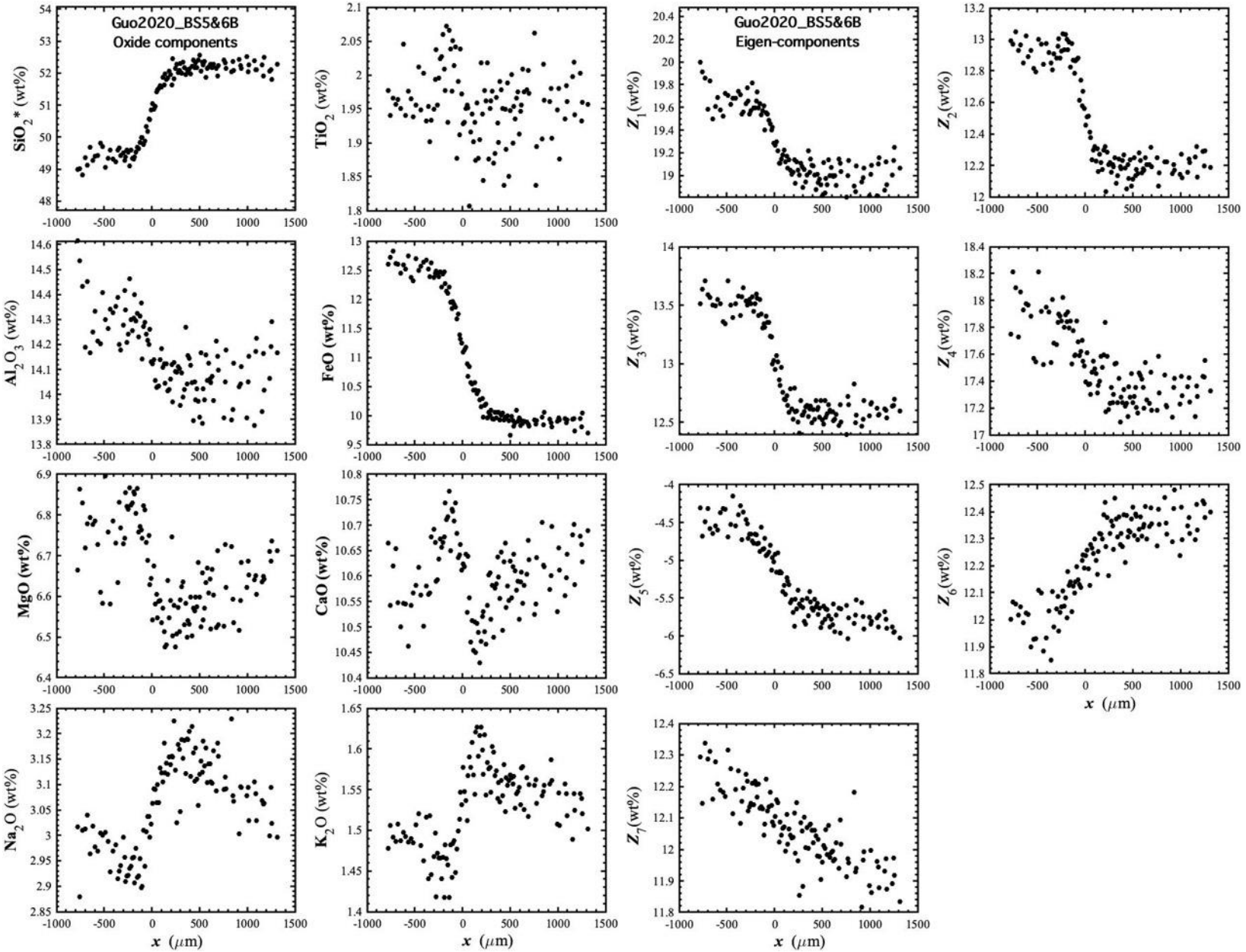

Figure 141. Concentration profiles of oxide components in wt% (left panel) and eigen-components (right panel) of Guo2020_BS5&6B, which is a diffusion couple experiment in basalt (Guo and Zhang, 2020).

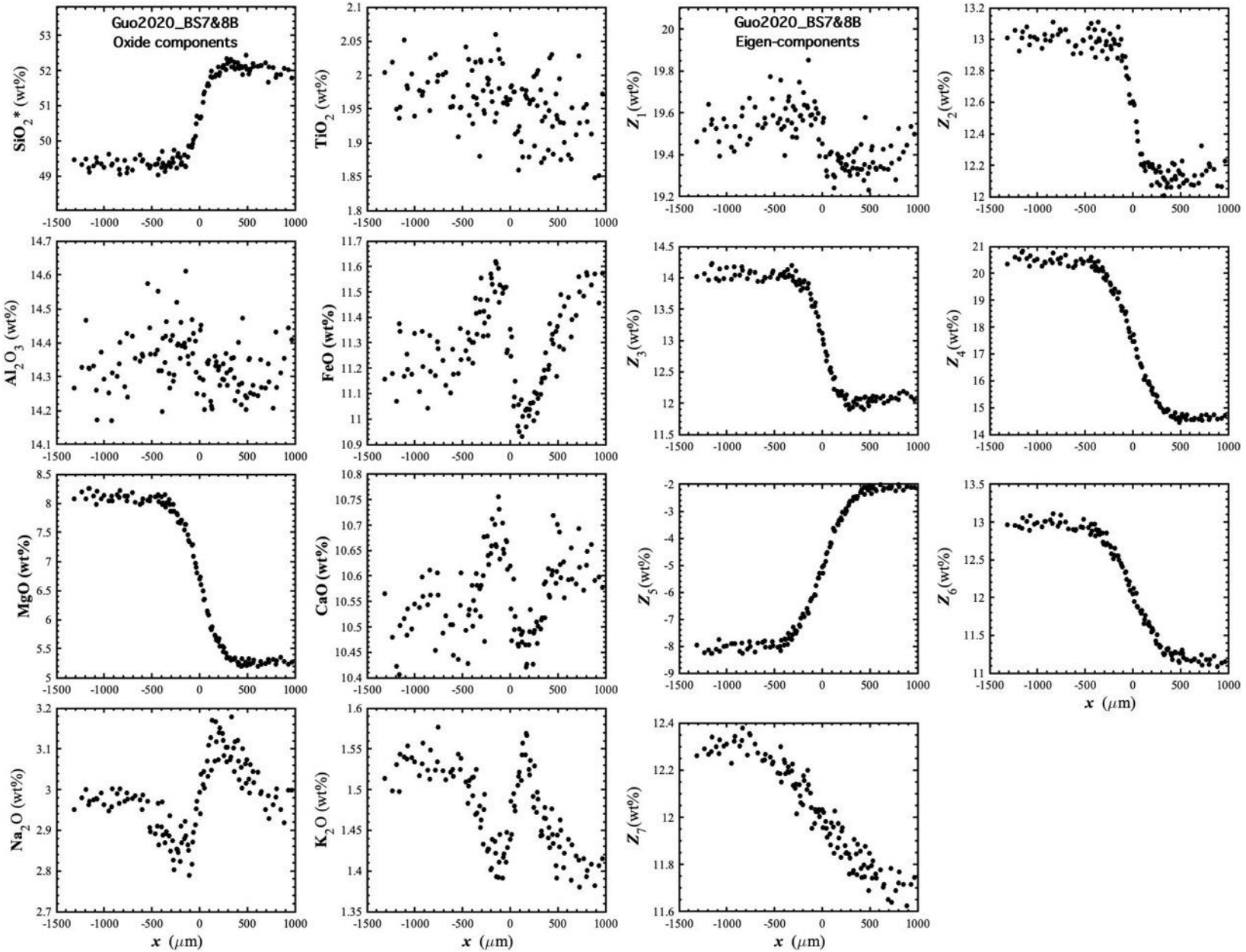

Figure 142. Concentration profiles of oxide components in wt% (left panel) and eigen-components (right panel) of Guo2020_BS7&8B, which is a diffusion couple experiment in basalt (Guo and Zhang, 2020).

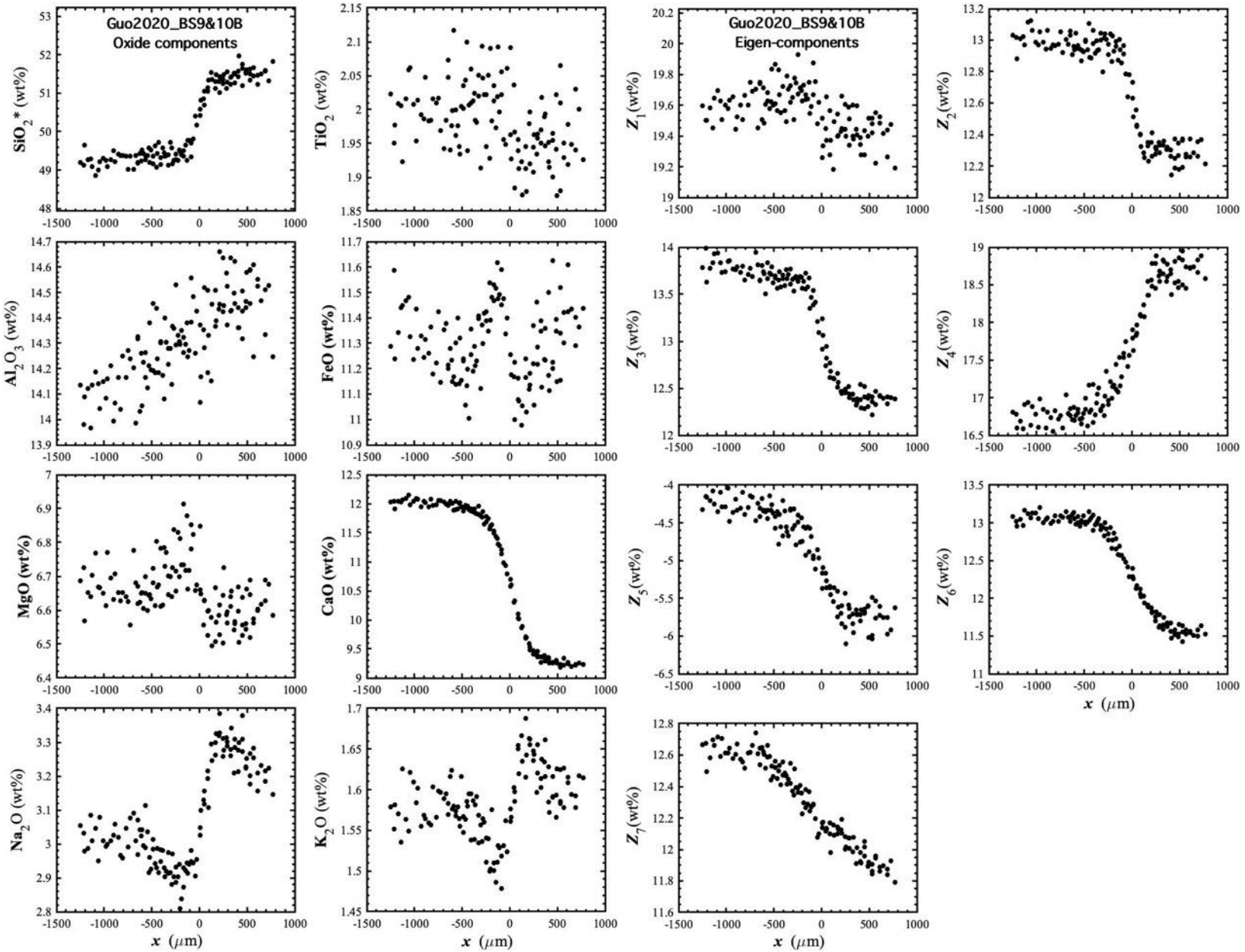

Figure 143. Concentration profiles of oxide components in wt% (left panel) and eigen-components (right panel) of Guo2020_BS9&10B, which is a diffusion couple experiment in basalt (Guo and Zhang, 2020).

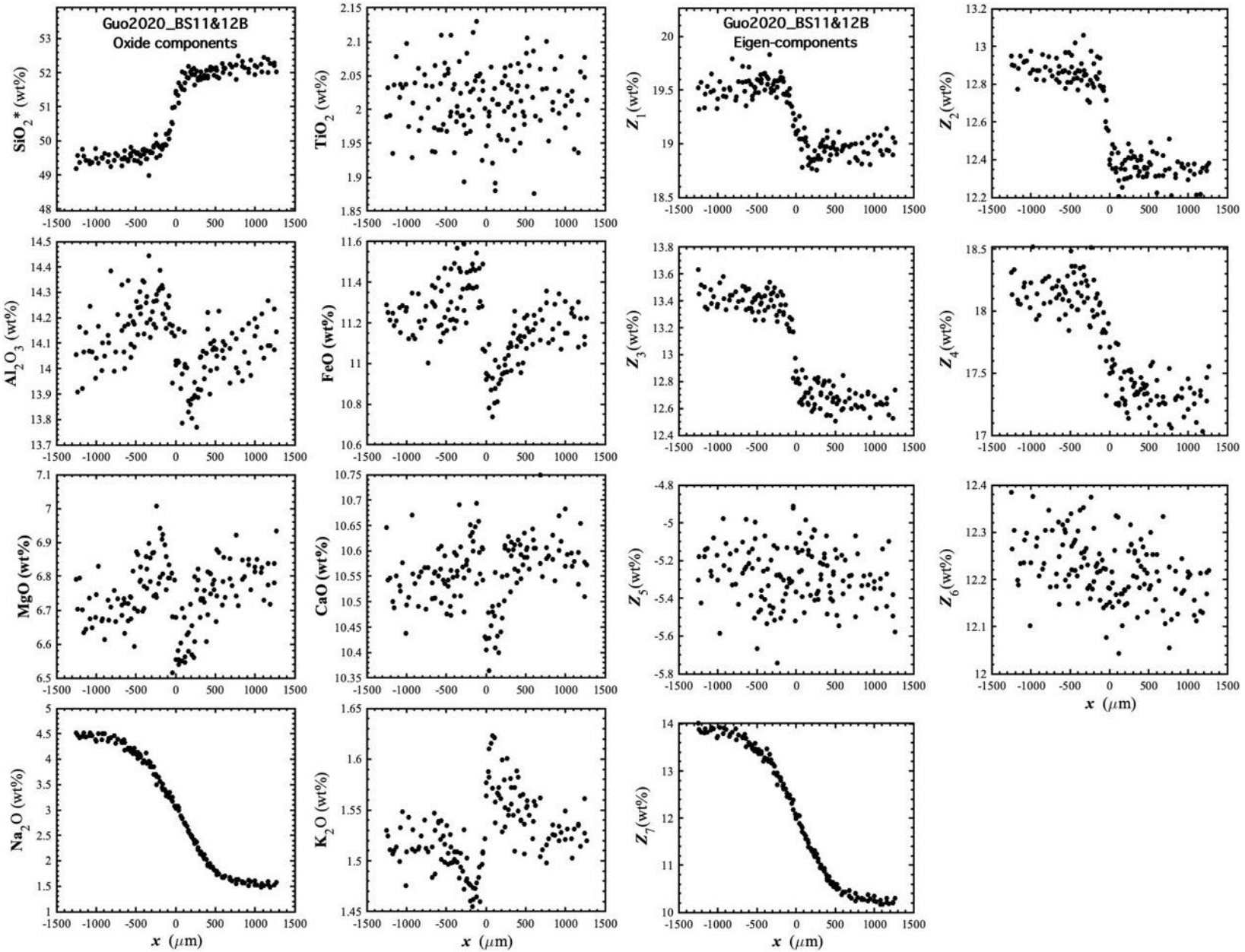

Figure 144. Concentration profiles of oxide components in wt% (left panel) and eigen-components (right panel) of Guo2020_BS11&12B, which is a diffusion couple experiment in basalt (Guo and Zhang, 2020).

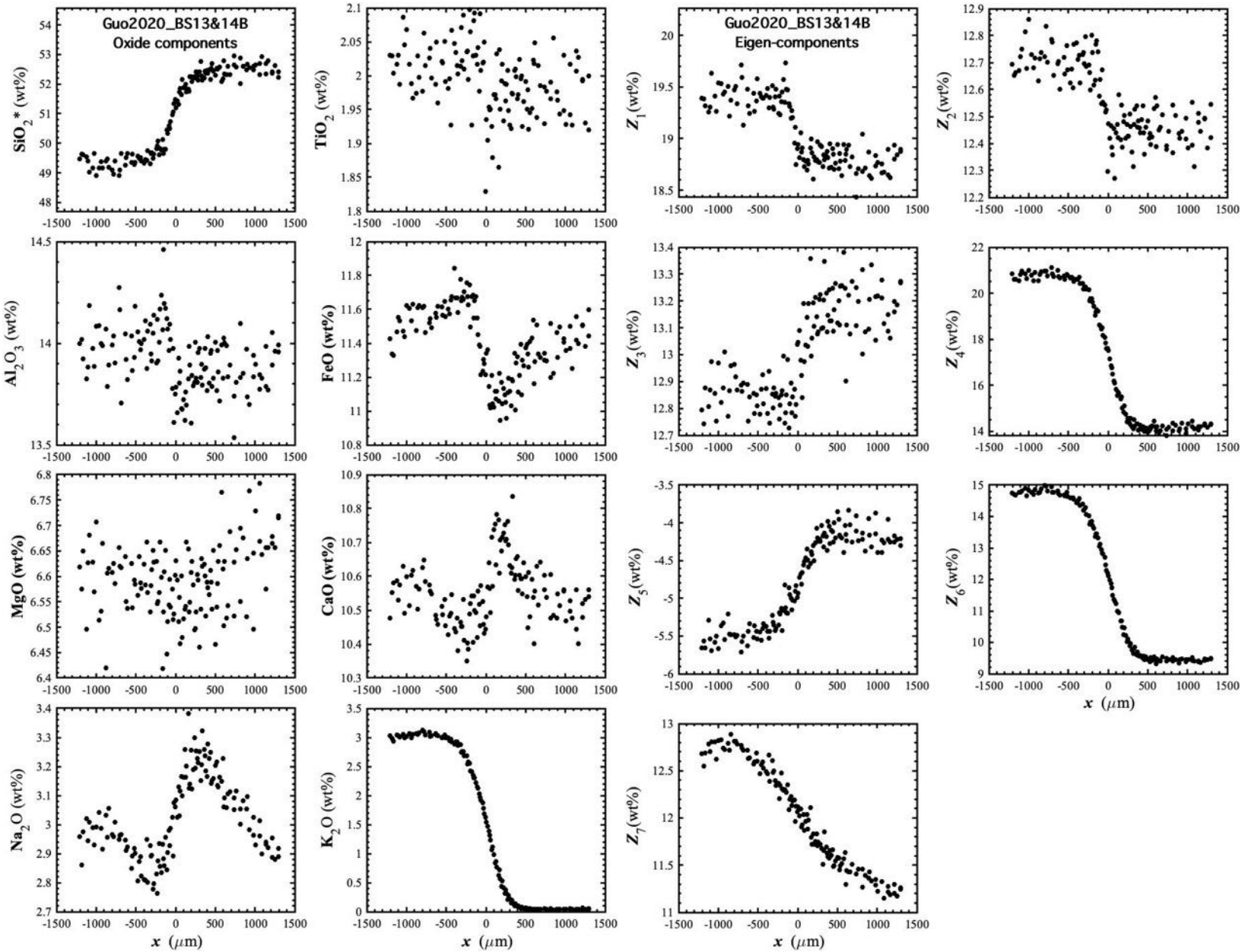

Figure 145. Concentration profiles of oxide components in wt% (left panel) and eigen-components (right panel) of Guo2020_BS13&14B, which is a diffusion couple experiment in basalt (Guo and Zhang, 2020).

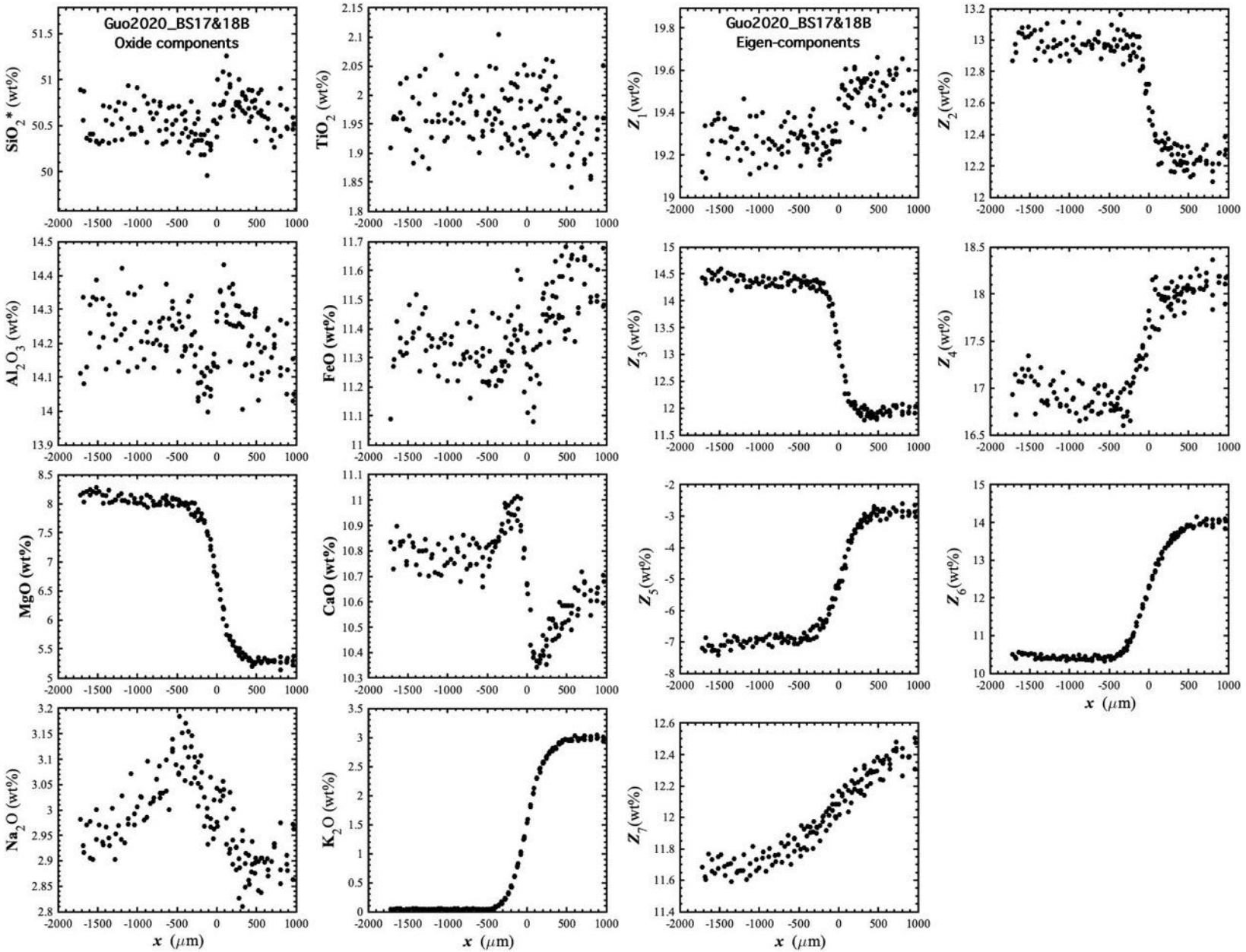

Figure 146. Concentration profiles of oxide components in wt% (left panel) and eigen-components (right panel) of Guo2020_BS17&18B, which is a diffusion couple experiment in basalt (Guo and Zhang, 2020).

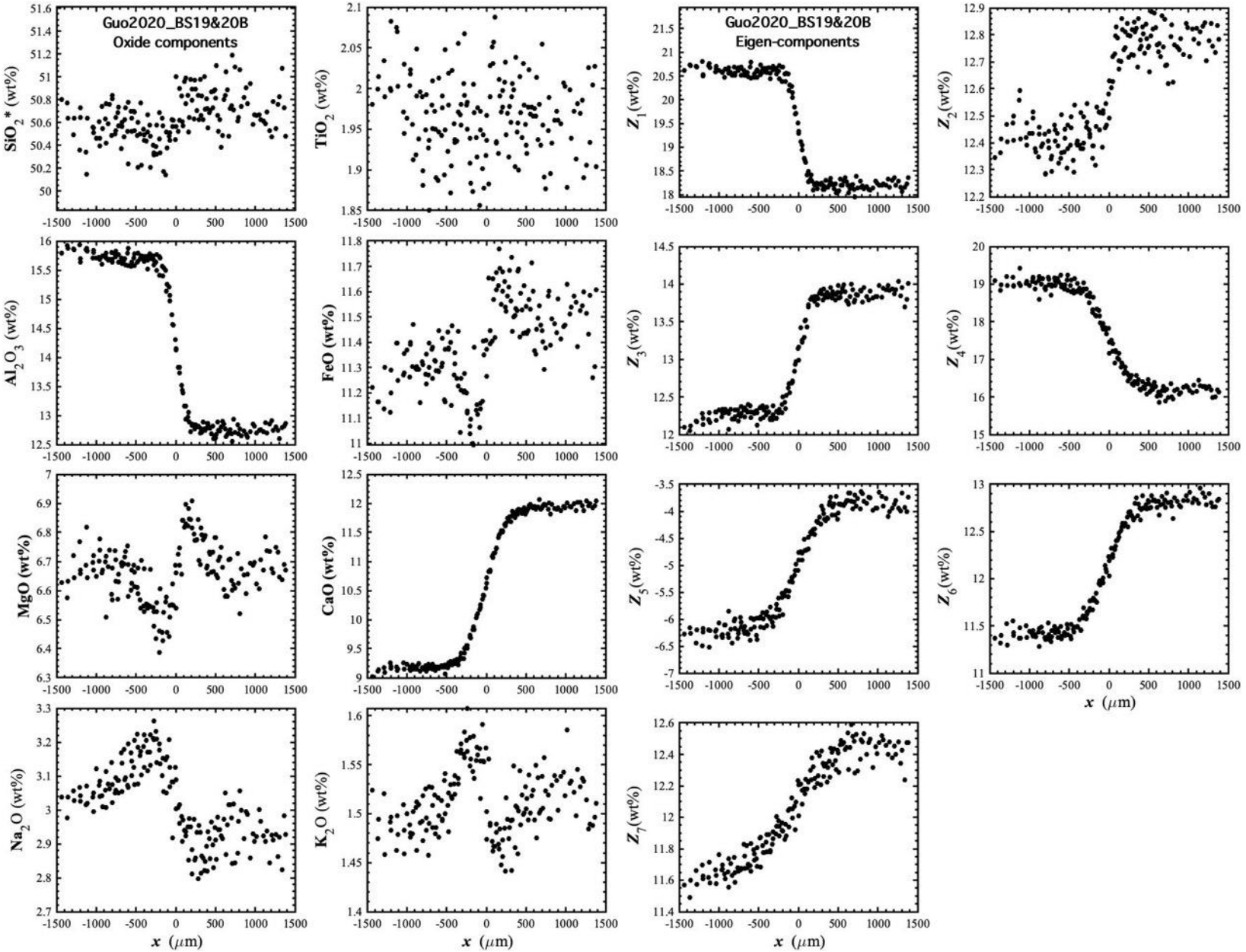

Figure 147. Concentration profiles of oxide components in wt% (left panel) and eigen-components (right panel) of Guo2020_BS19&20B, which is a diffusion couple experiment in basalt (Guo and Zhang, 2020).

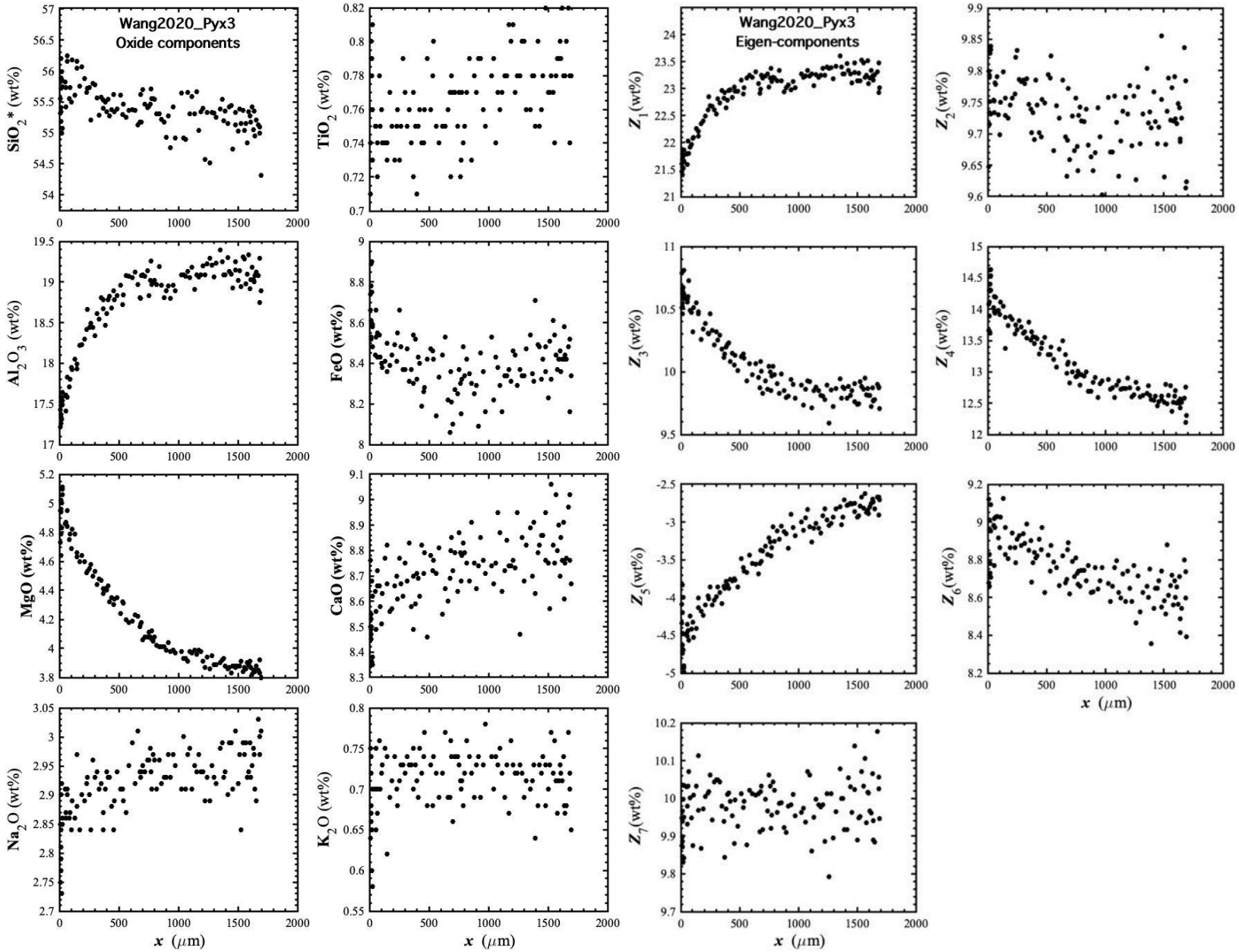

Figure 148. Concentration profiles of oxide components in wt% (left panel) and eigen-components (right panel) of Wang2020_Pyx3, which is a lherzolite dissolution experiment in basaltic andesite (Wang et al., 2020).

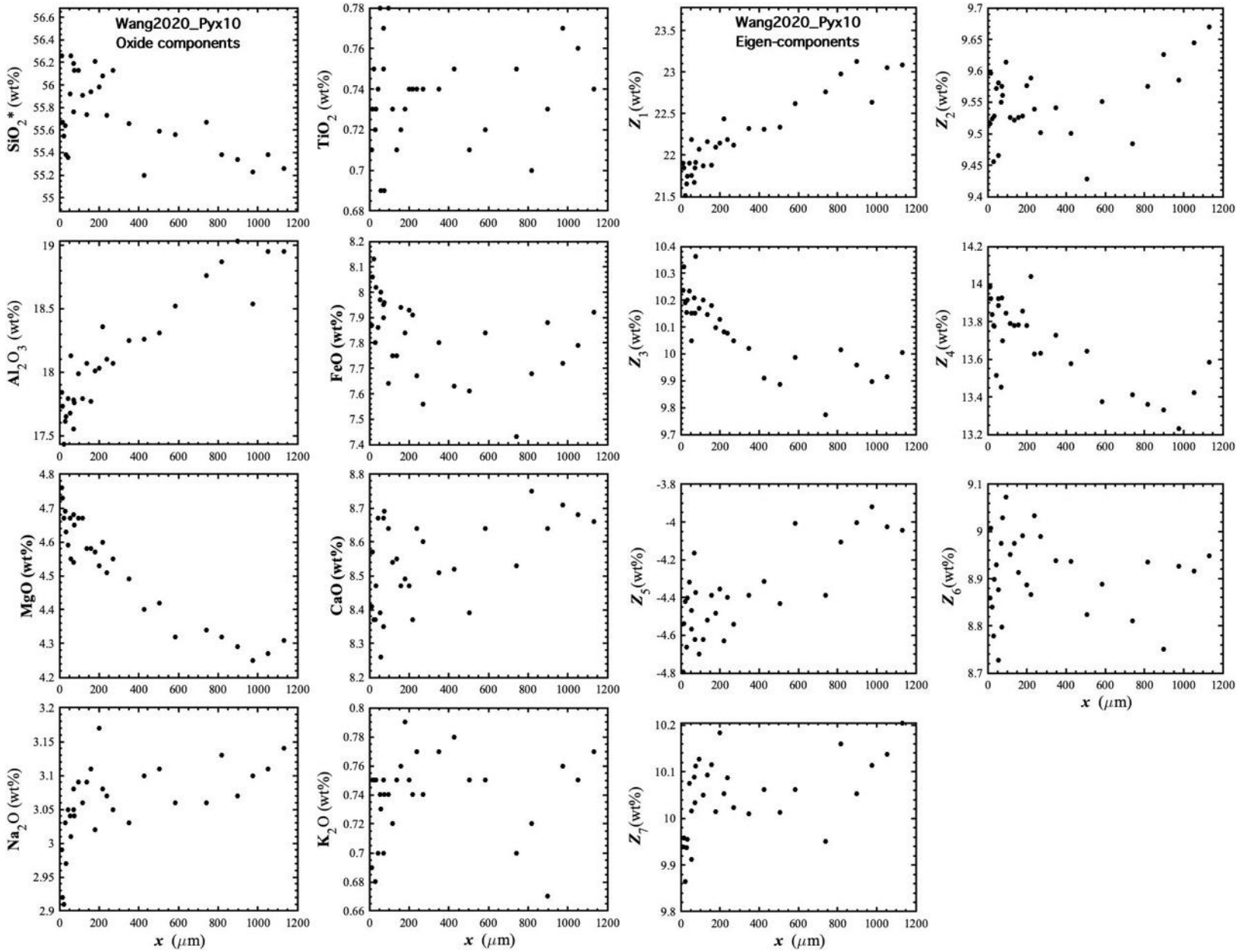

Figure 149. Concentration profiles of oxide components in wt% (left panel) and eigen-components (right panel) of Wang2020_Pyx10, which is a lherzolite dissolution experiment in basaltic andesite (Wang et al., 2020).

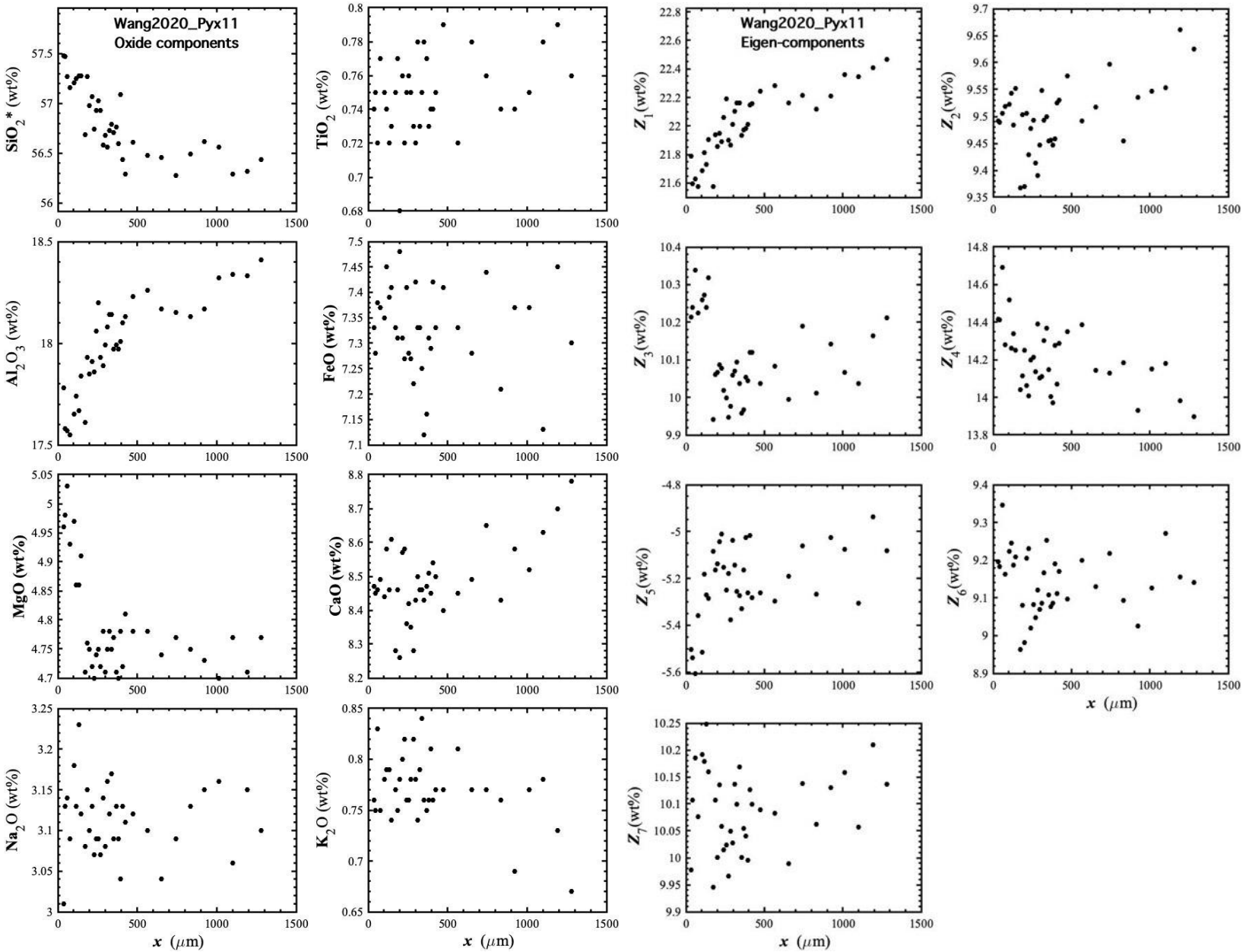

Figure 150. Concentration profiles of oxide components in wt% (left panel) and eigen-components (right panel) of Wang2020_Pyx11, which is a lherzolite dissolution experiment in basaltic andesite (Wang et al., 2020).

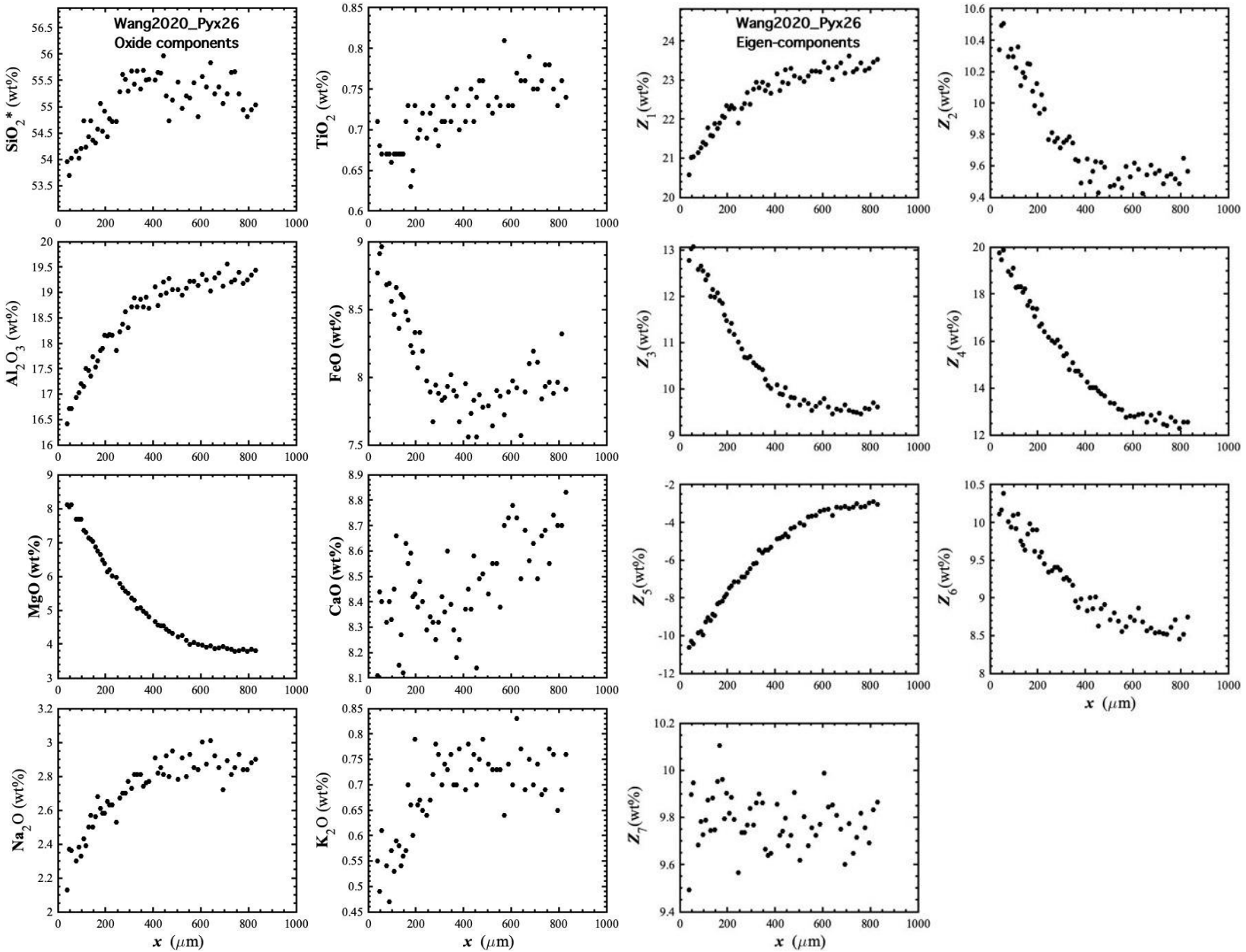

Figure 151. Concentration profiles of oxide components in wt% (left panel) and eigen-components (right panel) of Wang2020_Pyx26, which is a lherzolite dissolution experiment in basaltic andesite (Wang et al., 2020).

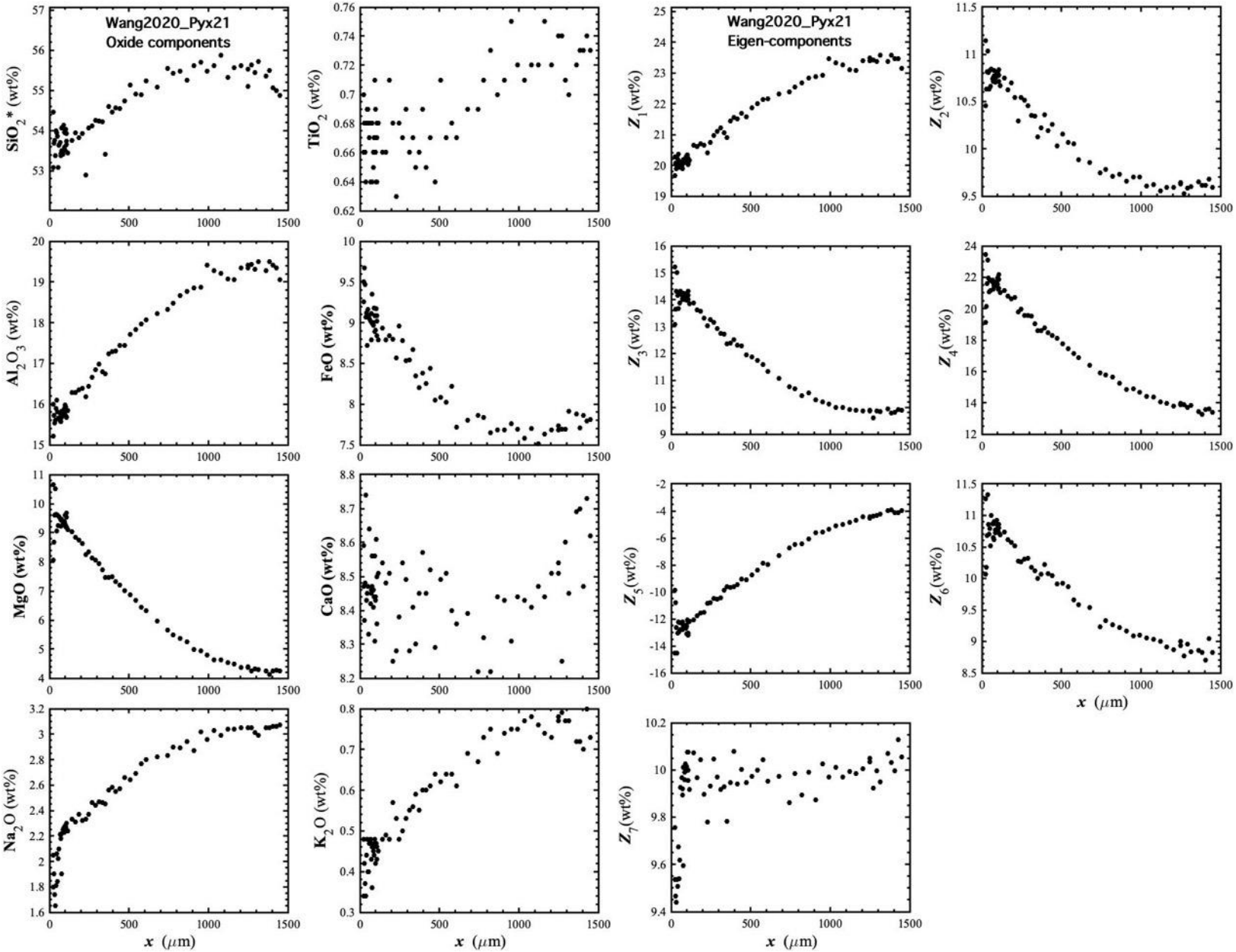

Figure 152. Concentration profiles of oxide components in wt% (left panel) and eigen-components (right panel) of Wang2020_Pyx21, which is a lherzolite dissolution experiment in basaltic andesite (Wang et al., 2020).

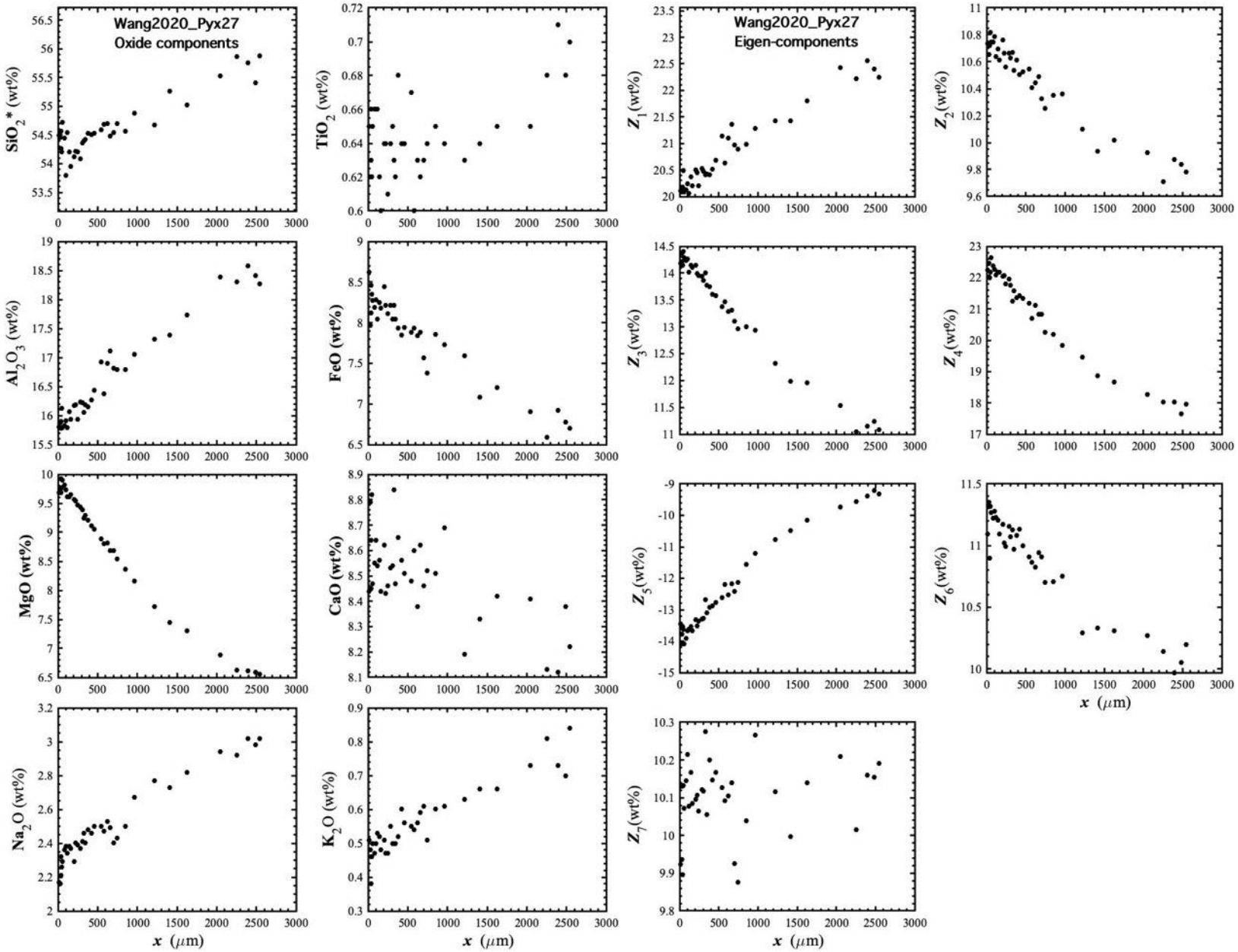

Figure 153. Concentration profiles of oxide components in wt% (left panel) and eigen-components (right panel) of Wang2020_Pyx27, which is a lherzolite dissolution experiment in basaltic andesite (Wang et al., 2020).

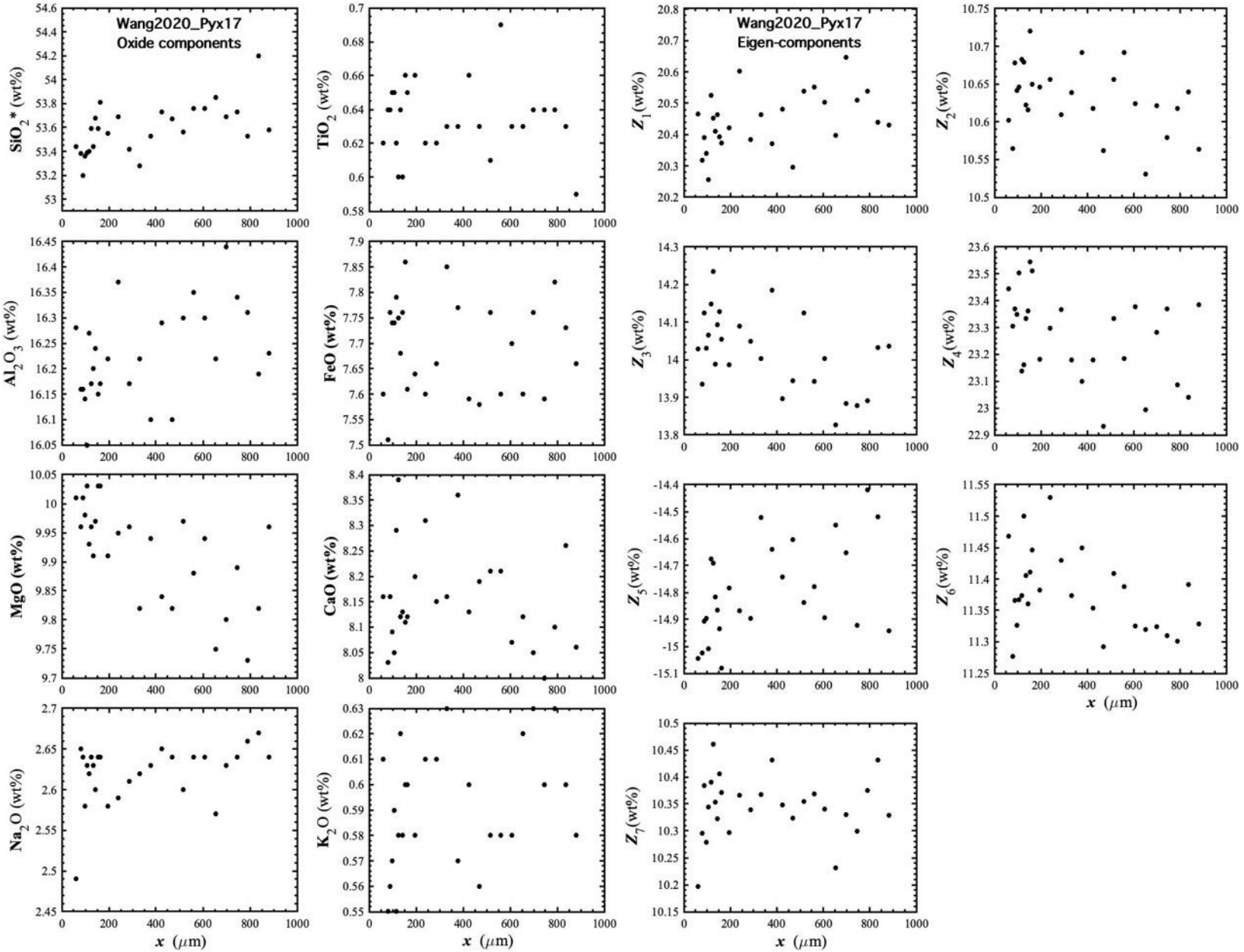

Figure 154. Concentration profiles of oxide components in wt% (left panel) and eigen-components (right panel) of Wang2020_Pyx17, which is a lherzolite dissolution experiment in basaltic andesite (Wang et al., 2020).

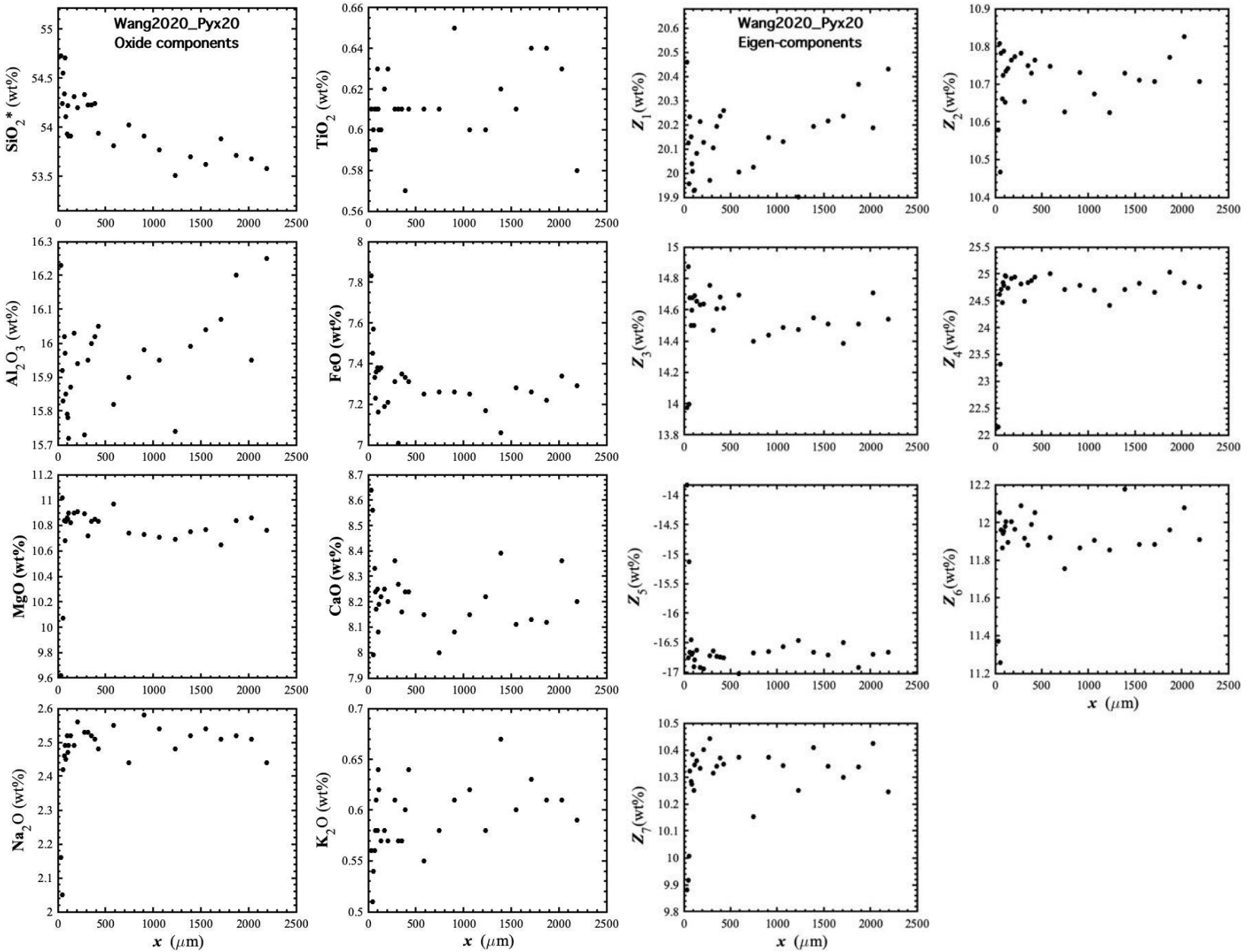

Figure 155. Concentration profiles of oxide components in wt% (left panel) and eigen-components (right panel) of Wang2020_Pyx20, which is a lherzolite dissolution experiment in basaltic andesite (Wang et al., 2020).

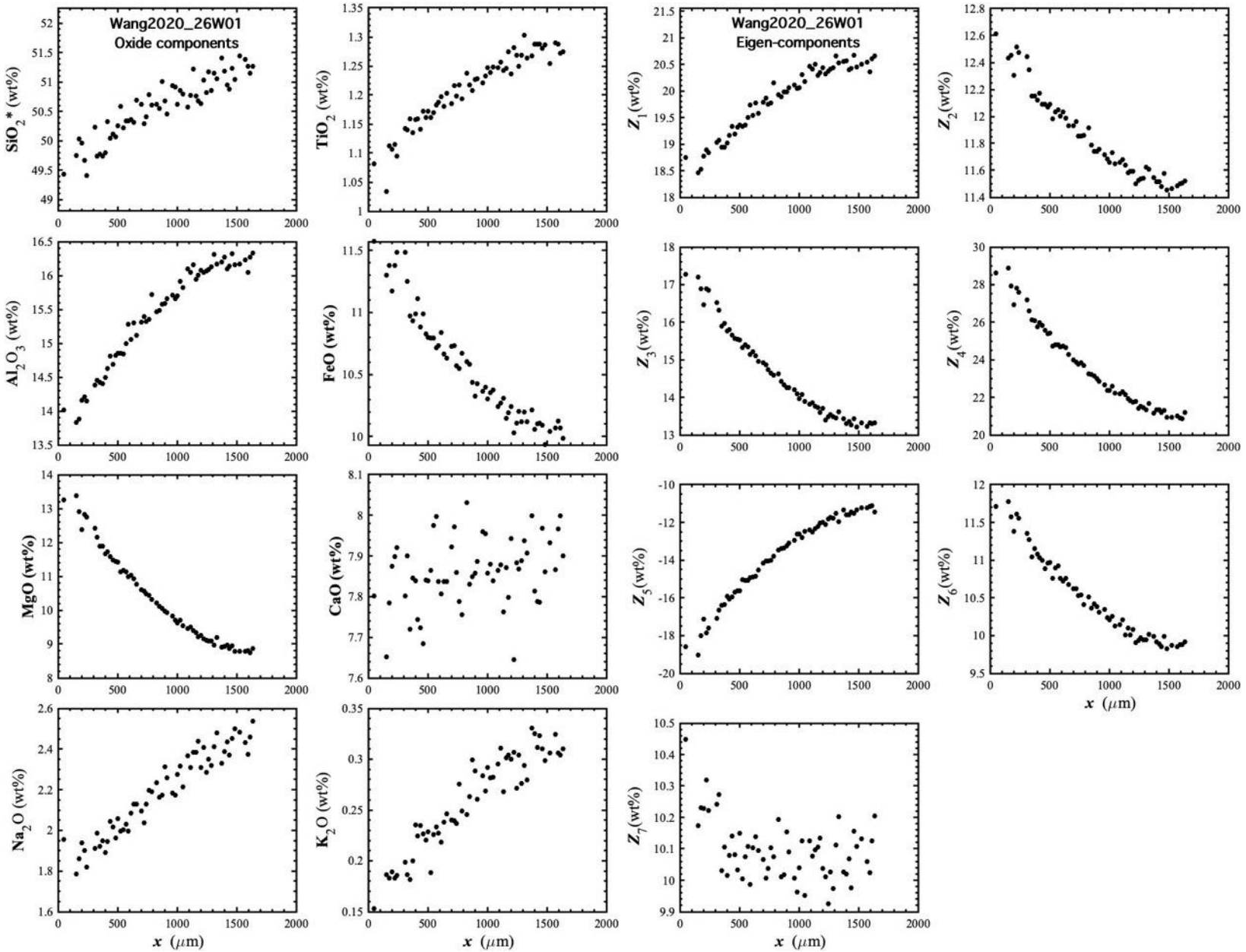

Figure 156. Concentration profiles of oxide components in wt% (left panel) and eigen-components (right panel) of Wang2020_26W01, which is a lherzolite dissolution experiment in basaltic andesite (Wang et al., 2020).

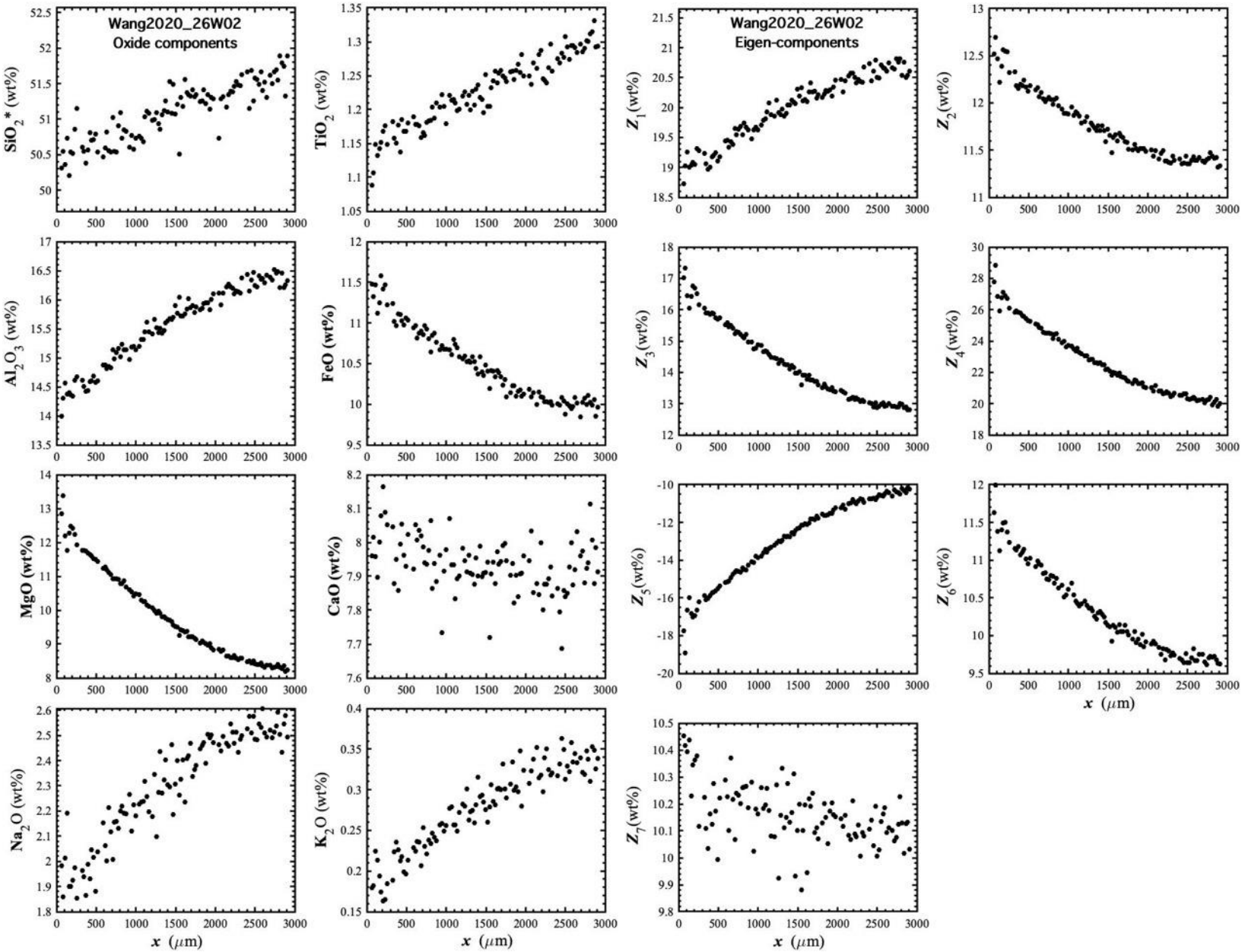

Figure 157. Concentration profiles of oxide components in wt% (left panel) and eigen-components (right panel) of Wang2020_26W02, which is a lherzolite dissolution experiment in basaltic andesite (Wang et al., 2020).

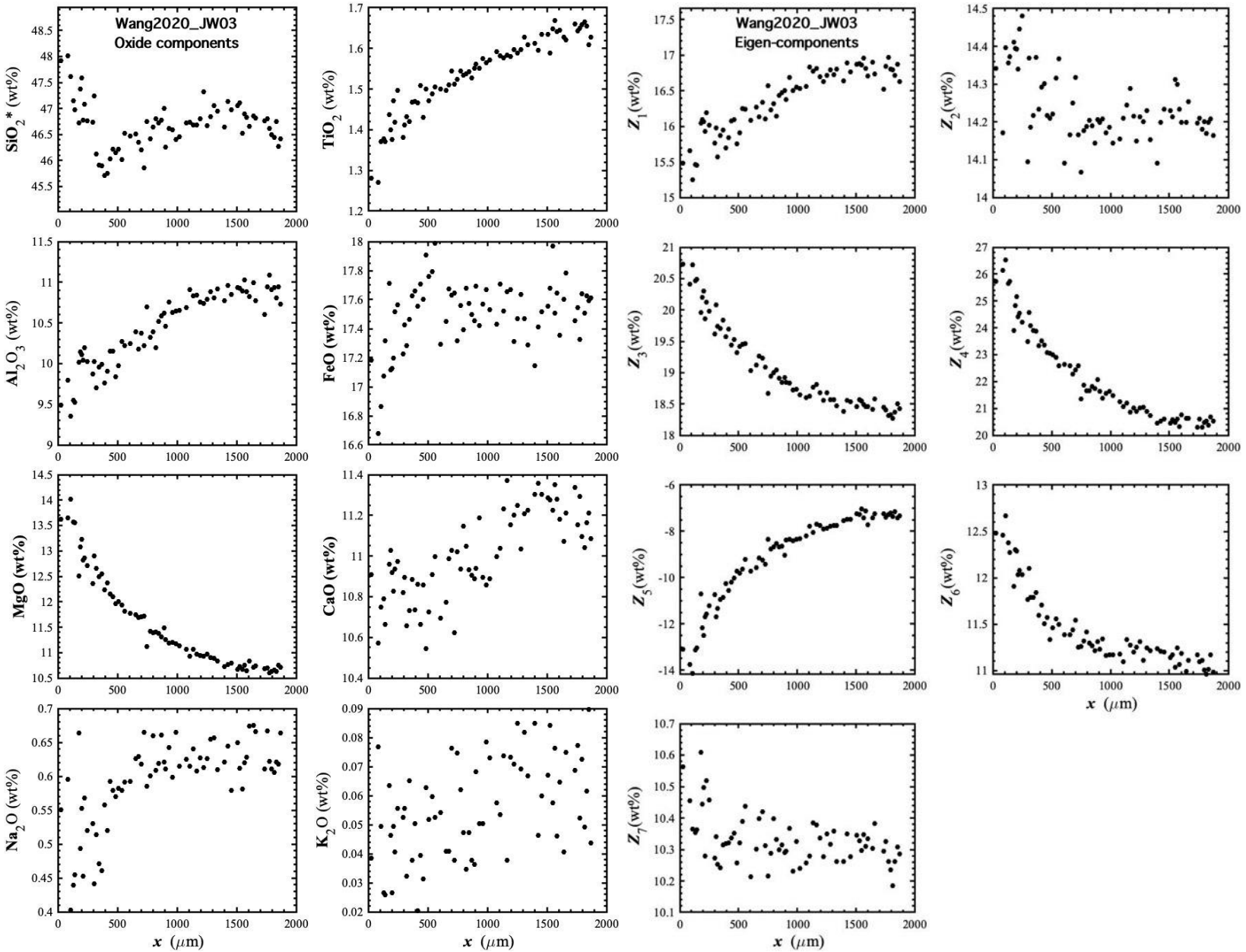

Figure 158. Concentration profiles of oxide components in wt% (left panel) and eigen-components (right panel) of Wang2020_JW03, which is a lherzolite dissolution experiment in ferro-basalt (Wang et al., 2020).

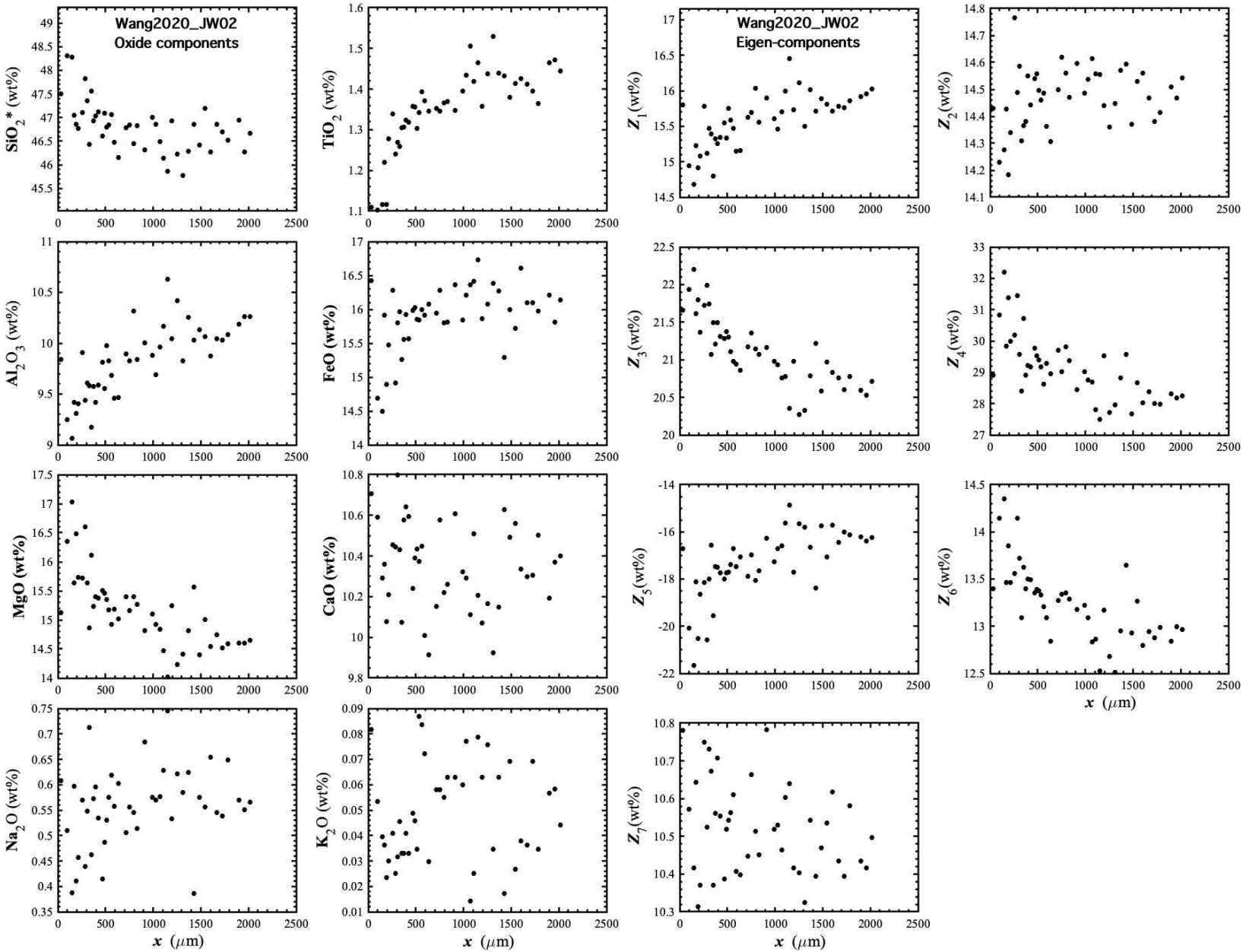

Figure 159. Concentration profiles of oxide components in wt% (left panel) and eigen-components (right panel) of Wang2020_JW02, which is a lherzolite dissolution experiment in ferro-basalt (Wang et al., 2020).

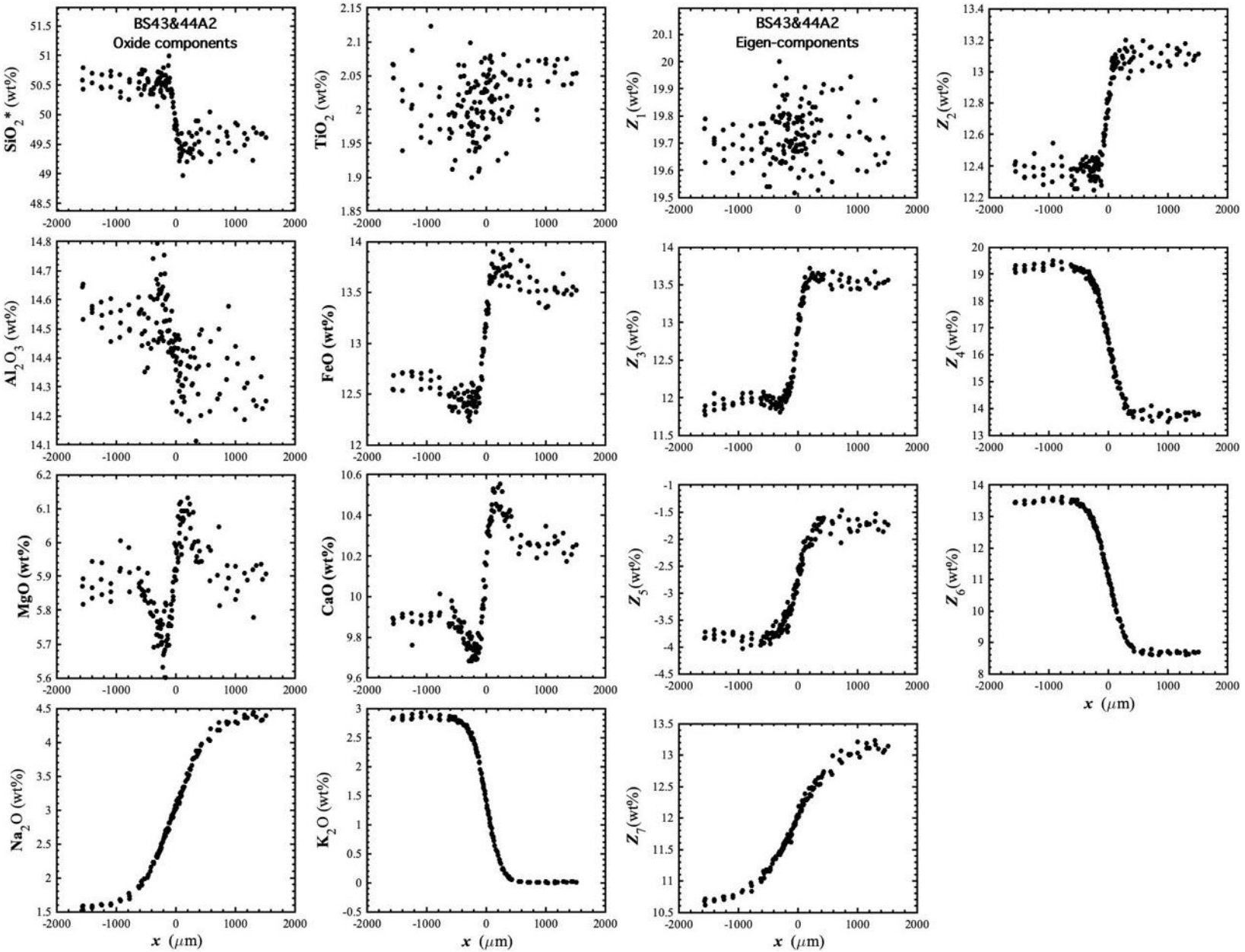

Figure 160. Concentration profiles of oxide components in wt% (left panel) and eigen-components (right panel) of BS43&44A2, which is a diffusion couple experiment in basalt, conducted in this work.